

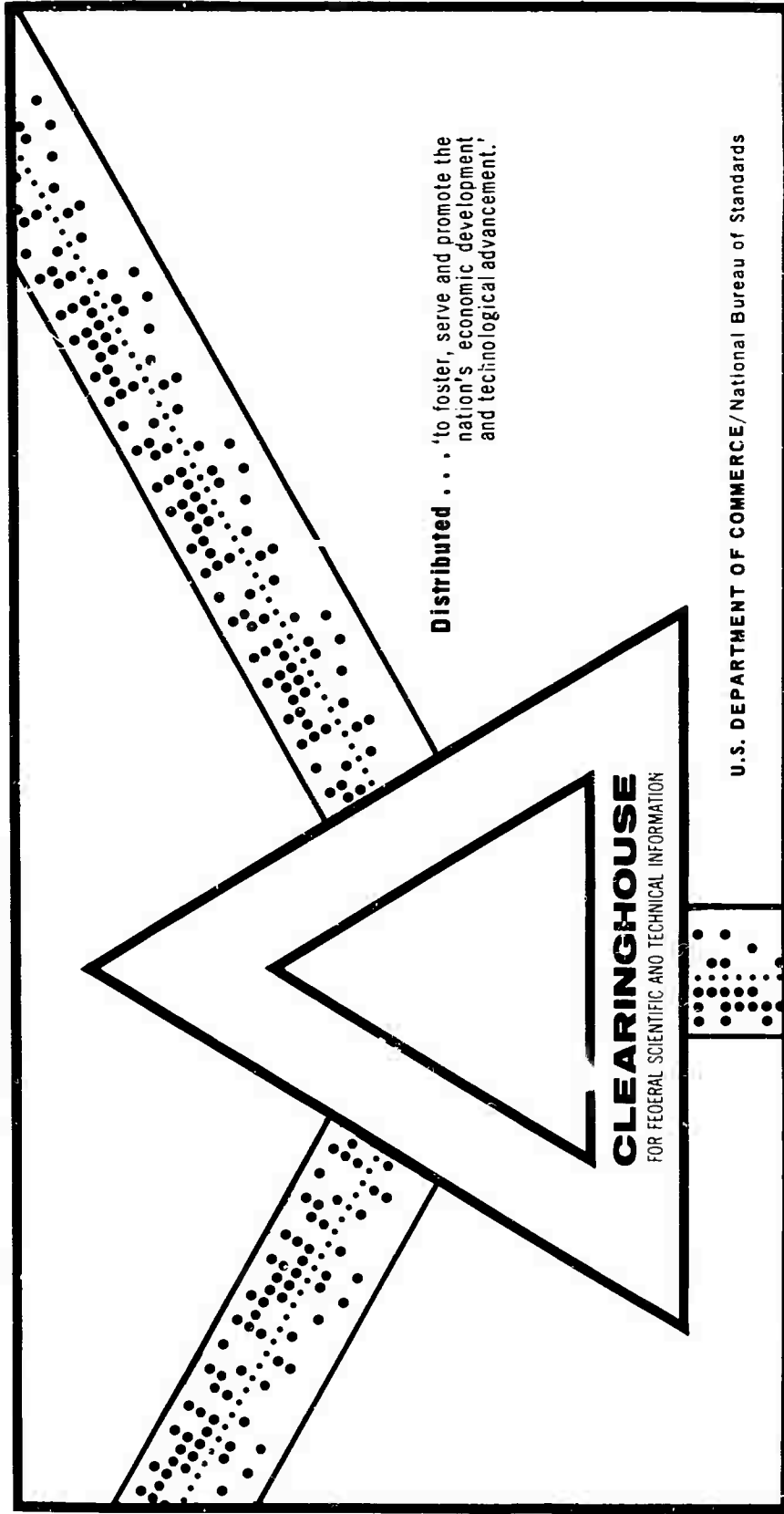
AD 697 729

DUAL INPUT DESCRIBING FUNCTIONS

Gordon D. Welford

Army Missile Command
Redstone Arsenal, Alabama

28 October 1969



Distributed . . . 'to foster, serve and promote the nation's economic development and technological advancement.'

CLEARINGHOUSE
FOR FEDERAL SCIENTIFIC AND TECHNICAL INFORMATION

U.S. DEPARTMENT OF COMMERCE/National Bureau of Standards

This document has been approved for public release and sale.

AD 697729

AD

REPORT NO. RG-TR-69-16

DUAL INPUT DESCRIBING FUNCTIONS

by

Gordon D. Welford

October 1969

This document has been approved for public release and sale; its distribution is unlimited.



U.S. ARMY MISSILE COMMAND

Redstone Arsenal, Alabama

Reproduced by the
CLEARINGHOUSE
for Federal Scientific & Technical
Information, Springfield Va. 22151

U S A R M Y
D E C 8 1969
G

108

ACCESSION for		
CPSTI	WRITE SECTION <input checked="" type="checkbox"/>	
DOC	BUFF SECTION <input type="checkbox"/>	
UNANNOUNCED <input type="checkbox"/>		
JUSTIFICATION		
BY		
DISTRIBUTION/AVAILABILITY CODES		
DIST.	AVAIL.	and/or SPECIAL
/		

DISPOSITION INSTRUCTIONS

*Destroy this report when it is no longer needed.
Do not return it to the originator.*

DISCLAIMER

The findings in this report are not to be construed as an official Department of the Army position unless so designated by other authorized documents.

28 October 1969

Report No. RG-TR-69-16

DUAL INPUT DESCRIBING FUNCTIONS

by

Gordon D. Welford

*This document has been approved for public release
and sale; its distribution is unlimited.*

Army Inertial Guidance and Control Laboratory and Center
Research and Engineering Directorate (Provisional)
U. S. Army Missile Command
Redstone Arsenal, Alabama 35809

ABSTRACT

A study was made of Dual Input Describing Functions (DIDF) for nonlinear elements with a view toward the synthesis problem where the characteristics of the DIDF are specified a priori. The study included a literature survey and an analytical investigation of the DIDF.

Improved methods for calculating DIDF's were sought. The problem of defining the DIDF in such a way that it is valid for multivalued nonlinear elements was also considered and one method of solution is proposed. The effect of changes in the secondary signal waveform on the DIDF for nonlinear elements was also investigated.

ACKNOWLEDGEMENTS

The author would like to express his gratitude to Professor C. D. Johnson for his many helpful suggestions while supervising and guiding this research program. The author also gratefully acknowledges the support of the Army Missile Command and in particular Mr. J. B. Huff and Mr. W. A. Griffith of the Army Guidance and Control Laboratory and Center and Mr. J. J. Fagan of the Office of the Director, Research and Engineering Directorate.

CONTENTS

	Page
Chapter I. INTRODUCTION	1
Chapter II. METHODS OF OBTAINING THE DIDF FOR DETERMINISTIC INPUTS	13
2.1 The DIDF of West, Douce, and Livesley	13
2.2 The Modified Nonlinear Element Concept	14
2.3 Power Series Method (TSIDF)	18
2.4 Methods of Stochastic Processes	19
2.5 Methods of Determining the DIDF for Multivalued Nonlinear Elements	20
2.6 A New Average DIDF Method for Deterministic Inputs	21
Chapter III. DEFINITION AND SOLUTION OF AN INVERSE DIDF PROBLEM FOR A PARTICULAR CLASS OF NONLINEAR ELEMENTS	31
Chapter IV. THE MODIFIED NONLINEAR ELEMENTS AND DUAL INPUT DF'S FOR TEN NONLINEAR ELEMENTS	53
4.1 Absquare	56
4.2 Relay	61
4.3 Preload	66
4.4 Relay with Dead Band	71
4.5 Dead Band	84
4.6 Limiter	92
4.7 Limiter with Dead Band	100
4.8 Relay with Dead Band and Hysteresis	111
4.9 Relay with Hysteresis	120
4.10 Limiter with Hysteresis	129
Chapter V. TWO-SINUSOID INPUT DF FOR RELAY WITH HYSTERESIS	148

CONTENTS (Concluded)

	Page
Chapter VI. CONCLUSIONS AND RECOMMENDATIONS FOR FUTURE WORK	162
Appendix. EXAMPLE CALCULATIONS OF THE MODIFIED NONLINEAR ELEMENT AND DIDF	166
REFERENCES	177
BIBLIOGRAPHY	181

ILLUSTRATIONS

Figure		Page
1.1	Replacement of the Original Nonlinear Element N by Its DF $\hat{K}(A)$	2
1.2	Actual Input and Output Signals of Nonlinear Element with Characteristic N(e)	3
1.3	Example Showing Nonlinear Element Replaced by Its DIDF	5
2.1	Diagram Showing the Error Term R(x,y,z) and Equivalent Representation of a Three-Input Nonlinear Element Where R(x,y,z) Is Neglected	15
3.1	Diagram Illustrating the Inverse DIDF Problem	33
3.2	Region over Which $\hat{N}[A_0; \sigma(\beta t)]$ May Be Varied by Changing $\sigma(\beta t)$	35
3.3	The Composite Signal $\sigma(\beta t) + A_0$	37
3.4	Modified Nonlinear Element and Secondary Signal for Perfect Relay Where N^* Is Given by $k_1\sqrt{A_0}$ over a Positive Range of A_0	40
3.5	A Secondary Signal Which Linearizes the Absquare	41
3.6	Sketch of the Secondary Signal $\sigma(\beta t) = B\left(\frac{2}{B}\beta t\right)$ and the Corresponding Modified Nonlinear Element for the Relay with Dead Band	46
3.7	Approximate Secondary Signal	47

ILLUSTRATIONS (Continued)

Figure		Page
4.1	Absquare	56
4.2	Modified Nonlinear Element for Absquare, Sine Wave Secondary Signal	57
4.3	DIDF for Absquare, Sine Wave Secondary Signal	58
4.4	Modified Nonlinear Element for Absquare, Triangle Wave Secondary Signal	59
4.5	DIDF for Absquare, Triangle Wave Secondary Signal	60
4.6	Relay	61
4.7	Modified Nonlinear Element for Absquare, Square Wave Secondary Signal	62
4.8	DIDF for Absquare, Square Wave Secondary Signal	63
4.9	Modified Nonlinear Element for Perfect Relay, Sine Wave Secondary Signal	64
4.10	DIDF for Relay, Sine Wave Secondary Signal	65
4.11	Preload	66
4.12	Modified Nonlinear Element for Perfect Relay, Triangle Wave Secondary Signal	67
4.13	DIDF for Relay, Triangle Wave Secondary Signal	68
4.14	Modified Nonlinear Element for Perfect Relay, Square Wave Secondary Signal	69
4.15	DIDF for Relay, Square Wave Secondary Signal	70
4.16	Modified Nonlinear Element for Preload, Sine Wave Secondary Signal	72
4.17	DIDF for Preload, Sine Wave Secondary Signal	73
4.18	Modified Nonlinear Element for Preload, Triangle Wave Secondary Signal	74

ILLUSTRATIONS (Continued)

Figure	Page
4.19	DIDF for Preload, Triangle Wave Secondary Signal 75
4.20	Modified Nonlinear Element for Preload, Square Wave Secondary Signal 76
4.21	DIDF for Preload, Square Wave Secondary Signal 77
4.22	Modified Nonlinear Element for Relay with Dead Band, Sine Wave Secondary Signal 78
4.23	DIDF for Relay with Dead Band, Sine Wave Secondary Signal 79
4.24	Relay with Dead Band 80
4.25	Modified Nonlinear Element for Relay with Dead Band, Triangle Wave Secondary Signal 82
4.26	DIDF for Relay with Dead Band, Triangle Wave Secondary Signal 83
4.27	Dead Band 84
4.28	Modified Nonlinear Element for Relay with Dead Band, Square Wave Secondary Signal 85
4.29	DIDF for Relay with Dead Band, Square Wave Secondary Signal 86
4.30	Modified Nonlinear Element for Dead Band, Sine Wave Secondary Signal 87
4.31	DIDF for Dead Band, Sine Wave Secondary Signal 88
4.32	Modified Nonlinear Element for Dead Band, Triangle Wave Secondary Signal 90
4.33	DIDF for Dead Band, Triangle Wave Secondary Signal 91
4.34	Limiter 92
4.35	Modified Nonlinear Element for Dead Band, Square Wave Secondary Signal 93

ILLUSTRATIONS (Continued)

Figure		Page
4.36	DIDF for Dead Band, Square Wave Secondary Signal	94
4.37	Modified Nonlinear Element for Limiter, Sine Wave Secondary Signal	96
4.38	DIDF for Limiter, Sine Wave Secondary Signal	97
4.39	Modified Nonlinear Element for Limiter, Triangle Wave Secondary Signal	98
4.40	DIDF for Limiter, Triangle Wave Secondary Signal	99
4.41	Saturation with Dead Band	100
4.42	Modified Nonlinear Element for Limiter, Square Wave Secondary Signal	101
4.43	DIDF for Limiter, Square Wave Secondary Signal	102
4.44	Modified Nonlinear Element for Limiter with Dead Band, Sine Wave Secondary Signal	103
4.45	DIDF for Limiter with Dead Band, Sine Wave Secondary Signal	104
4.46	Modified Nonlinear Element for Limiter with Dead Band, Triangle Wave Secondary Signal	106
4.47	DIDF for Limiter with Dead Band, Triangle Wave Secondary Signal	107
4.48	Modified Nonlinear Element for Limiter with Dead Band, Square Wave Secondary Signal	109
4.49	DIDF for Limiter With Dead Band, Square Wave Secondary Signal	110
4.50	Relay with Dead Band and Hysteresis	111
4.51	Modified Nonlinear Element for Relay with Hysteresis and Dead Band, Sine Wave Secondary Signal	112

ILLUSTRATIONS (Continued)

Figure		Page
4.52	DIDF for Relay with Hysteresis and Dead Band, Sine Wave Secondary Signal	113
4.53	Modified Nonlinear Element	113
4.54	Modified Nonlinear Element for Relay with Hysteresis and Dead Band, Sine Wave Secondary Signal	117
4.55	DIDF for Relay with Dead Band and Hysteresis, Triangle Wave Secondary Signal	118
4.56	Relay with Hysteresis	120
4.57	Modified Nonlinear Element for Relay with Hysteresis and Dead Band, Square Wave Secondary Signal	121
4.58	DIDF for Relay with Dead Band and Hysteresis, Square Wave Secondary Signal	122
4.59	Phase of DIDF for Relay with Hysteresis and Dead Band	123
4.60	Modified Nonlinear Element for Relay with Hysteresis, Sine Wave Secondary Signal	125
4.61	DIDF for Relay with Hysteresis, Sine Wave Secondary Signal	126
4.62	Modified Nonlinear Element for Relay with Hysteresis, Triangle Wave Secondary Signal	127
4.63	DIDF for Relay with Hysteresis, Triangle Wave Secondary Signal	128
4.64	Modified Nonlinear Element for Relay with Hysteresis, Square Wave Secondary Signal	130
4.65	DIDF for Relay with Hysteresis, Square Wave Secondary Signal	131
4.66	Phase of DIDF for Relay with Hysteresis	132
4.67	Modified Nonlinear Element for Limiter with Hysteresis, Sine Wave Secondary Signal	133

ILLUSTRATIONS (Continued)

Figure		Page
4.68	DIDF for Limiter with Hysteresis, Sine Wave Secondary Signal	134
4.69	Phase of DIDF for Limiter with Hysteresis, Sine Wave Secondary Signal	135
4.70	Limiter with Hysteresis	136
4.71	Modified Nonlinear Element When $B < b$	136
4.72	Modified Nonlinear Element When $B > b$	138
4.73	Modified Nonlinear Element for Limiter with Hysteresis, Triangle Wave Secondary Signal	140
4.74	DIDF for Limiter with Hysteresis, Triangle Wave Secondary Signal	141
4.75	Modified Nonlinear Element for Limiter with Hysteresis, Square Wave Secondary Signal	144
4.76	DIDF for Limiter with Hysteresis, Square Wave Secondary Signal	145
4.77	Modified Nonlinear Element When $B < b$ for the Square Wave Secondary Signal	146
4.78	Modified Nonlinear Element When $B > b$ for the Square Wave Secondary Signal	147
5.1	Relay with Hysteresis	148
5.2	Composite Input Signal for Defining Switching Point	151
5.3	Magnitude of DIDF of Relay with Hysteresis When $B/a = 0.5$	152
5.4	Phase of DIDF of Relay with Hysteresis When $B/a = 0.5$	153
5.5	Phase of DIDF of Relay with Hysteresis When $B/a = 0.5$	154
5.6	Magnitude of DIDF of Relay with Hysteresis When $B/a = 1.0$	155

ILLUSTRATIONS (Concluded)

Figure		Page
5.7	Phase of DIDF of Relay with Hysteresis When $B/a = 1.0$	156
5.8	Magnitude of DIDF of Relay with Hysteresis When $B/a = 2.0$	157
5.9	Phase of DIDF of Relay with Hysteresis When $B/a = 2.0$	158
5.10	Magnitude of DIDF of Relay with Hysteresis When $B/a = 4.0$	159
5.11	Phase of DIDF of Relay with Hysteresis When $B/a = 4.0$	160
A-1	Input and Output Signals of Absquare for Computing Modified Nonlinear Element	170
A-2	Input and Output Signals of Absquare Nonlinear Element for Determining the Modified Nonlinear Element	172
A-3	Modified Nonlinear Element for Absquare with Triangle Wave Secondary Signal, Shown with Primary Input Signal	173
A-4	Bias and Square Wave Secondary Signal	175

SYMBOLS

a	parameter associated with nonlinear element
b	parameter associated with nonlinear element
c	parameter associated with nonlinear element
e	input to a nonlinear element
k	the modulus in elliptic integrals
n	frequency ratio of nonlinear element input components
t	time
y	output of nonlinear element
A	amplitude of primary component in the nonlinear element input
A_0	bias or dc component in the nonlinear element input
B	amplitude of secondary component in the nonlinear element input
E	complete elliptic integral of the second kind
F	complete elliptic integral of the first kind
\hat{K}	DIDF
M	parameter associated with nonlinear element
N	nonlinear element
\hat{N}	modified nonlinear element
R	unwanted components in the nonlinear element output

SYMBOLS (Concluded)

α	parameter associated with elliptic integral of third kind
β	fundamental frequency of secondary input component to nonlinear element
γ_i	functions associated with the DIDF
Δ	incremental phase angle of an approximate secondary input
θ_i	functions associated with the modified nonlinear element
π	3.1416
σ	the secondary component of the input to a nonlinear element
ϕ	phase angle associated with the secondary component of nonlinear element input
ω	frequency of primary component of nonlinear element input

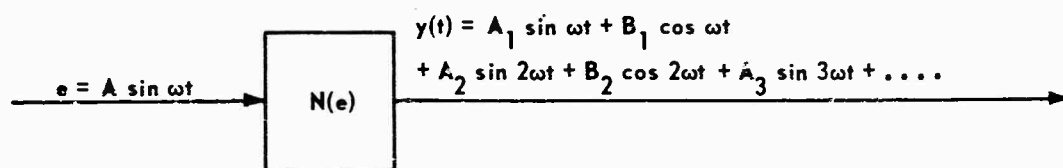
CHAPTER I

INTRODUCTION

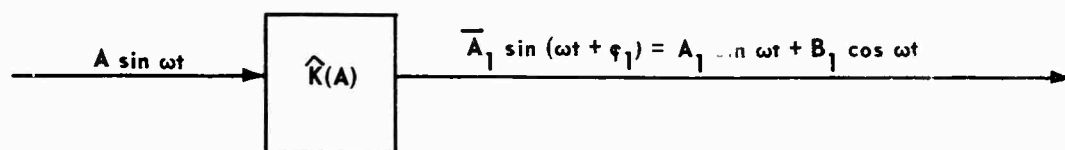
A typical nonlinear element N , as encountered in automatic control applications, may be characterized mathematically as a nonlinear operator which acts on a scalar input signal e and produces a scalar output signal $y = N(e)$ where, in general, $N(e)$ is a nonlinear function. In many cases, $N(e)$ is a multiple or even infinitely valued "function" and may possess a number of simple jump discontinuities. Hereafter the function $N(e)$ is referred to as the "characteristic" of the nonlinear element N .

One method commonly used to analyze electrical networks and feedback control systems containing such nonlinear elements is the Method of Describing Functions (DF). This method consists of a linearizing process whereby the nonlinear operator $N(e)$ is replaced by a (possibly complex) parameter dependent linear operator called the describing function. The DF method originated in the sinusoidal analyses of feedback control systems containing nonlinear elements and was therefore originally developed only for sinusoidal inputs. The DF for that case can be explained by Figure 1.1. The constant (possibly complex) gain $\hat{K}(A)$ is chosen so that the output $A_1 \sin(\omega t + \phi_1)$ of the linearized representation is precisely equal to the fundamental component

of the actual output $y(t)$ of the nonlinear element, the latter being determined by an ordinary Fourier Series analysis of $y(t)$. The remainder, $R(t) = A_2 \sin 2\omega t + B_2 \cos 2\omega t + \dots$, of the actual output $y(t)$ is, in effect, neglected.



(a) Actual Output of Nonlinear Element N



(b) Linearized Representation of Nonlinear Element N

Figure 1.1. Replacement of the Original Nonlinear Element N by Its DF $\hat{K}(A)$

Thus, the approximation of N by its DF is useful primarily in applications where the signal $y(t)$ subsequently passes through a filtering process such that the contribution of $R(t)$ at the filter output is negligible. In fact, it was situations of this type which prompted the original applications of the DF. As the filtering action more closely approximates that of a perfect low pass filter [low pass with respect to the fundamental frequency ω of $y(t)$], the DF approximation of N becomes more exact. It is remarked that the ordinary DF analysis is valid only if the nonlinear element output $y(t)$ has zero average value and the fundamental component of $y(t)$ has the same frequency ω as

the input $e(t) = A \sin \omega t$.

The intuitive (original) approach to the DF analysis described above leads one to the following definition of the parameter dependent gain $\hat{K}(A)$

$$\hat{K}(A) = \frac{A_1 + jB_1}{A} \triangleq \hat{K}_R + j\hat{K}_I, \quad (1.1)$$

where $\hat{K}(A)$ is defined in complex variable notation ($j = \sqrt{-1}$). The terms A_1 and B_1 are the magnitudes of the fundamental in-phase and quadrature components of the output $y(t)$.

The DF described above can also be derived by means of a seemingly different approach to the problem. In this approach the unwanted harmonics $R(t)$ are minimized in the root-mean-squared (RMS) sense. In other words, one seeks the function $\hat{K}(A)$ which gives the minimum RMS value of $R(t)$ in Figure 1.2.

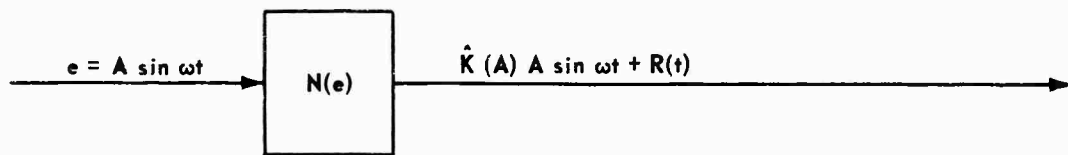


Figure 1.2. Actual Input and Output Signals of Nonlinear Element with Characteristic $N(e)$

The RMS value of $R(t)$ is given by

$$\begin{aligned} \bar{R} &= \left\{ \frac{1}{2\pi} \int_0^{2\pi} [N(A \sin \omega t) - \hat{K} A \sin \omega t]^2 d\omega t \right\}^{1/2} \\ &= \left\{ \frac{1}{2\pi} \int_0^{2\pi} [N(A \sin \omega t) - \hat{K}_R A \sin \omega t - \hat{K}_I A \cos \omega t]^2 d\omega t \right\}^{1/2}. \end{aligned} \quad (1.2)$$

It is not difficult to show that the minimum value of \bar{R} results when

$$\hat{K}_R = \frac{1}{\pi A} \int_0^{2\pi} N(A \sin \omega t) \sin \omega t \, d\omega t \quad (1.3)$$

$$\hat{K}_I = \frac{1}{\pi A} \int_0^{2\pi} N(A \sin \omega t) \cos \omega t \, d\omega t \quad (1.4)$$

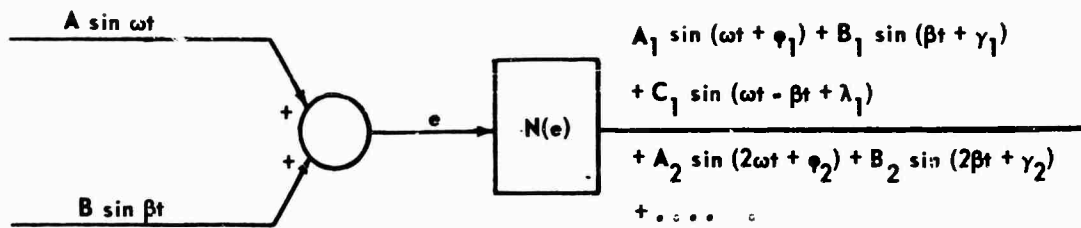
The result [Equations (1.3) and (1.4)] gives precisely the same DF previously described and illustrated in Figure 1.1. However, the derivation of DF's by minimization of the RMS value of $R(t)$ provides a convenient means for accommodating more general (non-sinusoidal) periodic inputs to N .

The conventional Dual Input Describing Function (DIDF) is defined for an input e which is the sum of two (possibly independent) components e_i where the e_i are typically chosen as constant, sinusoidal, or random noise signals. In this case, a DIDF or "equivalent linear gain" can be defined for each input component $e_i(t)$. Figure 1.3 illustrates how a nonlinear element with two sine wave input components can be replaced by two DIDF's.

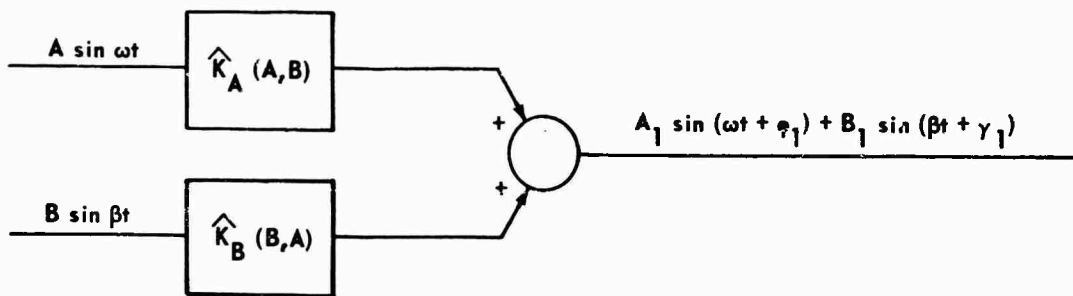
It is useful at this point to introduce, in a simplified way, the underlying principle of the DIDF for a nonlinear element with two independent input components. A more complete mathematical description of the DIDF and one means of deriving it for deterministic input components is given in Chapter II.

If the primary component of the input to the nonlinear element is denoted by e_1 and the secondary input component is e_2 , the DIDF for the component e_1 is defined as the coefficient of the term e_1 in the output $y(t)$, where $y(t)$ is written in the form

$$y(t) = \hat{K}_1 e_1(t) + R(t) \quad (1.5)$$



(a) Original Representation



(b) Equivalent Representation

Figure 1.3. Example Showing Nonlinear Element Replaced by Its DIDF

and $R(t)$ does not contain terms linear in $e_1(t)$. Since superposition does not hold, the presence of e_2 has the effect of "altering" the value of \hat{K}_1 , which in turn is chosen so that $R(t)$ is minimized in the RMS sense. In general the output $y(t)$ of the nonlinear element consists of terms involving e_1^p , e_2^q , and $e_1^p e_2^q$ where p and q are integers.

The observation that the characteristic $N(e)$ of a nonlinear element is, in effect, "altered" by addition of a secondary high frequency sinusoidal signal $e_2(t)$ to the primary component $e_1(t)$ was observed some time ago. In 1945 McColl [1] noted the apparent linearizing effect of the "extra oscillation" on a relay control system. He also mentioned the idea of replacing the original

relay element with a new "effectively linear" element and, by so doing, avoiding all explicit mention of the extra oscillation. McColl attributes this latter idea to Lozier [2]. These two ideas are the basic notions of the DIDF technique; they actually had their beginning prior to any published work on the "single input" DF.

Some of the earliest studies of describing function techniques were conducted independently by Goldfarb [3], Tustin [4], and Kochenburger [5]. These early researchers were evidently inspired by the so-called method of "harmonic balance" developed somewhat earlier by Kryloff and Bogoliuboff [6]. The success and wide acceptance of both the DF and DIDF can be attributed to the good low pass filtering characteristics of most practical controlled plants. This is true even though the definition of both the DF and the DIDF depends only upon the nonlinear element and input signals.

The use of a triangle wave secondary component $e_2(t)$ to provide "precisely linear" signal amplification, in the sense of the DIDF for carrier-controlled relay servos, was probably first proposed by Lozier [2]. The basic concepts involved in the DIDF for two sinusoidal components, where the ratio of frequencies is an irrational number, were clearly outlined by Lozier. West, Douce, and Livesly [7] first introduced the term "Dual Input Describing Function" and made a major contribution toward the development of practical computational procedures. However, the DIDF of West et al. is valid only for two sinusoidal components where the frequency ratio of the two sinusoids is a rational number. In practice this frequency ratio is usually taken as an integer or the reciprocal of an integer. The DIDF of West et al. is very cumbersome

because of the many parameters involved. In a later study, Oldenburger [8] noted the stabilizing effect brought about by the addition of a high frequency sinusoidal secondary signal into the nonlinear element input in certain unstable nonlinear feedback control systems. Somrervil' and Atherton [9] proposed a very appealing approximate method for calculating multiple input describing functions or equivalent gains \hat{K} which are valid for several input components with different waveforms including dc, sinusoidal, and gaussian noise. When the input consists of only two independent components, they propose and outline a method for obtaining the DIDF by a two-stage evaluation process in which the first step involves the calculation of an effective or modified nonlinear element. Oldenburger and Boyer [10] utilized a modified nonlinear element approach to derive many useful DIDF curves for the restricted case of two sinusoidal components where the frequency of the secondary component is high compared to the primary component. The modified nonlinear element concept was later shown, by Gibson and Sridhar [11], to give exact answers (subject of course to the accuracy of computational methods and equipment) for two sine wave components where the frequency ratio is an irrational number. The DIDF considered by Gibson and Sridhar was derived using the theory of random functions and is valid only for single valued nonlinear elements. Much earlier, however, Bennett [12], and later Kalb and Bennett [13], used a double Fourier Series expansion of a nonlinear element output in analyzing modulation products. Later Amsler and Gorozdos [14] used the method of Bennett and Kalb in the analysis of bistable control systems and derived what was later called the

DDIF for a relay with two sinusoidal input components with irrational frequency ratio.

Other investigators such as Sridhar and Oldenburger [15] and Atherton and Turnbull [16] have proposed alternative approaches to the DIDF based upon statistical methods. Gelb and Vander Velde [17] make use of a simpler dc equivalent gain as an approximation to the DIDF for two sinusoidal components in the analysis of limit cycling control systems. In a recent book, Gelb and Vander Velde [18] have applied the integral representation of nonlinear elements used by Gibson and Sridhar to the calculation of a DIDF for two sinusoidal input components (two-sinusoid input describing function or TSIDF). However, in their book Gelb and Vander Velde use purely deterministic arguments rather than the theory of random functions. In this same book Gelb and Vander Velde also disclose a very appealing power series TSIDF calculation for odd nonlinear elements with input sinusoids whose frequency ratio is irrational. This power series of the TSIDF is easily generated from an algebraic form of the ordinary DF.

All of the methods discussed above, with the exception of the DIDF of West, Douce, and Livesly [7] apply only to single valued nonlinear elements. Recently, Mahalanabis and Nath [19-21] have proposed a method of calculating the DIDF which, they assert, holds for multivalued nonlinear elements with multiple inputs. However, Atherton [22] has subsequently pointed out that this proposed method is valid only when the nonlinear element may be described by the function $f(e, \dot{e})$, where e is the input to the nonlinear element [23]. Often a function $f(e, \dot{e})$, although incorrectly describing the characteristic of a given

multivalued nonlinear element, may be successfully employed when the derivative of the input signal does not change signs within the hysteresis or multivalued region. This condition cannot, in general, be guaranteed for two independent input components regardless of any stipulations on the amplitude of these signals. Consequently, the method proposed by Mahalanabis and Nath is incorrect for two input components even when the restriction is added that the difference in amplitudes of the two components must be greater than the hysteresis width. For this reason, many subsequent articles [24-28] relating to such a method are incorrect. Mohan and Krishna [29] have correctly used this approach to find DIDF's for some multivalued nonlinear elements for which the function $f(e, \dot{e})$ is an exact representation. This rather special class of nonlinear elements excludes many of the important multivalued nonlinear elements encountered in practice, however.

Since frequencies and the frequency ratio of the two periodic components of the input to a nonlinear element are mentioned quite often in this report, standard symbols will be adopted for these terms. Hereafter the frequency of the primary input component (usually a sine wave) will be defined as ω and the fundamental frequency of the deterministic secondary input component will be defined as β . The term "frequency ratio" will refer to the ratio $= \beta/\omega$.

One may successfully apply the modified nonlinear element method of determining the DIDF for multivalued nonlinear elements when certain restrictions are placed on the input components. Atherton and Turnbull [16] have demonstrated that good approximate answers may be obtained when $\beta/\omega \gg 1$ or when $\beta/\omega \ll 1$. The first case ($\beta/\omega \gg 1$) requires only a straightforward

application of the method, whereas the latter case ($\beta/\omega \ll 1$) requires a slight modification of the method as originally outlined by Sommerville and Atherton [9].

Cook [30] has given the DIDF of some multivalued nonlinear elements for both sinusoidal and statistical secondary input components by using the modified nonlinear element method. Cook considered only the more straightforward application of the modified nonlinear element method where $\beta/\omega \gg 1$.

In another recent paper [31], Mahalanabis and Oldenburger have proposed an approximate method of calculating the DIDF of a multivalued nonlinear element by the use of statistical methods. They assert that the frequency of the secondary signal component may be either higher or lower (β/ω irrational) than that of the regular (primary) input component. The latter statement conflicts with the findings of this study and will be discussed in more detail in Chapter II.

To the author's knowledge, the papers cited above include the major part of the published original work on the DIDF's of multivalued nonlinear elements. Only Mahalanabis and Oldenburger [31] assert that their proposed DIDF applies generally to multivalued nonlinear elements and their DIDF appears to be incorrect. Even the restrictive case where the nonlinear element input consists of two sinusoidal components with irrational frequency ratio β/ω has not been satisfactorily solved.

Some of the studies cited above were concerned with stability considerations and others were concerned with the signal transmission properties of nonlinear elements. The primary concern of this study is the manner in which the effective nonlinear characteristic is altered in the presence of various

deterministic secondary signals. The possibility of changing the apparent gain characteristics of a nonlinear element by injection of various "stabilizing" signal waveforms has been considered by other authors [16,32,33]. Also of concern is an effective method of dealing with multivalued nonlinear elements without the severe restrictions of the modified nonlinear element concept.

Since it is known that the injection of secondary signals of different waveforms at the input of a nonlinear element results in different DIDF's, a related synthesis problem may be posed. This synthesis problem is stated as follows: Given a nonlinear element with characteristic $N(e)$, find a waveform (if one exists) of a periodic secondary input component $e_2(t)$ which will result in a specified DIDF. With added qualifications, this problem will be defined as the inverse DIDF problem. Gibson, Hill, Ibrahim, and di Tada [34] have proposed an inverse DF problem where it is desired to find the nonlinear characteristic which has a specified describing function. Although the inverse DIDF problem is not a logical extension of the inverse DF problem defined by Gibson et al., it is perhaps a more practical one for the two-input component case. It is with this inverse DIDF problem that part of this report is concerned. An unsuccessful attempt was made to find a general solution to this problem. As will be seen, specific classes of nonlinear elements lend themselves to relatively simple solutions. In the absence of a general approach to the inverse DIDF problem, considerable use could be made of curves showing the DIDF's of the nonlinear element for several specific secondary signal waveforms. The derivation of a catalog of several such DIDF's and the development

of new and shorter methods for obtaining them comprises another contribution of this report. The specific secondary signals considered are the sine wave, triangle wave, and square wave.

In summary, it is felt that this report makes some contribution in the following specific areas:

- a. The historical aspects of the DIDF
- b. The inverse DIDF problem
- c. A new method of obtaining the DIDF (The proposed method holds for a broad class of multivalued nonlinear elements and simplifies to a very compact form for single valued nonlinear elements with sinusoidal input components.)
- d. Calculation of DIDF's for several specific secondary signals.

CHAPTER II

METHODS OF OBTAINING THE DIDF FOR DETERMINISTIC INPUTS

2.1 The DIDF of West, Douce, and Livesly

The most general DIDF for the case in which the input to a single valued nonlinear element is the sum of two sine waves, $e = A \sin (\omega t + \phi) + B \sin (n\omega t + \psi)$, is given by the expression

$$\hat{K}(A, B, n, \phi, \psi) = \frac{1}{\pi A} \int_0^{2\pi} N[A \sin (\omega t + \phi) + B \sin (n\omega t + \psi)] \sin (\omega t + \phi) d\omega t. \quad (2.1)$$

Such a DIDF¹ has five variables, A, B, n, ϕ , and ψ , and is therefore somewhat complicated to use in practical problems. West, Douce, and Livesly [7] developed a simplification of the DIDF given by Equation (2.1) by assuming the parameter n to be a rational number. In fact the investigations of West et al. led them to consider the even more restrictive case where n is an integer or

¹Hereafter, the order of the indicated parameters in the DIDF $\hat{K}(A, B, a, b, n, \phi, \dots)$ has implied meaning. The first parameter A is the amplitude of the primary input signal for which the DIDF is derived. The second, B, is the peak value of the secondary input signal¹. Then follow the parameters a, b, c, etc., associated with the nonlinearity itself. The fourth group (n, ϕ , ψ , etc.) consists of the frequency ratio and phase angles associated with the two input signals. These comments also apply to the modified nonlinearity $\hat{N}(A, B, a, b, c, n, \dots)$.

the reciprocal of an integer. With this added restriction, the inclusion of two phase shift quantities ϕ and ψ becomes redundant and one of those parameters was eliminated. In this way, the simplified DIDF of West, Douce, and Livesly was obtained in the form

$$\hat{K}(A, B, n, \phi) = \frac{1}{\pi A} \int_0^{2\pi} N[A \sin(\omega t + \phi) + B \sin n\omega t] \sin(\omega t + \phi) d\omega t. \quad (2.2)$$

when $N(e)$ is single valued. The four parameters A , B , n , and ϕ in the DIDF of West, Douce, and Livesly still require a very large amount of data to give a complete representation. For this reason, and because of the restrictions on n , its use has been limited primarily to investigations of stability, subharmonic (superharmonic) oscillations, and jump phenomena in nonlinear systems. As pointed out by West et al., when $N(e)$ is adequately described by a low order polynomial the DIDF is most easily found by a direct expansion to obtain the terms in the output with frequency ω . Of course, the direct expansion technique works equally well when the frequency ratios of the input sinusoidal components are irrational.

2.2 The Modified Nonlinear Element Concept

The concept of the equivalent nonlinear element or the modified nonlinear element probably originated with Nikiforuk and West [35]. However, their modified, normalized, input-output characteristic was defined only for a sinusoidal input when noise was added to this input. Sommerville and Atherton [9] extended this concept to give a more meaningful "effective nonlinear element." This effective nonlinear element came about as a result

of the two-stage evaluation of the equivalent gain of a nonlinear element with respect to a primary signal in the presence of several other deterministic or random input components. The restriction was imposed that the cross correlation function of any two of the random input components must be zero and the frequency ratio for periodic input components must be irrational. The process is shown diagrammatically in Figure 2.1.

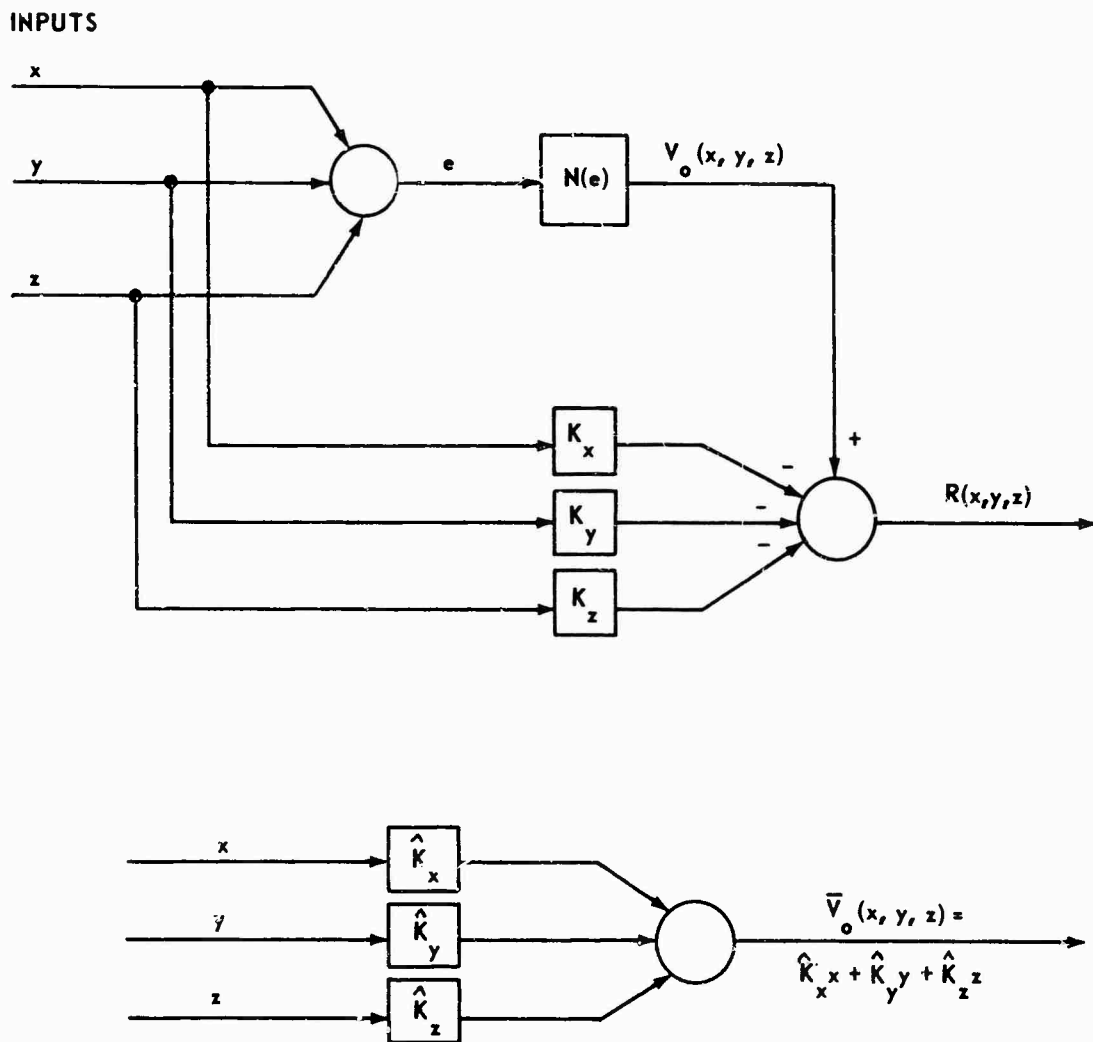


Figure 2.1. Diagram Showing the Error Term $R(x, y, z)$ and Equivalent Representation of a Three-Input Nonlinear Element Where $R(x, y, z)$ Is Neglected

In general, the spectrum of the output $V_o(x, y, z)$ consists of the sum of all the frequencies contained in x , y , and z plus harmonics of these frequencies and frequencies resulting from various cross-products of x , y , and z . The equivalent gain \hat{K}_x is that value of K_x (possibly complex) which gives a minimum value of $R(x, y, z)$ in the RMS sense as K_x is allowed to vary. The other equivalent gains \hat{K}_y and \hat{K}_z are found independently in the same manner. Of course, if only the equivalent gain to one input component (primary input component) is desired, as is the case in this study, it is not necessary to calculate the equivalent gains for the secondary components. When the primary input component x is a dc or sinusoidal signal it turns out that the required output $\hat{K}_x x$ is simply the corresponding dc or fundamental Fourier periodic components of $V_o(x, y, z)$ at the frequency of x . Sommerville and Atherton [9] have shown that precisely the same equivalent gain \hat{K}_x results when a two-stage method of evaluation is used. The intermediate step is to define an effective nonlinear element (modified nonlinear element) by considering a dc signal A_o instead of the primary signal x together with the other input components. The function $\hat{N}(A_o)$ relating the average dc output as a function of A_o is defined as the new effective nonlinear element. If the primary input component x is then applied to the new effective nonlinear element \hat{N} , the signal $\hat{K}_x x$ will appear at the output. This concept of the modified nonlinear element gives the engineer a very helpful physical insight into the mechanism of "signal stabilization" or equivalent linearization via high frequency signal injection [33]. When the number of inputs is reduced to two, the equivalent gains \hat{K} are called DIDF's. As mentioned earlier, when the input consists of a sum of sinusoidal

components, an equivalent gain or DIDF may be defined with respect to each component in the input. If there are only two components, both of which are sinusoidal, then the resulting equivalent gains have been called [36] TSIDF's. Although the equivalent gains of Sommerville and Atherton were defined and formulated to include stochastic components in the input signals, their formulation, as cited in this report, will be restricted to inputs in which the secondary components are deterministic periodic signals. Gelb and Vander Velde [36] have discussed such a formulation for the TSIDF. Suppose the two sinusoidal components of the input are given by $B \sin \beta t$ and $A \sin \omega t$, where β/ω is an irrational number. Then the equivalent gain or TSIDF with respect to the component $A \sin \omega t$ becomes

$$\hat{K}(A, B) = \frac{1}{2\pi^2 A} \int_0^{2\pi} \sin \omega t \, d\omega t \int_0^{2\pi} N(A \sin \omega t + B \sin \beta t) \, d\beta t \quad (2.3)$$

A similar expression defines $\hat{K}(B, A)$ with respect to the component $B \sin \beta t$. It should be pointed out that Equation (2.3) holds only for odd, single valued, nonlinear elements. As remarked earlier, the derivation of $\hat{K}(A, B)$ may be carried out in a two-stage process by first defining a modified nonlinear element $\hat{N}(A_0, B)$ for the case in which the input consists of the sum of a dc signal A_0 and a sinusoid $B \sin \beta t$. The characteristic function of the modified nonlinear element then becomes

$$\hat{N}(A_0, B) = \frac{1}{2\pi} \int_0^{2\pi} N(A_0 + B \sin \beta t) \, d\beta t \quad (2.4)$$

and the TSIDF is given by

$$\hat{K}(A, B) = \frac{1}{\pi A} \int_0^{2\pi} \hat{N}(A \sin \omega t, B) \sin \omega t \, d\omega t \quad (2.5)$$

This same two-stage process will be used in this thesis except that the secondary signal is not restricted to be sinusoidal. Oldenburger and Boyer [10] have outlined a semi-intuitive procedure for calculating the TSIDF which closely parallels the modified nonlinear element method proposed by Sommerville and Atherton. In the outline of their method, Oldenburger and Boyer emphasize the concepts which underlie the experimental measurement of the modified nonlinear element and the TSIDF.

The double Fourier Series expansion method given by Gelb and Vander Velde [18] and credited to Bennett [12] was mentioned in Chapter I. The TSIDF expression given by this method is exactly that of Equation (2.3) which results from the modified nonlinear element method and will not be discussed further.

The modified nonlinear element method given by Equations (2.3), (2.4), and (2.5) will be derived in section 2.6 of this chapter by an approach which differs from the random noise approach used by Sommerville and Atherton [9] or the intuitive approach used by Oldenburger and Boyer [10].

2.3 Power Series Method (TSIDF)

The power series method of obtaining the TSIDF mentioned in Chapter I is valid for odd nonlinear elements when the frequency ratio of the input components is irrational. This method is the result of expanding $\hat{K}(A, B)$ in a Taylor series about $B = 0$. Gelb and Vander Velde [18] have

shown that, provided the necessary derivatives exist, the TSIDF may be written as

$$\hat{K}(A, B) = \sum_{p=0}^{\infty} \frac{B^{2p}}{2^{2p} (p!)^2} V_p(A) ; \quad A > B , \quad (2.6)$$

where $V_p(A)$ is found by the recursive equation

$$V_{p+1}(A) = \frac{d^2 V_p(A)}{dA^2} + \frac{3}{A} \frac{dV_p(A)}{dA} , \quad (2.7)$$

with the first term being,

$$V_0(A) = \hat{K}(A) . \quad (2.8)$$

the ordinary DF. Likewise,

$$\hat{K}(A, B) = \sum_{p=0}^{\infty} \frac{A^{2p}}{2^{2p} p! (p+1)!} W_p(B) ; \quad A < B , \quad (2.9)$$

where

$$W_{p+1}(B) = \frac{d^2 W_p(B)}{dB^2} + \frac{1}{B} \frac{dW_p(B)}{dB} , \quad (2.10)$$

with the first term being found by the relation

$$W_0(B) = \hat{K}(B) + \frac{B}{2} \frac{d\hat{K}(B)}{dB} . \quad (2.11)$$

The function $\hat{K}(B)$ is the ordinary DF, when $B \sin \beta t$ is the input sinusoid. The power series method is easy to apply and is very useful when closed form solutions for the TSIDF cannot be found.

2.4 Methods of Stochastic Processes

Many authors [9, 11, 15, 16, 20, 22, 24, 27, 28, 29, 31, 37] have used the

mathematics of random functions to formulate and derive equivalent gains and DIDF's. Some of these studies differ in the method of approach but all involve the same fundamental ideas. Gibson and Sridhar [11] used this approach to derive an exact DIDF for single valued nonlinear elements with an input consisting of two sine wave components (TSIDF). Mahalarabis and Nath [37] proposed a more direct approach to calculating the TSIDF via the techniques of random process theory.

The TSIDF for single valued nonlinear elements was shown by Gibson and Sridhar [11] and Gelb and Vander Velde [18] to be

$$\hat{K}(A, B) = \frac{j}{\pi A} \int_{-\infty}^{\infty} y(ju) J_0(Bu) J_1(Au) du \quad , \quad (2.12)$$

where

$$y(ju) = \int_{-\infty}^{\infty} y(x) \exp[-jux] dx \quad (2.13)$$

is the Fourier Integral Transform of the nonlinear element output $y(x)$ with x as the input. The functions $J_0(Bu)$ and $J_1(Au)$ are Bessel functions of order zero and one respectively.

2.5 Methods of Determining the DIDF for Multivalued Nonlinear Elements

As already discussed in Chapter I, relatively few results have been published on effective methods of obtaining the minimum RMS error DIDF for multivalued nonlinear elements. One possible exception is the application [16,30,33] of the modified nonlinear element concept, which theoretically applies [16] to the multivalued nonlinear element case only as n or $1/n$

approaches infinity. It is plausible that the DIDF obtained by this approach is accurate enough for practical purposes when $1 \ll n \ll \infty$. However, to the author's knowledge, no previously published work has dealt with the inaccuracies involved in this finite case ($1 \ll n \ll \infty$) or with the question of possible ranges of finite n for which the method is accurate enough for practical purposes. In respect to the application of the modified nonlinear element method to multivalued nonlinear elements, Cook [30] has suggested a method of keeping track of the phase. A new approach to the question of finding the DIDF for multivalued nonlinear elements is offered in the following section. This approach may be useful in determining the exact DIDF for multivalued nonlinear elements with deterministic inputs.

2.6 A New Average DIDF Method for Deterministic Inputs

Consider the general TSIDF given by Equation (2.1) and let n be restricted to be an irrational number. This is the case considered [9,10,11,16,25,26,27,31,32,33,36,37] where the random input approach was used to derive the TSIDF for deterministic inputs. In such applications, the random input approach merely provides a convenient method for averaging out the relative phase angles ϕ and ψ . This is easily understood when one considers the very practical problem of trying to experimentally determine the TSIDF. When n is irrational, the phase angles ϕ and ψ lose their physical importance and it becomes impractical to even include them in the TSIDF. Consider the accurate experimental setup to measure the TSIDF given by Equation (2.1). It is obvious that if the two signal generators which generate the components

$A \sin(\omega t + \phi)$ and $B \sin(n\omega t + \psi)$ are allowed to run continuously, a different value of \hat{K} will be observed with each succeeding 2π interval of the primary input component $A \sin(\omega t + \phi)$. What is actually desired is the average value of \hat{K} as the observation time increases without bound. Therefore, this "average TSIDF" will not include ϕ and ψ as parameters. In other words, the actual TSIDF which is desired is given by

$$\hat{K}(A, B, n) = \lim_{p \rightarrow \infty} \frac{1}{p\pi A} \int_0^{2p\pi} N(A \sin \omega t + B \sin n\omega t) \sin \omega t \, d\omega t \quad (2.14)$$

where p is an integer.

Equation (2.14) is equivalent, in the measurement problem, to evaluating

$$\hat{K}(A, B, n, \phi, \psi) = \frac{1}{\pi} \int_0^{2\pi} N[A \sin(\omega t + \psi) + B \sin(n\omega t + \phi)] \sin(\omega t + \psi) \, d\omega t \quad (2.15)$$

for all possible combinations of "phase" or zero crossings of the two input components and averaging these values of $\hat{K}(A, B, n, \phi, \psi)$.

Thus, there is another way to calculate the TSIDF. Let one of the sinusoidal input components contain a relative phase angle ϕ , then average the resulting set of "instantaneous DIDF's" as ϕ ranges over 2π . The above arguments are more rigorously developed in the ensuing discussion. Define an equivalent gain K_A and K_B for each input component $A \sin \omega t$ and $B \sin(n\omega t + \phi)$ respectively. The "linearized" output is given by the expression $K_A A \sin \omega t + K_B B \sin(n\omega t + \phi)$. However, K_A and K_B are complex functions of A , B , and n , in general, and can therefore be expressed in the form

$$\begin{aligned}
 K_A &= K_{ar} + jK_{ai} \\
 K_B &= K_{br} + jK_{bi}
 \end{aligned}
 \tag{2.16}$$

The RMS value of the difference between the actual output and the linearized output over all time is

$$\begin{aligned}
 \bar{R} = & \left(\lim_{p \rightarrow \infty} \frac{1}{2p\pi} \int_0^{2\pi p} \{ N[A \sin \omega t + B \sin (n\omega t + \phi)] \right. \\
 & - K_{ar} A \sin \omega t - K_{ai} A \cos \omega t \\
 & - K_{br} B \sin (n\omega t + \phi) \\
 & \left. - K_{bi} B \cos (n\omega t + \phi) \}^2 d\omega \right)^{1/2},
 \end{aligned}
 \tag{2.17}$$

where p is an integer. Since n is restricted to be an irrational number, Equation (2.17) may be written in the following double integral form,

$$\begin{aligned}
 \bar{R} = & \left(\frac{1}{2\pi} \frac{1}{2\pi} \int_0^{2\pi} d\phi \int_0^{2\pi} \{ N[A \sin \omega t + B \sin (n\omega t + \phi)] \right. \\
 & - K_{ar} A \sin \omega t - K_{ai} A \cos \omega t - \\
 & - K_{br} B \sin (n\omega t + \phi) \\
 & \left. - K_{bi} B \cos (n\omega t + \phi) \}^2 d\omega \right)^{1/2}.
 \end{aligned}
 \tag{2.18}$$

The value of the real part of K_A (minimum RMS TSIDF) which minimizes \bar{R} is characterized by the condition

$$\frac{\partial \bar{R}}{\partial K_{ar}} = 0.
 \tag{2.19}$$

The indicated differentiation may be taken under the integral signs since the integrand is single valued, continuous, and differentiable with respect to the variable K_{ar} even though $N(e)$ may be discontinuous and multivalued. This value of K_{ar} , defined as \hat{K}_{ar} , is found to be

$$\hat{K}_{ar}(A, B, n) = \frac{1}{2\pi^2 A} \int_0^{2\pi} d\phi \int_0^{2\pi} N[A \sin \omega t + B \sin (n\omega t + \phi)] \sin \omega t d\omega t \quad (2.20)$$

Likewise the imaginary part of the DIDF is found to be

$$\hat{K}_{ai}(A, B, n) = \frac{1}{2\pi^2 A} \int_0^{2\pi} d\phi \int_0^{2\pi} N[A \sin \omega t + B \sin (n\omega t + \phi)] \cos \omega t d\omega t \quad (2.21)$$

The independent nature of the two input components (n-irrational) is emphasized by changing the variables ωt and $n\omega t$ to θ_1 and θ_2 , respectively.

If $N(e)$ is now restricted to be single valued, the imaginary part K_{ai} of the TSIDF goes to zero and θ_2 does not appear in the answer for K_{ar} .

Therefore, Equation (2.20) may be reduced to the following form

$$\hat{K}_A(A, B) = \frac{1}{2\pi^2 A} \int_0^{2\pi} d\phi \int_0^{2\pi} N(A \sin \theta_1 + B \sin \phi) \sin \theta_1 d\theta_1 \quad (2.22)$$

The role of ϕ and θ_2 may also be interchanged to give a similar expression for the DIDF,

$$\hat{K}_A(A, B) = \frac{1}{2\pi^2 A} \int_0^{2\pi} d\theta_2 \int_0^{2\pi} N(A \sin \theta_1 + B \sin \theta_2) \sin \theta_1 d\theta_1 \quad (2.23)$$

Since the integrand is single valued with at most a finite number of finite discontinuities, the order of integration may be interchanged. That is, Equation (2.23) may be written as

$$\hat{K}_A(A, B) = \frac{1}{2\pi^2 A} \int_0^{2\pi} \sin \theta_1 d\theta_1 \int_0^{2\pi} N(A \sin \theta_1 + B \sin \theta_2) d\theta_2 \quad (2.24)$$

Equation (2.24) is equivalent to (2.3) which in turn is a result of the modified nonlinear element method. Equation (2.24) is also the form of the TSIDF given by Gelb and Vander Velde [36]. The two-step evaluation of Equation (2.24) may be carried out as indicated in Equations (2.4) and (2.5).

Although the order of integration is not important, the integral forms resulting from Equation (2.23) may be easier to integrate than those of Equation (2.24), or vice versa.

Although the minimum RMS TSIDF was derived above under the assumption that the secondary component in the input was a sine wave, $B \sin(n\omega t + \phi)$, this restriction is not necessary. In fact, any periodic secondary signal $\sigma(\beta t)$ could have been chosen without affecting the form of the answer. This result will be used in Chapter V to show how the DIDF is affected by changing the wave shape of the periodic signal $\sigma(\beta t)$. Equations (2.22) through (2.24) also emphasize that the TSIDF of single valued nonlinear elements is independent of the frequency ratio n . It appears that such a simplification cannot be made when considering multivalued nonlinear elements. This latter statement is not in agreement with the assertion recently made by Mahalanabis and Oldenburger[31]. Further discussion of this point is made in Chapter IV where the DIDF for the relay with hysteresis is found by use of Equations (2.20) and (2.21) and is compared with the published results of Mahalanabis and Oldenburger.

Since the frequency ratio n does not enter into the TSIDF for single valued nonlinear elements, Equation (2.20) suggests an alternative approach to the calculation of the TSIDF. For instance, when n is very close to one, the DIDF may be written in the form

$$\hat{K}(A, B) = \frac{1}{2\pi^2 A} \int_0^{2\pi} d\phi \int_0^{2\pi} N[D \sin(\omega t + \psi)] \sin \omega t d\omega t \quad , \quad (2.25)$$

where

$$D = D(A, B, \phi) = \sqrt{A^2 + B^2 + 2AB \cos \phi} \quad (2.26)$$

$$\psi = \begin{cases} \sin^{-1} \left(\frac{B \sin \phi}{\sqrt{A^2 + B^2 + 2AB \cos \phi}} \right) ; & B \cos \phi + A \geq 0 \\ \pi - \sin^{-1} \left(\frac{B \sin \phi}{\sqrt{A^2 + B^2 + 2AB \cos \phi}} \right) ; & B \cos \phi + A \leq 0 \end{cases} \quad (2.27)$$

Now evaluate $\hat{K}(A, B)$ by a two-stage process, similar to that used in the modified nonlinear element concept, where

$$g(A, B, \phi) = \frac{1}{\pi A} \int_0^{2\pi} N[D \sin(\omega t + \psi)] \sin \omega t d\omega t \quad (2.28)$$

and

$$\hat{K}(A, B) = \frac{1}{2\pi} \int_0^{2\pi} g(A, B, \phi) d\phi \quad . \quad (2.29)$$

The function $g(A, B, \phi)$ simply defines a special case of the DIDF of West, Douce, and Livesly where $n = 1$. Equation (2.29) shows that $\hat{K}(A, B)$ is the average of $g(A, B, \phi)$ as ϕ ranges over 2π . This implies that the average value of the DIDF of West, Douce, and Livesly as ϕ ranges over $(0, 2\pi)$ is the same regardless of the value of n . The function $g(A, B, \phi)$ has the appearance

of the conventional DF with the additional parameter ψ . It will be shown below that the computation of $g(A, B, \phi)$ requires the same effort as the computation of the DF. It may be considerably more difficult to perform the integration indicated in Equation (2.29) than that in Equation (2.28). Since the characteristic $N(e)$ is single valued, the phase ψ is preserved through the nonlinear operation indicated in Equation (2.28). Therefore, Equation (2.28) may be rewritten as

$$g(A, B, \phi) = \frac{\cos \psi}{\pi A} \int_0^{2\pi} N(D \sin \omega t) \sin \omega t \, d\omega t \quad (2.30)$$

Substituting Equation (2.27) in Equation (2.30) gives

$$g(A, B, \phi) = \frac{A + B \cos \phi}{\sqrt{A^2 + B^2 + 2AB \cos \phi}} \frac{1}{\pi A} \int_0^{2\pi} N(D \sin \omega t) \sin \omega t \, d\omega t \quad (2.31)$$

and

$$\hat{K}(A, B) = \frac{1}{2\pi^2} \int_0^{2\pi} \frac{(1 + B/A \cos \phi) \, d\phi}{\sqrt{A^2 + B^2 + 2AB \cos \phi}} \int_0^{2\pi} N(\sqrt{A^2 + B^2 + 2AB \cos \phi} \cdot \sin \omega t) \sin \omega t \, d\omega t \quad (2.32)$$

It is interesting to note that this formulation leads to a general expression, Equation (2.32), which has the appearance of an elliptic integral. However, it appears that this integral may be difficult or impossible to reduce to one of the standard or tabulated elliptic integrals. The functional $\cos[\psi(A, B, \phi)]$ does not depend upon the nonlinear element and is symmetrical about $\phi = \pi$. In fact $g(A, B, \phi)$ is symmetrical about $\phi = \pi$ as well. In some cases approximate algebraic solutions may be desired rather than graphs of the TSIDF. If

trapezoidal integration or other approximate techniques are used, accuracy sufficient for practical application is usually achievable with very few terms. In the modified nonlinear element method, the function $\hat{N}(A_0, B)$ is ordinarily not difficult to obtain. The main task consists of determining the fundamental component of the output when the primary component of the input is operated upon by the function $\hat{N}(A_0, B)$.

Example: DIDF of Relay

In order to demonstrate the utility of the average DIDF method, consider the DIDF of the perfect relay. The relay is described by the equation:

$$y = M \operatorname{sgn}(e) = \begin{cases} M; & e > 0 \\ -M; & e < 0 \end{cases}, \quad (2.33)$$

where, for the present case, $e = A \sin \omega t + B \sin \beta t$. Equation (2.30) is simply the conventional DF times $\cos \psi$ with $D \sin \omega t$ as the input. Thus,

$$\text{DF} = \frac{1}{\pi A} \int_0^{2\pi} M \operatorname{sgn}(D \sin \omega t) \sin \omega t \, d\omega t = \frac{4M}{\pi A} \quad (2.34)$$

and

$$g(A, B, \phi) = \frac{4M}{\pi} \left(\frac{1 + B/A \cos \phi}{\sqrt{A^2 + B^2 + 2AB \cos \phi}} \right). \quad (2.35)$$

The second integration indicated by Equation (2.29) gives

$$\hat{K}(A, B) = \frac{4M}{\pi^2} \int_0^\pi \frac{1 + B/A \cos \phi}{\sqrt{A^2 + B^2 + 2AB \cos \phi}} \, d\phi. \quad (2.36)$$

This integral may be evaluated [38].

$$\hat{K}(A, B) = \frac{8M}{\pi^2} \frac{1}{A+B} \left[\left(1 + \frac{B}{A} \frac{k^2 - 2}{k^2} \right) F(k) + 2 \frac{B}{A} \frac{1}{k^2} E(k) \right], \quad (2.37)$$

where $F(k)$ is the complete elliptic integral of the first kind and $E(k)$ is the complete elliptic integral of the second kind. The modulus k is given by

$$k = \frac{2\sqrt{B/A}}{1 + B/A}. \quad (2.38)$$

Equation (2.37) is valid for all A and B . However, a modulus transformation may be applied [39] whereby

$$E(k) = \frac{2E(k) - (1 - k^2) F(k)}{1 + k} \quad (2.39)$$

$$F(k) = (1 + k) F(k), \quad (2.40)$$

when

$$\begin{aligned} k &= B/A; & B < A \\ k &= A/B; & B > A \end{aligned} \quad (2.41)$$

When Equations (2.38) through (2.41) are substituted in Equation (2.37), the following expressions for the DIDF of the perfect relay results:

$$\hat{K}(A, B) \begin{cases} \frac{8M}{\pi^2} E(B/A); & B < A \\ \frac{8M}{\pi^2 A} \frac{B}{A} \left[E(A/B) - \left(1 - \frac{A^2}{B^2} \right) K(A/B) \right]; & A < B \end{cases} \quad (2.42)$$

Equation (2.42) coincides exactly with the expressions obtained by Gibson and Sridhar [11] and Mahalanabis and Nath [37], who used essentially different methods of calculations.

When the secondary input component is nonsinusoidal, a simplified form of the average DIDF method comparable to that given in Equation (2.32) cannot be

found. However, either of the expressions given in Equations (2.23) and (2.24) may be used when $N(e)$ is single valued. Expressions similar to Equations (2.20) and (2.21) are used when $N(e)$ is a multivalued function. In order to include a more general periodic secondary signal $\sigma(\beta t)$, Equation (2.23) can be written as follows:

$$\hat{K}[A; \sigma(\theta_2)] = \frac{1}{2\pi^2 A} \int_0^{2\pi} d\theta_2 \int_0^{2\pi} N[A \sin \theta_1 + \sigma(\theta_2)] \sin \theta_1 d\theta_1 \quad (2.43)$$

The evaluation of Equation (2.43) may be carried out in two steps, following the modified nonlinear element approach, to give

$$\hat{N}[A_0; \sigma(\theta_2)] = \frac{1}{2\pi} \int_0^{2\pi} N[A_0 + \sigma(\theta_2)] d\theta_2 \quad (2.44)$$

$$\hat{K}[A; \sigma(\theta_2)] = \frac{1}{\pi A} \int_0^{2\pi} N[A \sin \theta_1; \sigma(\theta_2)] d\theta_1 \quad (2.45)$$

CHAPTER III

DEFINITION AND SOLUTION OF AN INVERSE DIDF PROBLEM FOR A PARTICULAR CLASS OF NONLINEAR ELEMENTS

Although a large portion of this report is devoted to the analysis of the output of a nonlinear element when the input contains a secondary signal of various waveforms, the motivation for this study was provided by the somewhat more difficult synthesis problem of finding the secondary signal $\sigma(\beta t)$ which will produce a prescribed modified nonlinear function $\hat{N}(A, B)$ for a given nonlinear function $N(e)$. It is assumed that the given nonlinear element is an inherent part of a system and cannot itself be changed or replaced. Perhaps the first logical step in a synthesis procedure is to define the desired DIDF $\hat{K} = \hat{K}[A; \sigma(\beta t)]$ where the primary component of the input signal is a sine wave. If one then attempts to work backward, using the modified nonlinear element concept, the second step consists of finding the equivalent nonlinear element $\hat{N} = \hat{N}[A_0; \sigma(\beta t)]$ which gives the desired DIDF. This, of course, is exactly analogous to the inverse describing function problem posed and largely solved by Gibson, Hill, Ibrahim, and di Tada [34]. Even though a method exists which may be used to solve this second step, one might proceed alternatively by first defining the desired $\hat{N}[A_0; \sigma(\beta t)]$ rather than the desired

$\hat{K}[A; \sigma(\beta t)]$. This latter problem is important in its own right and, in most practical situations, might just as well be the starting point. A logical extension of the ideas of the inverse DF problem mentioned above would lead one to define the inverse DIDF problem as one of finding a nonlinear element which corresponds to a given TSIDF. However, it is felt that the inverse DIDF definition given here is probably a more practical one. The inverse DIDF problem to be considered here may be precisely stated as follows:

The Inverse DIDF Problem

Given: A time invariant nonlinear element with characteristic $N(e)$ and the desired modified nonlinear characteristic

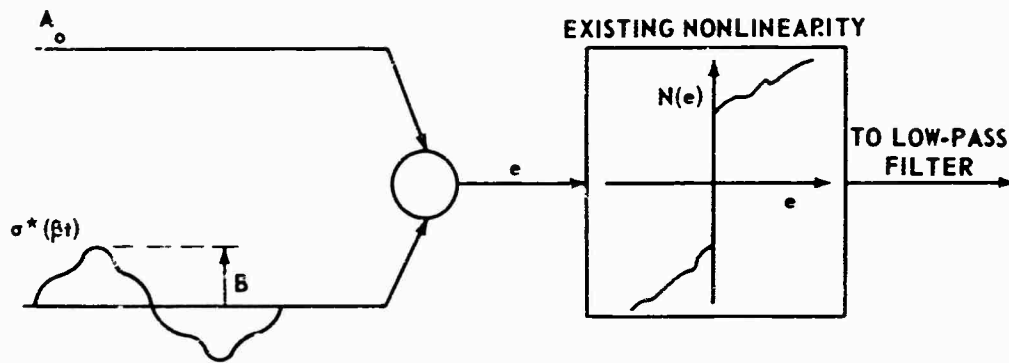
$$N^* = \hat{N}[A_0; \sigma(\beta t)]$$

Find: The periodic secondary signal $\sigma^*(\beta t)$ which will produce the modified nonlinear characteristic N^* .

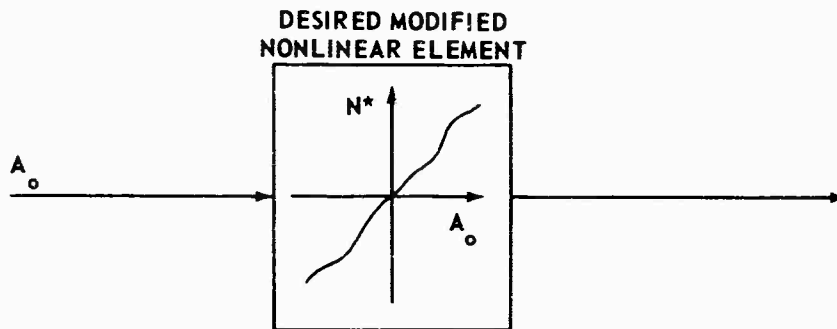
The diagram of Figure 3.1 shows the essential elements and signals required in the development.

In the present discussion, only odd, single valued nonlinear elements whose characteristic is not a function of frequency will be considered. In order to conveniently choose and restrict the class of secondary signals which should be considered, the following observation on integrals of functions is made: Let $f(t)$ be a given function of time, A_0 be an arbitrary constant, and $N(e)$ be a time invariant single valued nonlinear function. In addition, let

$$\int_0^{t_1} N[A_0 + f(t)] dt = X < \infty \quad . \quad (3.1)$$



(a) Exact Representation



(b) Equivalent Representation

Figure 3.1. Diagram Illustrating the Inverse DIDF Problem

Then there exists a function $g(t)$ such that

$$\frac{dg(t)}{dt} \geq 0 ; \quad 0 \leq t \leq t_1 \quad (3.2)$$

and

$$\int_0^{t_1} N[A_0 + g(t)] dt = X \quad (3.3)$$

Therefore, following the definition of the modified nonlinear element given by Equation (2.44), one may consider only secondary components $\sigma(\beta t)$ belonging to the class Σ where

$$\sigma(\beta t) = -\sigma(-\beta t)$$

$$\sum: \sigma(\pi/2 + t) = \sigma(\pi/2 - \beta t)$$

$$\frac{d\sigma(\beta t)}{dt} \geq 0 ; \quad 0 \leq \beta t \leq \pi/2 .$$

This restriction does not eliminate from consideration any modified characteristic function $\hat{N}[A_o; \sigma(\beta t)]$ which might otherwise be considered.

The restriction to the class Σ greatly simplifies the search for a solution $\sigma^*(\beta t)$ and does not eliminate any useful solutions. It is obvious that a secondary signal can alter the modified nonlinear characteristic only over certain regions. Such a region in the $\hat{N}[A_o; \sigma(\beta t)]$ versus A_o plane might be as shown in Figure 3.2. In addition there will be limits on the derivatives of \hat{N} in this region R. That is, the values of the derivatives $\frac{d^m \hat{N}}{dA_o^m}$ cannot be arbitrarily specified. To define the region R and the limits on the derivatives $\frac{d^m \hat{N}}{dA_o^m}$ which may be achieved by a secondary component in the input is a large task. However, with the exception of specifying the region R a priori, this is what is required in the inverse DIDF problem. Curves showing the DIDF's of nonlinear elements for several specific secondary signal waveforms should lend some insight into what may be expected from the inverse problem. A catalog of several such DIDF's is given in Chapter IV.

Consider the class of nonlinear elements defined by the equation

$$N(e) = Ke^m \text{sgn}(e) \quad (3.5)$$

where m is a non-negative even integer. Let the class of desired equivalent nonlinear elements, N^* , be defined by the relation

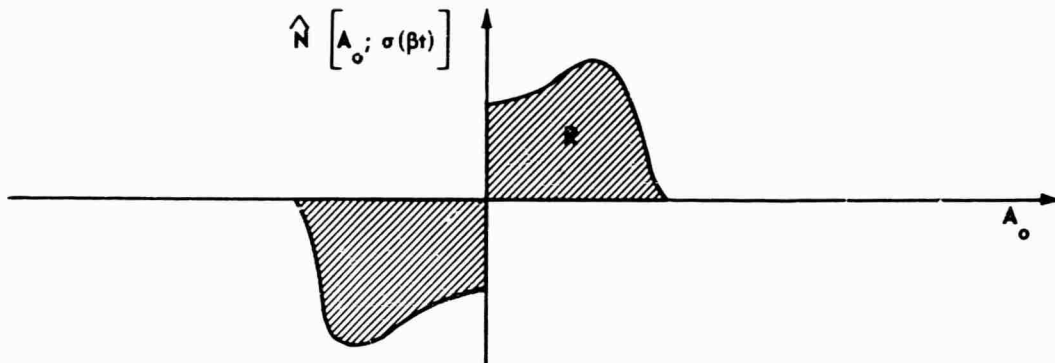


Figure 3.2. Region over Which $\hat{N}[A_0; \sigma(\beta t)]$
May Be Varied by Changing $\sigma(\beta t)$

$$N^* = \hat{N}[A_0; \sigma^*(\beta t)] = k_1 |A_0|^n \operatorname{sgn}(A_0) \quad (3.6)$$

This equation holds for some as yet undefined region about the origin $A_0 = 0$.

The equation for the equivalent nonlinear element with any secondary signal and a single valued nonlinear element is given by the functional

$$\hat{N}[A_0; \sigma(\beta t)] = \frac{1}{2\pi} \int_0^{2\pi} N[A_0 + \sigma(\beta t)] d\beta t \quad (3.7)$$

The class of problems under consideration can be solved with some degree of success in a very straightforward manner by defining only the m^{th} derivative of N^* . Of the nonlinear elements described by Equation (3.5), only the perfect relay and absquare will be considered. However, the method proposed here may be carried further without defining the nonlinear element to be considered. Substitution of Equation (3.5) into (3.7) results in the following desired modified nonlinear element:

$$\hat{N}[A_0; \sigma^*(\beta t)] = \frac{K}{2\pi} \int_0^{2\pi} [A_0 + \sigma^*(\beta t)]^m \operatorname{sgn}[A_0 + \sigma^*(\beta t)] d\beta t \quad (3.8)$$

It is necessary to separate the integral of Equation (3.8) into two integrals, where the limits then involve θ_1 (Figure 3.3), in order to perform the integration. By use of Leibnitz rule for integrals, it may be shown that the m^{th} and next lower order derivatives of N^* are given by

$$\frac{d^m N^*}{dA_o^m} = \frac{m!}{2\pi} \int_0^{2\pi} K \operatorname{sgn} [A_o + \sigma^*(\beta t)] d\beta t \quad (3.9)$$

and

$$\frac{d^{m-1} N^*}{dA_o^{m-1}} = \frac{(m-1)!}{2\pi} \int_0^{2\pi} K [A_o + \sigma^*(\beta t)] \operatorname{sgn} [A_o + \sigma(\beta t)] d\beta t \quad (3.10)$$

In addition, the desired expressions for these derivatives are as follows:

$$\frac{d^m N^*}{dA_o^m} = n(n-1)(n-2) \dots (n-m+1) k_1 |A_o|^{n-m} \operatorname{sgn}(A_o) \quad (3.11)$$

$$\frac{d^{m-1} N^*}{dA_o^{m-1}} = n(n-1)(n-2) \dots (n-m+2) k_1 |A_o|^{n-m+1} \operatorname{sgn}(A_o) + C_1 \quad (3.12)$$

where C_1 is a constant. Equation (3.9) may be solved in terms of the angle θ_1 as defined in Figure 3.3. When $\sigma(\beta t)$ is assumed to belong to the class of signals defined by Equation (3.4), the angle θ_1 may be found from the equation

$$\sigma(\theta_1) = A_o ; \quad A_o < B \quad (3.13)$$

Therefore, the solution of Equation (3.9) in terms of θ_1 is

$$\frac{d^m N^*}{dA_o^m} = m! \left(\frac{2K\theta_1}{\pi} \right) \quad (3.14)$$

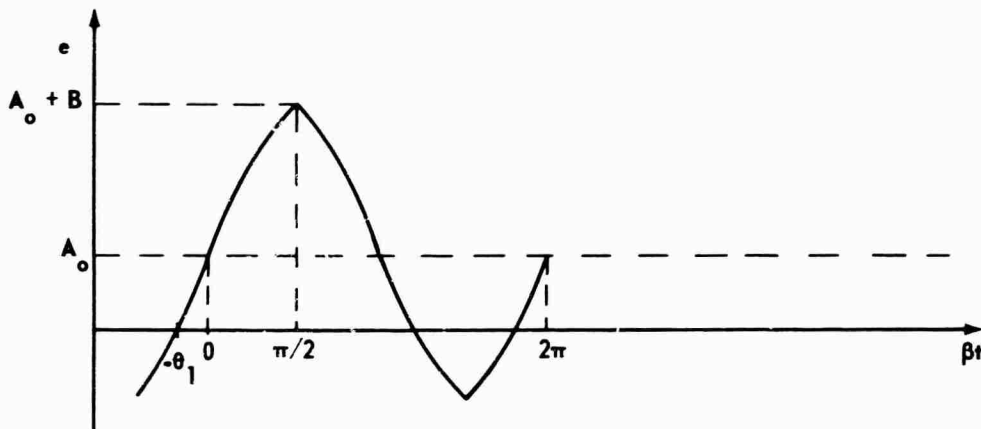


Figure 3.3. The Composite Signal $\sigma(\beta t) + A_0$

Equating the right-hand side of Equations (3.11) and (3.14) gives

$$m! \left(\frac{2K\theta_1}{\pi} \right) = n(n-1)(n-2) \dots (n-m+1) k_1 |A_0|^{n-m} \text{sgn}(A_0) . \quad (3.15)$$

However, in an equation which involves both A_0 and θ_1 , one may substitute the relation given by Equation (3.13). Thus

$$|\sigma^*(\theta_1)|^{n-m} \text{sgn}[\sigma(\theta_1)] = \frac{m!}{n(n-1)(n-2) \dots (n-m+1)} \frac{K}{k_1} \left(\frac{\theta_1}{\pi/2} \right) . \quad (3.16)$$

When $0 \leq \beta t \leq \pi/2$, Equation (3.16) may be rewritten more generally with βt as the independent variable to give

$$|\sigma^*(\beta t)|^{n-m} = \frac{m!}{n(n-1)(n-2) \dots (n-m+1)} \frac{K}{k_1} \left(\frac{\beta t}{\pi/2} \right) ; \quad (3.17)$$

$$0 \leq \beta t \leq \pi/2 .$$

Of course, only the highest nonzero derivative of N^* has been specified and there is no guarantee that the signal given by Equation (3.17) will result in the desired lower order derivatives.

It is evident from Equations (3.9) and (3.14) that

$$\frac{d^m N^*}{dA_0^m} \geq 0 \quad . \quad (3.18)$$

The latter relation, in conjunction with Equation (3.11), requires that

$$n \geq m - 1 \quad , \quad (3.19)$$

except when $m = 0$. Therefore, the order of the equation describing the modified nonlinear element cannot be made lower than $m - 1$. However, the order of the equation describing $\hat{N}[A_0; \sigma(\beta t)]$ may be larger than m . Equation (3.10) describes the average output of an absolute value circuit and is always positive when A_0 and $\sigma(\beta t)$ are not identically zero. Thus, the constant of Equation (3.12) is nonzero except possibly when $r \equiv m - 1$. The proposed method is further illustrated by the following examples:

Example 1 (Perfect Relay)

In this case, $m = 0$ and only the 0th derivative of \hat{N} is required to find the secondary signal. From Equation (3.17) the required secondary signal is

$$\sigma^*(\beta t) = \left(\frac{K}{k_1}\right)^{\frac{1}{n}} \left(\frac{\beta t}{\pi/2}\right)^{\frac{1}{n}} ; \quad 0 \leq \beta t \leq \pi/2 \quad . \quad (3.20)$$

When $n = 1$, that is when the relay is "linearized," the signal $\sigma^*(\beta t)$ is a triangle wave. The range over which Equation (3.2) holds is limited by the amplitude B^* of the secondary signal. The amplitude B^* for the relay case is readily seen from Equation (3.20) to be

$$B^* = \left(\frac{K}{k_1}\right)^{\frac{1}{n}} \quad . \quad (3.21)$$

The two degenerate cases where $n = 0$ and $k_1 = 0$ must be considered separately. When $n = 0$, $N^* = k_1 \operatorname{sgn}(A_0)$, which describes the original nonlinear element and $\sigma(\beta t) = 0$ is the only correct solution. If it is desired to make $k_1 = 0$, Equation (3.20) leads to a wave with infinite height. However, by referring to Equation (3.15) one obtains the relation

$$\frac{2K\theta_1}{\pi} = k_1 \triangleq 0 ; \quad A_0 < B^* . \quad (3.22)$$

The last equation implies that $\theta_1 = 0$ for nonzero values of A_0 . One signal $\sigma^*(\beta t)$ satisfying this equation is a symmetric square wave of arbitrary amplitude B^* . The resulting \hat{N} is, of course, a relay with dead band width $2B^*$ [16]. Notice that a negative n implies a negative $\frac{dN^*}{dA_0}$. Solving Equation (3.8) when $m = 0$ gives

$$N^* = \frac{K}{2\pi} \int_0^{2\pi} \operatorname{sgn} [A_0 + \sigma^*(\beta t)] d\beta t = \frac{2K}{\pi} \theta_1 . \quad (3.23)$$

Thus

$$\frac{dN^*}{dA_0} = \frac{2K}{\pi} \frac{d\theta_1}{dA_0} , \quad (3.24)$$

which cannot be negative, as is easily seen in Figure 3.3. The inequality $n \geq 0$ must therefore be imposed in the relay problem. A typical plot of N^* for $n = 1/2$ and $k_1 = K$ is shown in Figure 3.4.

Example 2 (Absquare)

The solution for the absquare problem is obtained by simply setting $m = 2$ in Equation (3.17). The equation for the first $1/4$ wave of the secondary signal is

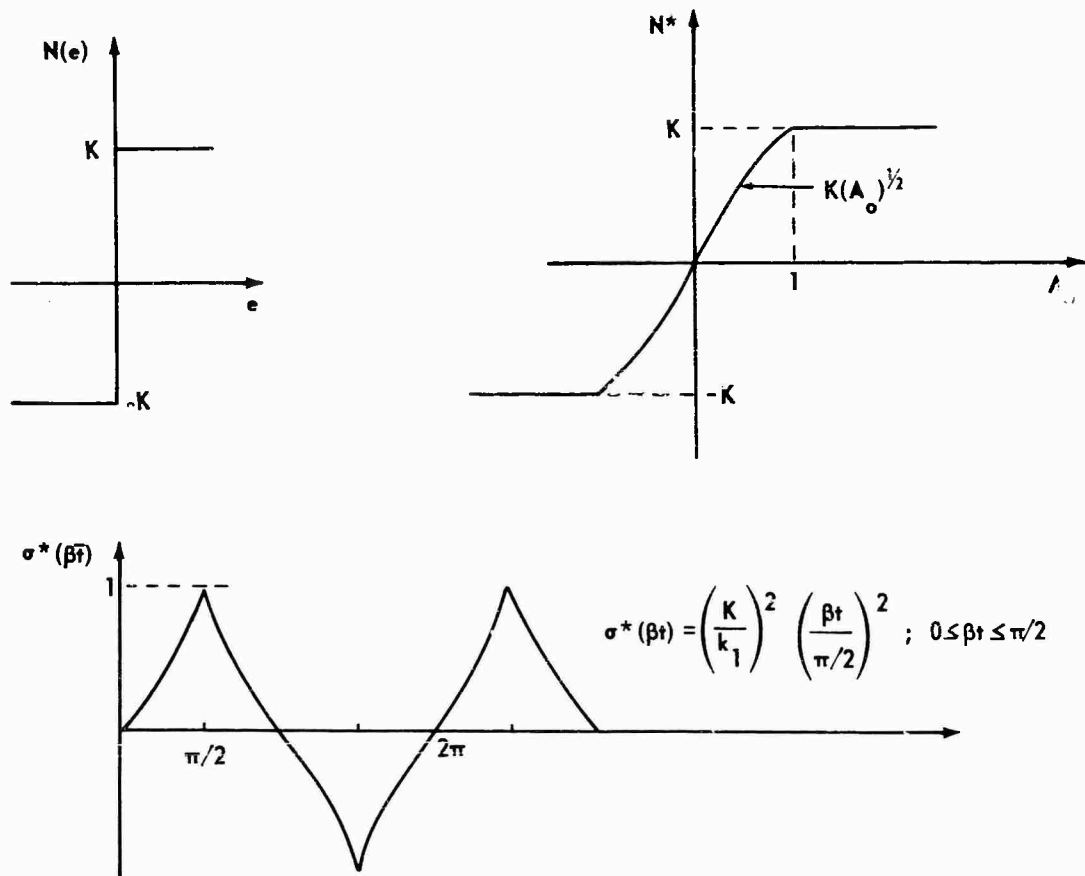


Figure 3.4. Modified Nonlinear Element and Secondary Signal for Perfect Relay Where N^* is Given by $k_1 \sqrt{A_0}$ over a Positive Range of A_0

$$\sigma(\beta t) = \left[\frac{2K}{k_1 n(n-1)} \right]^{\frac{1}{n-2}} \left(\frac{\beta t}{\pi/2} \right)^{\frac{1}{n-2}} ; \quad 0 \leq \beta t \leq \pi/2 \quad (3.25)$$

By specifying the second derivative to be

$$\frac{d^2 N^*}{dA_0^2} = n(n-1)k_1 |A_0|^{n-2} \text{sgn } A_0 \quad (3.26)$$

it is only possible to guarantee that

$$\frac{dN^*}{dA_0} = nk_1 |A_0|^{n-1} \text{sgn } A_0 + C_1 \quad (3.27)$$

and

$$N^* = k_1 |A_0|^n \operatorname{sgn}(A_0) + C_1 A_0 + C_2, \quad (3.28)$$

where C_1 and C_2 are constants. However, solution of Equation (3.8) when $A_0 = 0$ shows that $\hat{N}[0, \sigma^*(\beta t)] = 0$ for allowable $\sigma^*(\beta t)$, and thus $C_2 = 0$.

Three degenerate cases occur when $n = 0, 1, 2$. The first one, $n = 0$, is eliminated by Equation (3.19). When $n = 1$, that is when the absquare is linearized, it is convenient to use Equation (3.15) from which one may write

$$\theta_1 = 0; \quad A_0 \neq 0. \quad (3.29)$$

In addition, Equation (3.13) requires that

$$\sigma(0) = A_0; \quad A_0 < M, \quad (3.30)$$

where M is arbitrary. The only secondary signal which satisfies the requirements of Equations (3.29) and (3.30) is one with infinite slope for $\sigma(\beta t) < M$. For example, the secondary signal of Figure 3.5 results in the modified non-linear element of Equation (3.31) which is linear in A_0 .

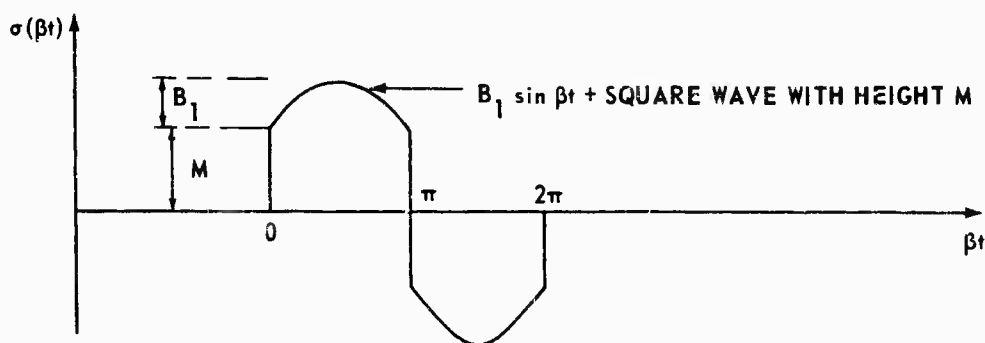


Figure 3.5. A Secondary Signal Which Linearizes the Absquare

$$\hat{N}[A_0; \sigma^*(\beta t)] = K \left[2M + \frac{4B_1}{\pi} \right] A_0 ; \quad A_0 < M . \quad (3.31)$$

The family of curves for \hat{N} and \hat{K} are given in Chapter IV when $B_1 = 0$ and M takes on different values. As stated above, the constant C_1 of Equation (3.28) is not zero for values of n other than one. The case where $n = 2$ describes the original nonlinear element and $\sigma(\beta t) = 0$ is the only correct solution. The exponent $\frac{1}{n-2}$ in Equation (3.5) causes the secondary signal to have infinite amplitude when $n < 2$. Therefore the specified \hat{N} cannot be physically realized for the admissible range $1 < n < 2$.

The last case which will be considered under the absquare example occurs when $n = 3$. The secondary signal becomes

$$\sigma(\beta t) = \frac{1}{3k_1} \left(\frac{\beta t}{\pi/2} \right) ; \quad 0 \leq \beta t \leq \pi/2 , \quad (3.32)$$

which is a triangle wave with amplitude $B^* = \frac{1}{3k_1}$. Substituting this wave for $\sigma(\beta t)$ in Equation (3.23) gives the following equations for \hat{N} :

$$\hat{N}[A_0; \sigma(\beta t)] = K \left[\frac{1}{3B^*} A_0^3 + B^* A_0 \right] ; \quad A_0 \leq B^* \quad (3.33)$$

$$\hat{N}[A_0; \sigma(\beta t)] = K \left[A_0^2 + \frac{1}{3} B^{*2} \right] ; \quad A_0 \geq B^* . \quad (3.34)$$

Therefore the gain factor k_1 in Equation (3.27) becomes $\frac{K}{3B^*}$ and the constant C_1 becomes KB^* . Although the $k_1 A_0^3$ term does appear in the expression for $\hat{N}[A_0; \sigma(\beta t)]$, it is not large compared with the $C_1 A_0$ term except when $B \ll 1$, in which case the usable range is much less than one. The results in this case are not very satisfactory. It is suspected, however, that not any other secondary signal will give an \hat{N} closer to the one specified.

Consider next the nonlinear elements which are defined by

$$N(e) = Ke^p, \quad (3.35)$$

where p is an odd positive integer. It will be shown that all secondary signals give the same structural form of \hat{N} . Differences in secondary signals alter only the magnitude of certain parameters in \hat{N} . The modified nonlinear element is given by

$$\hat{N}[A_o; \sigma(\beta t)] = \frac{1}{2\pi} \int_0^{2\pi} K [A_o + \sigma(\beta t)]^p d\beta t. \quad (3.36)$$

The p^{th} and lower order derivatives are computed as follows:

$$\frac{d^1 \hat{N}}{dA_o^p} = p! \frac{1}{2\pi} \int_0^{2\pi} K d\beta t = p! K \quad (3.37)$$

$$\frac{d^{p-1} \hat{N}}{dA_o^{p-1}} = p! \frac{K}{2\pi} \int_0^{2\pi} [A_o + \sigma(\beta t)] d\beta t = p! KA \quad (3.38)$$

$$\begin{aligned} \frac{d^{p-2} \hat{N}}{dA_o^{p-2}} &= \frac{p! K}{2} \frac{1}{2\pi} \int_0^{2\pi} [A_o + \sigma(\beta t)]^2 d\beta t \\ &= \frac{p! K}{2} [A_o^2 + C_1], \end{aligned} \quad (3.39)$$

where

$$C_1 = \frac{1}{2\pi} \int_0^{2\pi} [\sigma(\beta t)]^2 d\beta t \quad (3.40)$$

$$\frac{d^{p-3} \hat{N}}{dA_o^{p-3}} = \frac{p! K}{6} (A_o^3 + 3A_o C_1), \quad (3.41)$$

and so on for the lower order derivatives.

When $\sigma(\beta t) \neq 0$, all the constants which appear are of the form

$$C_n = \frac{1}{2\pi} \int_0^{2\pi} [\sigma(\beta t)]^{2n} d\beta t \quad (3.42)$$

and are nonzero. For example, the modified nonlinear element for the cubic is

$$\hat{N}[A_0; \sigma(\beta t)] = A_0^3 + 3A_0 C_1 \quad (3.43)$$

Thus by changing the waveform of $\sigma(\beta t)$ only the magnitude of C_1 is affected. It is found in practice that the equivalent dc gain $\hat{K}[A_0; \sigma(\beta t)]$ is often quite similar to the DIDF and can be obtained by dividing $\hat{N}[A_0; \sigma(\beta t)]$ by A_0 . The dc equivalent gain for the cubic is given by the relation

$$\hat{K}[A_0; \sigma(\beta t)] = A_0^2 + 3C_1 \quad (3.44)$$

Thus the gain for small inputs ($A_0 \rightarrow 0$) is changed from zero to $3C_1$. This is a peculiar class of nonlinear elements where the waveform of $\sigma(\beta t)$ does not affect the "shape" of \hat{N} . Therefore the secondary signal is not unique even within the restricted class of signals described by Equation (3.4). The values for the constant C_1 when $\sigma(\beta t)$ is a square wave, sine wave, and triangle wave, respectively, are

$$C_1 \text{ (square wave)} = B^2 \quad (3.45)$$

$$C_1 \text{ (sine wave)} = B^2/2 \quad (3.46)$$

$$C_1 \text{ (triangle wave)} = B^2/3 \quad (3.47)$$

The method of taking derivatives of \hat{N} to get simpler expressions with which to work is not limited entirely to the nonlinear elements defined by Equation (3.5). Limited success may be achieved where the nonlinear

element is piecewise constant or linear. For example, the "linearization" of the relay with dead band by the method presented above requires a triangle wave. The triangle wave is known to be a correct answer (Chapter IV). The method also gives the same answer for the relay with dead band and the perfect relay when $n = 2$. The secondary signal is computed to be

$$\sigma(\beta t) = \left(\frac{M}{k_1}\right)^{1/2} \left(\frac{\beta t}{\pi/2}\right)^{1/2}; \quad 0 \leq \beta t \leq \pi/2 \quad (3.48)$$

However, the process is much more tedious in the case of the relay with dead band and the resulting \hat{N} is not what one might expect. The specified structure $\left[\hat{N} = k_1 A_0^2 \operatorname{sgn}(A_0)\right]$ is achieved (within a constant) only in the region $a \leq |A_0| \leq B - a$. A linear range results when $|A_0| < a$ (Figure 3.6).

An important question which has been left unanswered by this procedure is: Does a secondary signal exist which gives the desired modified nonlinear element $\left[\hat{N} = A_0^2 \operatorname{sgn}(A_0)\right]$? The procedure used above also suffers from the fact that it cannot be used when a more general type nonlinear element is encountered.

A brute force method which offers some possibility for the general problem is now given. Only odd single valued nonlinear elements will be considered. The method is approximate and involves assuming the amplitude B of the secondary signal at the start. A digital computer solution will be required in most cases. The procedure is as follows:

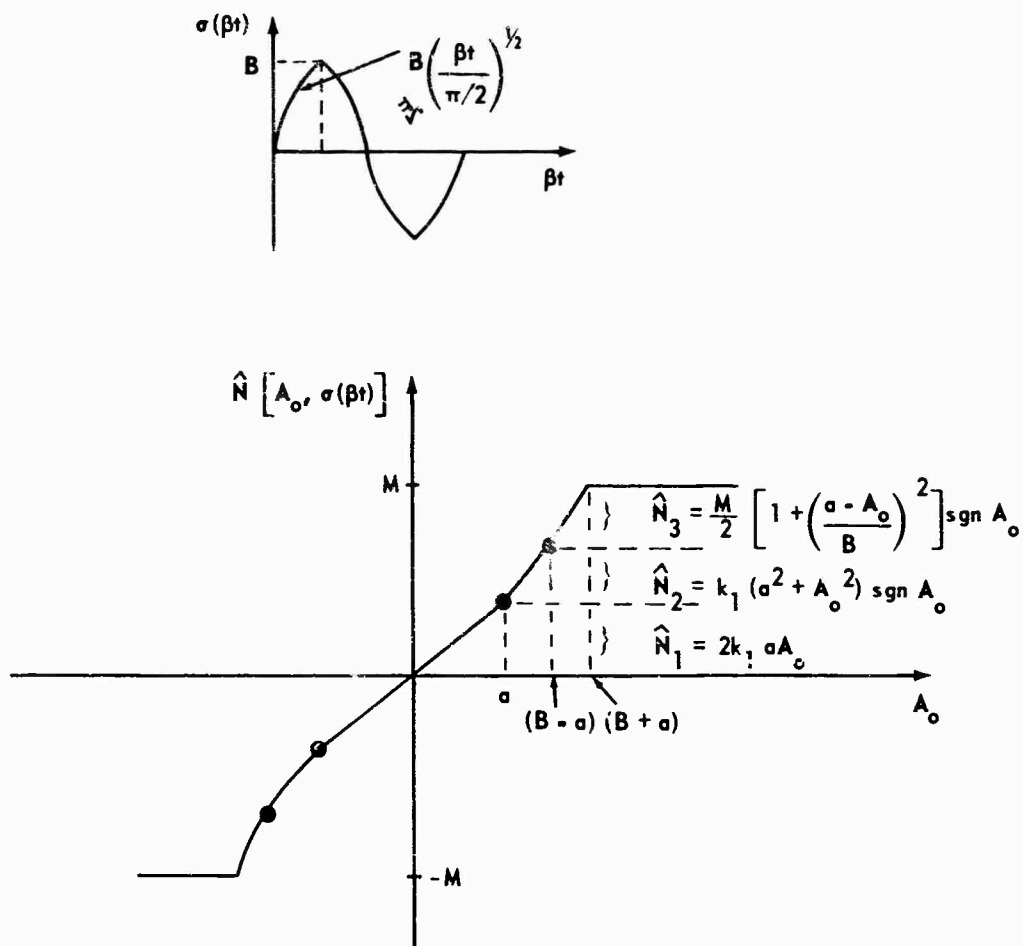


Figure 3.6. Sketch of the Secondary Signal $\sigma(\beta t) = B \left(\frac{2}{B} \beta t \right)$ and the Corresponding Modified Nonlinear Element for the Relay with Dead Band

Step 1

Assume an approximate secondary signal $\sigma(\beta t)$ of the staircase type shown in Figure 3.7. The signal $\bar{\sigma}(\beta t)$ has the same properties which have been assumed above and described by Equation (3.4). The amplitude B is divided into n equal increments ($B = n\Delta$). The width of the i^{th} increment is T_i and is unknown. Define the T_i so that

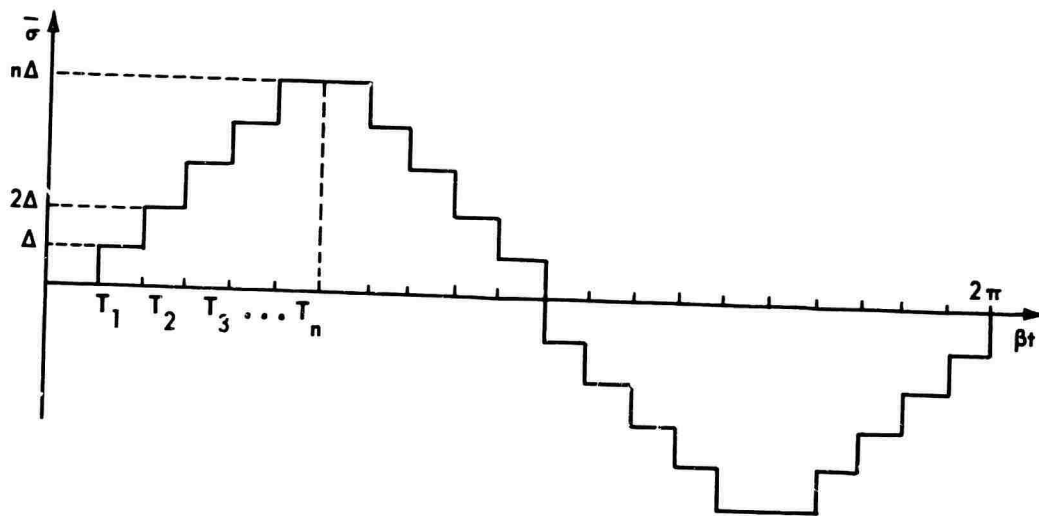


Figure 3.7. Approximate Secondary Signal

$$\sum_{i=1}^n T_i = \pi/2 \quad (3.49)$$

Step 2

Assume the composite signal $A_0 + \bar{\sigma}(\beta t)$ as an input to the nonlinear element where, for convenience, the bias A_0 is confined to the Δ increments as well. That is, let

$$A_0 = j\Delta \leq B \quad (3.50)$$

where

$$j \leq n \quad (3.51)$$

Both j and n are positive integers. Now, write out the algebraic equation for the average output of the nonlinear element over a complete cycle $\beta t = 2\pi$.

The equations take the following form:

$$\begin{aligned}
A_v = \frac{2}{2\pi} & \left[N(A_o + \Delta)T_1 + N(A_o + 2\Delta)T_2 + \dots + N(A_o + i\Delta)T_i + \dots \right. \\
& + N(A_o + n\Delta)T_n \left. \right] + \frac{2}{2\pi} \left[N(A_o - \Delta)T_1 + N(A_o - 2\Delta)T_2 + \dots \right. \\
& \left. + N(A_o - k\Delta)T_k + \dots + N(A_o - n\Delta)T_n \right] , \quad (3.52)
\end{aligned}$$

or

$$A_v = \frac{1}{\pi} \sum_{i=1}^n N(A_o + i\Delta)T_i + \frac{1}{\pi} \sum_{i=1}^n N(A_o - i\Delta)T_i . \quad (3.53)$$

Substituting the value for A_o given in Equation (3.50) and recognizing that A_v is really \hat{N} at this particular value A_o gives

$$\hat{N}_j = \frac{1}{\pi} \sum_{i=1}^n [N(j\Delta + i\Delta) + N(j\Delta - i\Delta)] T_i . \quad (3.54)$$

\hat{N}_j is defined by the equation

$$\hat{N}_j \triangleq \hat{N}(A_o = j\Delta) . \quad (3.55)$$

Step 3

Place the desired values of N^* on the left-hand side of Equation (3.54) and solve for the unknown T_i . There will, in general, be $(n - 1)$ linearly independent equations and the relation given in Equation (3.49) is required to complete the solution. If no negative or imaginary values are found for the T_i , this means that secondary signal $\bar{\sigma}(\beta t)$ has been found which approximates the desired signal $\sigma^*(\beta t)$. Since the amplitude B of the secondary signal is chosen a priori, it is advisable to have a variable k_1 multiplying the desired \hat{N} . For example,

$$N^* = k_1 |A_o|^m \text{sgn}(A_o) . \quad (3.56)$$

To specify k_1 initially would, in many cases, eliminate any possibility of obtaining a physically realizable answer. It is remarked that after the wave-form of $\sigma(\beta t)$ and the magnitude of \hat{N} have been determined, a second choice of B might lead to a better approximate solution.

Step 4

When $\bar{\sigma}(\beta t)$ has been found, draw a smooth curve through the midpoint of each increment. This should give the best approximate solution $\bar{\sigma}^*(\beta t)$. The value of n chosen will depend upon the desired accuracy. It is suggested that the first try be made with a small n .

A simple example of the linearization of the absquare will be given to show how the method may be used.

Example 3 (Absquare)

The absquare is described by the equation

$$N(e) = e^2 \operatorname{sgn}(e) \quad . \quad (3.57)$$

The desired modified nonlinear element is given by

$$N^* [A_o ; \sigma(\beta t)] = k_1 A_o ; \quad A_o \leq B \quad . \quad (3.58)$$

Since $N(e)$ is described by a one-term polynomial, it is not necessary to choose a specific value for B . Choose $n = 5$ for this example and the value of Δ becomes $B/5$. Equation (3.65) is written out as follows:

$$\Delta k_1 = \frac{1}{\pi} (4\Delta^2 T_1 + 8\Delta^2 T_2 + 12\Delta^2 T_3 + 16\Delta^2 T_4 + 20\Delta^2 T_5) \quad (3.59)$$

$$2\Delta k_1 = \frac{1}{\pi} (9\Delta^2 T_1 + 16\Delta^2 T_2 + 24\Delta^2 T_3 + 32\Delta^2 T_4 + 40\Delta^2 T_5) \quad (3.60)$$

$$3\Delta k_1 = \frac{1}{\pi} (20\Delta^2 T_1 + 40\Delta^2 T_2 + 50\Delta^2 T_3 + 64\Delta^2 T_4 + 60\Delta^2 T_5) \quad (3.61)$$

$$4\Delta k_1 = \frac{1}{\pi} (34\Delta^2 T_1 + 40\Delta^2 T_2 + 50\Delta^2 T_3 + 64\Delta^2 T_4 + 80\Delta^2 T_5) \quad (3.62)$$

$$5\Delta k_1 = \frac{1}{\pi} (50\Delta^2 T_1 + 58\Delta^2 T_2 + 68\Delta^2 T_3 + 82\Delta^2 T_4 + 100\Delta^2 T_5) \quad (3.63)$$

Successive elimination of the unknown terms shows that

$$T_1 = T_2 = T_3 = T_4 = 0 \quad (3.64)$$

This leaves finally

$$\Delta k_1 = \frac{20}{\pi} \Delta^2 T_5 \quad (3.65)$$

From Equation (3.49) it is seen that

$$T_5 = \pi/2 \quad (3.66)$$

Thus,

$$k_1 = 2B^* ; \quad A_0 \leq B^* \quad (3.67)$$

Equation (3.66) relates that $\sigma^*(\beta t)$ is a square wave and Equation (3.67) states that the resulting gain is $2B^*$ in the linear region. This answer has already been shown in Example 2 to be correct. When the nonlinear element is piecewise linear, the amplitude B does not have to be chosen first and the parameter Δ may be factored out of Equation (3.54) in a manner similar to the above example.

The examples given using the method of specifying the m^{th} derivative of $\hat{N}[A_0; \sigma(\beta t)]$ shows that only very limited success can be expected from any method where the nonlinear element is more general. This applies to the approximate method described above where the nonlinear element may exist only in graphical form. Although emphasis has been placed on the region $A_0 \leq B$ around the origin, this restriction is not necessary. The region of

\hat{N} for $A_0 > B$ may sometimes be altered in a specified manner by the presence of $\sigma(\beta t)$.

If the desired secondary signal cannot be found by any of the methods described above, there is an alternative method of modifying the nonlinear element which may prove effective [suggested to the author by C. D. Johnson]. In order to apply this alternative method, the desired K^* or N^* must lie in the region R which is attainable with some secondary signal. It is usually not difficult to establish R . The first step is to choose a convenient secondary signal $\bar{\sigma}(\beta t)$, perhaps a sine wave. Step 2 is to determine how the amplitude B of $\bar{\sigma}(\beta t)$ must be varied in accordance with the input signal amplitude A_0 in order to give the desired modified nonlinear element. This may be done by solving the equation

$$\hat{N}[A_0; \sigma(\beta t)] = N^*(A) \quad (3.68)$$

The unknown in Equation (3.68) is B and will only be function of A_0 once $\bar{\sigma}(\beta t)$ is chosen. This function $B(A)$ will then become a "variable gain box" which will premultiply $\bar{\sigma}(\beta t)$ before it is summed with the input A_0 . From a hardware implementation viewpoint, this alternative method is not appreciably more complex than shaping the secondary signal $\sigma^*(\beta t)$ in the inverse DDF method.

Oldenburger and Ikebe [40] have offered still another linearizing method where a relay function and a triangle wave secondary signal are placed in series ahead of the existing nonlinear element. In effect the insertion of the relay function in front of another nonlinear element in the signal flow path results in a relay function for the combination. It was seen in this chapter

that the relay is perhaps the most versatile nonlinear element when one is concerned with shaping the modified nonlinear element with an extra signal. Therefore, the approach presented in this chapter can be used to extend the method of Oldenburger and Labe to the more general problem of specifying $\hat{N}[A_0; \sigma(\beta t)]$ rather than strict linearization.

CHAPTER IV

THE MODIFIED NONLINEAR ELEMENTS AND DUAL INPUT DF'S FOR TEN NONLINEAR ELEMENTS

In this chapter the modified nonlinear element and the DIDF's (Chapter II) of ten common nonlinear elements are given for the case when the secondary signal is either a sine wave, a triangle wave, or a square wave. These secondary signal waveforms were chosen to show the qualitative trend in $\hat{N}[A; \sigma(\beta t)]$ as the waveform is changed. The specific nonlinear elements are as follows:

- a. Absquare
- b. Relay
- c. Relay with dead band
- d. Preload
- e. Dead band
- f. Limiter
- g. Limiter with dead band
- h. Relay with dead band and hysteresis
- i. Relay with hysteresis
- j. Limiter with hysteresis.

Closed form solutions for the modified nonlinear elements are given for all cases. Closed form solutions are also given for the DIDF's with the exception of five nonlinear elements with sine wave secondary signals. Approximate

solutions are given for some of these cases in the form of finite series obtained by trapezoidal integration tabulated along with the complete set of curves of both the modified nonlinear elements and the DIDF's. The average DIDF method as explained in Chapter II was used to calculate the TSIDF with the exception of the three memory type nonlinear elements. Otherwise, the modified nonlinear element method, also explained in Chapter II, was used to calculate the DIDF. When the modified nonlinear element is derived, no special effort is made to insure that the equation holds for negative inputs A_0 . It is simply necessary to recall that the modified nonlinear element is an odd function.

It is emphasized again that the DIDF's of the double valued nonlinear elements found by the modified nonlinear element method are valid only when the frequency of the secondary signal is very high compared to that of the primary input component. An example is given in the appendix to show the procedure used in deriving these modified nonlinear elements and DIDF's. Numerical answers for the DIDF's were obtained by digital computer evaluation of the given equations.

The following definitions describe angles and symbols used in the modified nonlinear element and DIDF equations:

$$|X| \triangleq \text{absolute value of } X \quad (4.1)$$

$$\text{sgn}(X) = \begin{cases} 1; & X > 1 \\ -1; & X < 1 \end{cases} \quad (4.2)$$

$$\text{sat}(X) = \begin{cases} X; & |X| \leq 1 \\ \text{sgn}(X); & |X| > 1 \end{cases} \quad (4.3)$$

$$\theta_1 = \sin^{-1} \operatorname{sat} \left(\frac{A}{B} \right)$$

$$\theta_2 = \sin^{-1} \operatorname{sat} \left(\frac{a - A}{B} \right)$$

$$\theta_3 = \sin^{-1} \operatorname{sat} \left(\frac{a + A}{B} \right)$$

$$\theta_4 = \sin^{-1} \operatorname{sat} \left(\frac{b - A}{B} \right)$$

$$\theta_5 = \sin^{-1} \operatorname{sat} \left(\frac{b + A}{B} \right)$$

$$\theta_{2T} = \frac{\pi}{2} \operatorname{sat} \left(\frac{a - A}{B} \right)$$

$$\theta_{3T} = \frac{\pi}{2} \operatorname{sat} \left(\frac{a + A}{B} \right)$$

$$\theta_{4T} = \frac{\pi}{2} \operatorname{sat} \left(\frac{b - A}{B} \right)$$

$$\theta_{5T} = \frac{\pi}{2} \operatorname{sat} \left(\frac{b + A}{B} \right)$$

$$\gamma_1 = \sin^{-1} \operatorname{sat} \left(\frac{B}{A} \right)$$

$$\gamma_2 = \sin^{-1} \operatorname{sat} \left(\frac{a - B}{A} \right)$$

$$\gamma_3 = \sin^{-1} \operatorname{sat} \left(\frac{a + B}{A} \right)$$

$$\gamma_4 = \sin^{-1} \operatorname{sat} \left(\frac{b - B}{A} \right)$$

$$\gamma_5 = \sin^{-1} \operatorname{sat} \left(\frac{b + B}{A} \right)$$

(4.4)

4.1. Absquare

$$N(e) = e^2 \operatorname{sgn}(e) \quad (4.5)$$

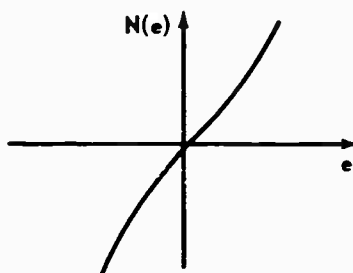


Figure 4.1. Absquare

Sine Wave Secondary Signal (Figures 4.2 and 4.3)

$$\hat{N}(A_0, B) = \begin{cases} \frac{1}{\pi} \left[\left(2A_0^2 + B^2 \right) \sin^{-1} \left(\frac{A_0}{B} \right) + 3A_0 B \sqrt{1 - \left(\frac{A_0}{B} \right)^2} \right] ; & A_0 < B \\ \left(A_0^2 + \frac{1}{2} B^2 \right) ; & A_0 \geq B \end{cases} \quad (4.6)$$

$$\hat{K}(A, B) = \frac{3(A+B)}{9\pi^2 A^2} \left[(7A^2 + B^2) E(k) - (A-B)^2 F(k) \right] \quad (4.7)^2$$

$$k = \frac{2\sqrt{AB}}{A+B} \quad (4.8)$$

Triangle Wave Secondary Signal (Figures 4.4 and 4.5)

$$\hat{N}_{A_0, B} = \begin{cases} A_0 B + \frac{A_0^3}{3B} ; & A_0 \leq B \\ A_0^2 + \frac{B^2}{3} ; & A_0 > B \end{cases} \quad (4.9)$$

${}^2F(k)$ denotes the complete elliptic integral of the first kind and $E(k)$ denotes the complete elliptic integral of the second kind. The modulus is defined as k .

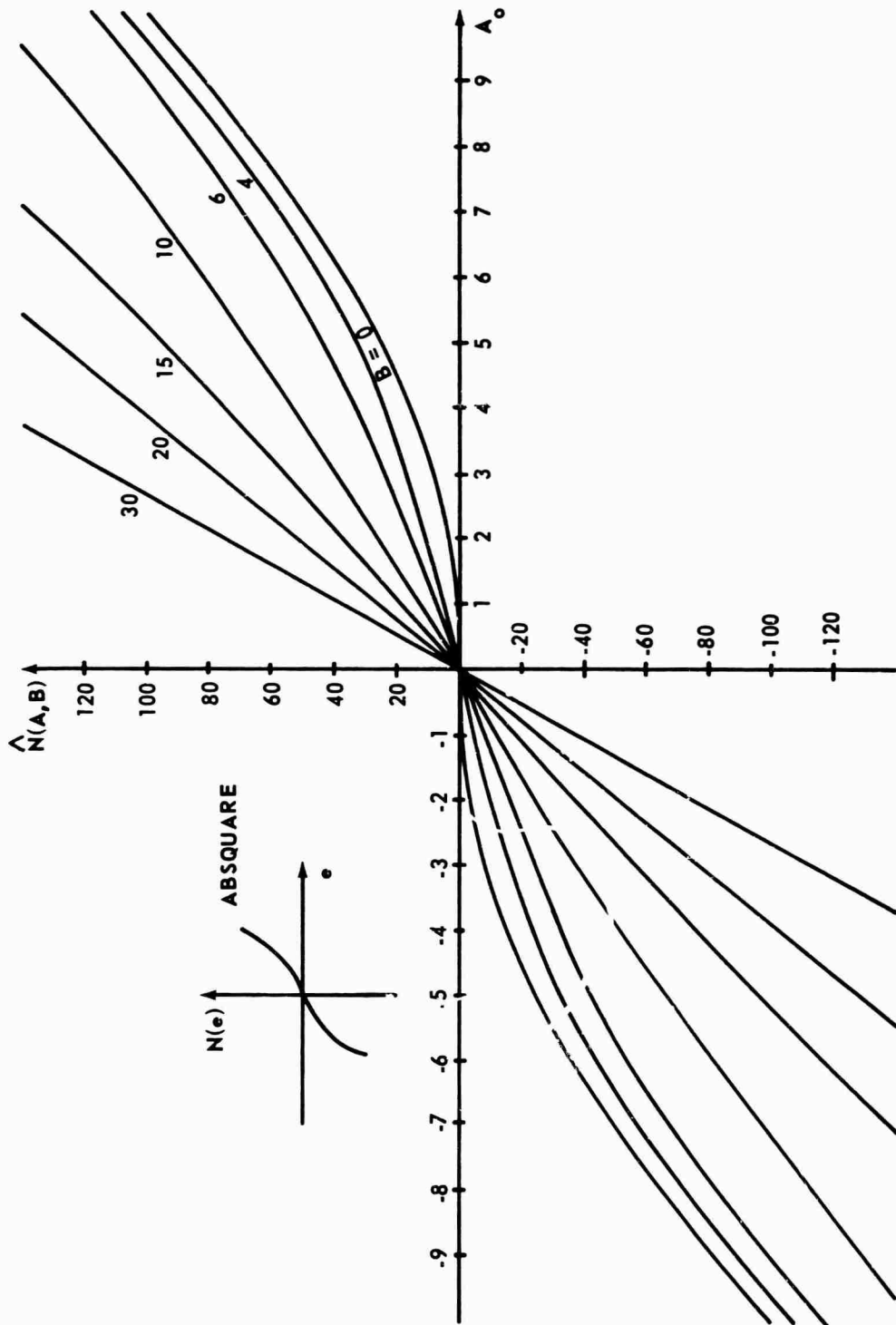


Figure 4.2. Modified Nonlinear Element for Absquare, Sine Wave Secondary Signal

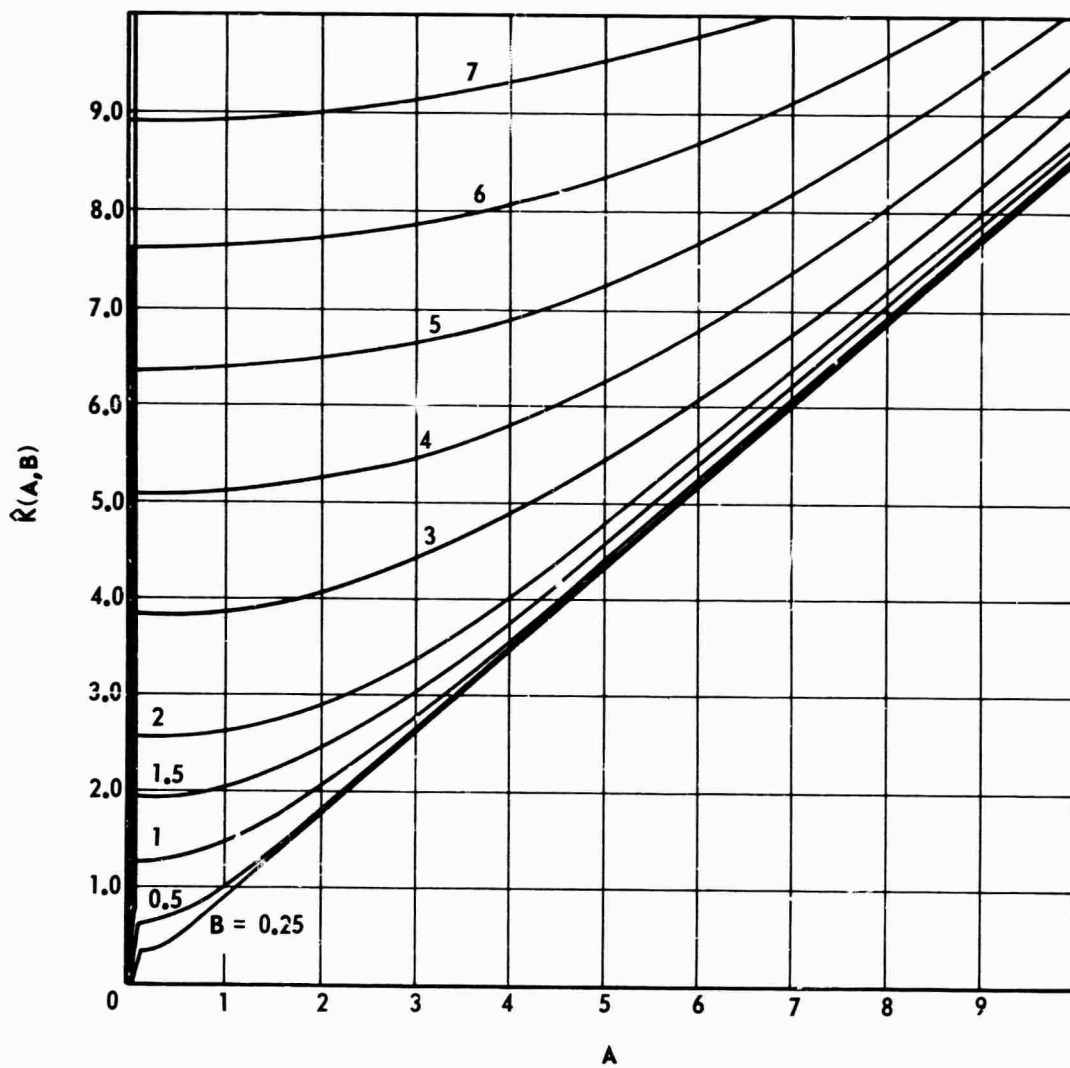


Figure 4.3. DIDF for Absquare, Sine Wave Secondary Signal

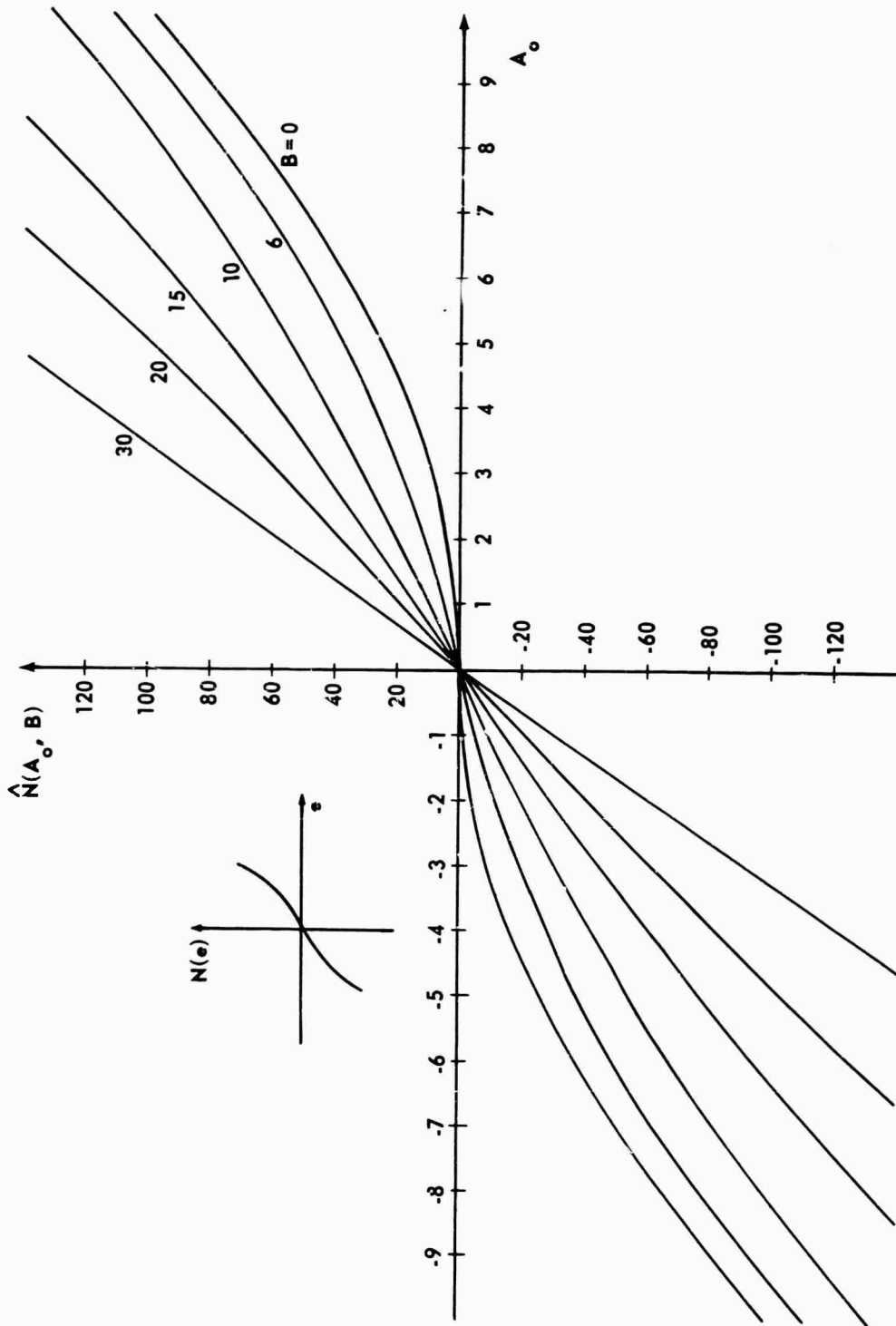


Figure 4.4. Modified Nonlinear Element for Absquare, Triangle Wave Secondary Signal

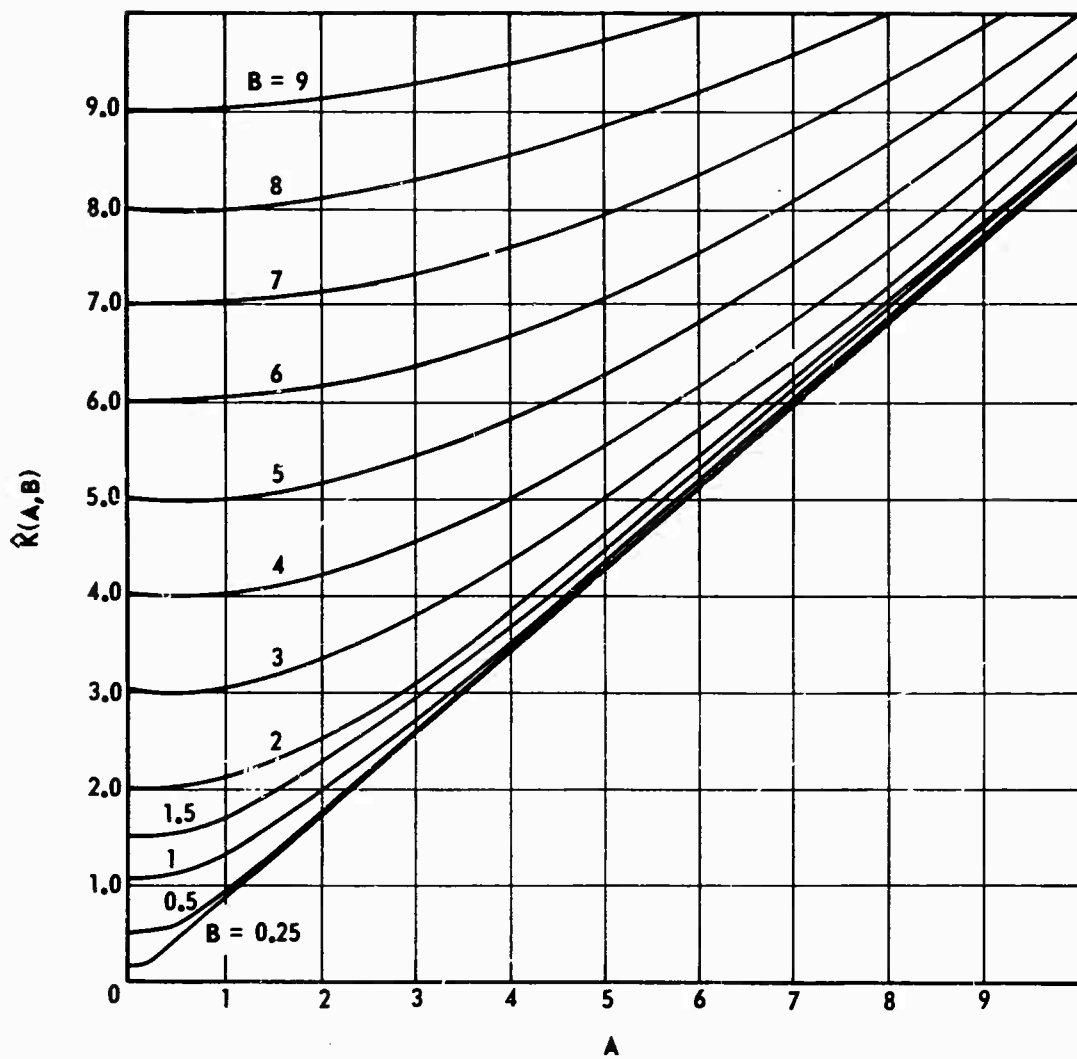


Figure 4.5. DIDF for Absquare, Triangle Wave Secondary Signal

$$\hat{K}(A, B) = \begin{cases} \frac{1}{\pi} \left[\left(2B + \frac{A^2}{2B} \right) \sin^{-1} \left(\frac{B}{A} \right) + \sqrt{1 + \frac{B}{A} \left(\frac{B^2}{3A} + \frac{13}{6} A \right)} \right] ; & A > B \\ B + \frac{A^2}{4B} ; & A \leq B \end{cases} \quad (4.10)$$

Square Wave Secondary Signal (Figures 4.7 and 4.8)

$$\hat{N}(A_o, B) = \begin{cases} 2BA_o ; & A_o \leq B \\ A_o^2 + B^2 ; & A_o > B \end{cases} \quad (4.11)$$

$$\hat{K}(A_o, B) = \begin{cases} \frac{4}{\pi} \left[B \sin^{-1} \left(\frac{B}{A} \right) + \frac{1}{3} \left(2A + \frac{B^2}{A} \right) \sqrt{1 - \left(\frac{B}{A} \right)^2} \right] ; & A > B \\ 2B ; & A \leq B \end{cases} \quad (4.12)$$

4.2 Relay

$$N(e) = M \operatorname{sgn}(e) \quad (4.13)$$

Sine Wave Secondary Signal (Figures 4.9 and 4.10)

$$\hat{N}(A_o, B) = \frac{2M}{\pi} \sin^{-1} \operatorname{sat} \left(\frac{A_o}{B} \right) \quad (4.14)$$

$$\hat{K}(A, B) = \frac{4M}{\pi^2} \frac{1}{A^2} [(A - B)K(k) + (A + B)E(k)] ; \quad (4.15)$$

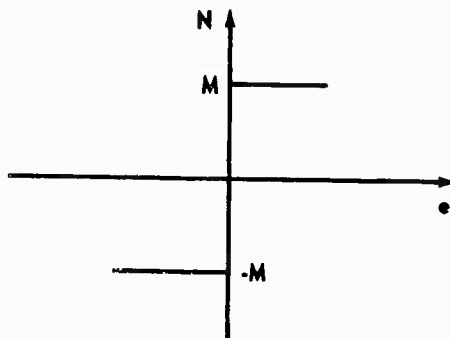


Figure 4.6. Relay

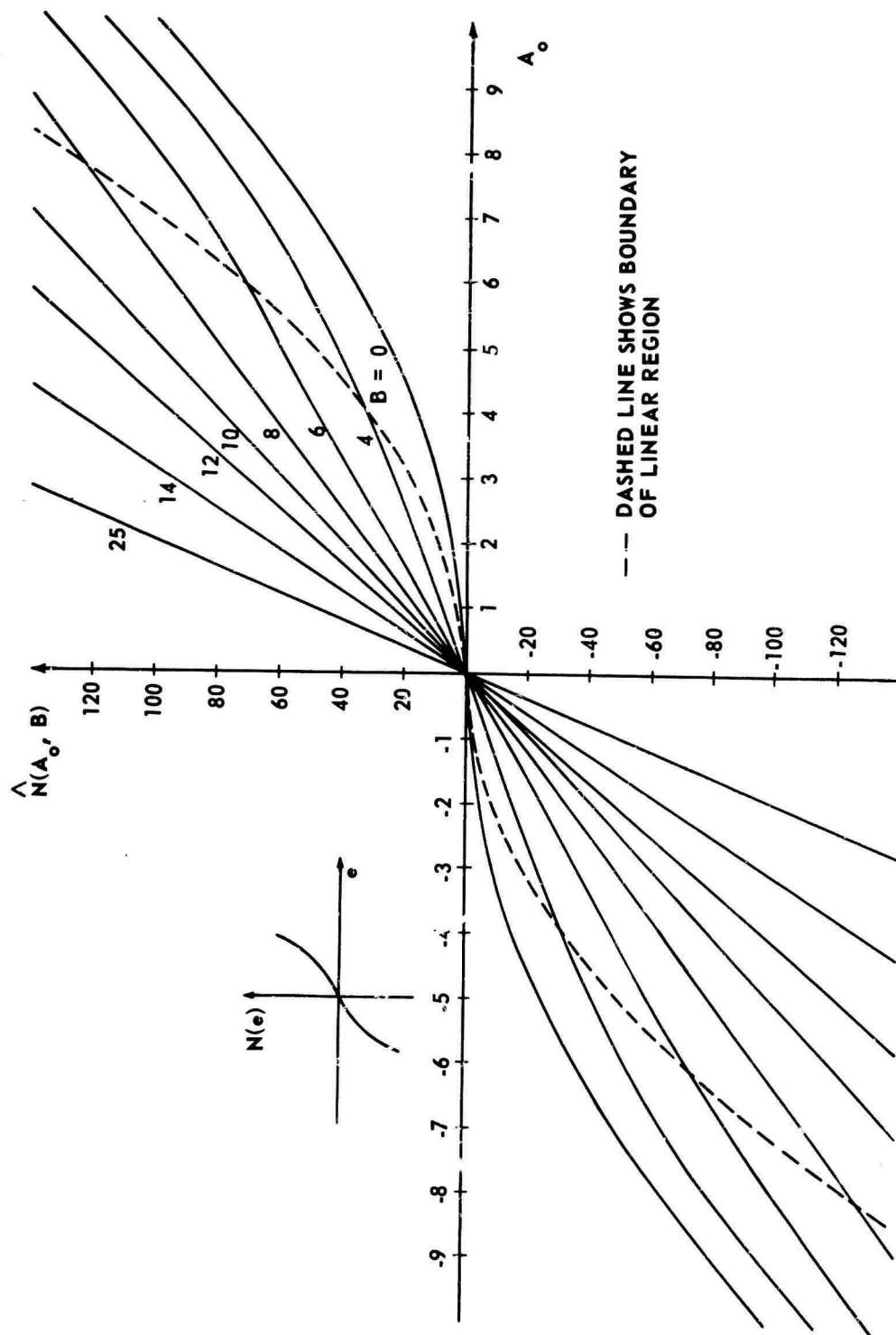


Figure 4.7. Modified Nonlinear Element for Absquare, Square Wave Secondary Signal

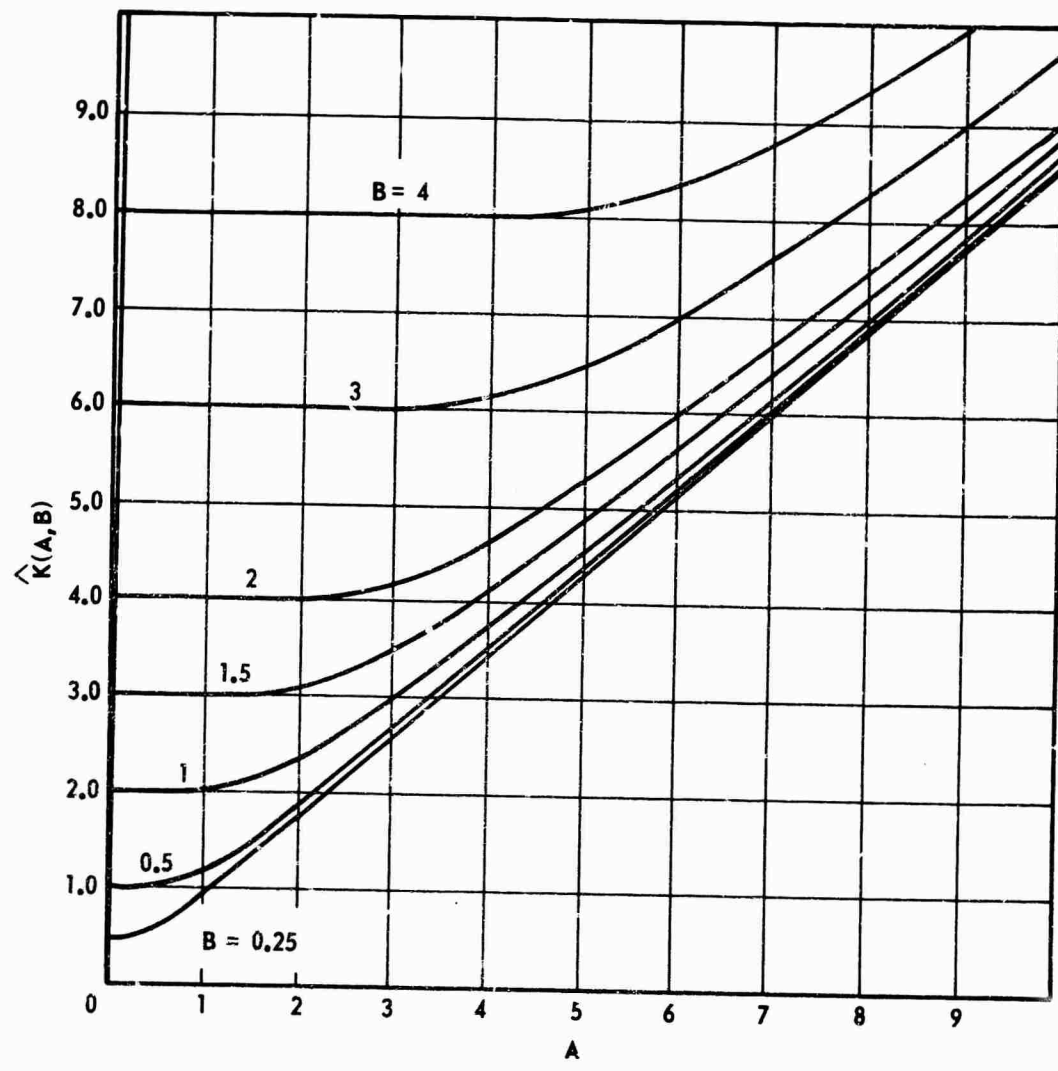


Figure 4.8. DIDF for Absquare, Square Wave Secondary Signal

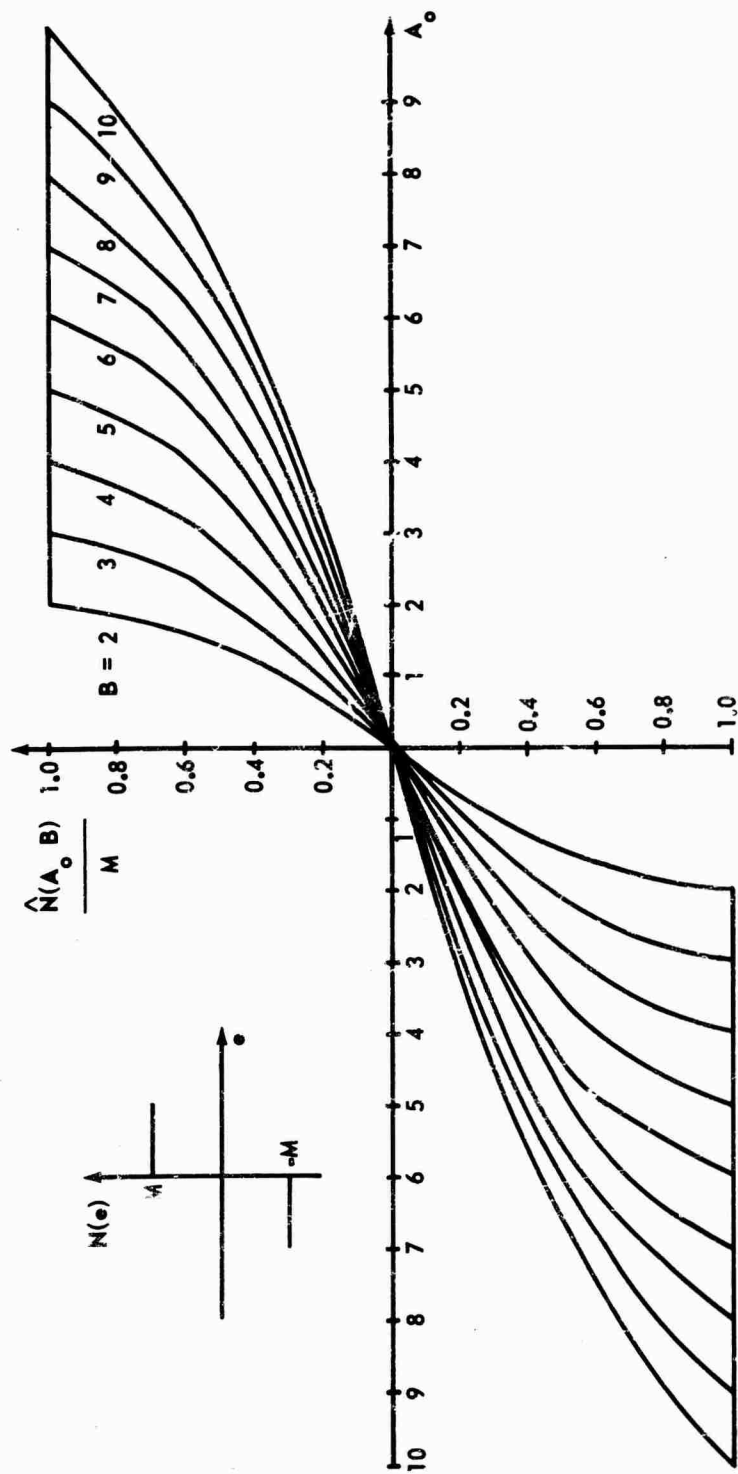


Figure 4.9. Modified Nonlinear Element for Perfect Relay, Sine Wave Secondary Signal

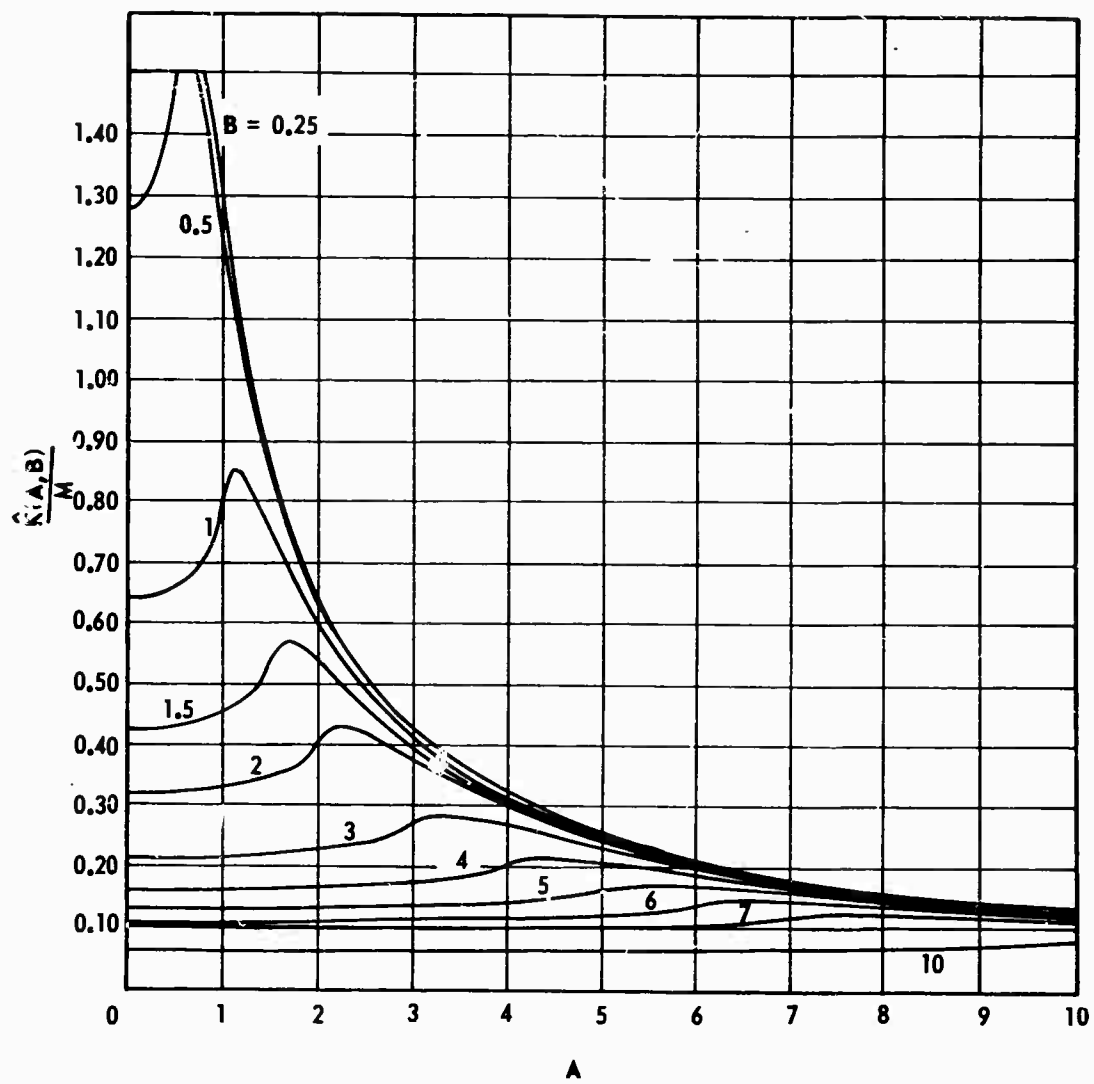


Figure 4.10. DIDF for Relay, Sine Wave Secondary Signal

where

$$k^2 = \frac{4AB}{(A + B)^2} \quad (4.16)$$

Triangle Wave Secondary Signal (Figures 4.12 and 4.13)

$$\hat{N}(A_o, B) = M \operatorname{sat} \left(\frac{A_o}{B} \right) \quad (4.17)$$

$$\hat{K}(A, B) = \frac{M}{B\pi} (2\gamma_1 - \sin 2\gamma_1) + \frac{4M}{\pi A} \cos \gamma_1 \quad (4.18)$$

Square Wave Secondary Signal (Figures 4.14 and 4.15)

$$\hat{N}(A_o, B) = \begin{cases} 0 & ; \quad A_o < B \\ M & ; \quad A_o \geq B \end{cases} \quad (4.19)$$

$$\hat{K}(A, B) = \frac{4M}{\pi A} \sqrt{1 - \operatorname{sat} \left(\frac{B}{A} \right)^2} \quad (4.20)$$

4.3 Preload

$$N(e) = Ce + M \operatorname{sgn}(e) \quad (4.21)$$

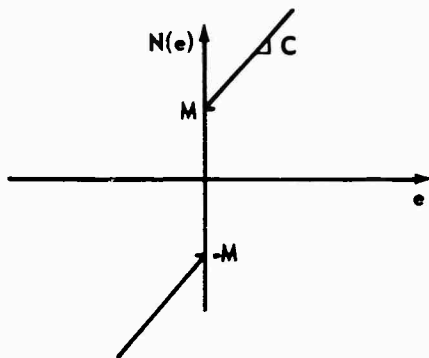


Figure 4.11. Preload

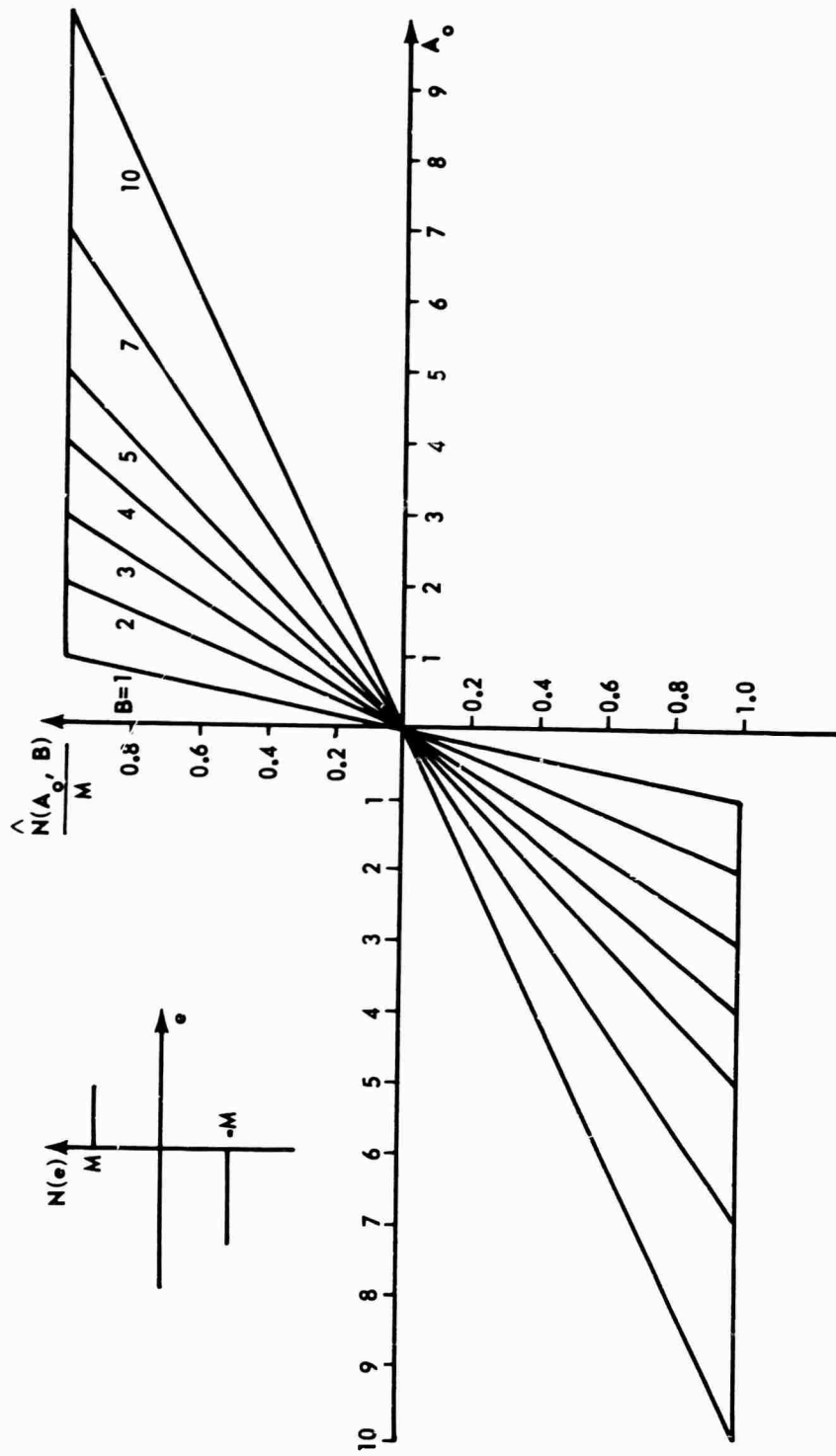


Figure 4.12. Modified Nonlinear Element for Perfect Relay, Triangle Wave Secondary Signal

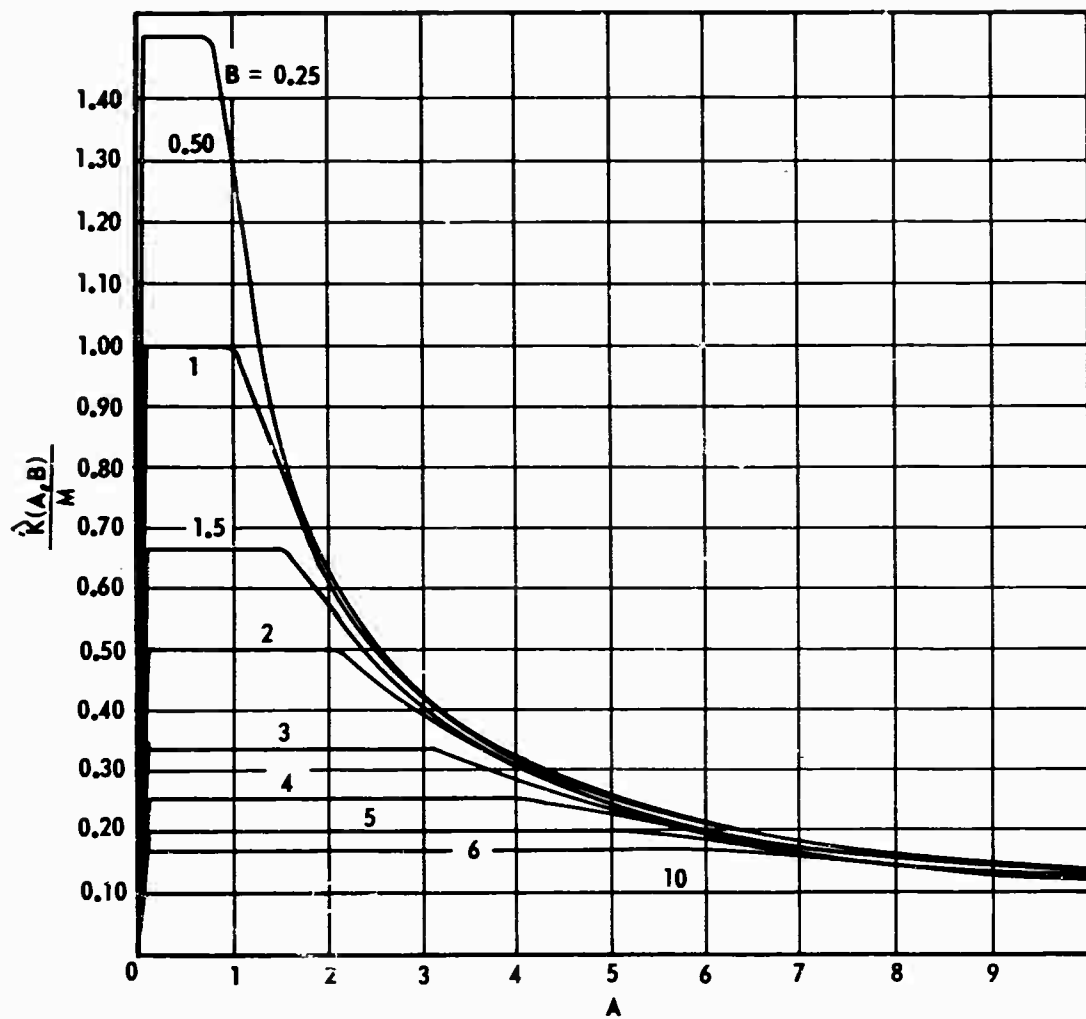


Figure 4.13. DIDF for Relay, Triangle Wave Secondary Signal

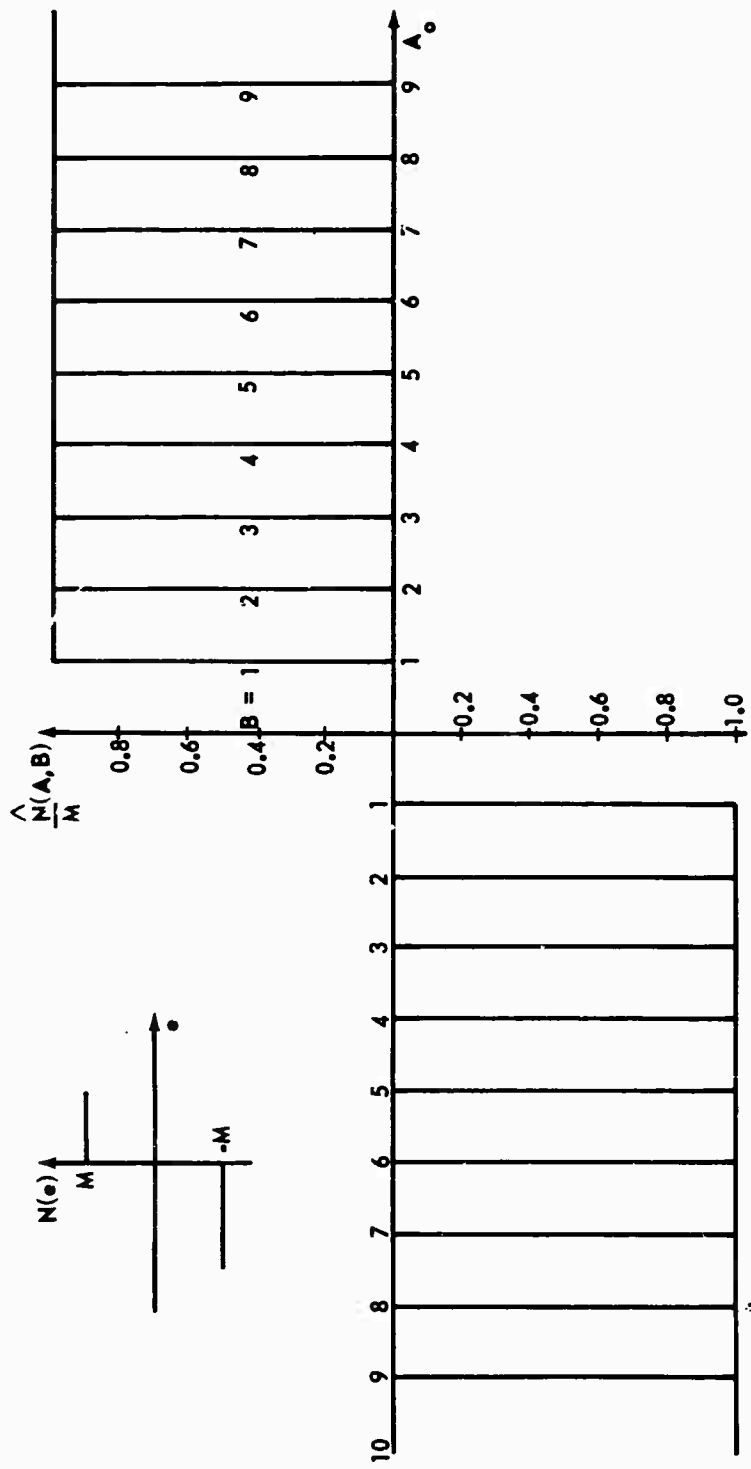


Figure 4.14. Modified Nonlinear Element for Perfect Relay, Square Wave Secondary Signal

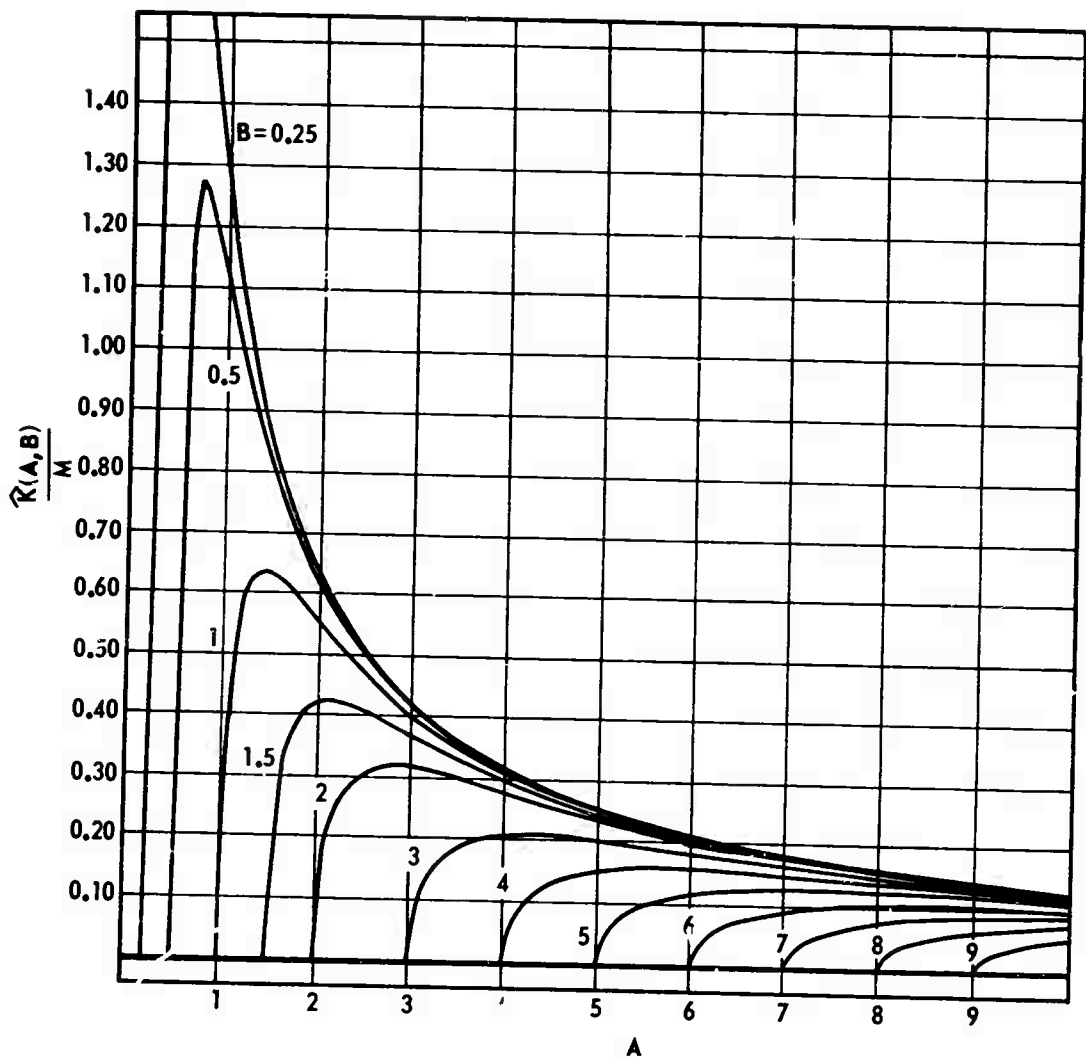


Figure 4. 15. DIDF for Relay, Square Wave Secondary Signal

Sine Wave Secondary Signal (Figures 4.16 and 4.17)

$$\hat{N}(A_o, B, C, M) = CA_o + \frac{2M}{\pi} \sin^{-1} \text{sat} \left(\frac{A_o}{B} \right) \quad (4.22)$$

$$\hat{K}(A, B, C, M) = C + \frac{4M}{\pi^2} \frac{1}{A^2} [(A - B)K(k) + (A + B)E(k)] ; \quad (4.23)$$

where

$$k^2 = \frac{4AB}{(A + B)^2} \quad (4.24)$$

Triangle Wave Secondary Signal (Figures 4.18 and 4.19)

$$\hat{N}(A_o, B, C, M) = CA_o + M \text{sat} \left(\frac{A_o}{B} \right) \quad (4.25)$$

$$\hat{K}(A, B, C, M) = C + \frac{M}{B\pi} (2\gamma_1 - \sin 2\gamma_1) + \frac{4M}{\pi A} \cos \gamma_1 \quad (4.26)$$

Square Wave Secondary Signal (Figures 4.20 and 4.21)

$$\hat{N}(A_o, B, C, M) = \begin{cases} CA_o ; & A_o < B \\ CA_o + M ; & A_o \geq B \end{cases} \quad (4.27)$$

$$\hat{K}(A, B, C, M) = C + \frac{4M}{\pi A} \sqrt{1 - \text{sat} \left(\frac{B}{A} \right)^2} \quad (4.28)$$

4.4 Relay with Dead Band

$$N(e) = \frac{M}{2} [\text{sgn}(e - a) + \text{sgn}(e + a)] \quad (4.29)$$

Sine Wave Secondary Signal (Figures 4.22 and 4.23)

$$\hat{N}(A_o, B, a) = \frac{M}{\pi} (\theta_3 - \theta_2) \quad (4.30)$$

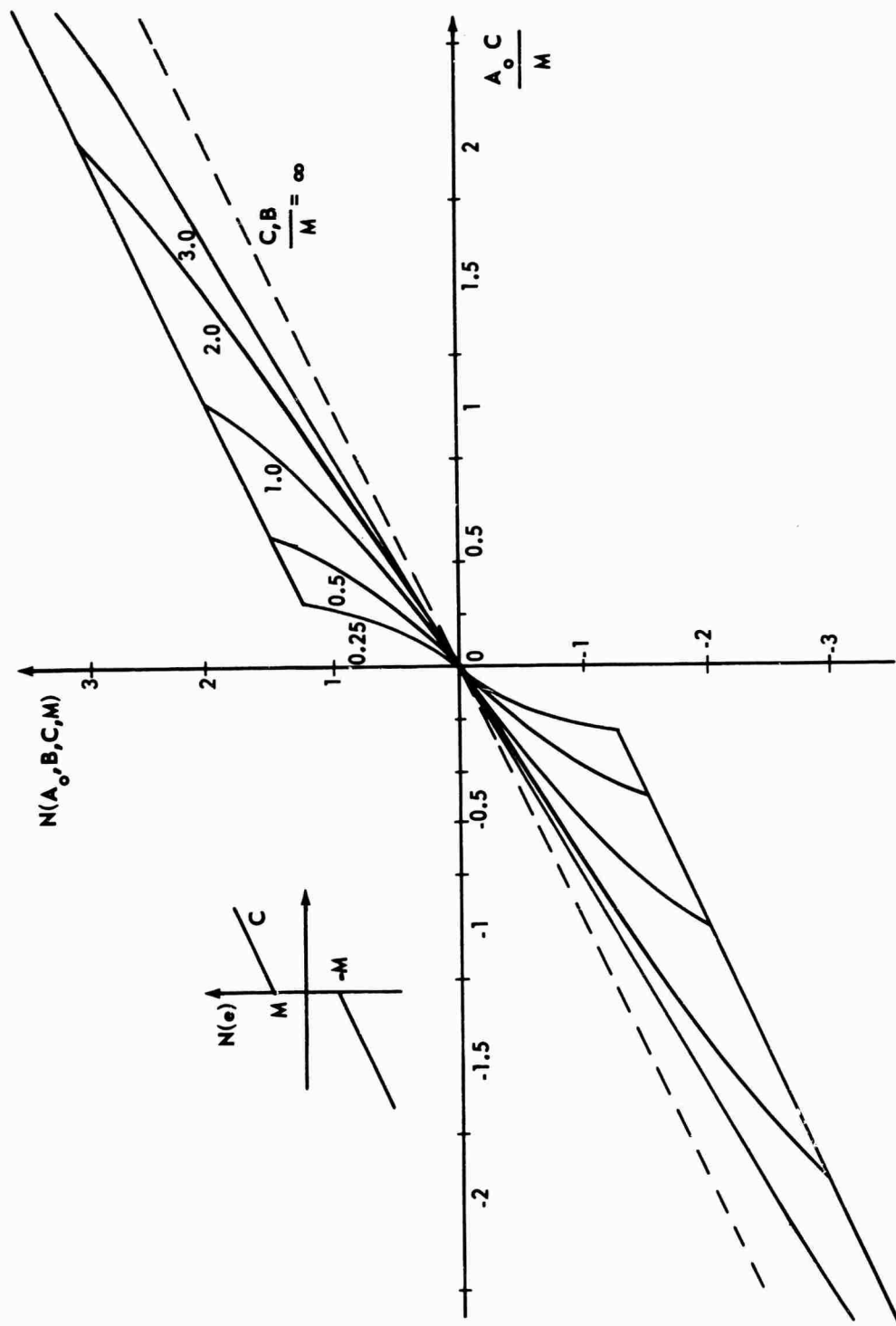


Figure 4.16. Modified Nonlinear Element for Preload, Sine Wave Secondary Signal

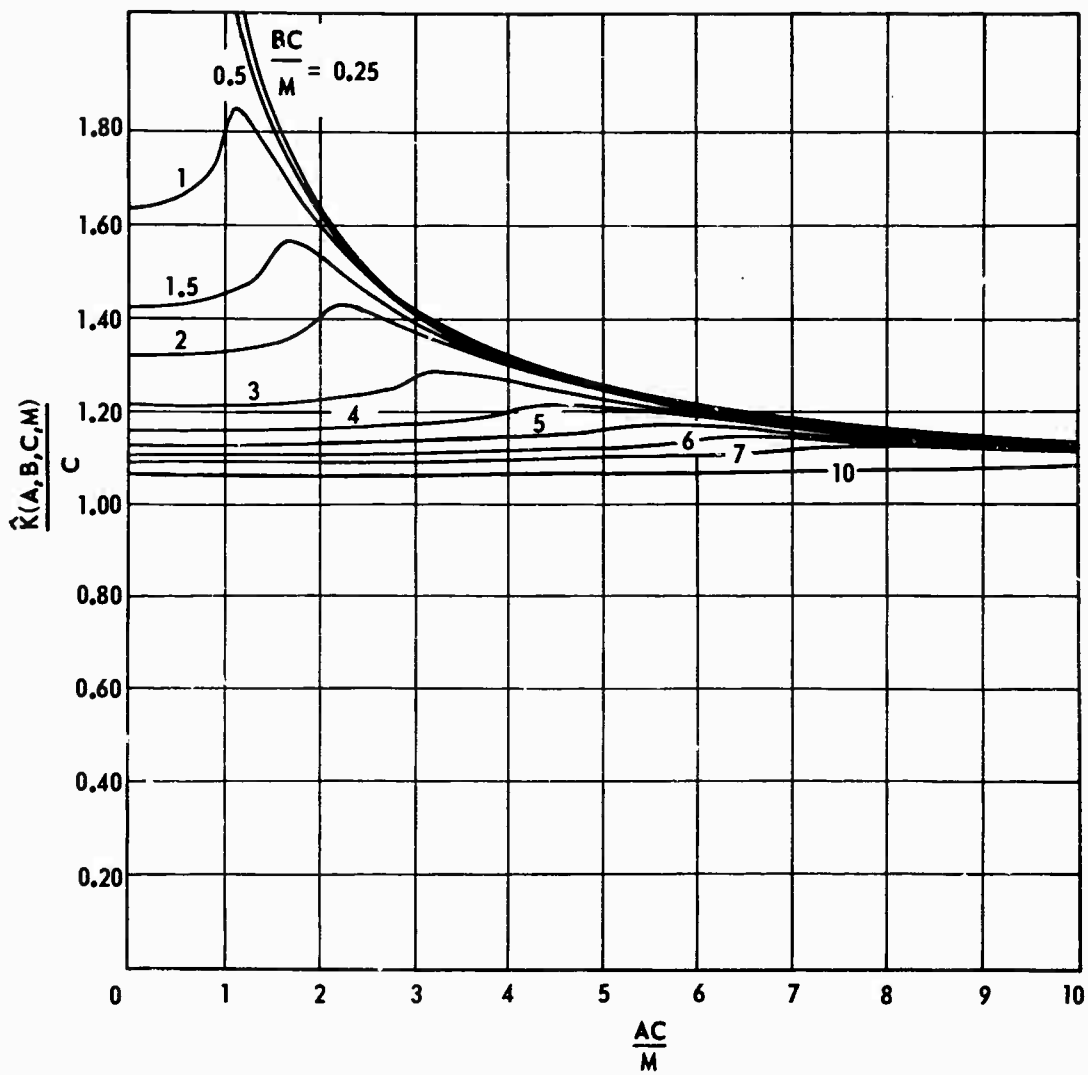


Figure 4.17. DIDF for Preload, Sine Wave Secondary Signal

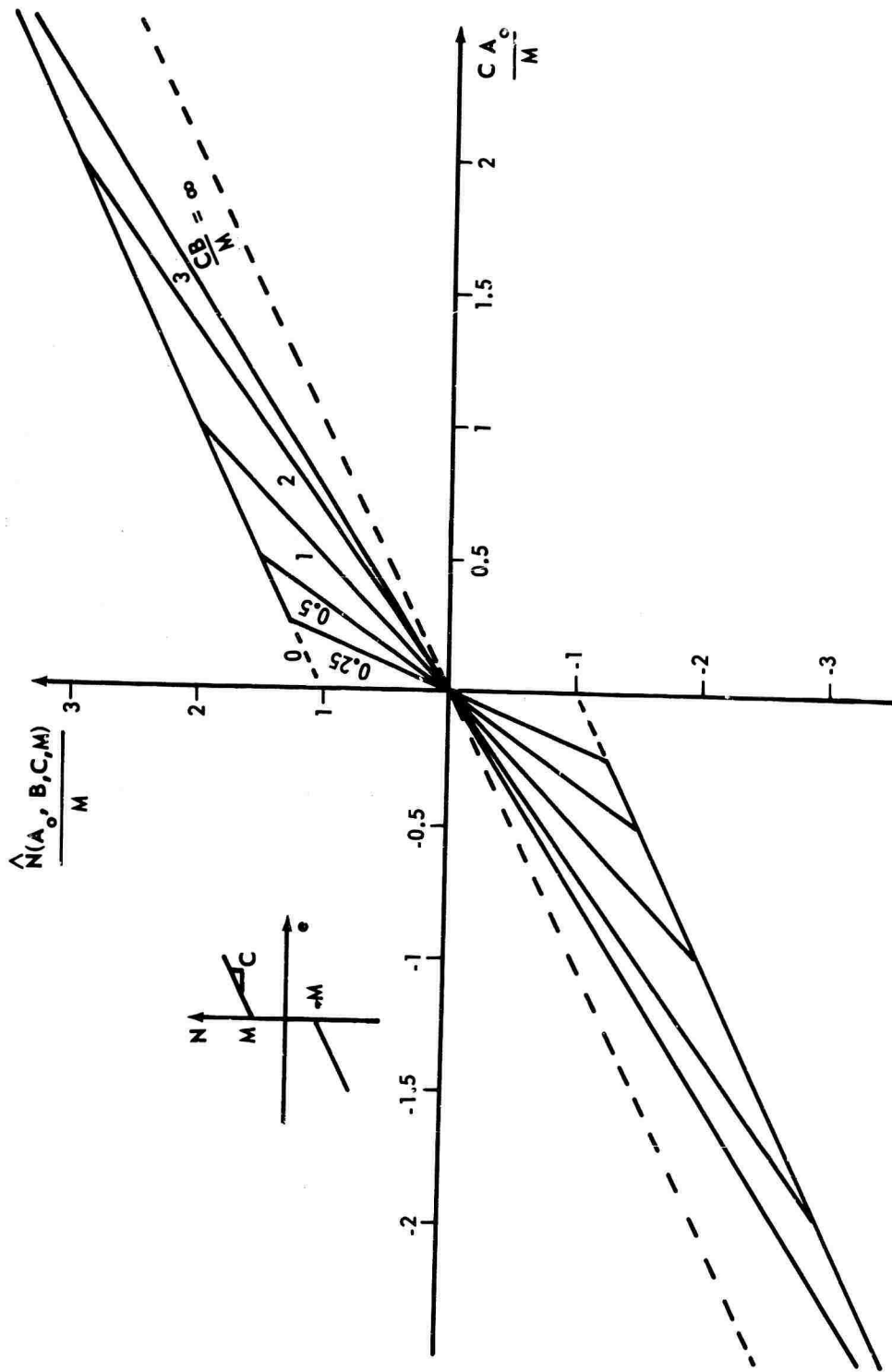


Figure 4.18. Modified Nonlinear Element for Preload, Triangle Wave Secondary Signal

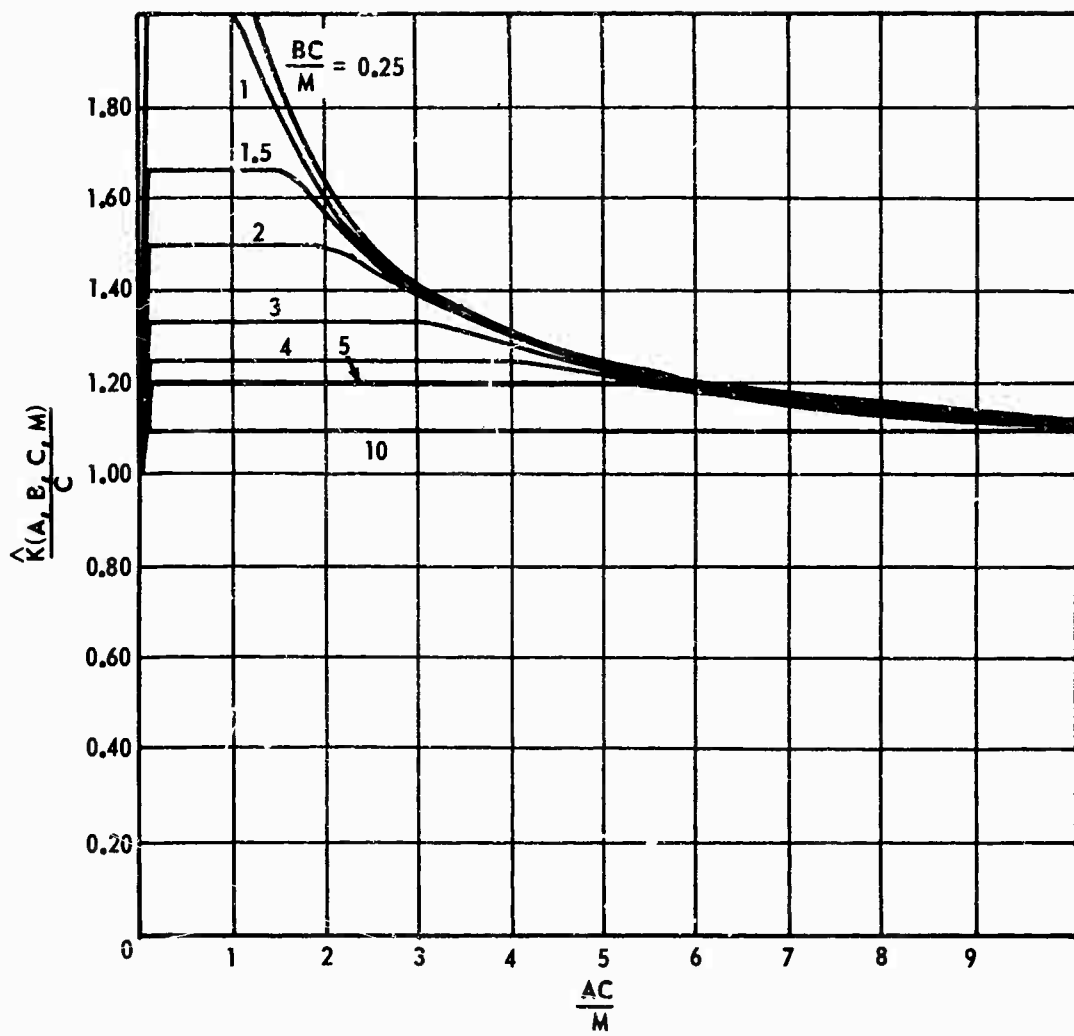


Figure 4.19. DIDF for Preload, Triangle Wave Secondary Signal

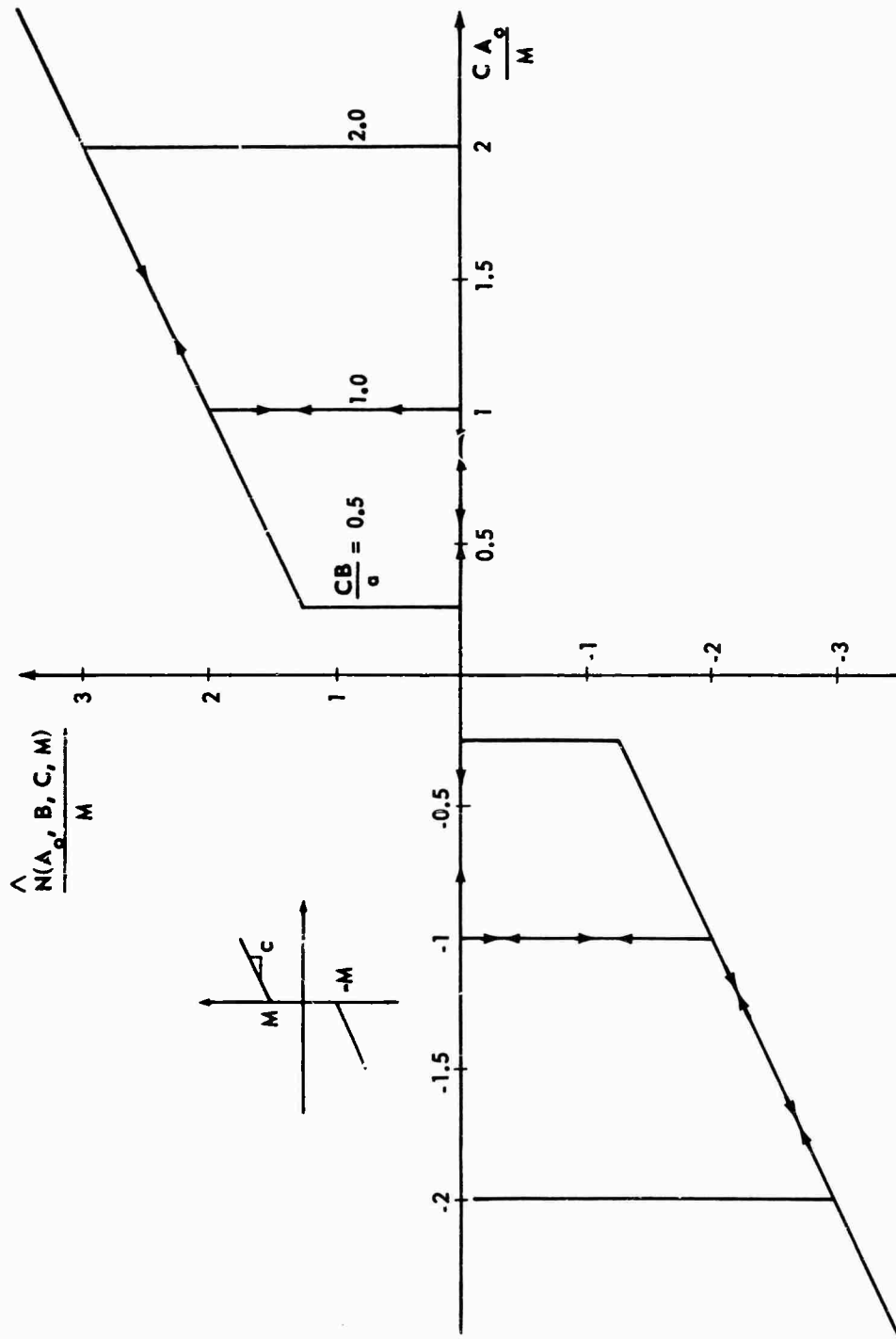


Figure 4.20. Modified Nonlinear Element for Preload, Square Wave Secondary Signal

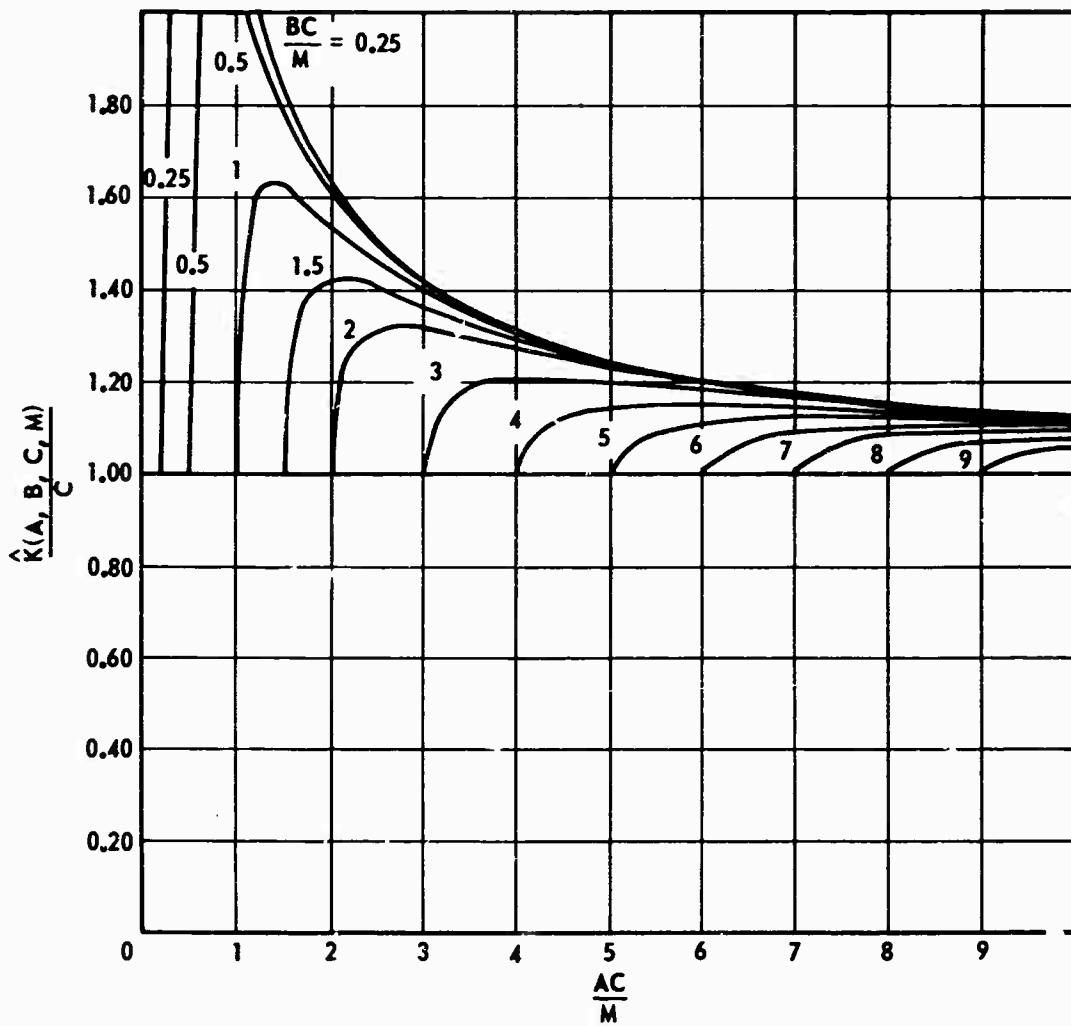


Figure 4. 21. DIF for Preload, Square Wave Secondary Signal

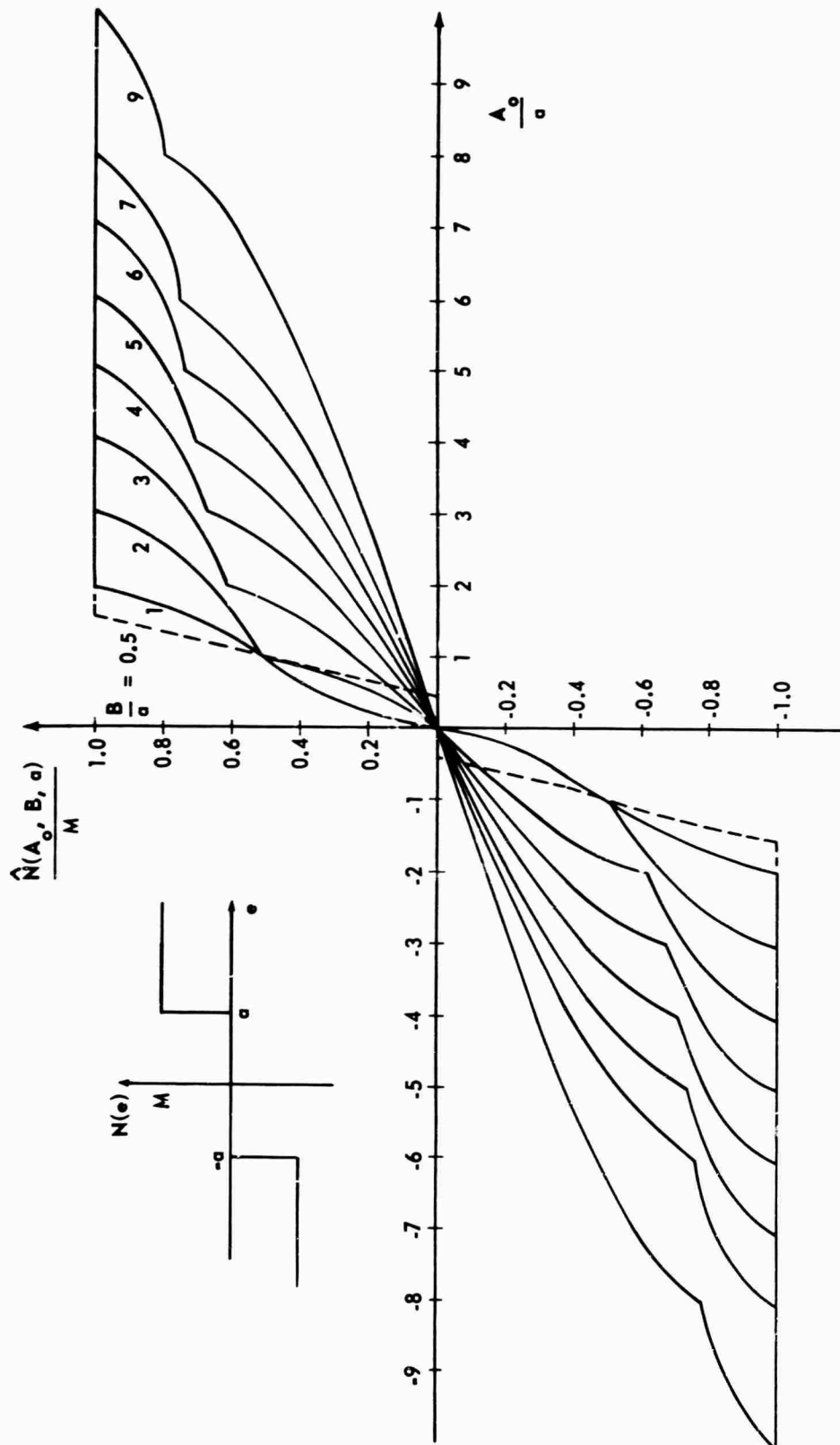


Figure 4.22. Modified Nonlinear Element for Relay with Dead Band, Sine Wave Secondary Signal

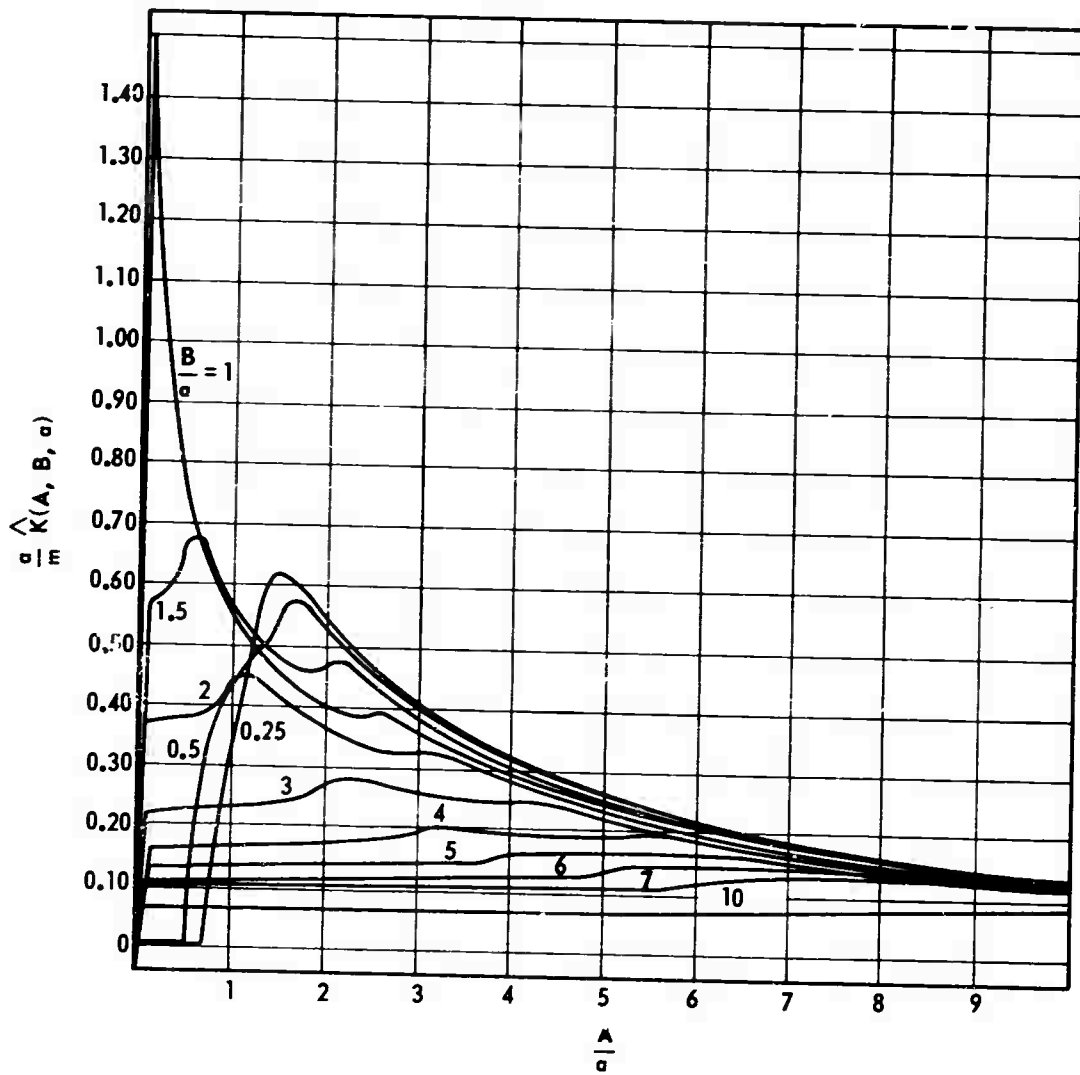


Figure 4.23. DIDF for Relay with Dead Band, Sine Wave Secondary Signal

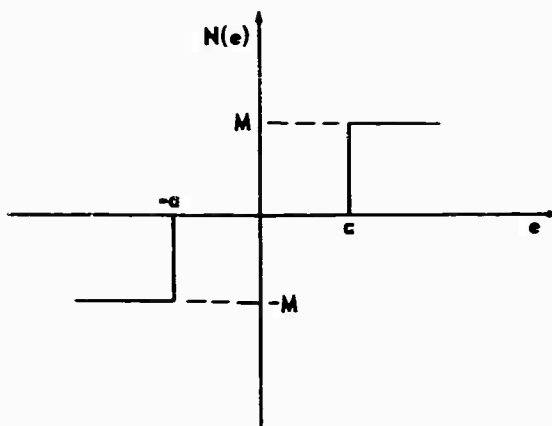


Figure 4.24. Relay with Dead Band

Case a

$$A + B < a$$

$$K(A, B, a) = 0$$

Case b

$$(A - B)^2 < a^2$$

$$(A + B)^2 > a^2 ,$$

$$\hat{K}(A, B, a) = \frac{4M}{\pi^2} \frac{1}{A} \sqrt{\frac{B}{A}} \left\{ 2E - F + \frac{2A^2 - a^2}{2AB} \left[\left(\frac{\alpha^2}{\alpha_1^2} - 1 \right) \Pi(\alpha^2, k) + F \right] \right\} ;$$

$$A \neq B , \quad (4.31)^3$$

where

$$\alpha_1^2 = \frac{1 + \frac{A^2 + B^2 - a^2}{2AB}}{1 - \frac{A}{B} \left(\frac{a^2 - A^2 - B^2}{2A^2 - a^2} \right)} \quad (4.32)$$

${}^3\Pi(\alpha^2, k)$ is the complete elliptic integral of the third kind and may be found in terms of F and F times the Jacobian zeta function $Z(\beta, k)$. The product $FZ(\beta, k)$ is also a tabulated function [30].

$$\alpha^2 = \frac{(A + B)^2 - a^2}{(A + B)^2} \quad (4.33)$$

$$\hat{K}(B, B, a) = \frac{4\sqrt{2}M}{\pi^2 B} \left[E(\xi, k) - \frac{a^2}{4B^2} F(\xi, k) \right] ; \quad A = B \quad (4.34)$$

where

$$k^2 = 1 - \frac{a^2}{4B^2} \quad (4.35)$$

$$\xi = \sin^{-1} \sqrt{\frac{a^2}{4B^2 - a^2}} \quad (4.36)$$

Case c

$$(A - B)^2 > a^2$$

$$\begin{aligned} \hat{K}(A, B, a) = \frac{4M}{\pi^2 A^2} \frac{1}{\sqrt{(A + B)^2 - a^2}} & \left\{ (A^2 - B^2)F + [(A + B)^2 - a^2]E \right. \\ & \left. + (2A^2 - a^2) \left(\frac{\alpha^2}{\alpha_1^2} - 1 \right) \Pi(\alpha^2, k) \right\} \end{aligned} \quad (4.37)$$

where

$$\alpha^2 = \frac{4AB}{(A + B)^2} \quad (4.38)$$

$$\alpha_1^2 = \frac{2}{1 - \frac{A}{B} \left(\frac{a^2 - A^2 - B^2}{2A^2 - a^2} \right)} \quad (4.39)$$

Triangle Wave Secondary Signal (Figures 4.25 and 4.26)

$$\hat{N}(A_o, B, a) = \frac{M}{2} \left[\text{sat} \left(\frac{a + A_o}{B} \right) - \text{sat} \left(\frac{a - A_o}{B} \right) \right] \quad (4.40)$$

$$\begin{aligned} \hat{K}(A, B, a) = \frac{M}{B\pi} & \left[\gamma_3 - \gamma_2 - \sin \gamma_3 \cos \gamma_3 + \sin \gamma_2 \cos \gamma_2 \right. \\ & \left. + \frac{2(a - B)}{A} (\cos \gamma_3 - \cos \gamma_2) + \frac{4B}{A} \cos \gamma_3 \right] \end{aligned} \quad (4.41)$$

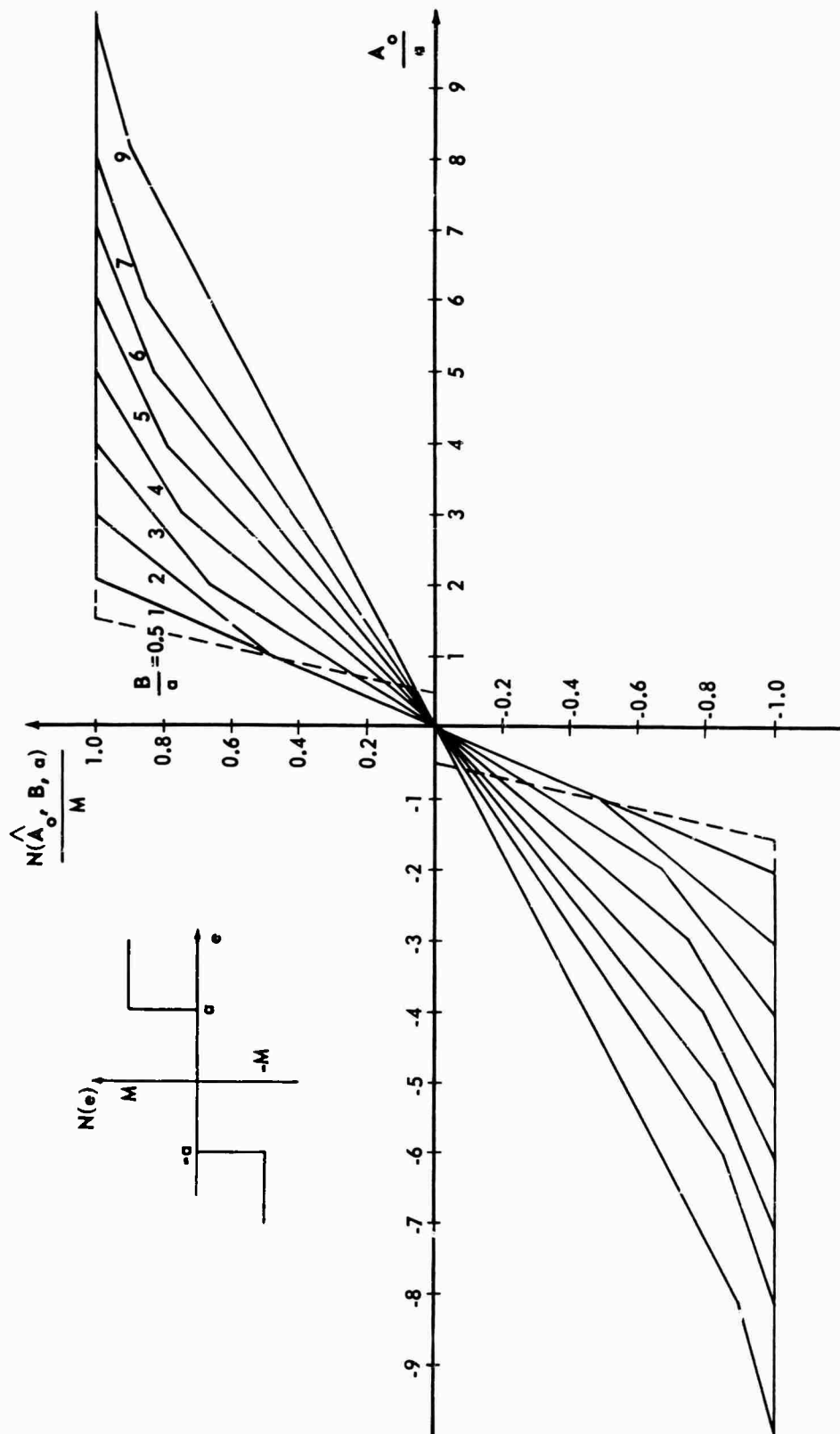


Figure 4.25. Modified Nonlinear Element for Relay with Dead Band, Triangle Wave Secondary Signal

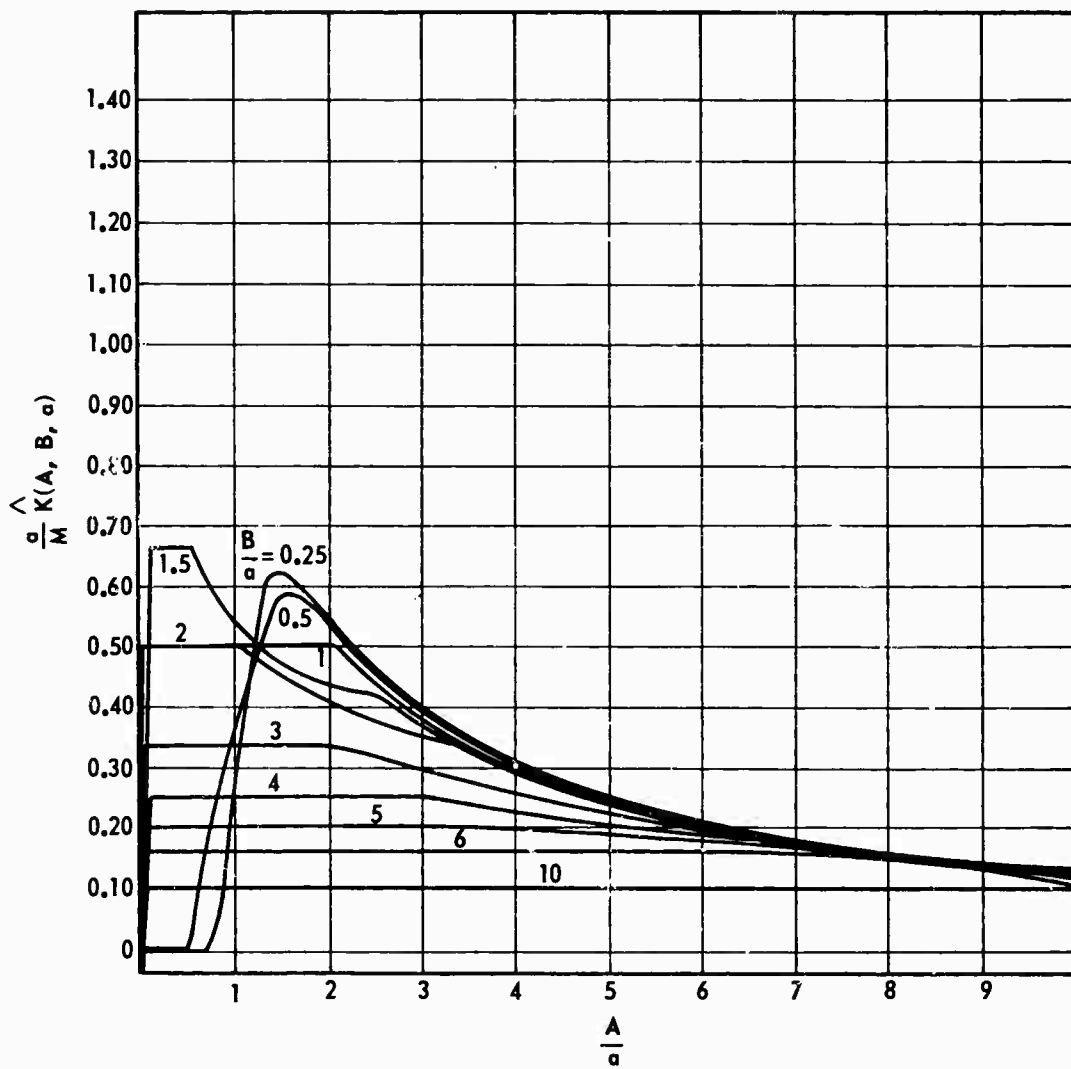


Figure 4.26. DIDF for Relay with Dead Band, Triangle Wave Secondary Signal

Square Wave Secondary Signal (Figures 4.28 and 4.29)

$$\hat{N}(A_o, B, a) = \frac{M}{4} \left[\text{sgn}(A_o + b) + \text{sgn}(A_o - b) + \text{sgn}(A_o + c) + \text{sgn}(A_o - c) \right] \quad (4.42)$$

$$\hat{K}(A, B, a) = \frac{2M}{\pi A} (\cos \gamma_2 + \cos \gamma_3) \quad (4.43)$$

4.5 Dead Band

$$N(e) = C[e - a \text{ sat}(e/a)] \quad (4.44)$$

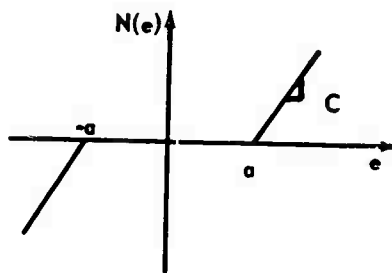


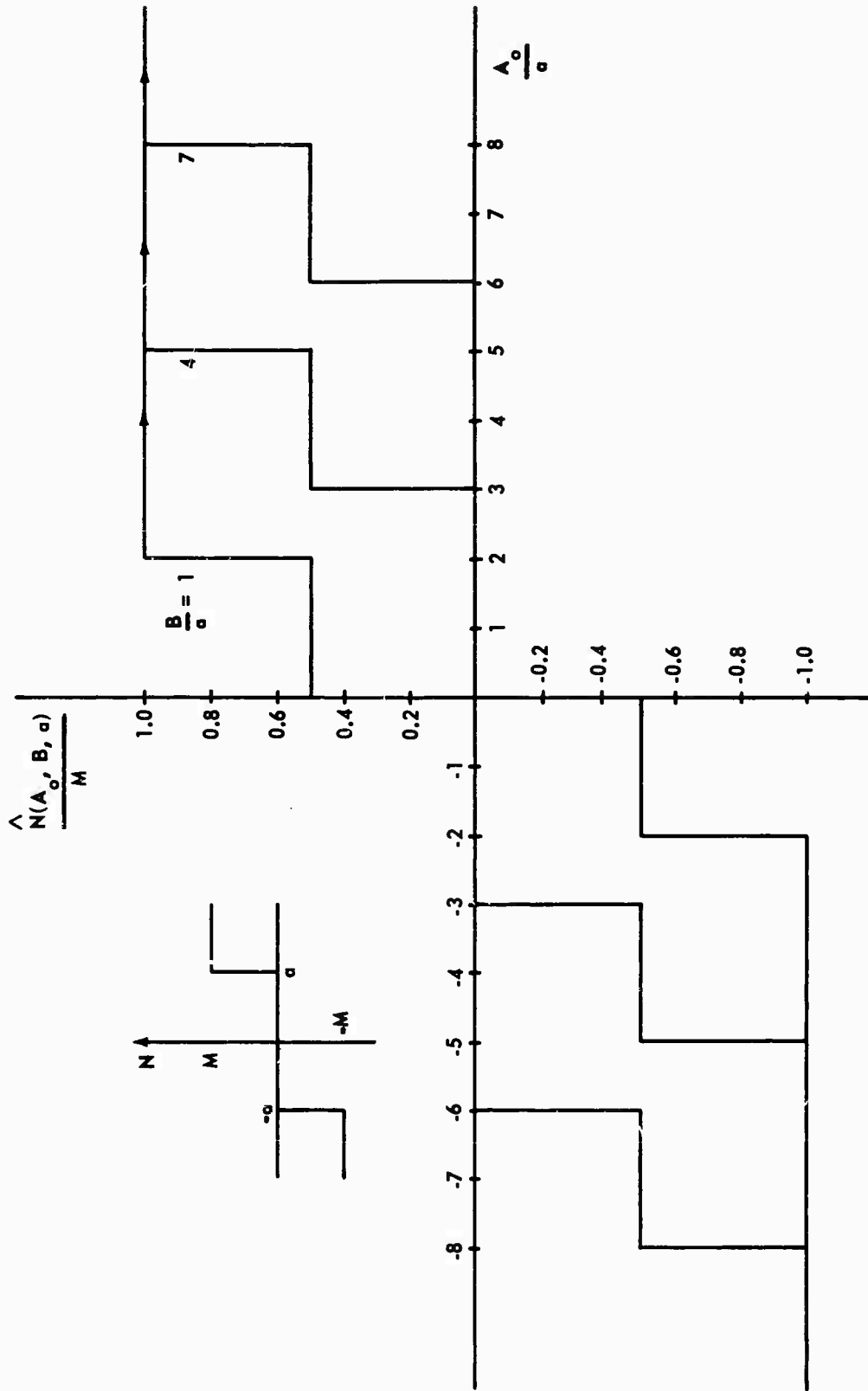
Figure 4.27. Dead Band

Sine Wave Secondary Signal (Figures 4.30 and 4.31)

$$\hat{N}(A_o, B, a) = CA_o - \frac{C}{\pi} [(\theta_2 + \theta_3)A_o + B(\cos \theta_3 - \cos \theta_2) + a(\theta_3 - \theta_2)] \quad (4.45)$$

The following approximate solution is derived by trapezoidal integration of the second integral in the average DIDF method as explained in Chapter II.

$$\frac{1}{C} \hat{K}(A, B, a) = \frac{1}{\pi} \left(\phi_s + \frac{B}{A} \sin \phi_s \right) + \frac{\phi_s}{\pi^2 n} \left(g_o + g_n + 2 \sum_{i=1}^{n-1} g_i \right) \quad (4.46)$$



85 Figure 4.28. Modified Nonlinear Element for Relay with Dead Band, Square Wave Secondary Signal

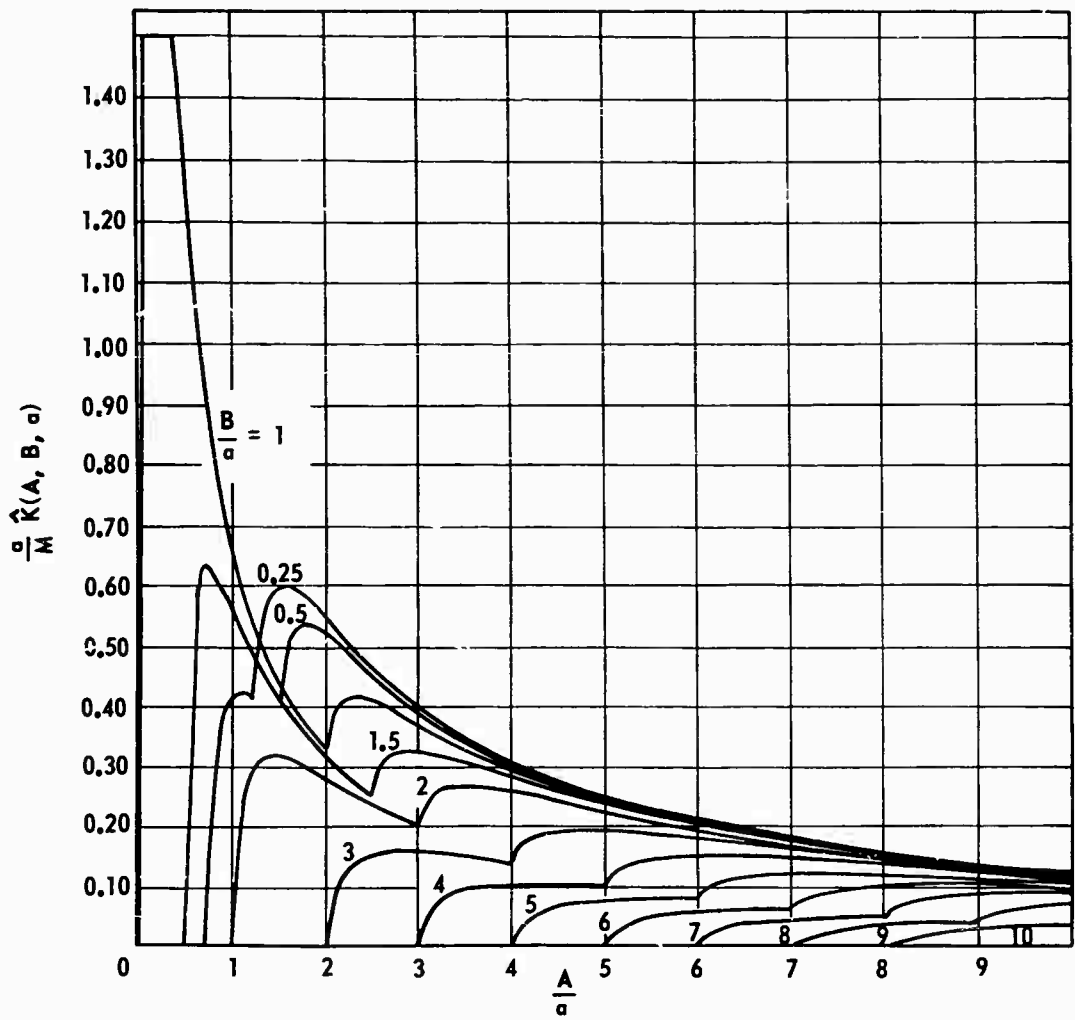


Figure 4.29. DIDF for Relay with Dead Band, Square Wave Secondary Signal

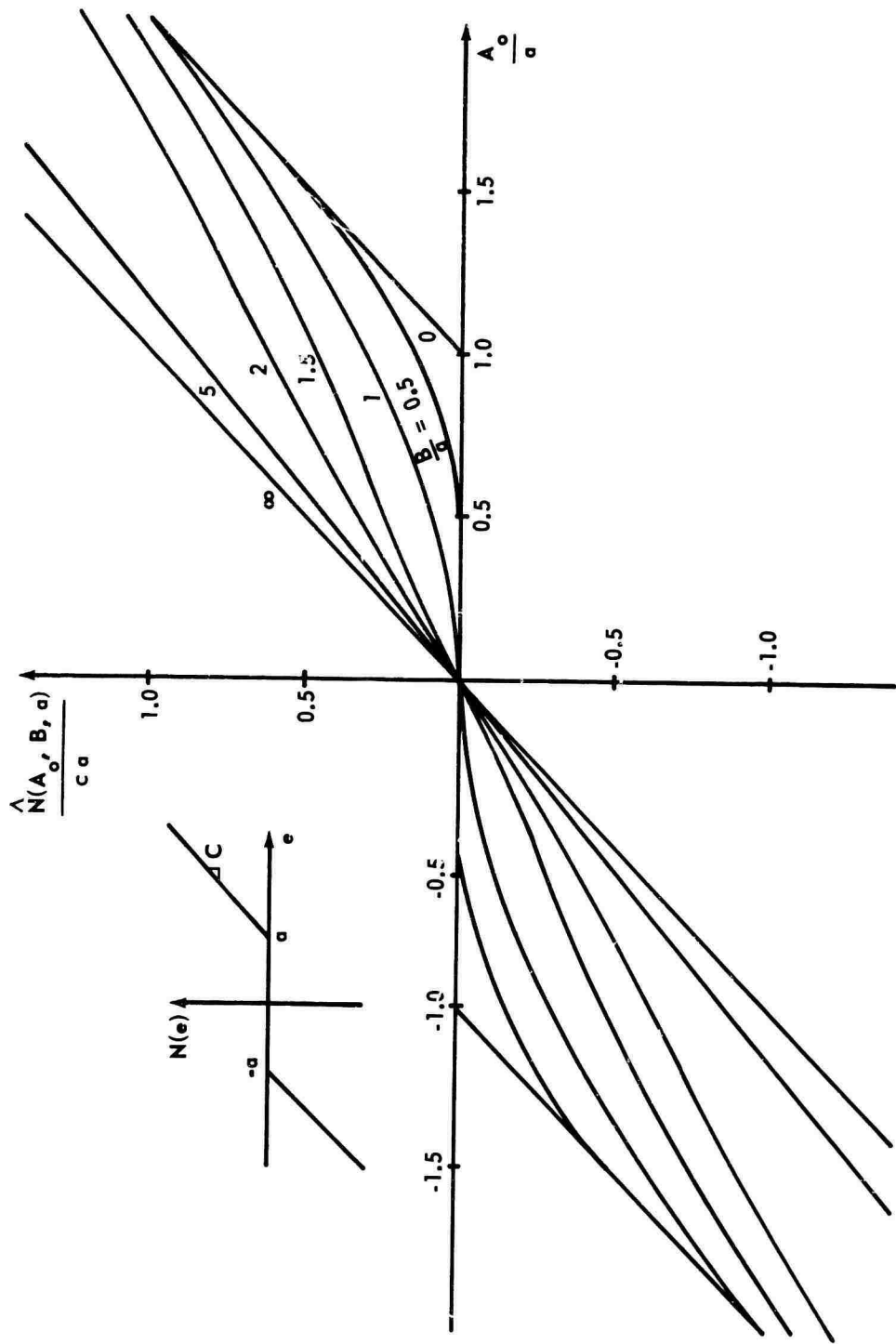


Figure 4.30. Modified Nonlinear Element for Dead Band, Sine Wave Secondary Signal

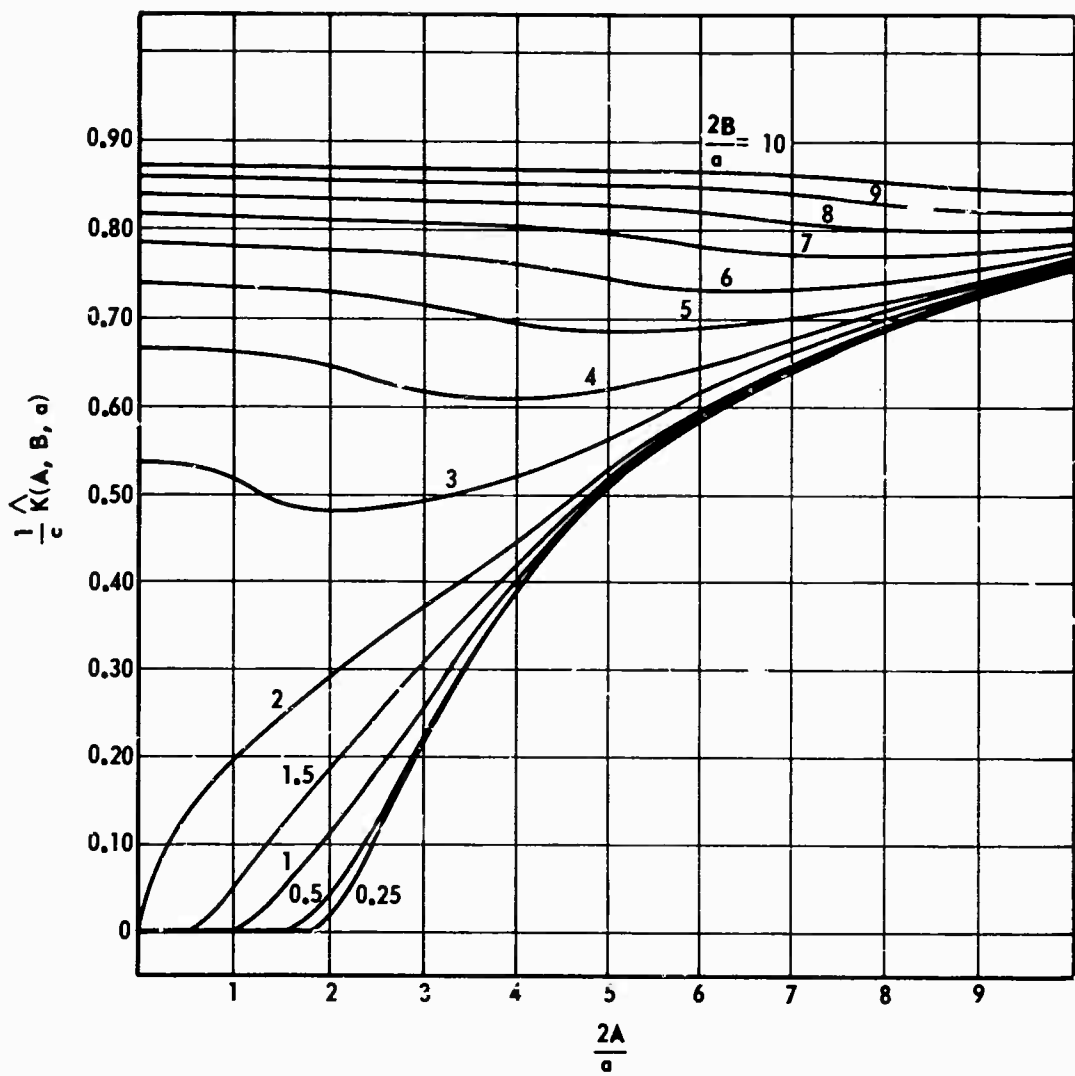


Figure 4.31. DIDF for Dead Band, Sine Wave Secondary Signal

where

$$g_i = \left(1 + \frac{B}{A} \cos \phi_i\right) \left[-\sin^{-1} \text{sat} \left(\frac{a}{D_i} \right) + \left(\text{sat} \frac{a}{D_i} - \frac{2a}{D_i} \right) \sqrt{1 - \text{sat} \left(\frac{a}{D_i} \right)^2} \right] \quad (4.47)$$

and

$$D_i \triangleq \sqrt{A^2 + B^2 + 2AB \cos \phi_i} \quad (4.48)$$

$$\phi_s = \cos^{-1} \text{sat} \left(\frac{a^2 - A^2 - B^2}{2AB} \right) \quad (4.49)$$

$$\phi_i = \frac{i}{n} \phi_s = \frac{i}{n} \cos^{-1} \text{sat} \left(\frac{a^2 - A^2 - B^2}{2AB} \right) \quad (4.50)$$

$$n = \text{integer} \geq 2 \quad (4.51)$$

The accuracy is increased as n is allowed to become larger.

Triangle Wave Secondary Signal (Figures 4.32 and 4.33)

$$\hat{N}(A_o, B, a) = \frac{C}{\pi} \left[\frac{B}{\pi} (\theta_{3T}^2 - \theta_{2T}^2) + A_o (\pi - \theta_{2T} - \theta_{3T}) + a (\theta_{2T} - \theta_{3T}) \right] \quad (4.52)$$

$$\hat{N}(A_o, B, a) = CA_o \left(1 + \frac{a}{B} \right) ; \quad B > A_o + a \quad (4.53)$$

$$\begin{aligned} \hat{K}(A, B, a) = & \frac{C}{\pi} \frac{B}{A} \left\{ \left[\left(1 - \frac{a}{B} \right)^2 + \left(\frac{A}{B} \right)^2 \right] (\cos \gamma_2 - \cos \gamma_3) \right. \\ & + \sin \gamma_3 \cos \gamma_3 \left(\frac{A}{B} + \frac{aA}{B^2} \right) + \sin \gamma_2 \cos \gamma_2 \left(\frac{A}{B} - \frac{aA}{B^2} \right) \\ & - \frac{4a}{B} \cos \gamma_3 - \gamma_3 \left(\frac{A}{B} + \frac{aA}{B^2} \right) - \gamma_2 \left(\frac{A}{B} - \frac{aA}{B^2} \right) \\ & \left. + \frac{1}{3} \left(\frac{A}{B} \right)^2 (\cos^3 \gamma_3 - \cos^3 \gamma_2) + \frac{A}{B} \pi \right\} \quad (4.54) \end{aligned}$$

$$\hat{K}(A, B, a) = C \left(1 + \frac{a}{B} \right) ; \quad B > A + a \quad (4.55)$$

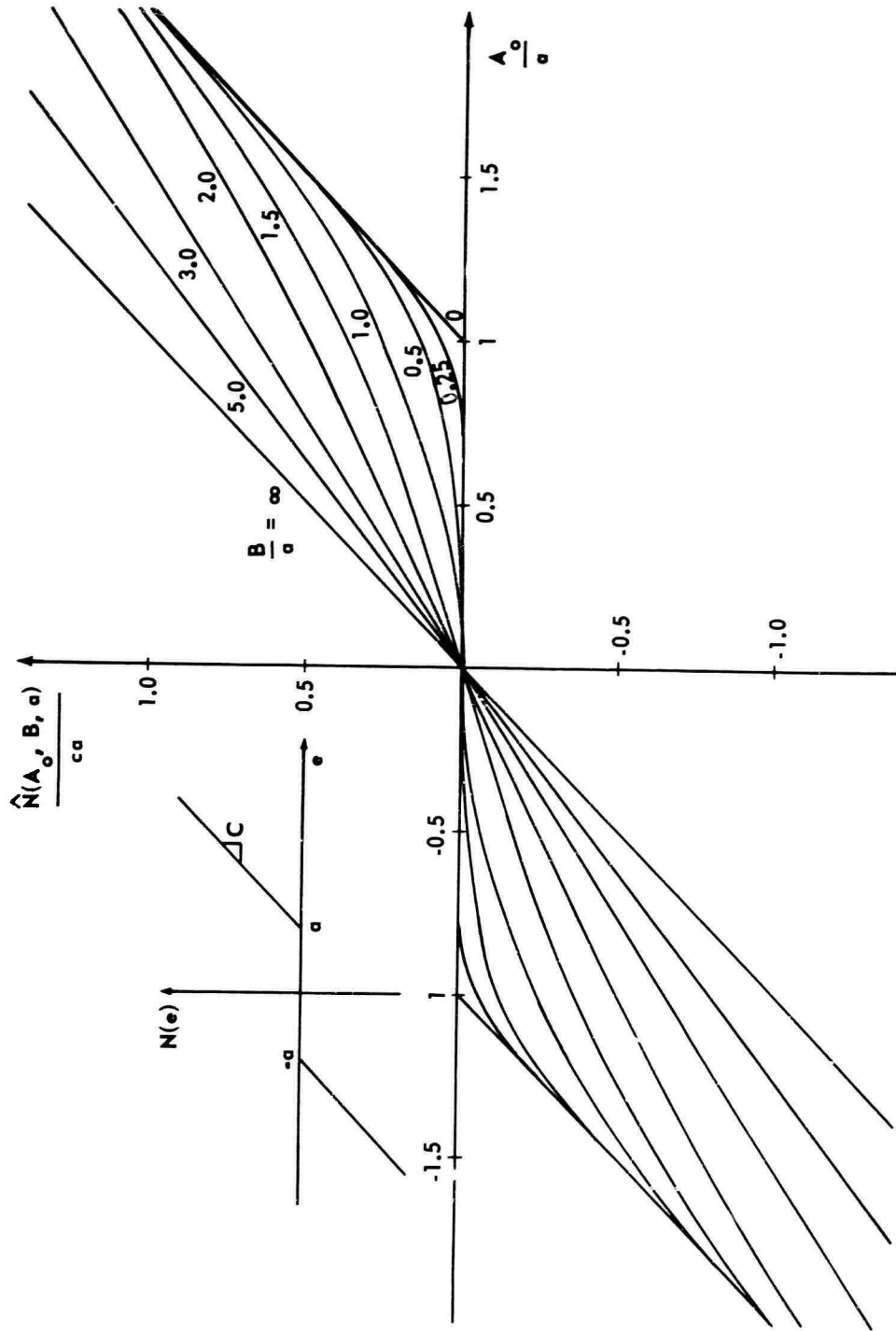


Figure 4.32. Modified Nonlinear Element for Dead Band, Triangle Wave Secondary Signal

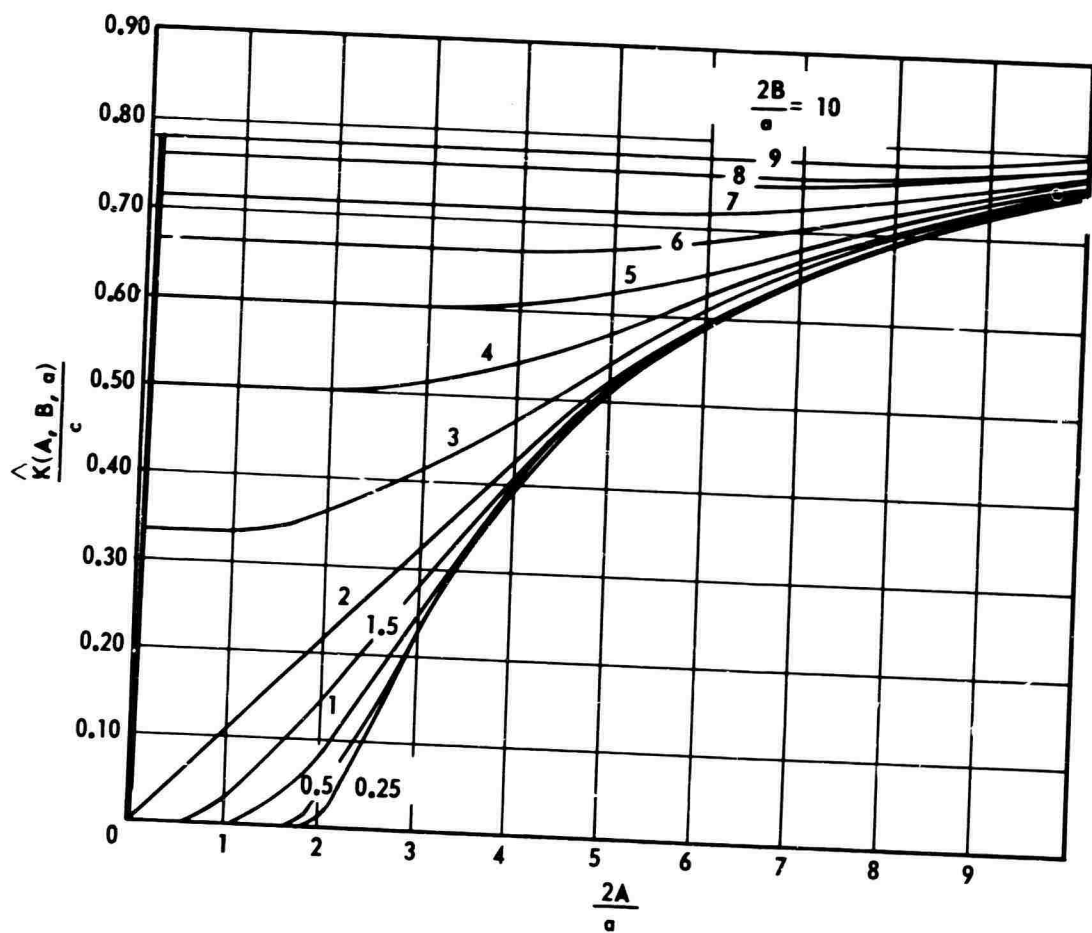


Figure 4.33. DIDF for Dead Band, Triangle Wave Secondary Signal

Square Wave Secondary Signal (Figures 4.35 and 4.36)

$$\begin{aligned} \hat{N}(A_o, B, a) = C & \left\{ A_o - \frac{B}{4} \left[2 + \operatorname{sgn}(a - B - A_o) - \operatorname{sgn}(a + B - A_o) \right] \right. \\ & + \frac{a - A_o}{4} \left[\operatorname{sgn}(a - B - A_o) + \operatorname{sgn}(a + B - A_o) \right] \\ & \left. + \frac{(B - a - A_o)}{4} \left[1 - \operatorname{sgn}(B - a - A_o) \right] \right\} \end{aligned} \quad (4.56)$$

$$\begin{aligned} \hat{K}(A, B, a) = \frac{C}{\pi} & \left[\pi - \gamma_3 - \gamma_2 + \sin \gamma_3 \cos \gamma_3 + \sin \gamma_2 \cos \gamma_2 \right. \\ & \left. + \frac{2B}{A} (\cos \gamma_3 - \cos \gamma_2) - \frac{2a}{A} (\cos \gamma_2 + \cos \gamma_3) \right] \end{aligned} \quad (4.57)$$

or

$$\hat{K}(A, B, a) = C ; \quad B > A + a \quad (4.58)$$

$$\hat{K}(A, B, a) = \frac{C}{2} ; \quad A < 2B, \quad B = a \quad (4.59)$$

4.6 Limiter

$$N(e) = aC \operatorname{sat} \left(\frac{e}{a} \right) \quad (4.60)$$

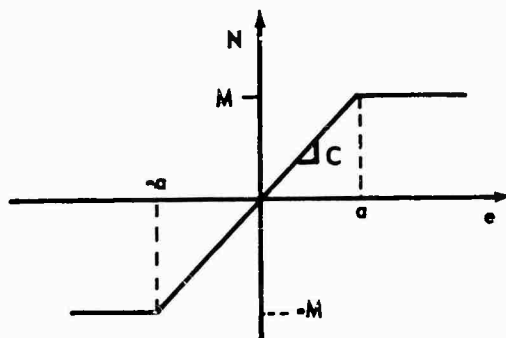


Figure 4.34. Limiter

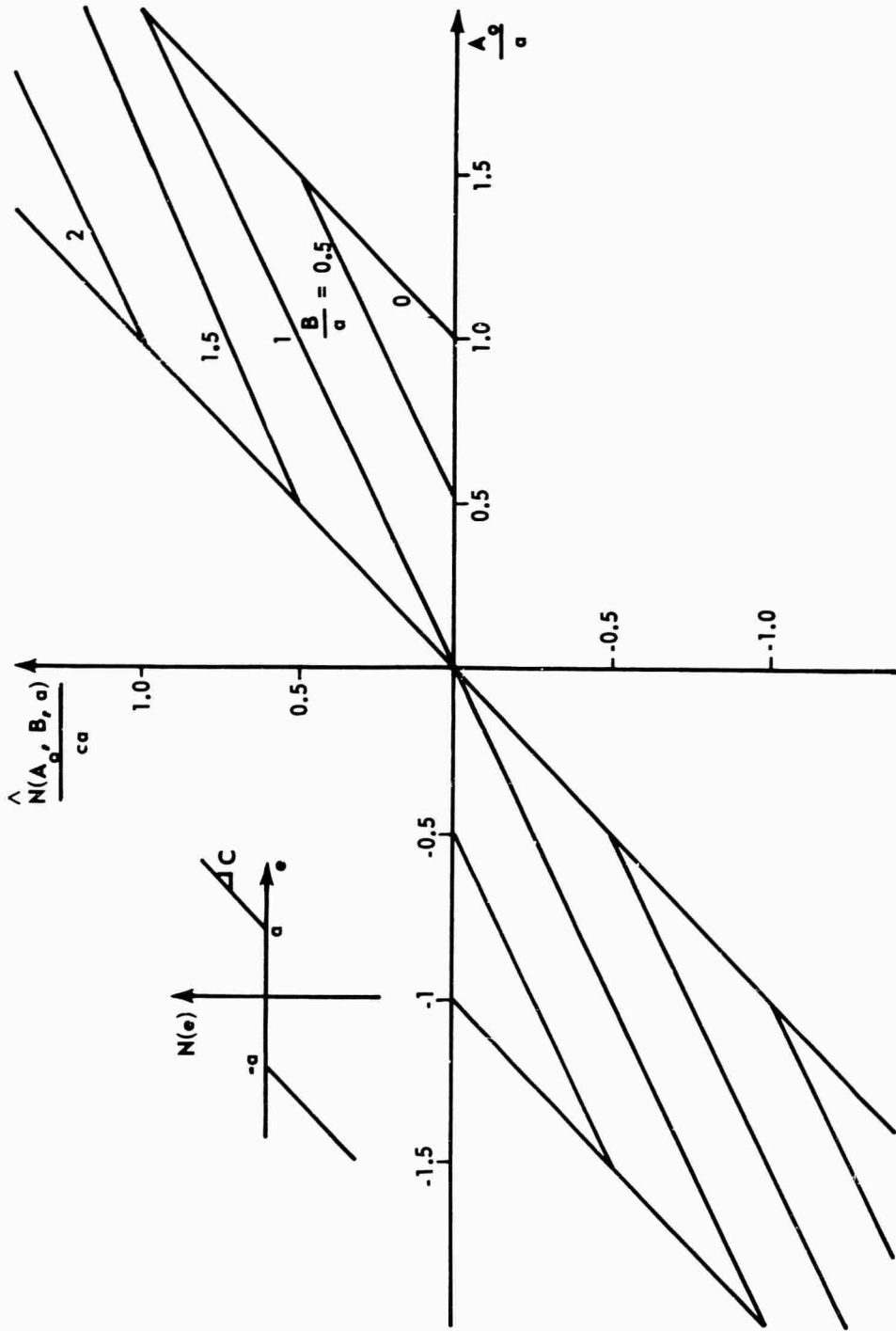


Figure 4.35. Modified Nonlinear Element for Dead Band, Square Wave Secondary Signal

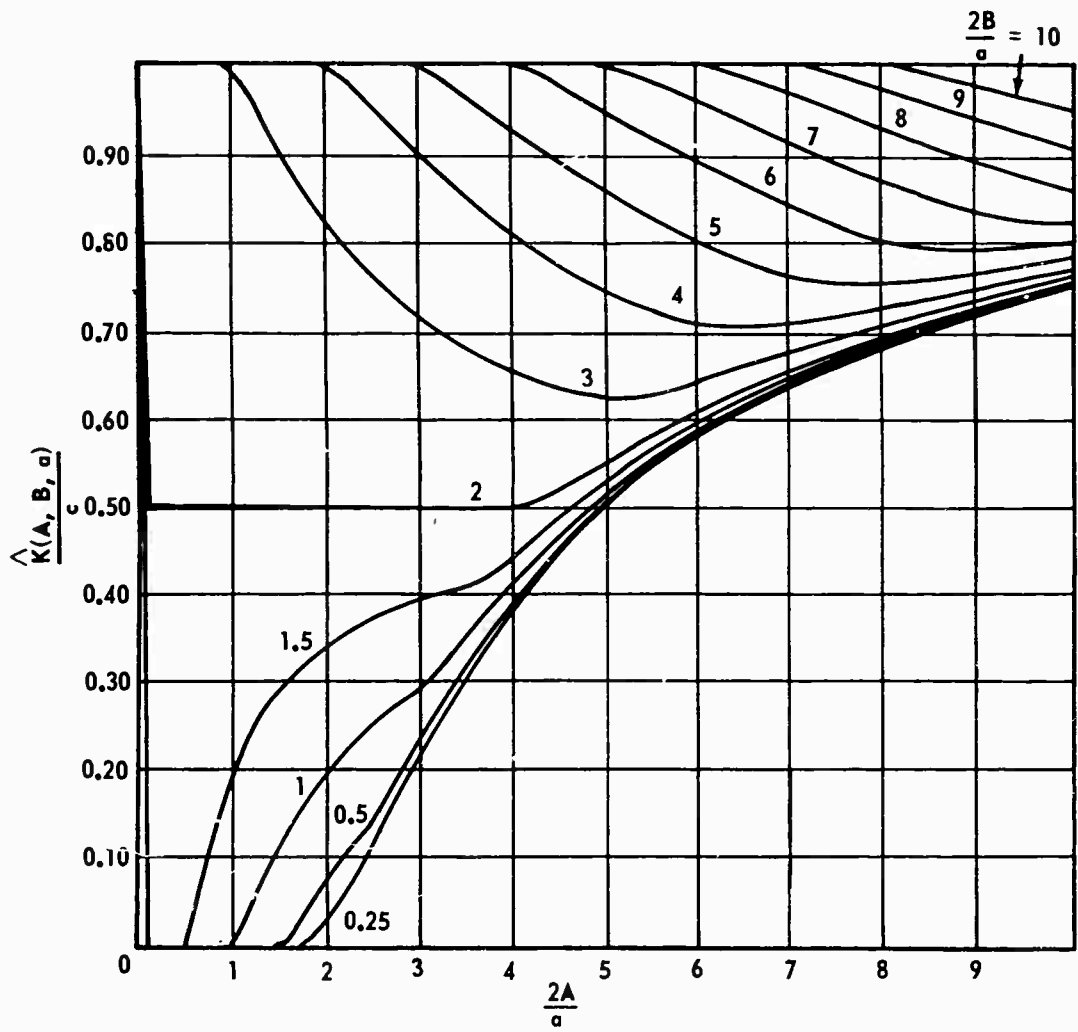


Figure 4.36. DIDF for Dead Band, Square Wave Secondary Signal

Sine Wave Secondary Signal (Figures 4.37 and 4.38)

$$\hat{N}(A_o, B, a) = \frac{C}{\pi} \left[(\theta_{2T} + \theta_{3T}) A_o + B (\cos \theta_{3T} - \cos \theta_{2T}) + a (\theta_{3T} - \theta_{2T}) \right] \quad (4.61)$$

$$\frac{\hat{K}(A, B, a)}{C} = 1 - \frac{1}{\pi} \left(\phi_s + \frac{B}{A} \sin \phi_s \right) - \frac{\phi_s}{\pi^2 n} \left(g_o + g_n + 2 \sum_{i=1}^{n-1} g_i \right) \quad (4.62)$$

where

$$g_i = \left(1 + \frac{B}{A} \cos \phi_i \right) \left[-\sin^{-1} \text{sat} \left(\frac{a}{D_i} \right) + \left(\text{sat} \frac{a}{D_i} - \frac{2a}{D_i} \right) \sqrt{1 - \text{sat} \left(\frac{a}{D_i} \right)^2} \right] \quad (4.47)$$

$$D_i = \sqrt{A^2 + B^2 + 2AB \cos \phi_i} \quad (4.63)$$

$$\phi_s = \cos^{-1} \text{sat} \left(\frac{a^2 - A^2 - B^2}{2AB} \right) \quad (4.64)$$

$$\phi_i = \frac{i}{n} \phi_s \quad (4.65)$$

$$n = \text{integer} \geq 2 \quad (4.66)$$

Triangle Wave Secondary Signal (Figures 4.39 and 4.40)

$$\hat{N}(A_o, B, a) = \frac{C}{\pi} \left[\frac{B}{\pi} (\theta_{2T}^2 - \theta_{3T}^2) + A_o (\theta_{2T} + \theta_{3T}) + a (\theta_{3T} - \theta_{2T}) \right] \quad (4.67)$$

$$\begin{aligned} \hat{K}(A, B, a) = \frac{C}{\pi} \frac{B}{A} \left\{ \left[\left(1 - \frac{a}{B} \right)^2 + \left(\frac{A}{B} \right)^2 \right] (\cos \gamma_3 - \cos \gamma_2) \right. \\ - \sin \gamma_3 \cos \gamma_3 \left(\frac{A}{B} + \frac{aA}{B^2} \right) + \sin \gamma_2 \cos \gamma_2 \left(\frac{aA}{B^2} - \frac{A}{B} \right) \\ + \frac{4a}{B} \cos \gamma_3 + \gamma_3 \left(\frac{A}{B} + \frac{aA}{B^2} \right) + \gamma_2 \left(\frac{A}{B} - \frac{aA}{B^2} \right) \\ \left. + \frac{1}{3} \left(\frac{A}{B} \right)^2 (\cos \gamma_3 - \cos^3 \gamma_3) \right\} \quad (4.68) \end{aligned}$$

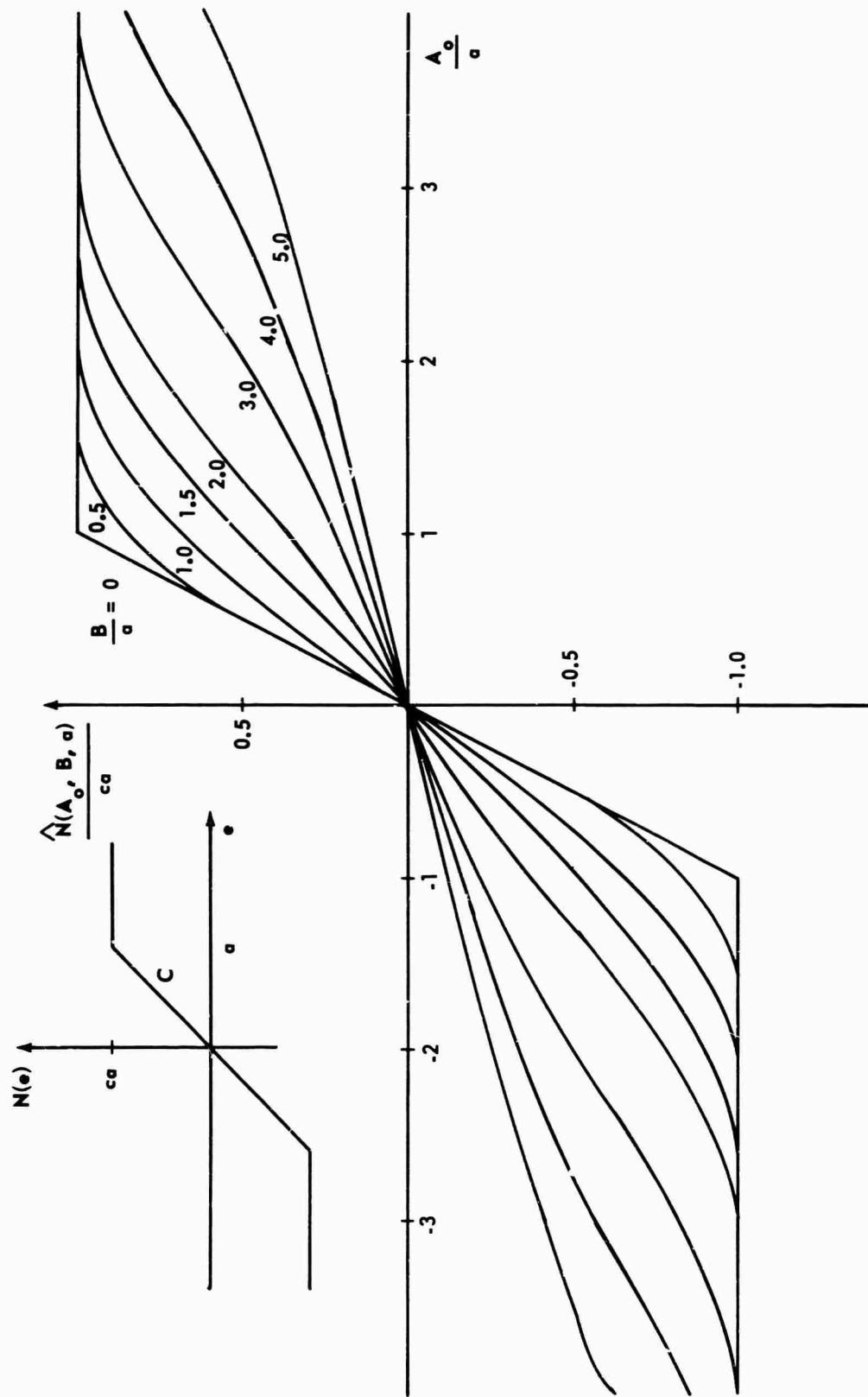


Figure 4.37. Modified Nonlinear Element for Limiter, Sine Wave Secondary Signal

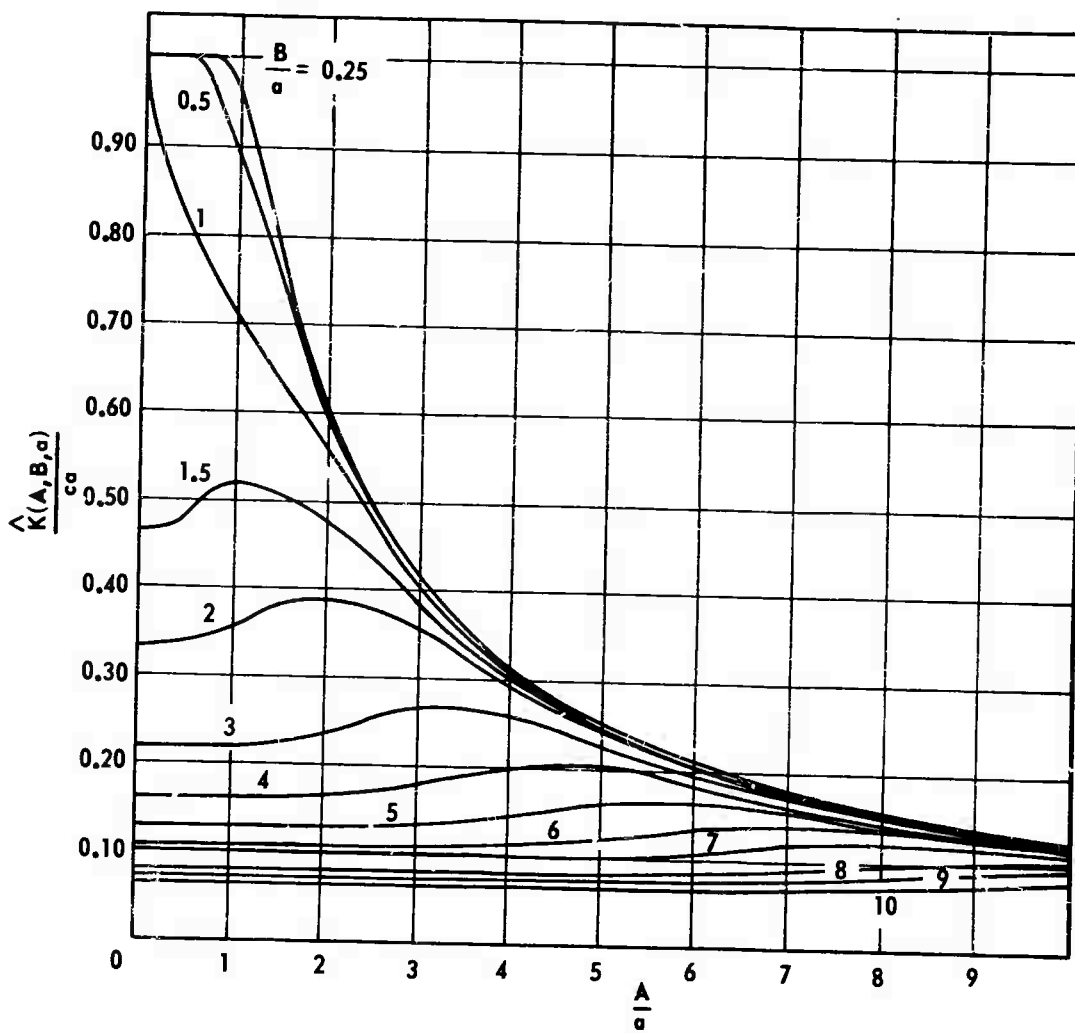


Figure 4.38. DIDF for Limiter, Sine Wave Secondary Signal

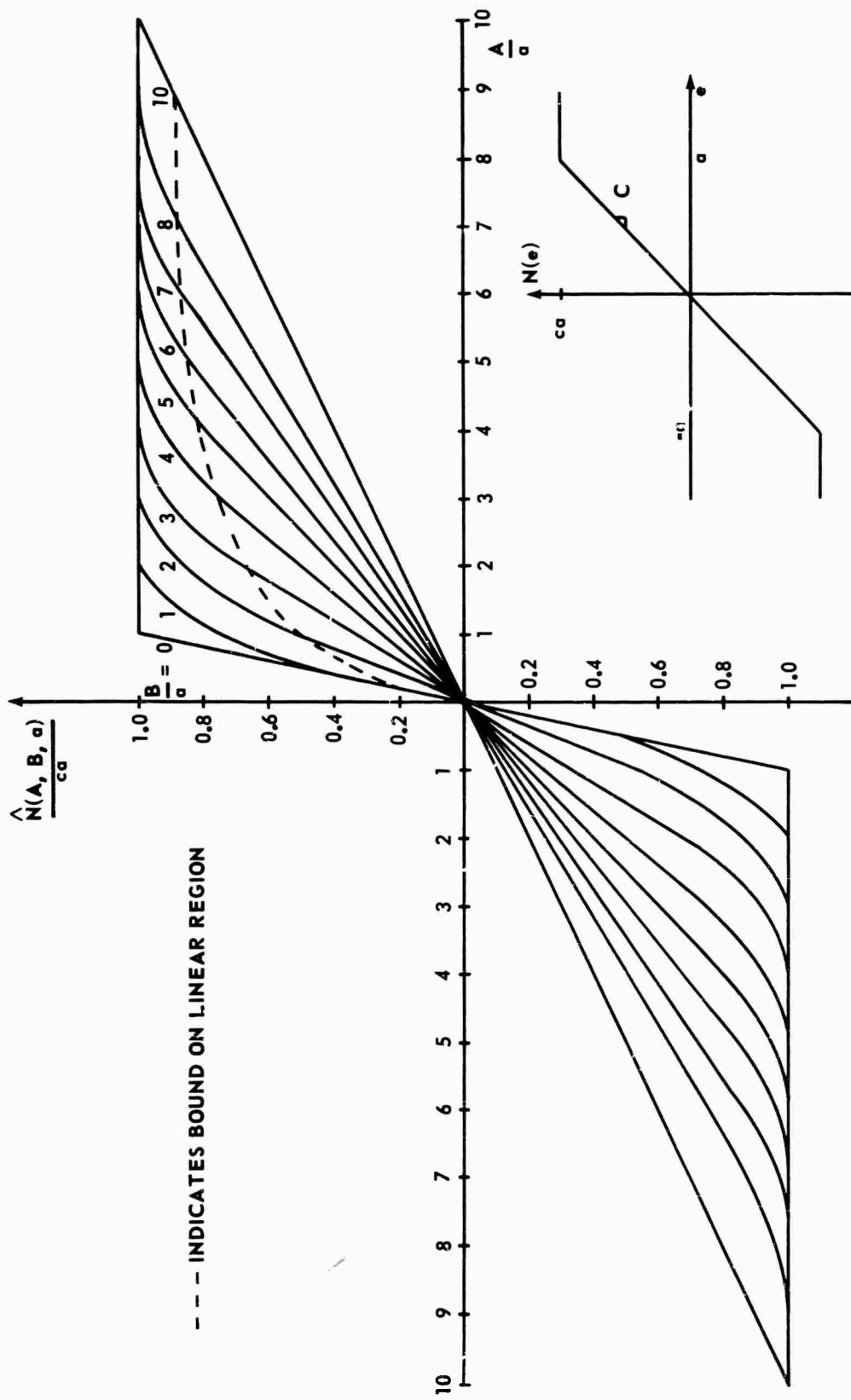


Figure 4.39. Modified Nonlinear Element for Limiter, Triangle Wave Secondary Signal

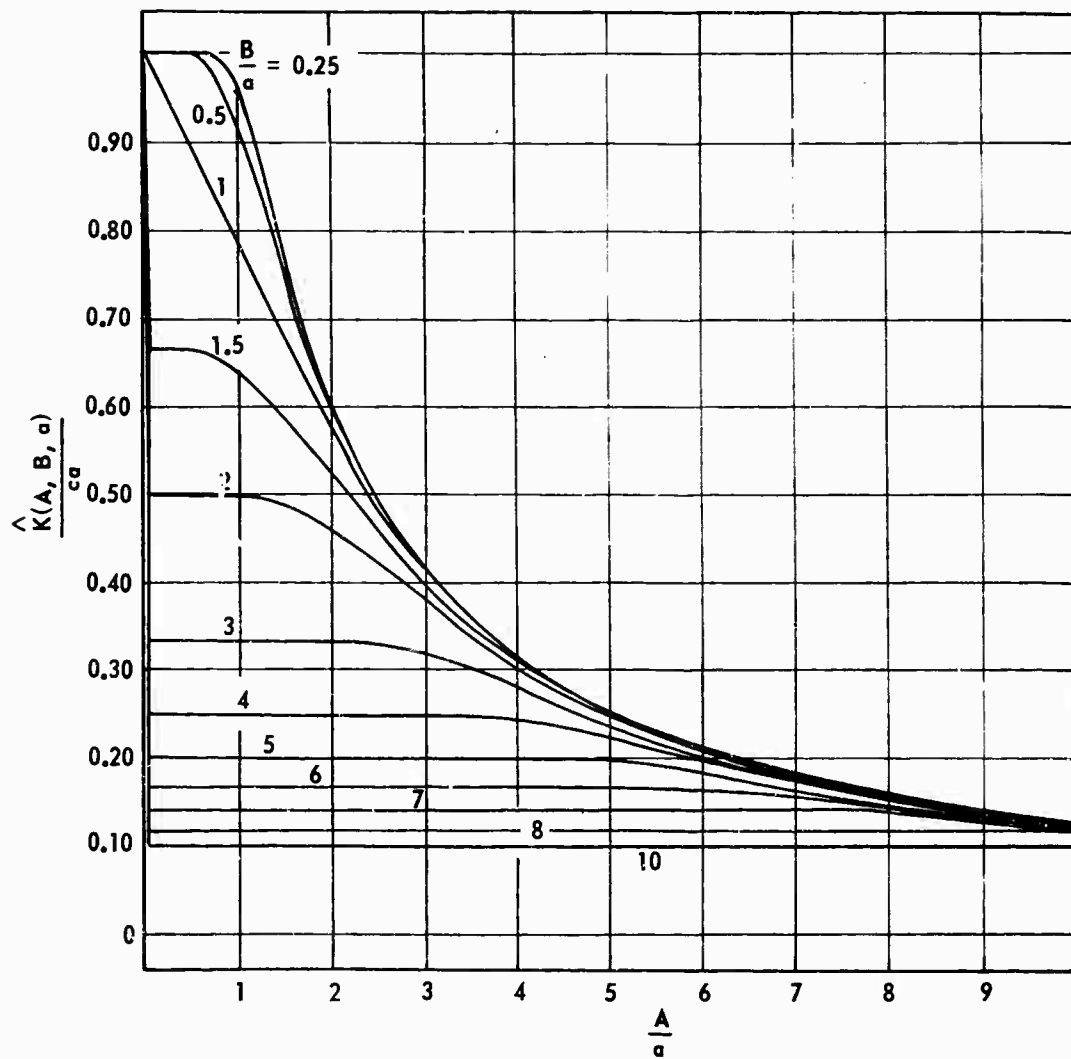


Figure 4.40. DIDF for Limiter, Triangle Wave Secondary Signal

Square Wave Secondary Signal (Figures 4.42 and 4.43)

$$\hat{N}(A_0, B, a) = \frac{C}{4} \left\{ B \left[2 + \operatorname{sgn}(a - B - A_0) - \operatorname{sgn}(a + B - A_0) \right] \right. \\ \left. + (A_0 - a) \left[\operatorname{sgn}(a - B - A_0) + \operatorname{sgn}(a + B - A_0) \right] \right. \\ \left. + (A_0 + a - B) \left[1 - \operatorname{sgn}(B - a - A_0) \right] \right\} \quad (4.69)$$

$$\hat{K}(A, B, a) = \frac{C}{\pi} \left[\gamma_3 + \gamma_2 - \sin \gamma_3 \cos \gamma_2 - \sin \gamma_2 \cos \gamma_3 \right. \\ \left. + \frac{2B}{A} (\cos \gamma_3 - \cos \gamma_2) + \frac{2a}{A} (\cos \gamma_3 + \cos \gamma_2) \right] \quad (4.70)$$

4.7 Limiter with Dead Band

$$N(e) = C \left[b \operatorname{sat} \left(\frac{e}{b} \right) - a \operatorname{sat} \left(\frac{e}{a} \right) \right] \quad (4.71)$$

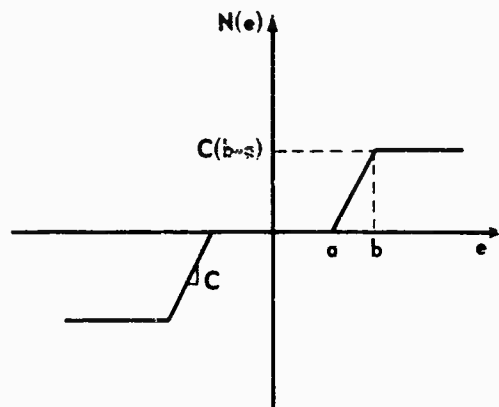


Figure 4.41. Saturation with Dead Band

Sine Wave Secondary Signal (Figures 4.44 and 4.45)

$$\hat{N}(A_0, B, a, b) = \frac{C}{\pi} \left[(\theta_4 + \theta_5 - \theta_2 - \theta_3) A_0 \right. \\ \left. + B(\cos \theta_5 - \cos \theta_4 - \cos \theta_3 + \cos \theta_2) \right. \\ \left. + b(\theta_5 - \theta_4) - a(\theta_3 - \theta_2) \right] \quad (4.72)$$

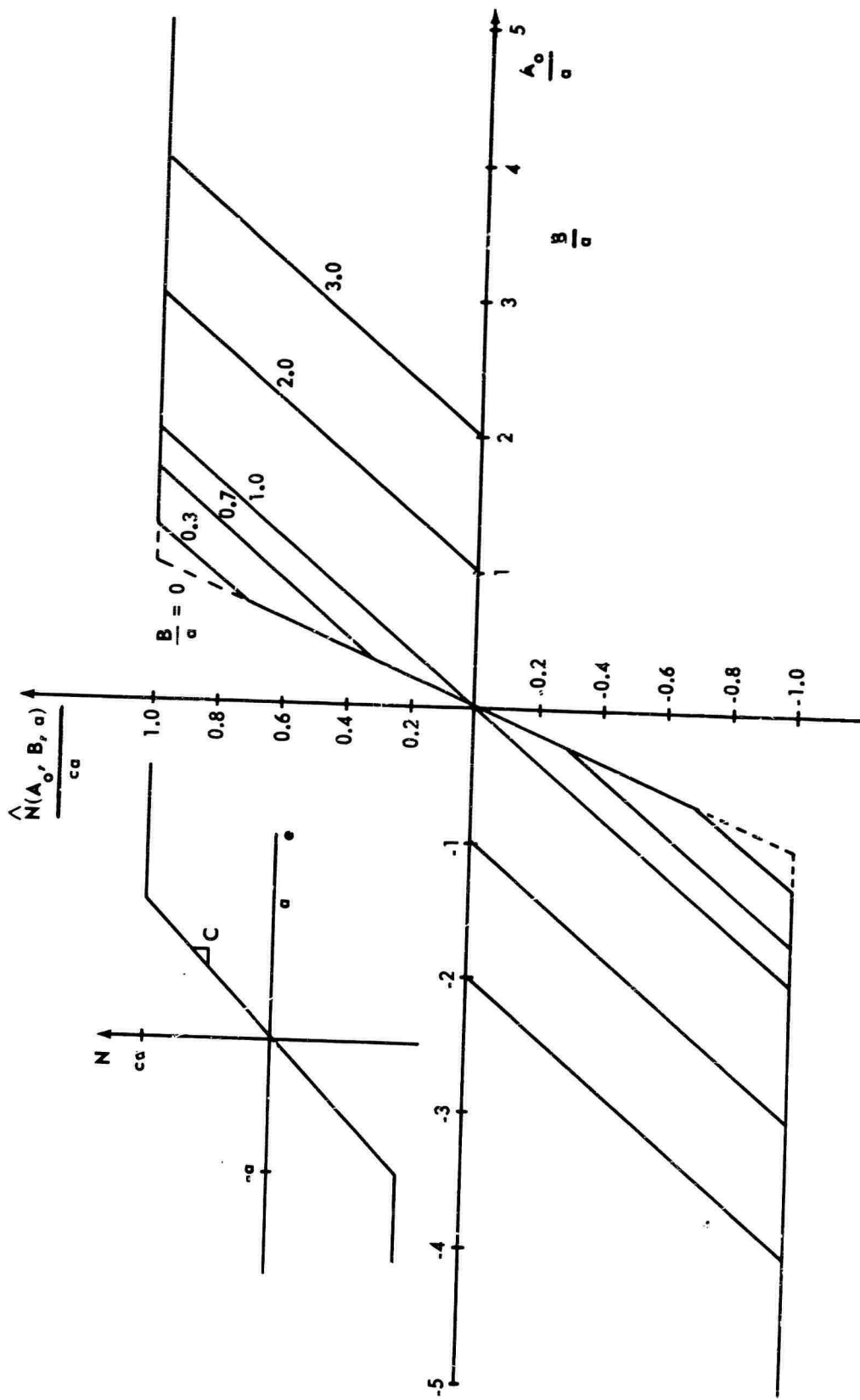


Figure 4.42. Modified Nonlinear Element for Limiter, Square Wave Secondary Signal

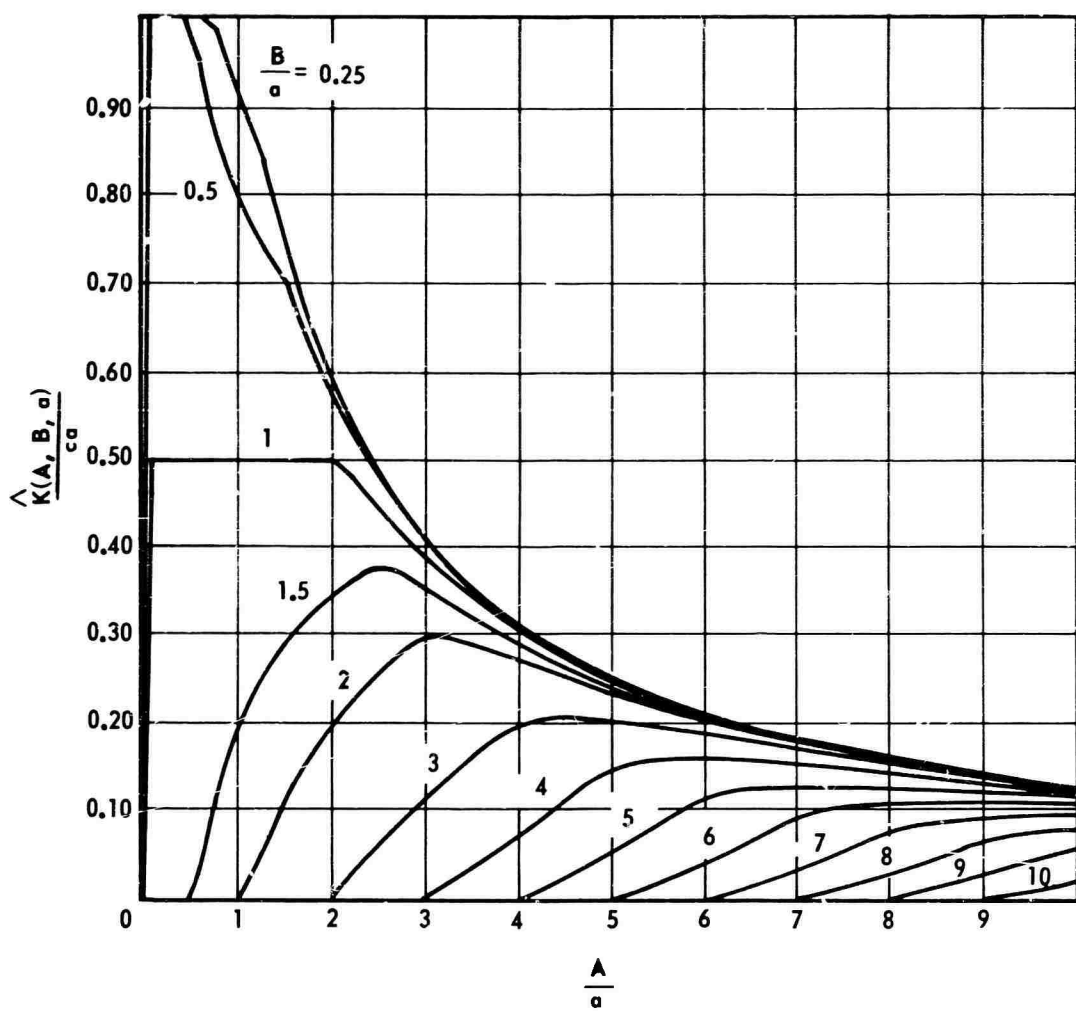


Figure 4.43. DIDF for Limiter, Square Wave Secondary Signal

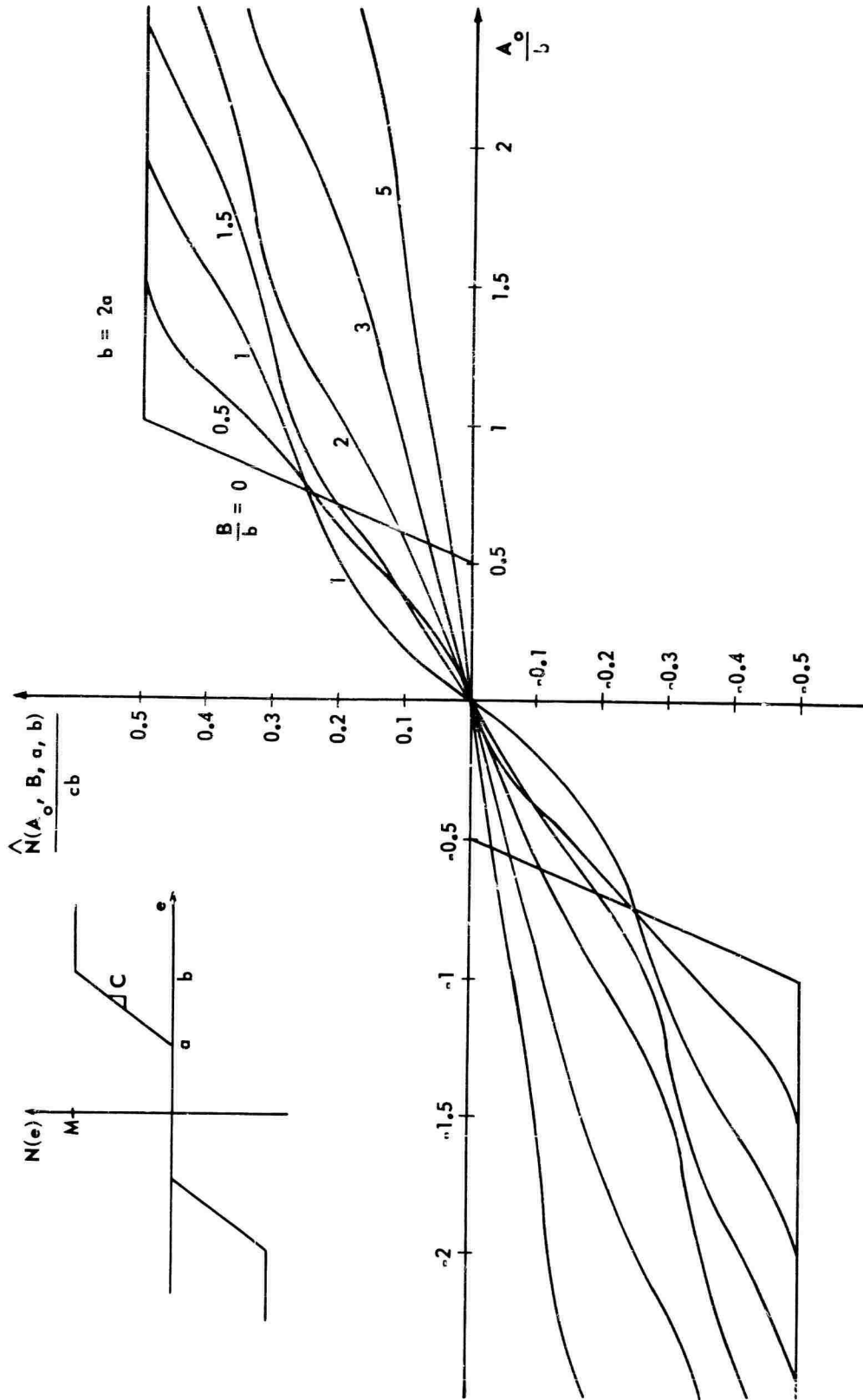


Figure 4.44. Modified Nonlinear Element for Limiter with Dead Band, Sine Wave Secondary Signal

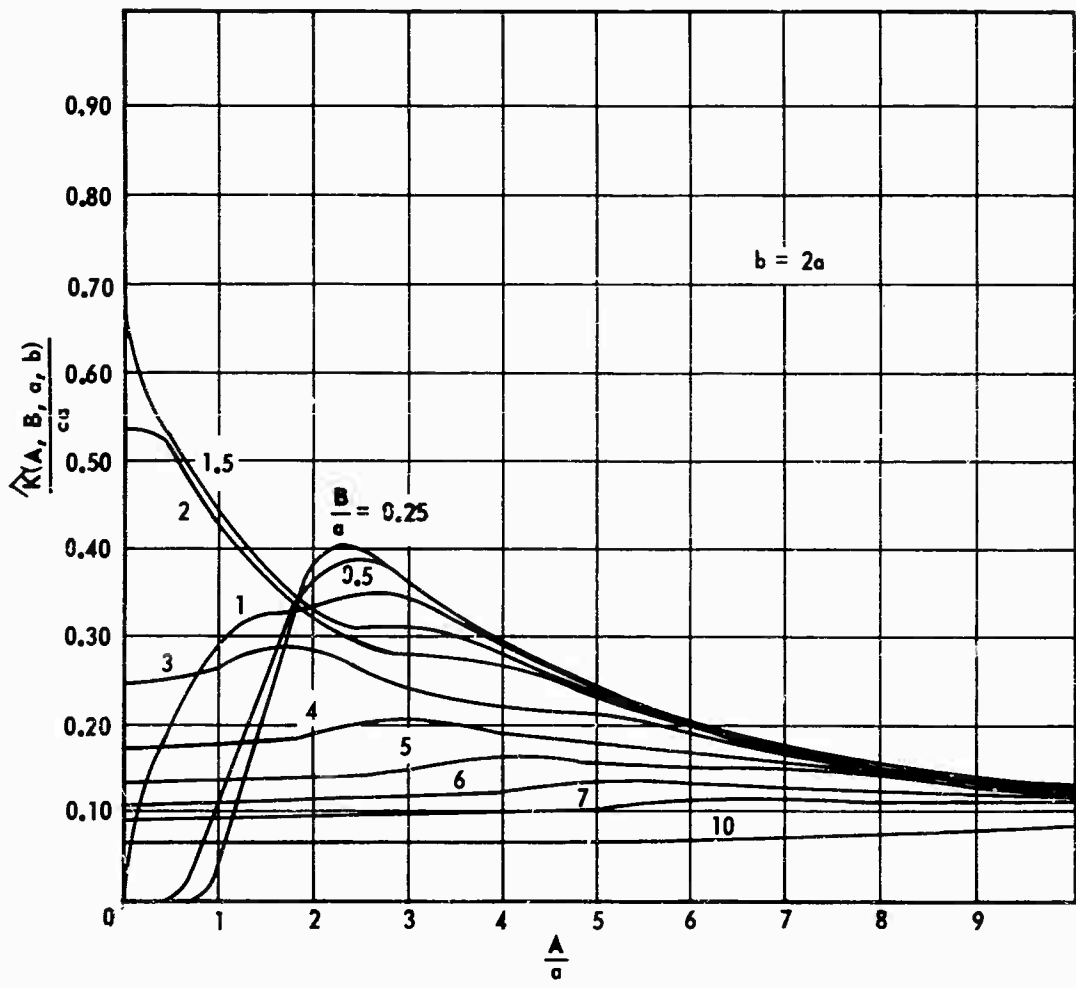


Figure 4.45. DIDF for Limiter with Dead Band, Sine Wave Secondary Signal

$$\begin{aligned} \frac{\hat{K}(A, B, a, b)}{C} &= \frac{1}{\pi} \left(\phi_{sa} - \phi_{sb} + \frac{B}{A} \sin \phi_{sa} - \frac{B}{A} \sin \phi_{sb} \right) \\ &+ \frac{\phi_{sa}}{\pi^2 n} \left(g_0 + g_n + 2 \sum_{i=1}^{n-1} g_i \right) \\ &+ \frac{\phi_{sb}}{\pi^2 n} \left(f_0 + f_n + 2 \sum_{j=1}^{n-1} f_j \right), \end{aligned} \quad (4.73)$$

where

$$\phi_{sa} = \cos^{-1} \text{sat} \frac{a^2 - A^2 - B^2}{2AB} \quad (4.74)$$

$$\phi_{sb} = \cos^{-1} \text{sat} \frac{b^2 - A^2 - B^2}{2AB} \quad (4.75)$$

$$g_i = \left(1 + \frac{B}{A} \cos \phi_{sa} \right) \left[-\sin^{-1} \text{sat} \frac{a}{D_i} + \left(\text{sat} \frac{a}{D_i} - \frac{2a}{D_i} \right) \sqrt{1 - \text{sat} \left(\frac{a}{D_i} \right)^2} \right] \quad (4.76)$$

$$f_j = \left(1 + \frac{B}{A} \cos \phi_{sb} \right) \left[-\sin^{-1} \frac{b}{D_j} + \left(\text{sat} \frac{b}{D_j} - \frac{2b}{D_j} \right) \sqrt{1 - \text{sat} \left(\frac{b}{D_j} \right)^2} \right] \quad (4.77)$$

$$D_i = \sqrt{A^2 + B^2 + 2AB \cos \phi_i} \quad (4.78)$$

$$D_j = \sqrt{A^2 + B^2 + 2AB \cos \phi_j} \quad (4.79)$$

$$n = \text{integer} \geq 2 \quad (4.80)$$

$$\phi_i = \frac{i}{n} \phi_{sa} \quad (4.81)$$

$$\phi_j = \frac{j}{n} \phi_{sb} \quad (4.82)$$

Triangle Wave Secondary Signal (Figures 4.46 and 4.47)

$$\begin{aligned} \hat{N}(A, B, a, b) &= \frac{C}{\pi} \left[\frac{B}{\pi} (\theta_{3T}^2 - \theta_{2T}^2 - \theta_{5T}^2 + \theta_{4T}^2) \right. \\ &+ A_0 (\theta_{4T} + \theta_{5T} - \theta_{2T} - \theta_{3T}) + a (\theta_{2T} - \theta_{3T}) - b (\theta_{4T} - \theta_{5T}) \left. \right] \end{aligned} \quad (4.83)$$

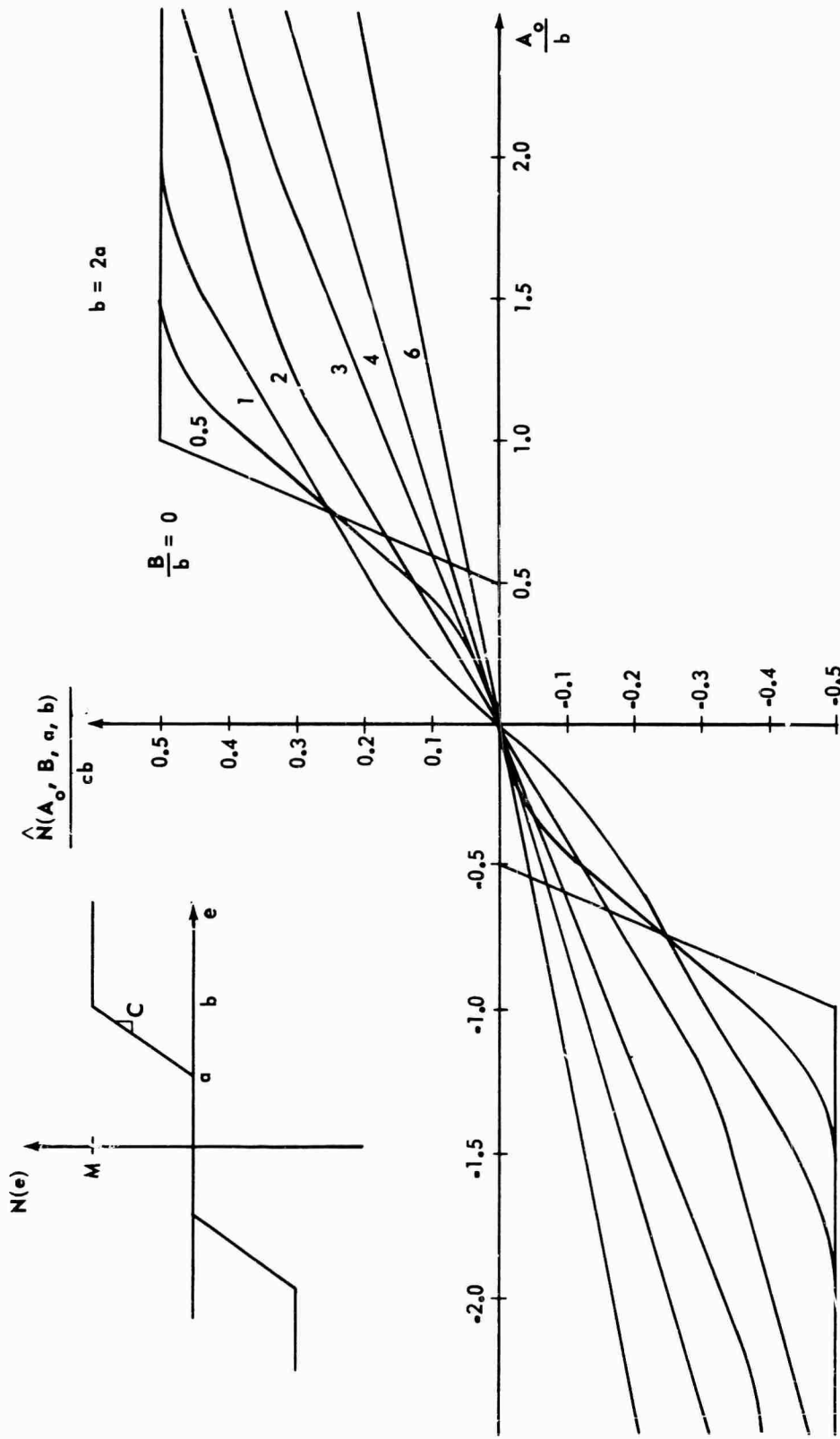


Figure 4.46. Modified Nonlinear Element for Limiter with Dead Band, Triangle Wave Secondary Signal

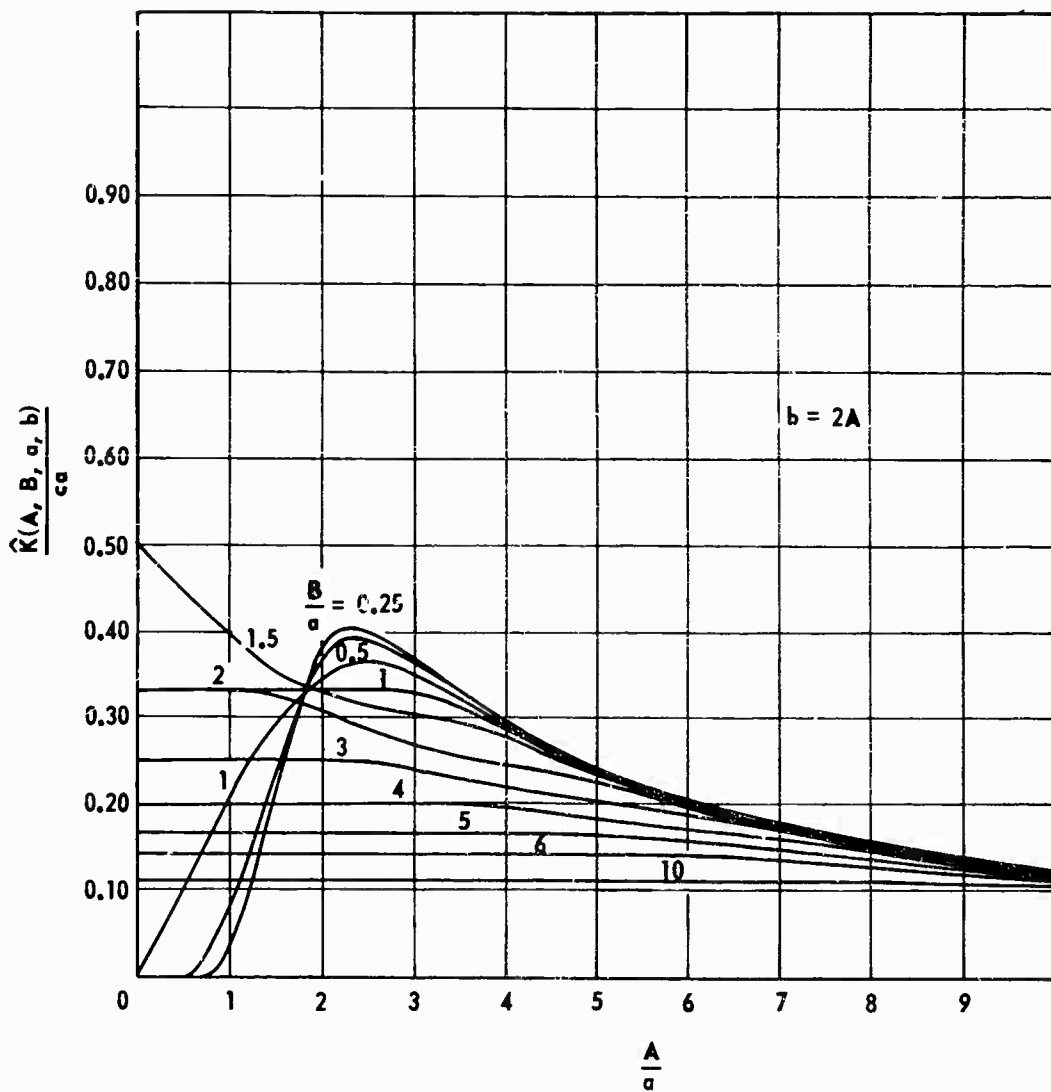


Figure 4.47. DIDF for Limiter with Dead Band, Triangle Wave Secondary Signal

$$\begin{aligned}
\hat{K}(A, B, a, b) = & \frac{C}{\pi} \frac{B}{A} \left\{ \left[\left(1 - \frac{a}{B}\right)^2 + \left(\frac{A}{B}\right)^2 \right] (\cos \gamma_2 - \cos \gamma_3) \right. \\
& - \left[\left(1 - \frac{b}{B}\right)^2 + \left(\frac{A}{B}\right)^2 \right] (\cos \gamma_4 - \cos \gamma_5) \\
& + \sin \gamma_3 \cos \gamma_3 \left(\frac{A}{B} + \frac{aA}{B^2}\right) - \sin \gamma_5 \cos \gamma_5 \left(\frac{A}{B} + \frac{bA}{B^2}\right) \\
& + \sin \gamma_2 \cos \gamma_2 \left(\frac{A}{B} - \frac{aA}{B^2}\right) - \sin \gamma_4 \cos \gamma_4 \left(\frac{A}{B} - \frac{bA}{B^2}\right) \\
& - \frac{4a}{B} \cos \gamma_3 + \frac{4b}{B} \cos \gamma_5 - \gamma_3 \left(\frac{A}{B} + \frac{aA}{B^2}\right) + \gamma_5 \left(\frac{A}{B} + \frac{bA}{B^2}\right) \\
& - \gamma_2 \left(\frac{A}{B} - \frac{aA}{B^2}\right) + \gamma_4 \left(\frac{A}{B} - \frac{bA}{B^2}\right) \\
& \left. + \frac{1}{3} \left(\frac{A}{B}\right)^2 (\cos^3 \gamma_3 - \cos^3 \gamma_2 - \cos^3 \gamma_5 + \cos^3 \gamma_4) \right\} \quad (4.84)
\end{aligned}$$

Square Wave Secondary Signal (Figures 4.48 and 4.49)

$$\begin{aligned}
\hat{N}(A_0, B, a, b) = & \frac{CB}{4} \left\{ \operatorname{sgn}(b - B - A_0) - \operatorname{sgn}(b + B - A_0) \right. \\
& - \operatorname{sgn}(a - B - A_0) + \operatorname{sgn}(a + B - A_0) \\
& + \left(\frac{a - A_0}{B}\right) \left[\operatorname{sgn}(a - B - A_0) + \operatorname{sgn}(a + B - A_0) \right] \\
& - \left(\frac{b - A_0}{B}\right) \left[\operatorname{sgn}(b - B - A_0) + \operatorname{sgn}(b + B - A_0) \right] \\
& + \left(\frac{B - a - A_0}{B}\right) \left[1 - \operatorname{sgn}(B - a - A_0) \right] \\
& \left. - \left(\frac{B - b - A_0}{B}\right) \left[1 - \operatorname{sgn}(B - b - A_0) \right] \right\} \quad (4.85)
\end{aligned}$$

$$\begin{aligned}
K(A, B, a, b) = & \frac{c}{\pi} \left[\gamma_5 + \gamma_4 - \gamma_3 - \gamma_2 + \sin \gamma_2 \cos \gamma_2 + \sin \gamma_3 \cos \gamma_3 \right. \\
& - \sin \gamma_4 \cos \gamma_4 - \sin \gamma_5 \cos \gamma_5 + \frac{2B}{A} (\cos \gamma_2 - \cos \gamma_3) \\
& \left. - \cos \gamma_4 + \cos \gamma_5 \right] - \frac{2a}{A} (\cos \gamma_2 + \cos \gamma_3)
\end{aligned}$$

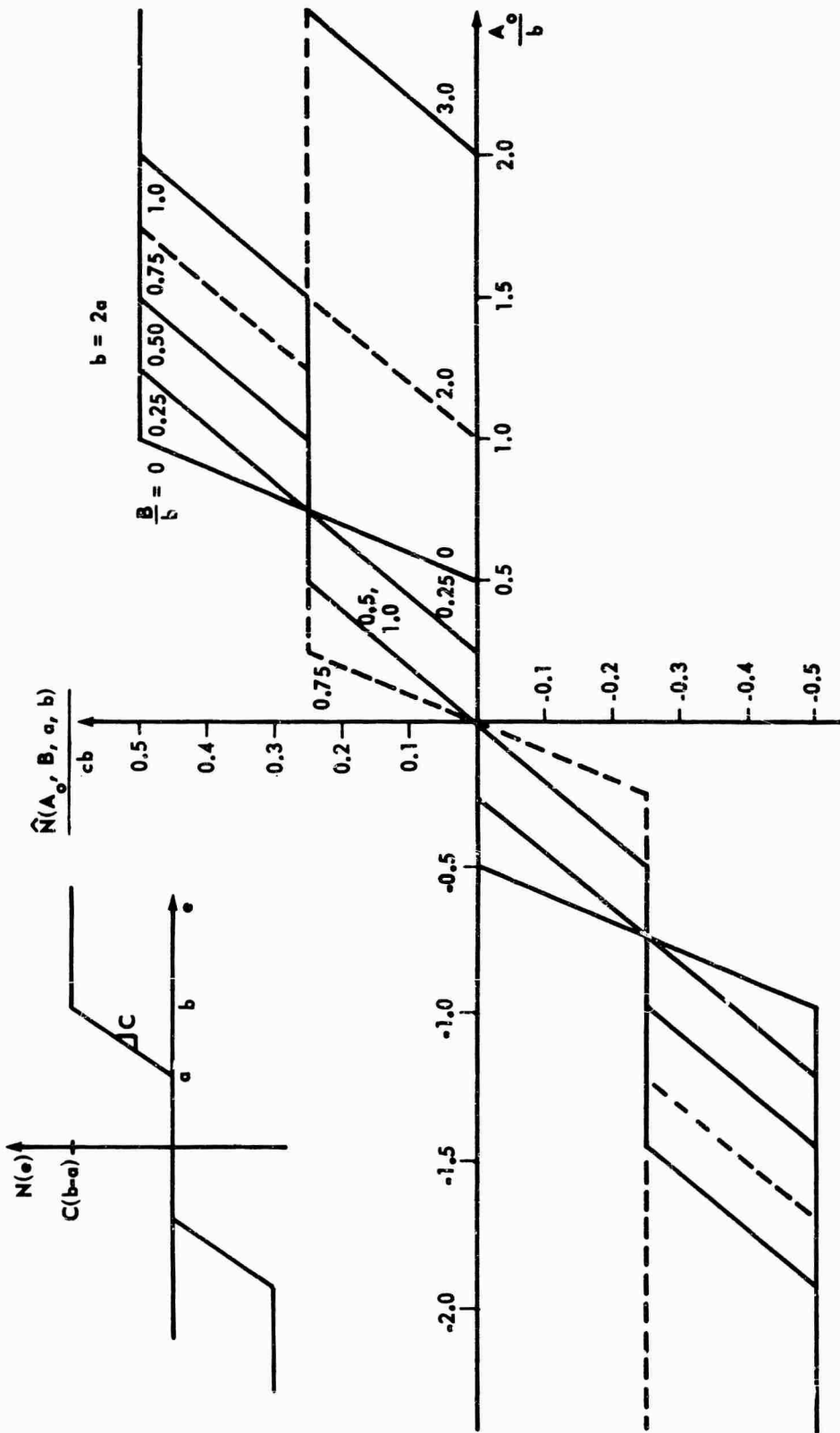


Figure 4.48. Modified Nonlinear Element for Limiter with Dead Band, Square Wave Secondary Signal

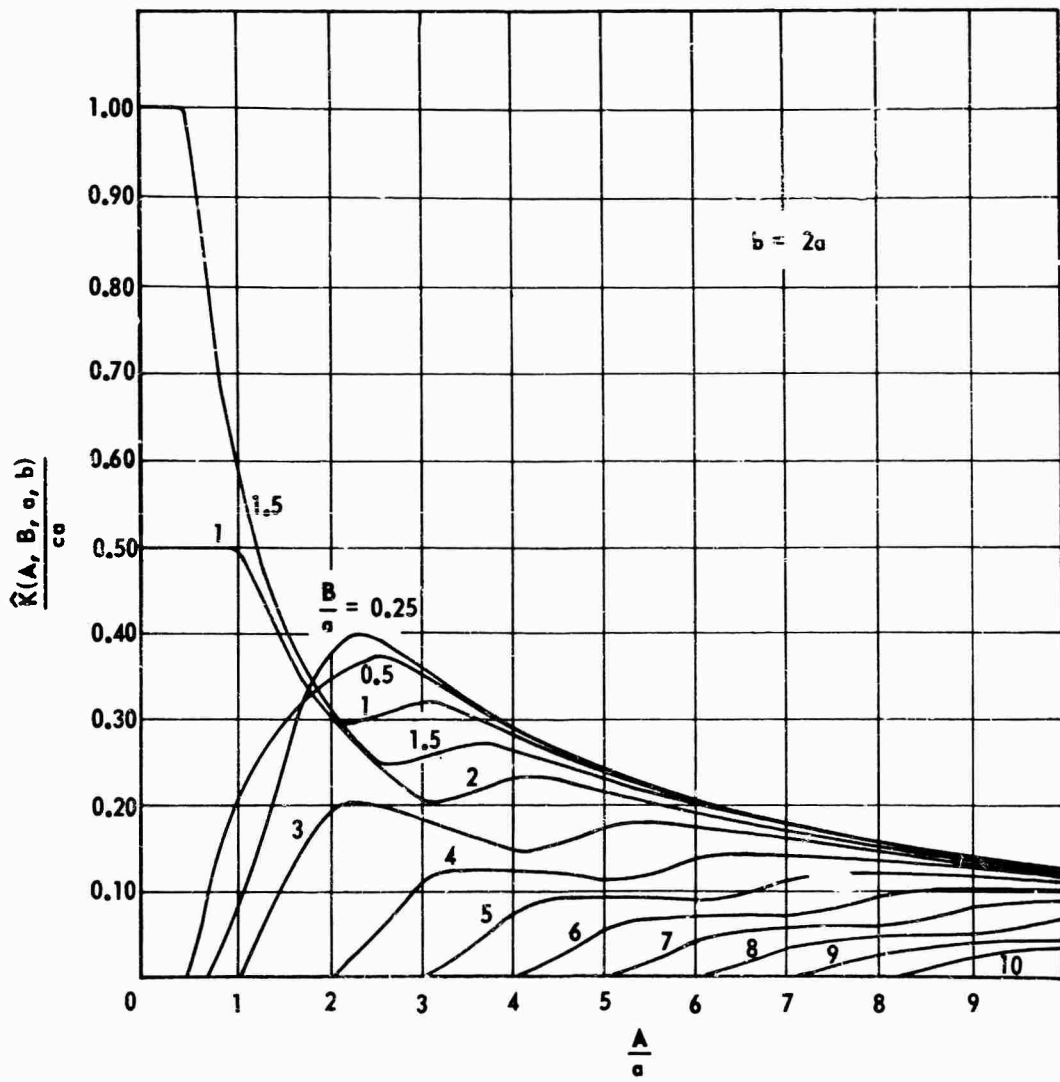


Figure 4.49. DIDF for Limiter with Dead Band,
Square Wave Secondary Signal

$$+ \frac{2b}{A} (\cos \gamma_4 + \cos \gamma_5) \quad (4.86)$$

4.8 Relay with Dead Band and Hysteresis

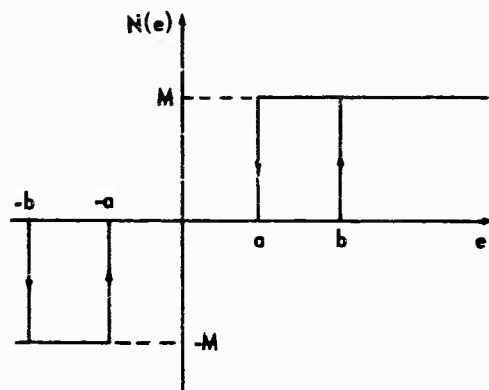


Figure 4.50. Relay with Dead Band and Hysteresis

Sine Wave Secondary Signal (Figures 4.51 and 4.52)

$$\hat{N}(A, B, a, b) = \frac{M}{2\pi} (\theta_5 + \theta_3 - \theta_4 - \theta_2) ; \quad B > \frac{b-a}{2}, \quad (4.87)$$

subject to the restrictions that

$$\theta_2 \text{ is set to } -\pi/2 \text{ when } \theta_4 = -\pi/2$$

$$\theta_4 \text{ is set to } +\pi/2 \text{ when } \theta_2 = \pi/2$$

$$\theta_3 \text{ is set to } +\pi/2 \text{ when } \theta_5 = \pi/2$$

$$\theta_5 \text{ is set to } -\pi/2 \text{ when } \theta_3 = -\pi/2 \quad (4.88)$$

$$\begin{aligned} \hat{K}(A, B, a, b) &= \frac{2M}{\pi^2 A} \int_0^{\gamma_4} \left[\sin^{-1} \left(\frac{a + A \sin \omega t}{B} \right) + \sin^{-1} \left(\frac{b + A \sin \omega t}{B} \right) \right] \sin \omega t \, d\omega t \\ &\quad - \frac{2M}{\pi^2 A} \int_0^{\gamma_3} \left[\sin^{-1} \left(\frac{a - A \sin \omega t}{B} \right) + \sin^{-1} \left(\frac{b - A \sin \omega t}{B} \right) \right] \sin \omega t \, d\omega t \\ &\quad + \frac{2M}{\pi A} (\cos \gamma_4 + \cos \gamma_3) \quad (4.89) \end{aligned}$$

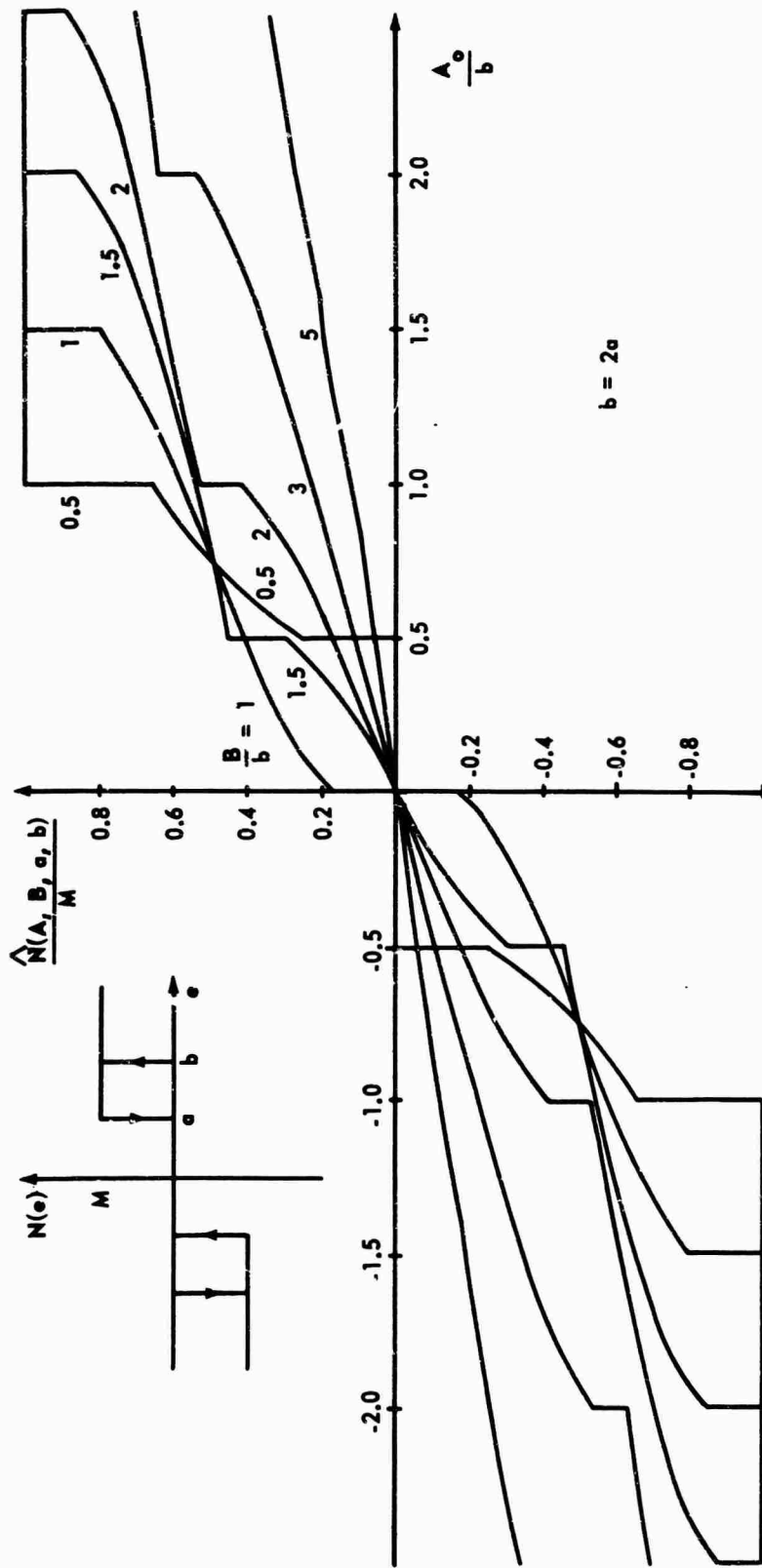


Figure 4.51. Modified Nonlinear Element for Relay with Hysteresis and Dead Band, Sine Wave Secondary Signal

Downloaded from <https://www.cambridge.org/core>. University of Cambridge, on 02 Jun 2018 at 10:00:00, subject to the Cambridge Core terms of use, available at <https://www.cambridge.org/core/terms>. <https://doi.org/10.1017/CBO9780511526457.008>

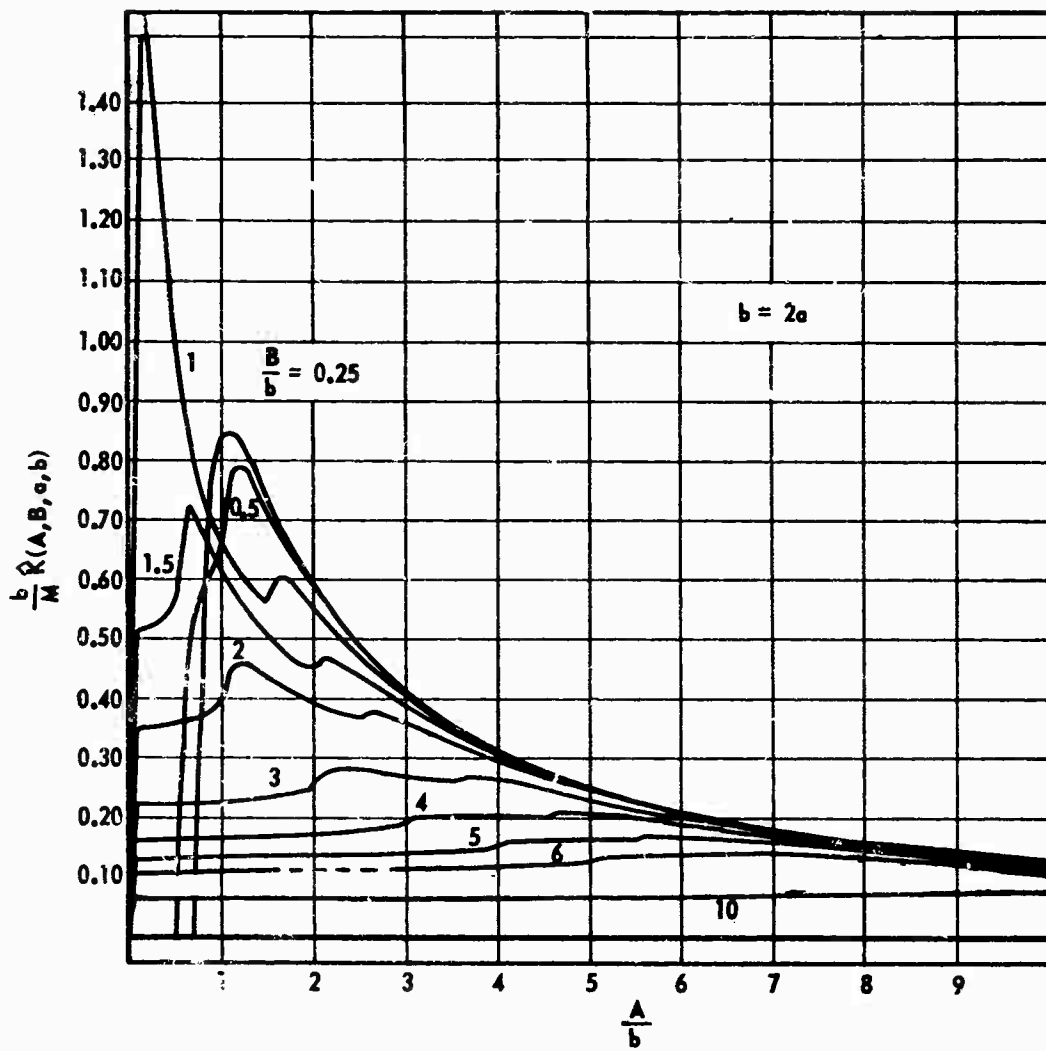


Figure 4.52. DIDF for Relay with Hysteresis and Dead Band, Sine Wave Secondary Signal

These integrals may be solved in closed form. There are two types to consider. Replacing a and b by c to give more generality, the two integral types become

$$K_1 = \frac{2M}{\pi^2 A} \int_0^{-\gamma_4} \sin^{-1} \left(\frac{c + A \sin \omega t}{B} \right) \sin \omega t \, d\omega t \quad (4.90)$$

$$K_2 = \frac{2M}{\pi^2 A} \int_0^{\gamma_3} \sin^{-1} \left(\frac{c - A \sin \omega t}{B} \right) \sin \omega t \, d\omega t \quad (4.91)$$

$$K_1 = \frac{2M}{\pi^2} \left[\frac{1}{A} \sin^{-1} \left(\frac{C}{B} \right) - \frac{\cos \gamma_4}{A} \sin^{-1} \left(\frac{c - A \sin \gamma_4}{B} \right) \right] + K_{11} \quad (4.92)$$

$$K_2 = \frac{2M}{\pi^2} \left[\frac{1}{A} \sin^{-1} \left(\frac{C}{B} \right) - \frac{\cos \gamma_3}{A} \sin^{-1} \left(\frac{c - A \sin \gamma_3}{B} \right) \right] + K_{21} \quad (4.93)$$

where

$$K_{11} = \int_0^{\gamma_1} \frac{\cos^2 \omega t \, d\omega t}{\sqrt{1 - \left(\frac{c + A \sin \omega t}{B} \right)^2}} \quad (4.94)$$

$$K_{21} = \int_0^{\gamma_2} \frac{\cos^2 \omega t \, d\omega t}{\sqrt{1 - \left(\frac{c - A \sin \omega t}{B} \right)^2}} \quad (4.95)$$

A general form of the solution for both K_{11} and K_{21} is given as follows:

$$K_x = \frac{\frac{B}{A} hg}{2(k^2 - \alpha^2)} \left[E(\phi, k) + \left(\frac{\alpha^2 - k^2}{\alpha^2} \right) F(\phi, k) \right. \\ \left. + \left(\alpha^2 - 2 + \frac{k^2}{\alpha^2} \right) \Pi(\phi, \alpha^2, k) \right] \quad (4.96)$$

$$- \frac{\alpha^2 \sin \phi \cos \phi \sqrt{1 - k^2 \sin^2 \phi}}{1 - \alpha^2 \sin^2 \phi} \left. \right] \quad (4.96)$$

The correct values of k , g , α^2 , ϕ , and h are given in Table 4-I.

Table 4.1. Variables Associated with the DIDF for Relay with Dead Band and Hysteresis with Sine Wave Secondary Signal

		K_{11}	K_{21}
Case a $\frac{B - C}{A} > 1$	k^2	$\frac{4AB}{(A + B - C)(A + B + C)}$	$\frac{4AB}{(A + B - C)(A + B + C)}$
	g	$\frac{2A}{\sqrt{(A + B - C)(A + B + C)}}$	$\frac{2A}{\sqrt{(A + B - C)(A + B + C)}}$
	α^2	$\frac{2A}{A + B - C}$	$\frac{2A}{A + B + C}$
	ϕ	$\sin^{-1} \sqrt{\frac{A + B - C}{2(B - C)}}$	$\sin^{-1} \sqrt{\frac{A + B + C}{2(B + C)}}$
	h	$\frac{2}{A}(B - C - A)$	$\frac{2}{A}(B + C - A)$
Case b $\frac{B - C}{A} < 1$ $\frac{B + C}{A} > 1$	k^2	$\frac{(A + B - C)(A + B + C)}{4AB}$	$\frac{(A + B - C)(A + B + C)}{4AB}$
	g	$\sqrt{A/B}$	$\sqrt{A/B}$
	α^2	$\frac{A + B - C}{2A}$	$\frac{A + B - C}{2B}$
	ϕ	$\sin^{-1} \sqrt{\frac{2(B - C)}{(A + B - C)}}$	$\sin^{-1} \sqrt{\frac{2AB}{(A + B - C)(B + C)}}$
	h	$\frac{1}{A^2}(A - B + C)(A + B - C)$	$\frac{1}{A^2}(B + C - A)(A + B - C)$
Case c $\frac{B + C}{A} < 1$	k^2	$\frac{4AB}{(A + B + C)(A + B - C)}$	$\frac{4AB}{(A + B + C)(A + B - C)}$
	g	$\frac{2A}{\sqrt{(A + B + C)(A + B - C)}}$	$\frac{2A}{\sqrt{(A + B + C)(A + B - C)}}$
	α^2	$\frac{2B}{(A + B + C)}$	$\frac{2B}{(A + B - C)}$
	ϕ	$\sin^{-1} \sqrt{\frac{(B - C)(A + B + C)}{2AB}}$	$\sin^{-1} \sqrt{\frac{(A + B - C)(B + C)}{2AB}}$
	h	$\frac{2B}{A^2}(A - B + C)$	$\frac{2B}{A^2}(A - B - C)$

$$\hat{N}(A, B, a, b) = \text{Relay with dead band } 2(a + b) \text{ and hysteresis } (b - a - 2B) \quad (4.97)$$

(Figure 4.53)

$$\text{for } B < \frac{b - a}{2} .$$

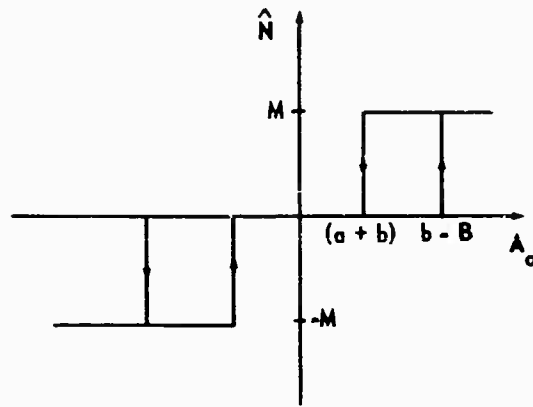


Figure 4.53. Modified Nonlinear Element

$$|\hat{K}(A, B, a, b)| = \frac{2M}{\pi A} \sqrt{2 + 2 \cos(\gamma_3 + \gamma_4)} ; \quad B < \frac{b - a}{2} \quad (4.98)$$

$$\angle \hat{K} = \tan^{-1} \left(\frac{\sin \gamma_1 - \sin \gamma_2}{\cos \gamma_1 + \cos \gamma_2} \right) = - \frac{(\gamma_4 - \gamma_3)}{2} ; \quad B < \frac{b - a}{2} \quad (4.99)$$

Triangle Wave Secondary Signal (Figures 4.54 and 4.55)

Case a

$$\left(B < \frac{b - a}{2} \right)$$

Both $\hat{N}(A_0, B, a, b)$ and $\hat{K}(A, B, a, b)$ are the same as in the sine wave case.

Case b

$$\left(\frac{b - a}{2} < B < b \right)$$

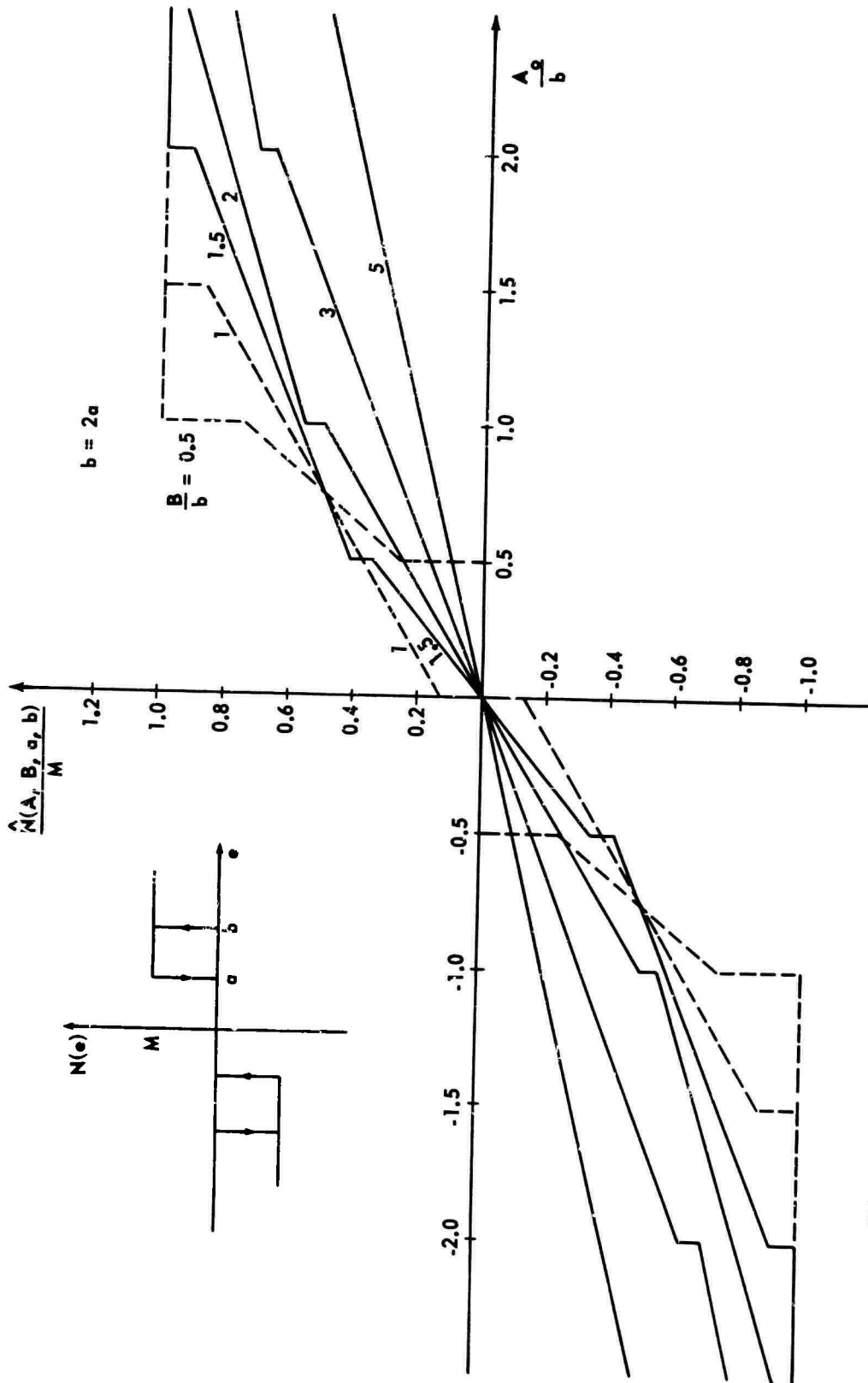


Figure 4.54. Modified Nonlinear Element for Relay with Hysteresis and Dead Band, Sine Wave Secondary Signal

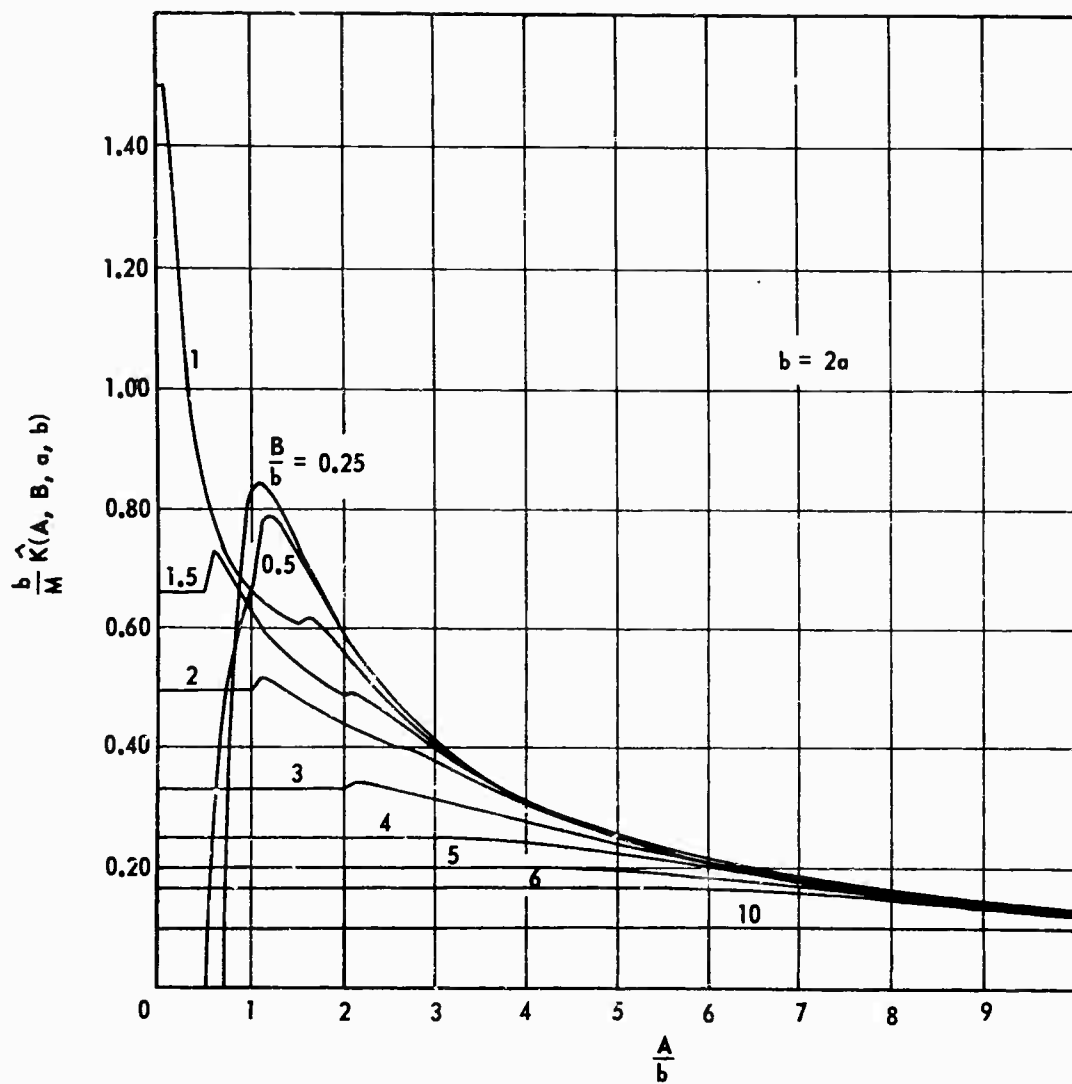


Figure 4.55. DIDF for Relay with Dead Band and Hysteresis, Triangle Wave Secondary Signal

$$\hat{N}(A_o, B, a, b) = \begin{cases} \frac{M}{B} A_o ; & B - A_o \geq b \\ \frac{M}{2} \left(1 - \frac{a+b}{2B} + \frac{A_o}{B} \right) ; & -b < A_o - B < a \\ M ; & a < A_o - B \end{cases} \quad (4.100)$$

$$\hat{N}(A_o, B, a, b) = \begin{cases} 0 ; & A_o < b - B \\ \frac{M}{2} \left(1 - \frac{a+b}{2B} + \frac{A_o}{B} \right) ; & b - B < A_o < B + a \\ M ; & A_o > B + a \end{cases} \quad (4.101)$$

or

$$\begin{aligned} \hat{N}(A_o, B, a, b) = & \frac{M}{4} \left[\operatorname{sgn}(A_o + b - B) - \operatorname{sgn}(A_o + B + a) \right. \\ & \left. + \operatorname{sgn}(A_o - b + B) - \operatorname{sgn}(A_o - B - a) \right] \left[1 \right. \\ & \left. + \frac{a+b}{2B} + \frac{A_o}{B} \right] + \frac{M}{2} \left[\operatorname{sgn}(A_o + b + a) \right. \\ & \left. + \operatorname{sgn}(A_o - B - a) \right] ; \end{aligned} \quad (4.102)$$

$$\begin{aligned} \hat{K}(A, B, a, b) = & \frac{M}{\pi B} (\gamma_3 - \gamma_4 + \sin \gamma_4 \cos \gamma_4 - \sin \gamma_3 \cos \gamma_3) \\ & + \frac{2M}{\pi A} \left(1 - \frac{a+b}{2B} \right) (\cos \gamma_4 - \cos \gamma_3) + \frac{4M}{\pi A} \cos \gamma_3 \end{aligned} \quad (4.103)$$

Case c

(B > b)

$$\hat{N}(A_o, B, a, b) = \begin{cases} \frac{M}{B} A_o ; & B - A_o \geq b \\ \frac{M}{2} \left(1 - \frac{a+b}{2B} + \frac{A_o}{B} \right) ; & -b < A_o - B < a \\ M ; & a < A_o - B \end{cases} \quad (4.104)$$

$$\hat{K}(A, B, a, b) = (\text{same as case b}) \quad (4.105)$$

Square Wave Secondary Signal (Figures 4.57 and 4.58)

Case a

$$\left(B < \frac{b - a}{2} \right)$$

See Case a for sine wave secondary signal.

Case b

$$\left(B > \frac{b - a}{2} \right)$$

$$\begin{aligned} \hat{N}(A_0, B, a, b) = \frac{M}{4} & \left[\operatorname{sgn}(A_0 + B + a) + \operatorname{sgn}(A_0 + B - b) \right. \\ & \left. + \operatorname{sgn}(A_0 - B + b) + \operatorname{sgn}(A_0 - B - a) \right] \quad (4.106) \end{aligned}$$

$$\hat{K}(A, B, a, b) = \frac{2M}{\pi A} [\cos \gamma_4 + \cos \gamma_3] \quad (4.107)$$

Figure 4.59 shows the phase of DIDF for relay with hysteresis and dead band.

4.9 Relay with Hysteresis

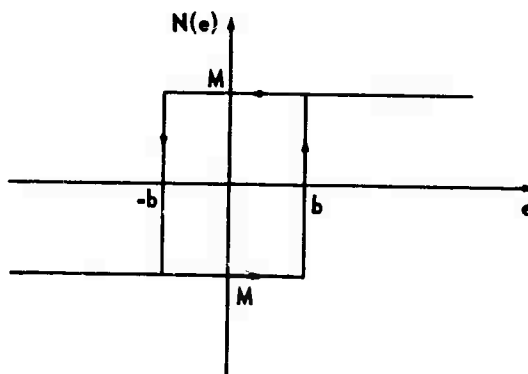


Figure 4.56. Relay with Hysteresis

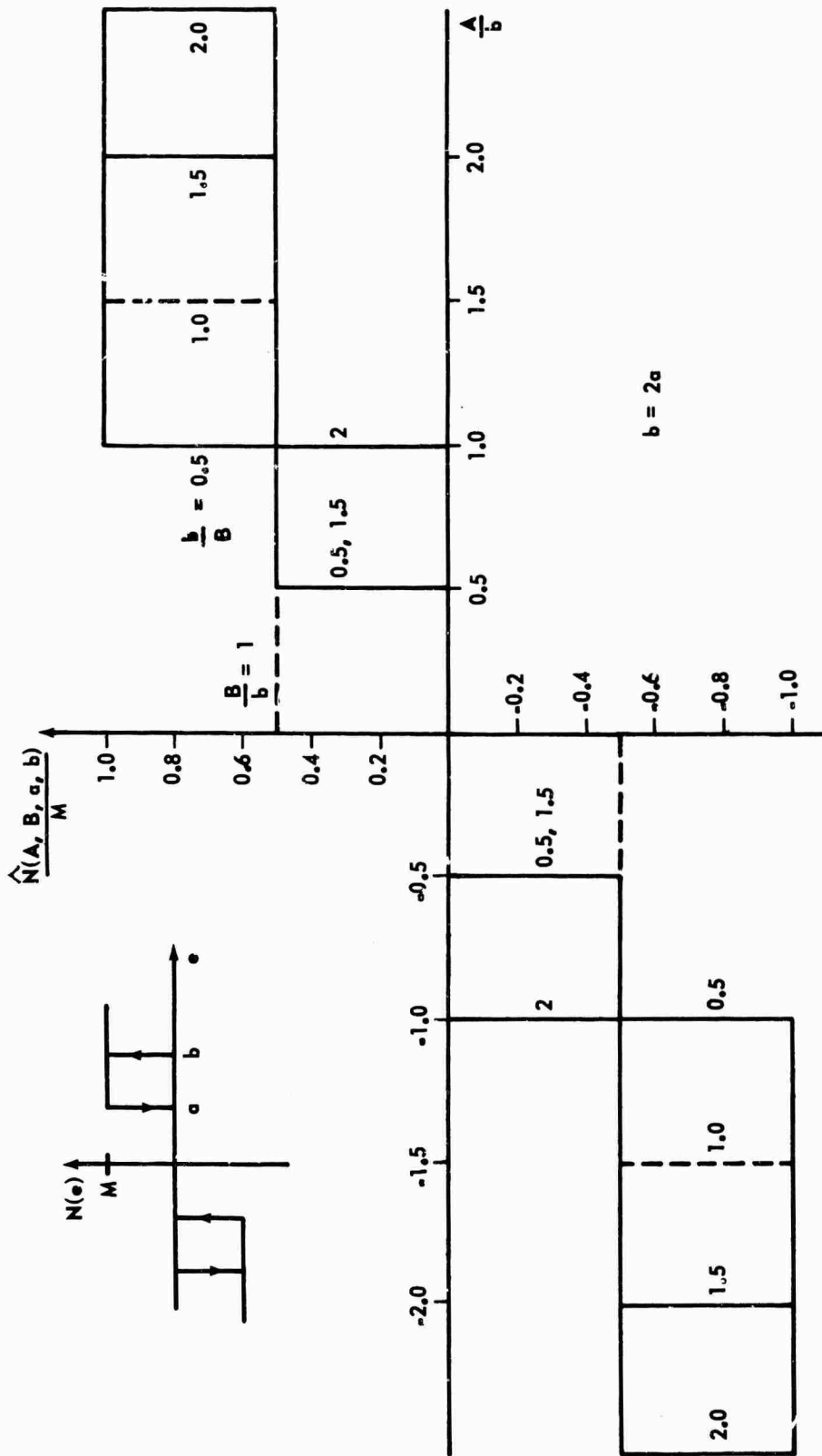


Figure 4.57. Modified Nonlinear Element for Relay with Hysteresis and Dead Band, Square Wave Secondary Signal

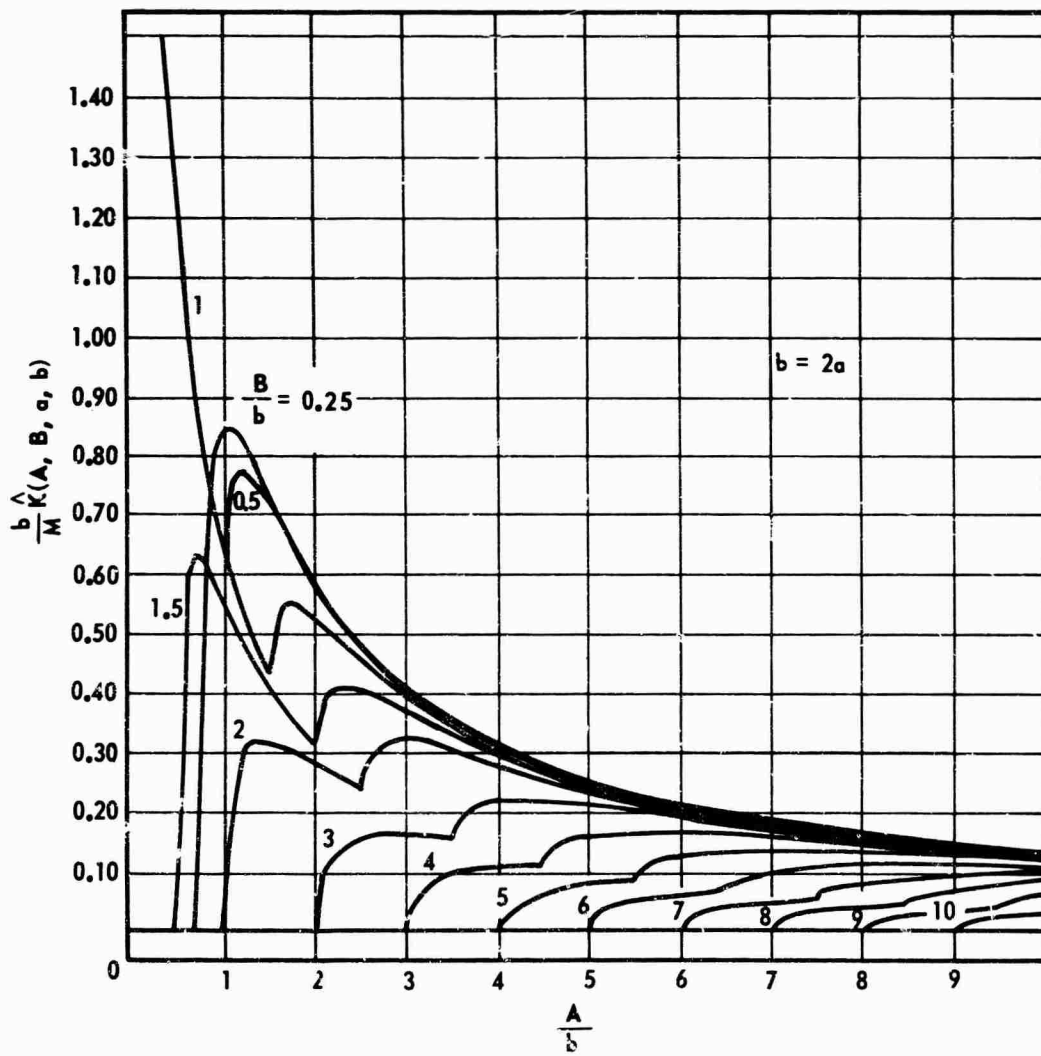


Figure 4.58. DIDF for Relay with Dead Band and Hysteresis, Square Wave Secondary Signal

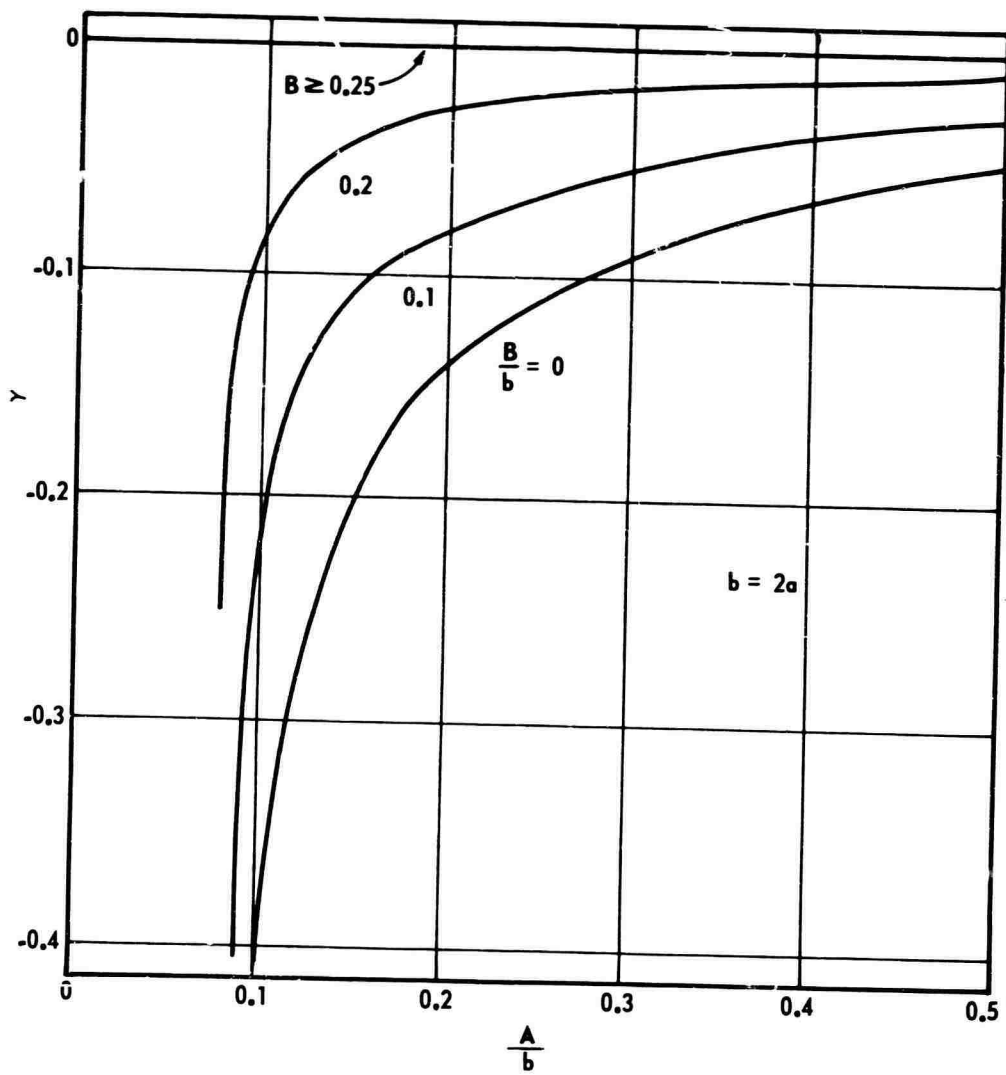


Figure 4. 59. Phase of DIDF for Relay with Hysteresis and Dead Band

Sine Wave Secondary Signal (Figures 4.60 and 4.61)

Case a

$$(B < b)$$

$$\hat{N}(A, B, a, b) = \text{Relay with hysteresis width } 2(b - B) \quad (4.108)$$

$$|\hat{K}(A, B, b)| = \frac{4M}{\pi A} \quad (4.109)$$

$$\angle \hat{K} = -\sin^{-1} \left(\frac{b - B}{A} \right) \quad (4.110)$$

Case b

$$(B > b)$$

$$\hat{N}_{A_o, B, b} = \begin{cases} \frac{M}{\pi} \left[\sin^{-1} \left(\frac{b + A_o}{B} \right) - \sin^{-1} \left(\frac{b - A_o}{B} \right) \right] & ; A_o < B - b \\ M & ; A_o > B - b \end{cases} \quad (4.111)$$

$$\hat{K}(A, B, b) = 2(K_{11} - K_{22}) \quad (4.112)$$

where K_{11} and K_{22} are defined for the relay with hysteresis and dead band, sine wave secondary signal. The variable c must be replaced by b in the equations for K_{11} and K_{21} .

Triangle Wave Secondary Signal (Figures 4.62 and 4.63)

Case a

$$(B < b)$$

See Case a for sine wave secondary signal.

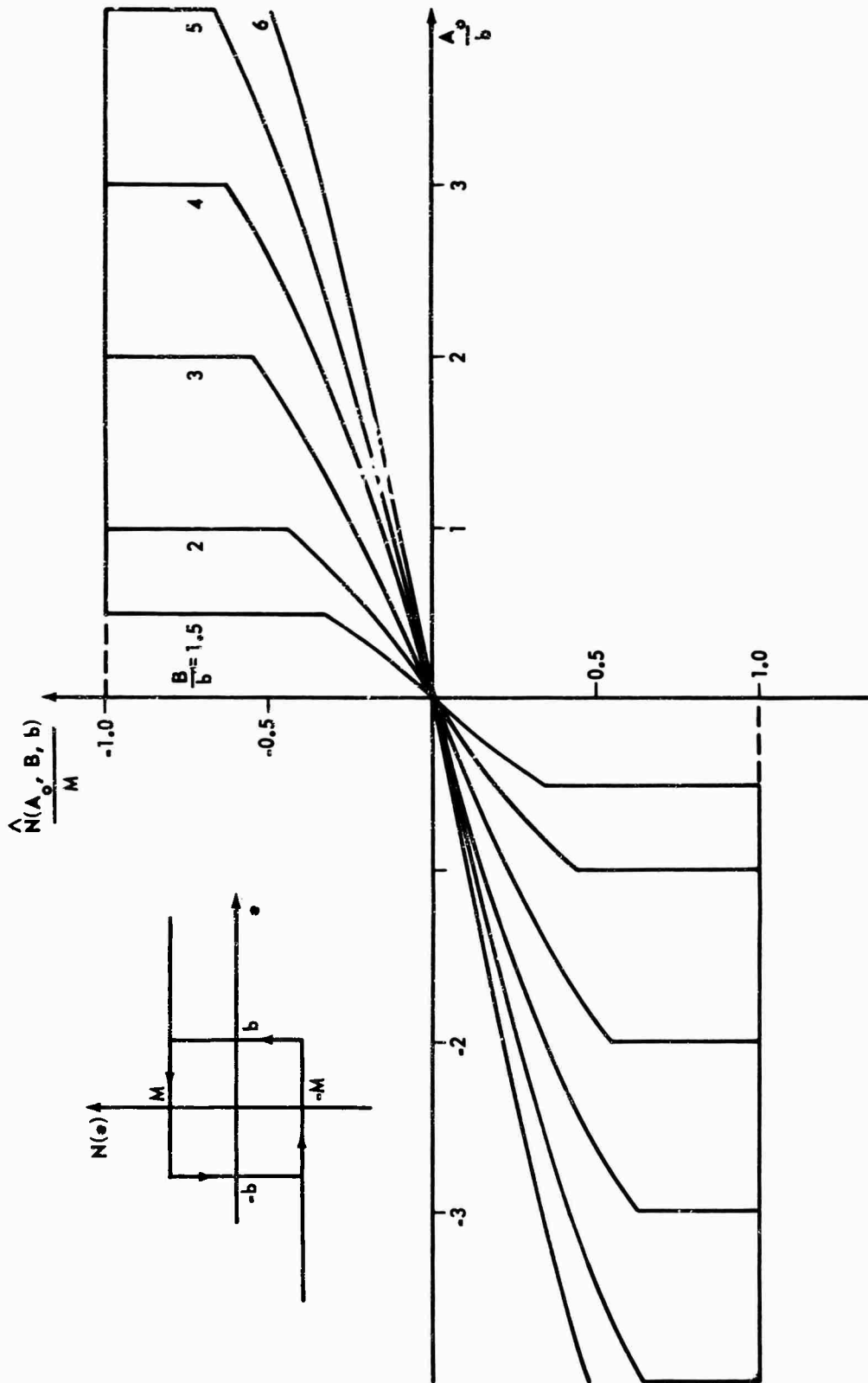


Figure 4.60. Modified Nonlinear Element for Relay with Hysteresis, Sine Wave Secondary Signal

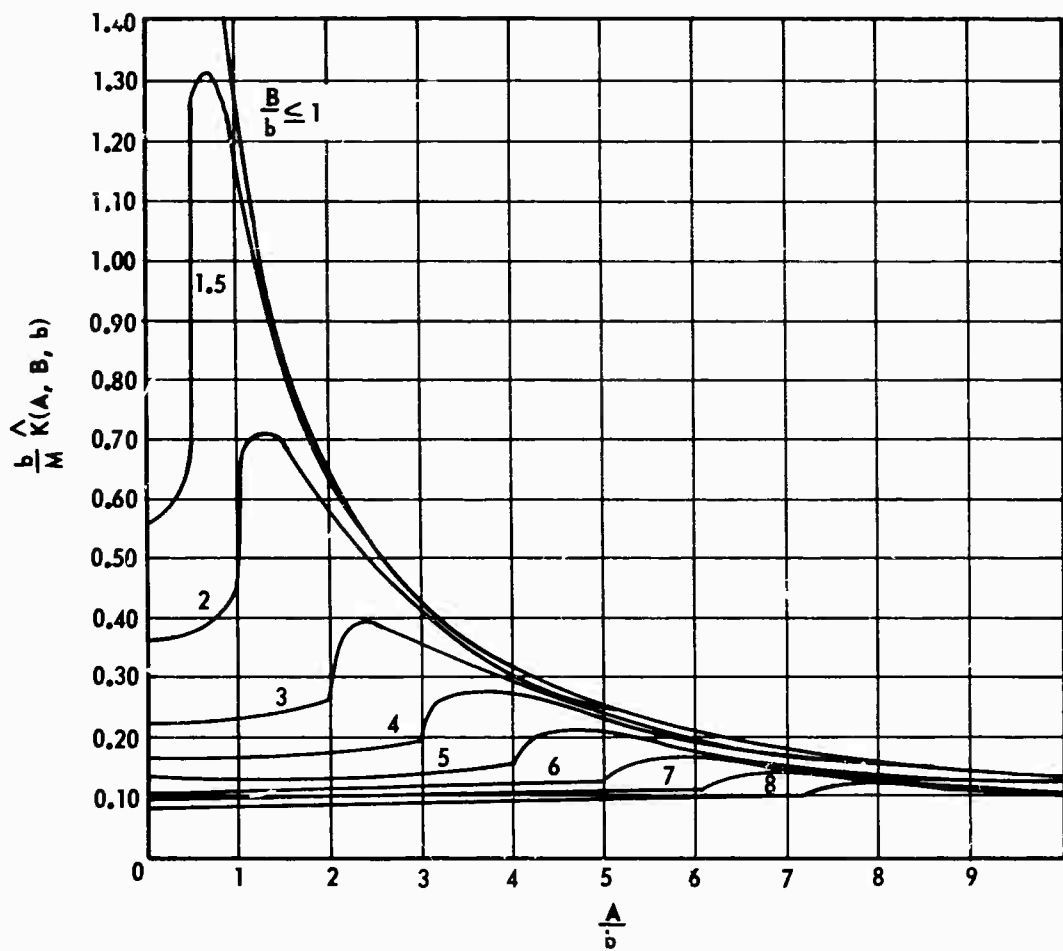


Figure 4.61. DIDF for Relay with Hysteresis, Sine Wave Secondary Signal

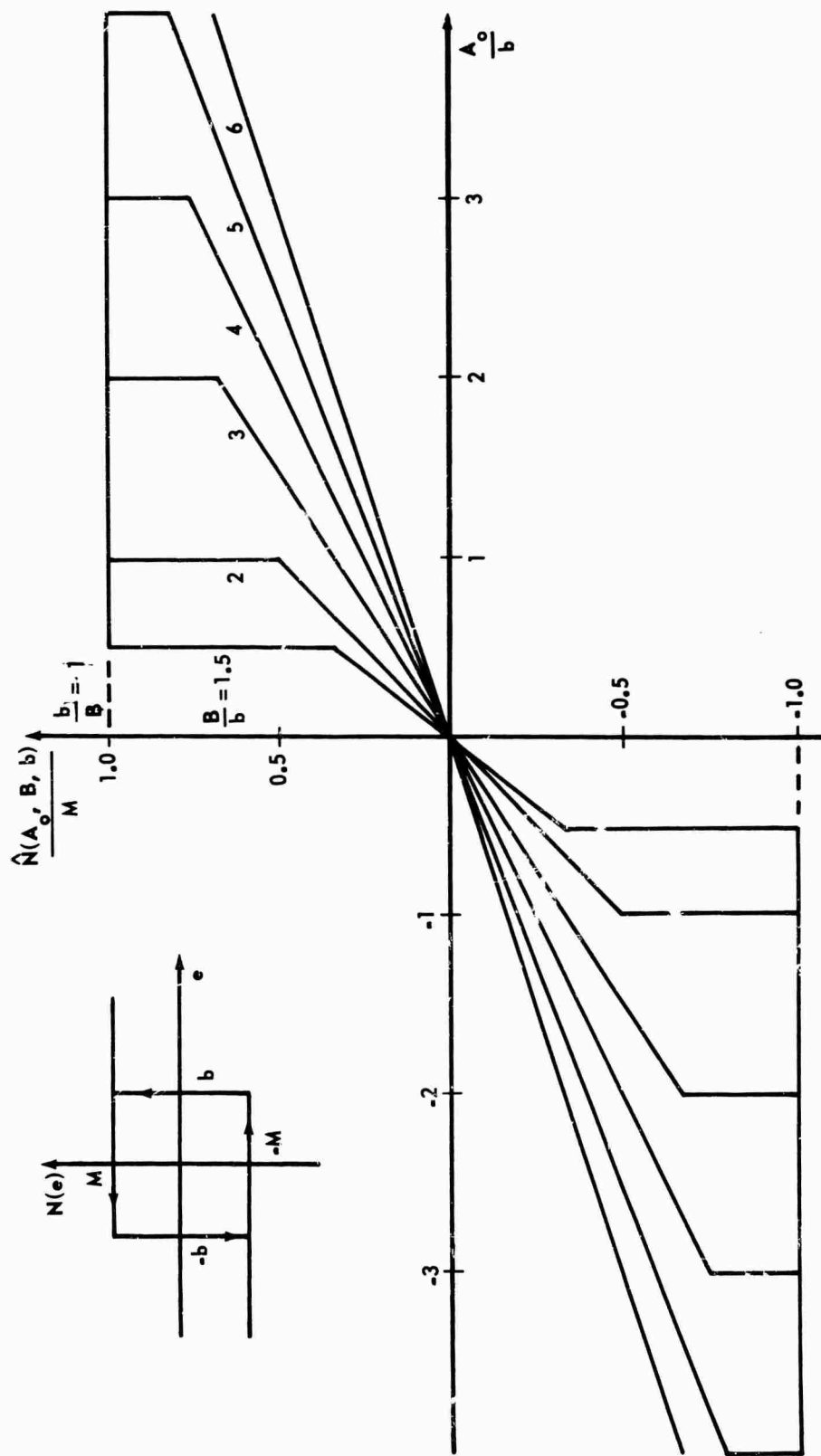


Figure 4.62. Modified Nonlinear Element for Relay with Hysteresis, Triangle Wave Secondary Signal

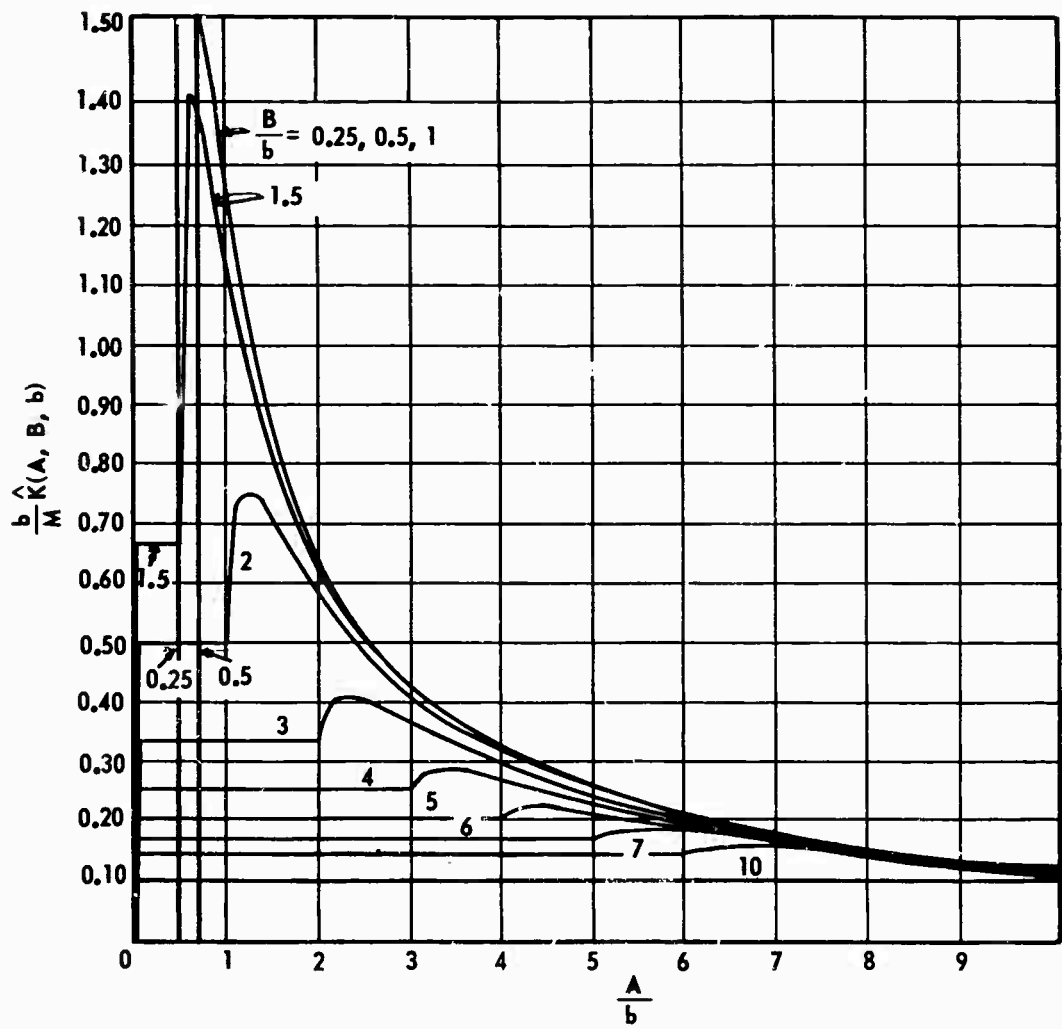


Figure 4.63. DIDF for Relay with Hysteresis, Triangle Wave Secondary Signal

Case b

$$(B > b)$$

$$\hat{N}(A_o, B, b) = \begin{cases} \frac{M}{B} A_o ; & A_o < B - b \\ M ; & A_o \geq B - b \end{cases} \quad (4.113)$$

$$\hat{K}(A_o, B, b) = \frac{2M}{\pi B} (\sin \gamma_4 \cos \gamma_4 - \gamma_4) + \frac{4M}{\pi A} \cos \gamma_4 \quad (4.114)$$

Square Wave Secondary Signal (Figures 4.64 and 4.65)

Case a

$$(B < b)$$

See Case a for sine wave secondary signal.

Case b

$$(B > b)$$

$$\hat{N}(A_o, B, b) = \frac{M}{2} \left[\text{sgn}(A_o + B - b) + \text{sgn}(A_o - B + b) \right] \quad (4.115)$$

$$\hat{K}(A, B, b) = \frac{4M}{\pi A} \cos \gamma_4 \quad (4.116)$$

Figure 4.66 shows the phase of DIDF for relay with hysteresis.

4.10 Limiter with Hysteresis

Sine Wave Secondary Signal (Figures 4.67 through 4.69)

Case a (Figure 4.71)

$$(B < b)$$

$$N_3 = \frac{c}{2\pi} \left[\pi b - 2a\theta_2 + A_o (\pi + 2\theta_2) - 2B \cos \theta_2 \right] \quad (4.117)$$

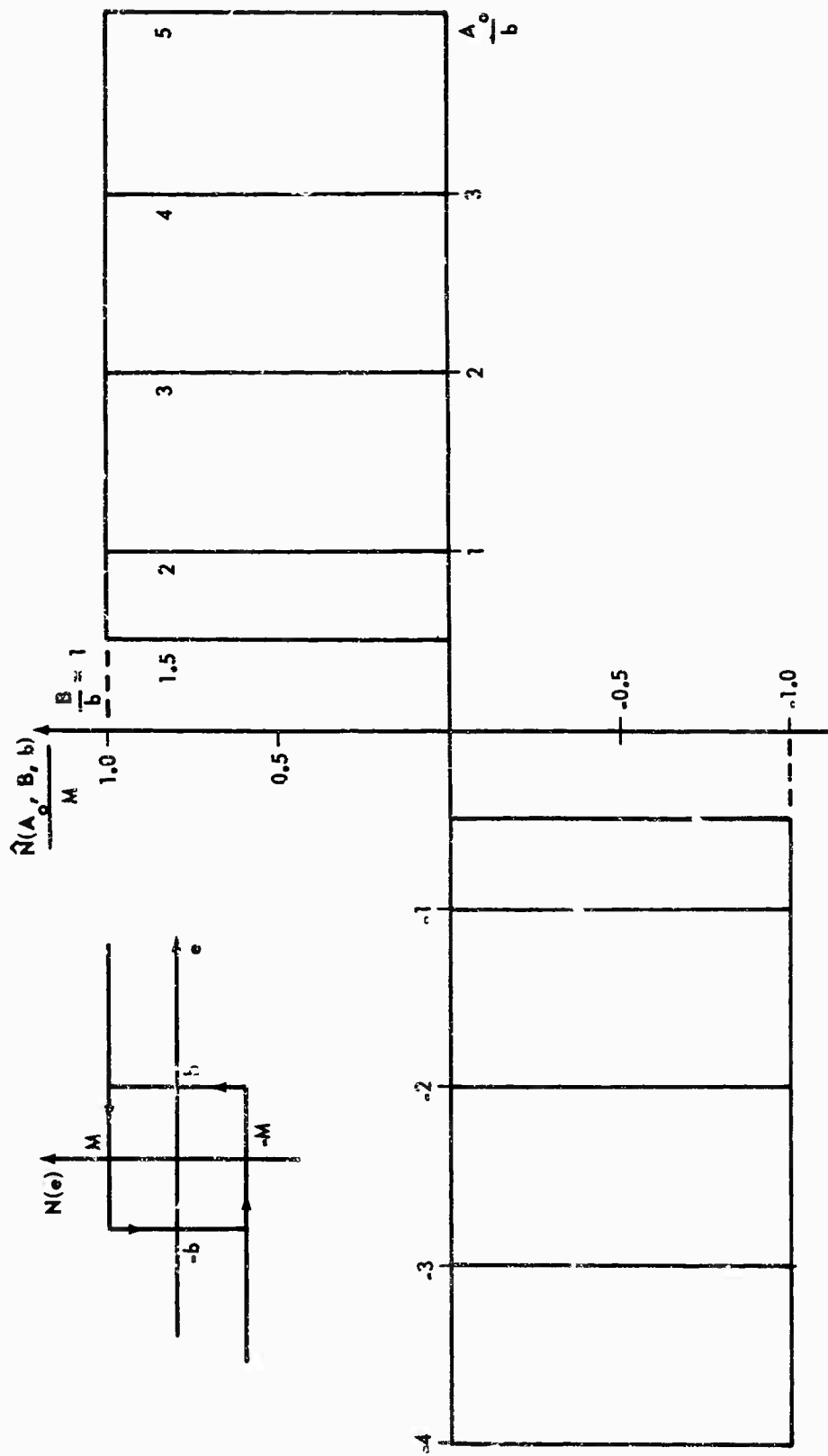


Figure 4.64. Modified Nonlinear Element for Relay with Hysteresis, Square Wave Secondary Signal

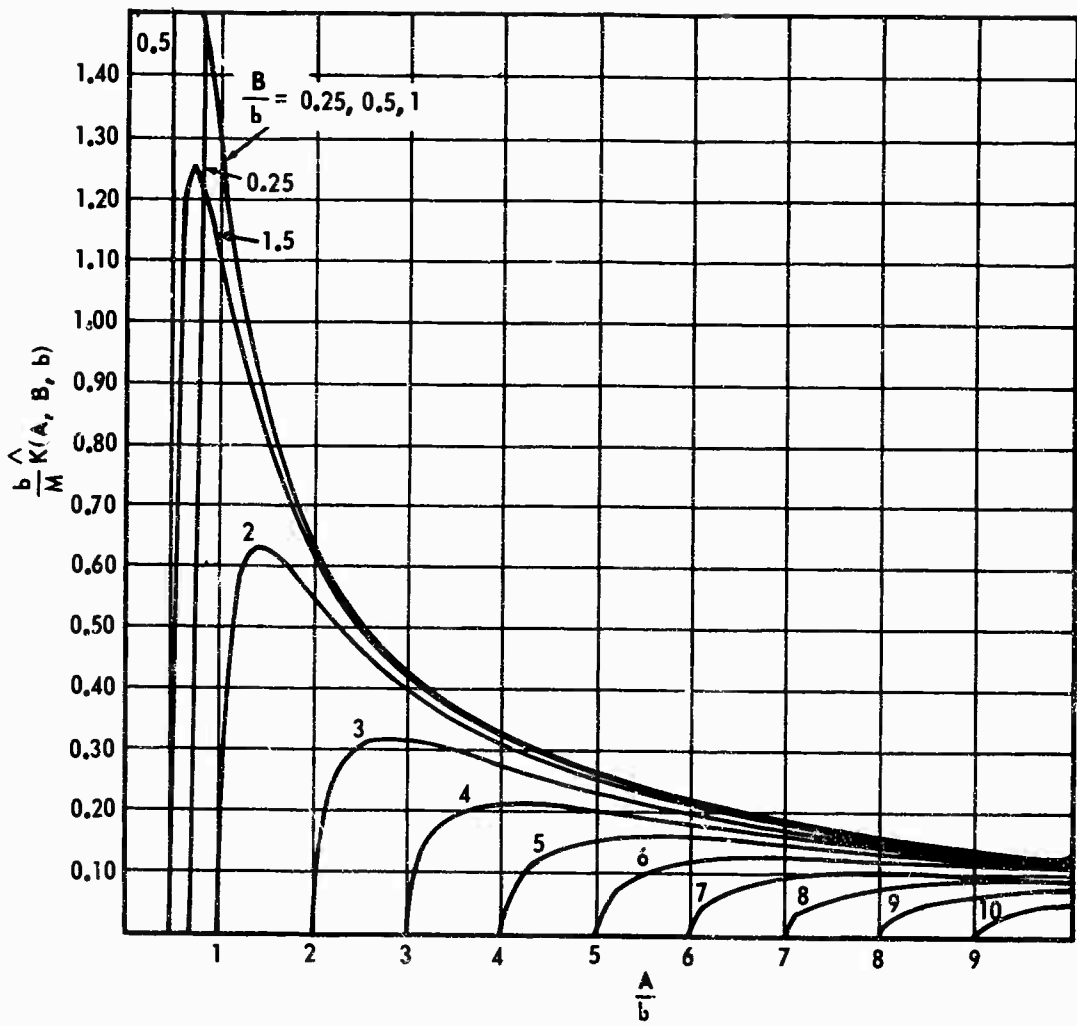


Figure 4.65. DIDF for Relay with Hysteresis,
Square Wave Secondary Signal

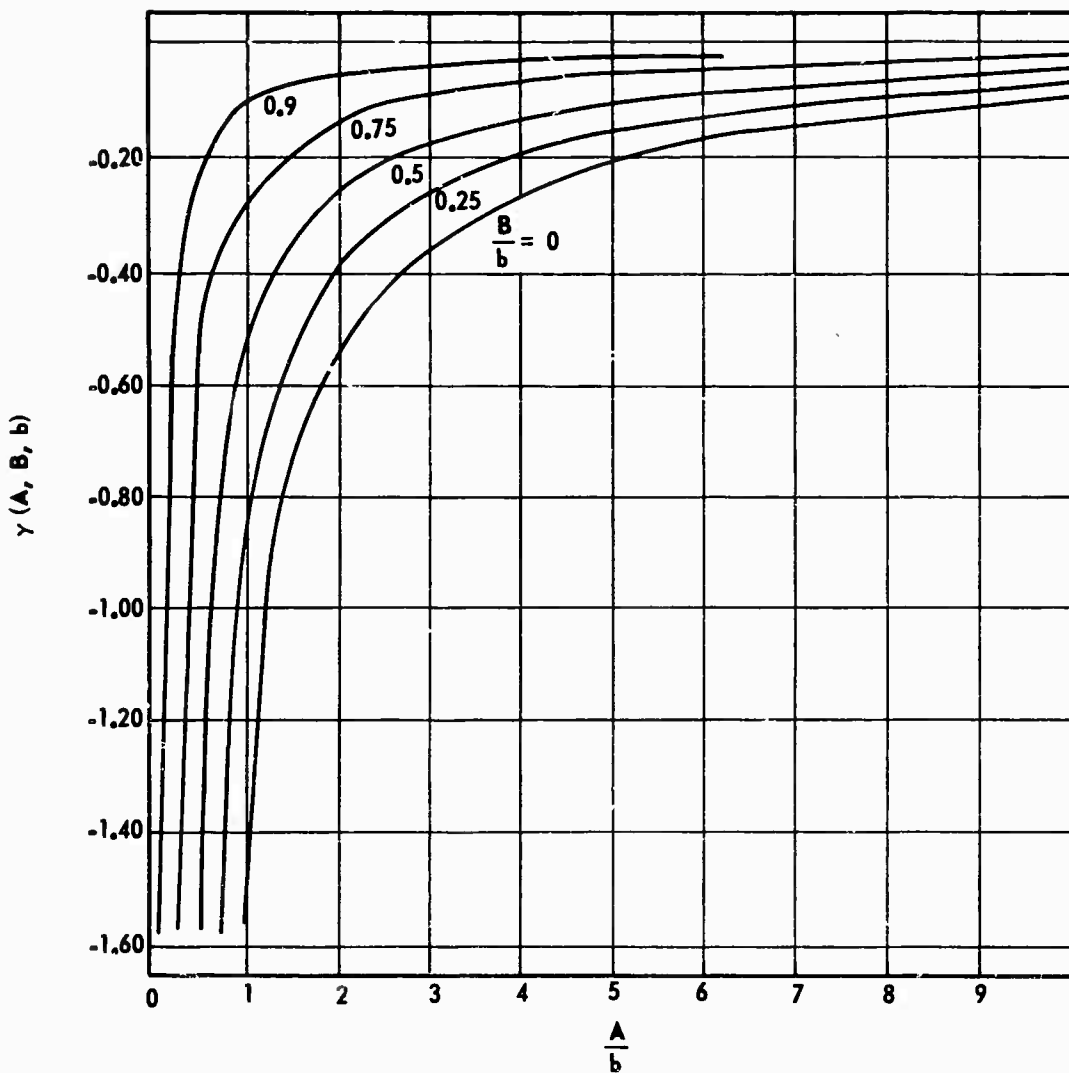


Figure 4.66. Phase of DIDF for Relay with Hysteresis

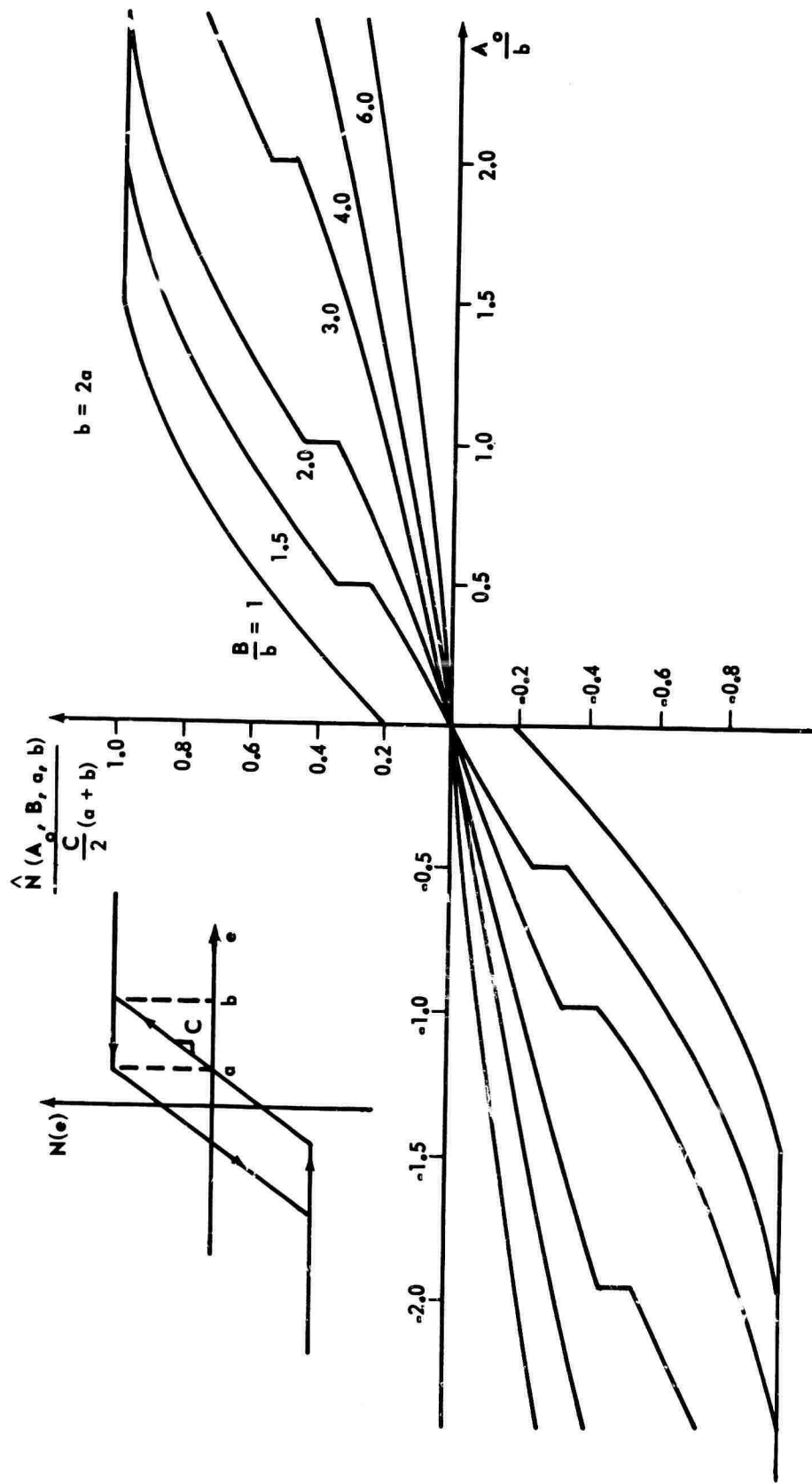


Figure 4.67. Modified Nonlinear Element for Limiter with Hysteresis, Sine Wave Secondary Signal

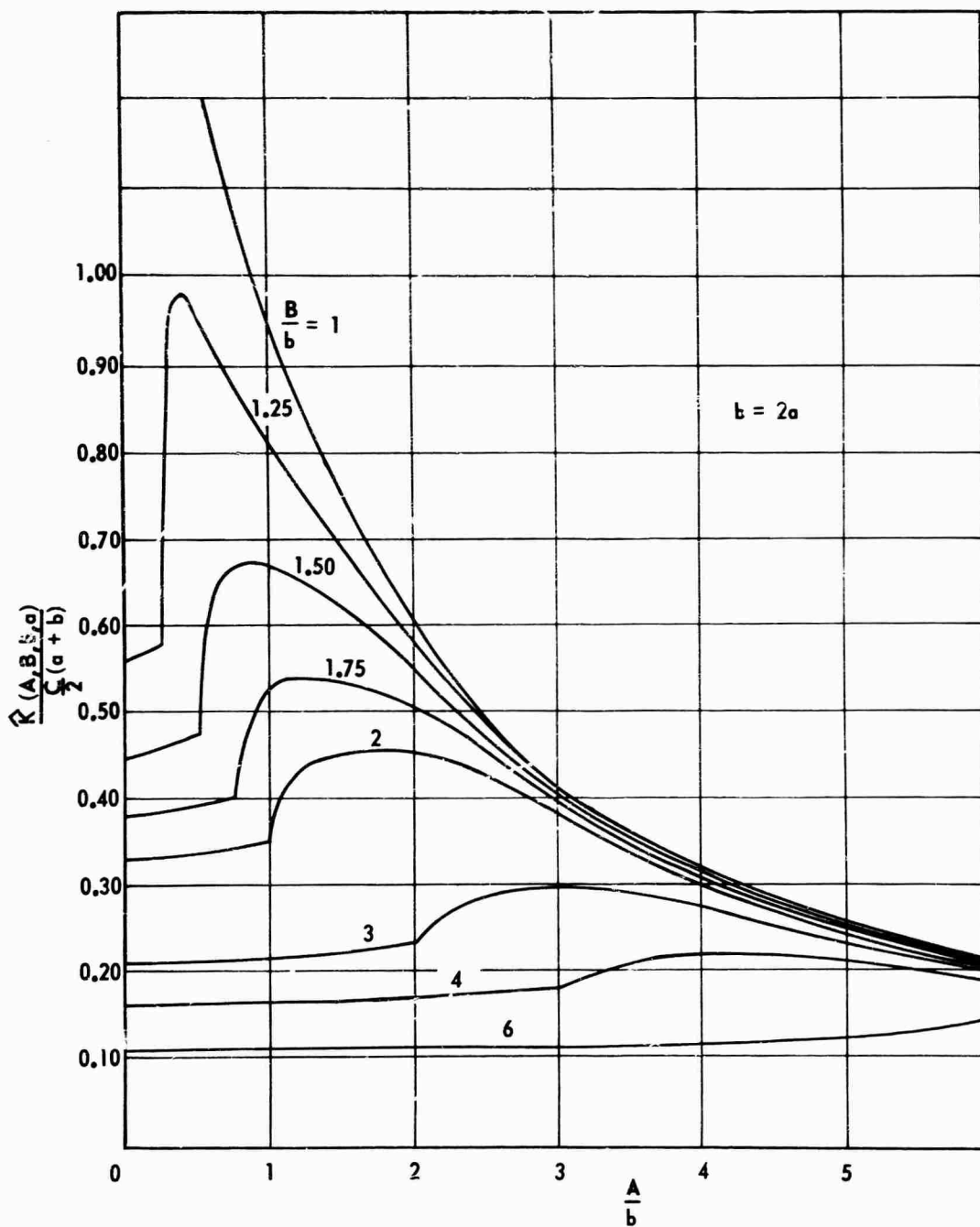


Figure 4.68. DIDF for Limiter with Hysteresis,
Sine Wave Secondary Signal

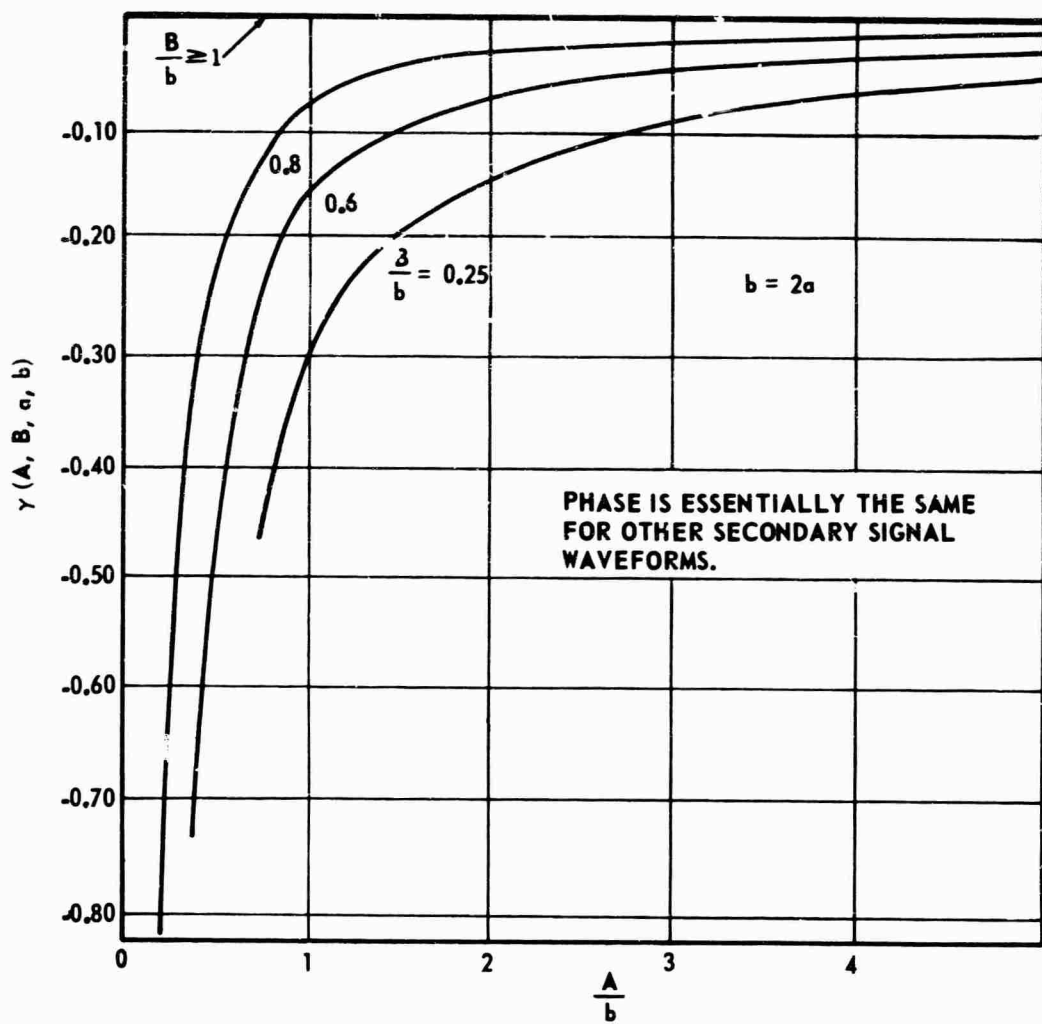


Figure 4.69. Phase of DIDF for Limiter with Hysteresis, Sine Wave Secondary Signal

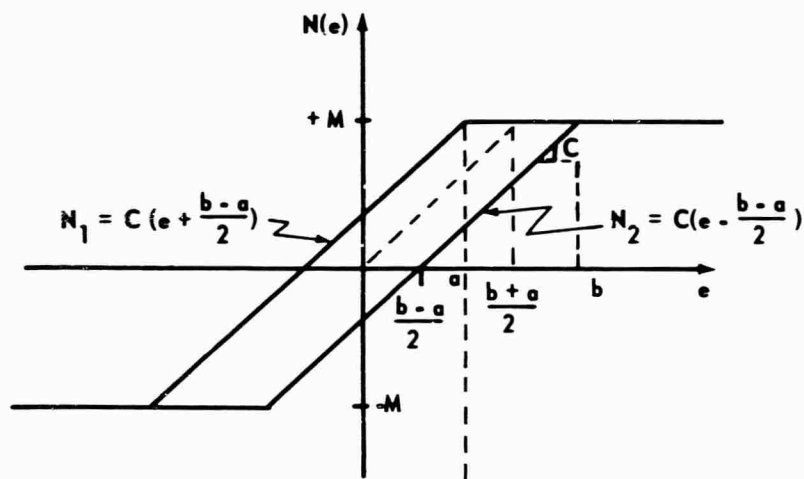


Figure 4.70. Limiter with Hysteresis

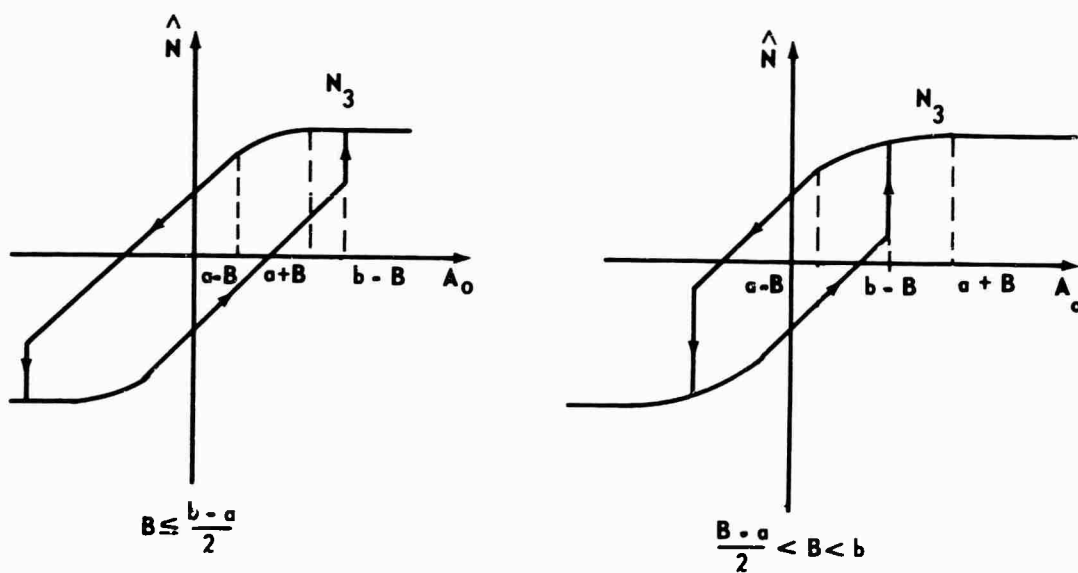


Figure 4.71. Modified Nonlinear Element When $B < b$

$$|\hat{K}(A, B, a, b)| = \sqrt{g_A^2 + h_A^2} \quad (4.118)$$

$$\angle \hat{K}(A, B, a, b) = \tan^{-1} \frac{h_A}{g_A} \quad (4.119)$$

where

$$\begin{aligned}
 g_A &= \frac{2}{\pi A} \int_{-\gamma_2}^{\gamma_4} C \left(A \sin \omega t - \frac{b-a}{2} \right) \sin \omega t \, d\omega t \\
 &+ \frac{2}{\pi A} \int_{\gamma_4}^{\pi-\gamma_2} \frac{C}{2\pi} \left[\pi b - 2a \sin^{-1} \text{sat} \left(\frac{a - A \sin \omega t}{B} \right) \right. \\
 &+ 2A \sin \omega t \sin^{-1} \text{sat} \left(\frac{a - A \sin \omega t}{B} \right) \\
 &\left. - 2B \sqrt{1 - \text{sat} \left(\frac{a - A \sin \omega t}{B} \right)^2} \right] \sin \omega t \, d\omega t \quad (4.120)
 \end{aligned}$$

and

$$\begin{aligned}
 h_A &= \frac{2}{\pi A} \int_{-\gamma_2}^{\gamma_4} C \left(A \sin \omega t - \frac{b-a}{2} \right) \cos \omega t \, d\omega t \\
 &+ \frac{2}{\pi A} \int_{\gamma_4}^{\pi-\gamma_2} \frac{C}{2\pi} \left[\pi b - 2a \sin^{-1} \text{sat} \left(\frac{a - A \sin \omega t}{B} \right) \right. \\
 &+ 2A \sin \omega t \sin^{-1} \text{sat} \left(\frac{a - A \sin \omega t}{B} \right) \\
 &\left. - 2B \sqrt{1 - \text{sat} \left(\frac{a - A \sin \omega t}{B} \right)^2} \right] \cos \omega t \, d\omega t \quad (4.121)
 \end{aligned}$$

Numerical or approximate solutions to the above integrals are required.

Case b (Figure 4.72)

$$(B > b)$$

$$\begin{aligned}
 N_4 &= \frac{C}{2\pi} \left[B(\cos \theta_5 + \cos \theta_3 - \cos \theta_4 - \cos \theta_2) + A_o (\theta_2 + \theta_3 + \theta_4 + \theta_5) \right. \\
 &\left. + b(\theta_5 - \theta_4) + a (\theta_3 - \theta_2) \right] ; \quad A_o < B - b \quad (4.122)
 \end{aligned}$$

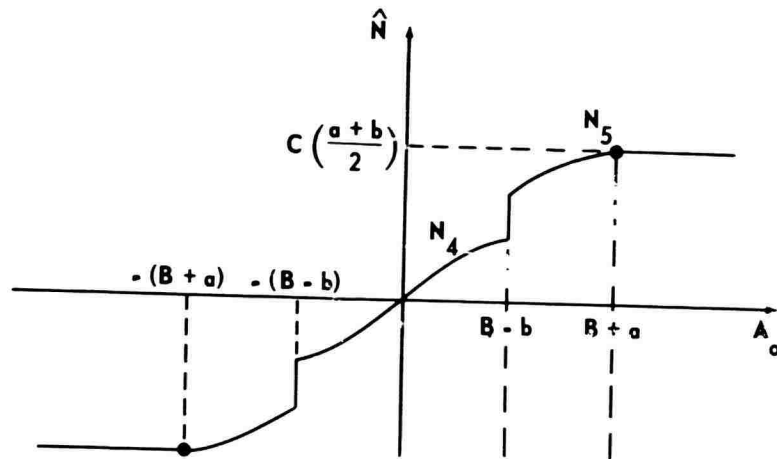


Figure 4.72. Modified Nonlinear Element When $B > b$

$$N_5 = \frac{C}{2\pi} \left[A_0 (\pi + 2\theta_2) + \pi b - 2a\theta_2 - 2B \cos \theta_2 \right] ;$$

$$B - b \leq A_0 . \quad (4.123)$$

$$\begin{aligned} \hat{K}(A, B, a, b) = & \frac{4}{\pi A} \int_0^{\gamma_4} \frac{C}{2\pi} \left\{ B \sqrt{1 - \left(\frac{b + A \sin \omega t}{B} \right)^2} + B \sqrt{1 - \left(\frac{a + A \sin \omega t}{B} \right)^2} \right. \\ & - B \sqrt{1 - \left(\frac{b - A \sin \omega t}{B} \right)^2} - B \sqrt{1 - \left(\frac{a - A \sin \omega t}{B} \right)^2} \\ & + A \sin \omega t \left[\sin^{-1} \left(\frac{a - A \sin \omega t}{B} \right) + \sin^{-1} \left(\frac{b - A \sin \omega t}{B} \right) \right. \\ & + \sin^{-1} \left(\frac{a + A \sin \omega t}{B} \right) + \sin^{-1} \left(\frac{b + A \sin \omega t}{B} \right) \\ & + b \sin^{-1} \left(\frac{b + A \sin \omega t}{B} \right) - b \sin^{-1} \left(\frac{b - A \sin \omega t}{B} \right) \\ & \left. + a \sin^{-1} \left(\frac{a + A \sin \omega t}{B} \right) - a \sin^{-1} \left(\frac{a - A \sin \omega t}{B} \right) \right\} \sin \omega t \, d\omega t \\ & + \frac{4}{\pi A} \int_{-\gamma_4}^{\gamma_3} \frac{C}{2\pi} \left\{ A \sin \omega t \left[\pi + 2 \sin^{-1} \left(\frac{a - A \sin \omega t}{B} \right) \right] \right\} \end{aligned}$$

$$\begin{aligned}
& + \pi b - 2a \sin^{-1} \left(\frac{a - A \sin \omega t}{B} \right) \\
& - 2B \sqrt{1 - \left(\frac{a - A \sin \omega t}{B} \right)^2} \left. \right\} \sin \omega t \, d\omega t + \frac{4M}{\pi A} \cos \gamma_3 \quad . \quad (4.124)
\end{aligned}$$

Triangle Wave Secondary Signal (Figures 4.73 and 4.74)

Case a (Figure 4.71)

$$(B < b)$$

$$N_3 = \frac{C}{4} \left[2 \left(1 + \frac{a}{B} \right) A_0 - \frac{A^2}{B} - B + 2b - \frac{a^2}{B} \right]; \quad (4.125)$$

$$a - B \leq A_0 \leq a + B \quad . \quad (4.126)$$

$$|\hat{K}(A, B, a, b)| = \sqrt{g_A^2 + h_A^2} \quad (4.126)$$

$$\angle \hat{K} = \tan^{-1} \frac{h_A}{g_A} \quad (4.127)$$

where

$$\begin{aligned}
g_A = \frac{C}{\pi A} & \left[A(\gamma_4 + \gamma_2 - \sin \gamma_2 \cos \gamma_2 - \sin \gamma_4 \cos \gamma_4) \right. \\
& + 2b(\cos \gamma_3 + \cos \gamma_4) + a(\cos \gamma_2 + \cos \gamma_3) \\
& + \frac{A}{2} \left(1 + \frac{a}{B} \right) (\gamma_2 + \gamma_3 + \sin \gamma_2 \cos \gamma_2 - \sin \gamma_3 \cos \gamma_3) \\
& + \frac{A^2}{2B} \left(\cos \gamma_3 - \cos \gamma_2 + \frac{1}{3} \cos^3 \gamma_3 - \frac{1}{3} \cos^3 \gamma_2 \right) \\
& \left. + \frac{1}{2} \left(B + \frac{a^2}{B} \right) (\cos \gamma_3 - \cos \gamma_2) \right]; \quad B < \frac{b-a}{2} \quad (4.128)
\end{aligned}$$

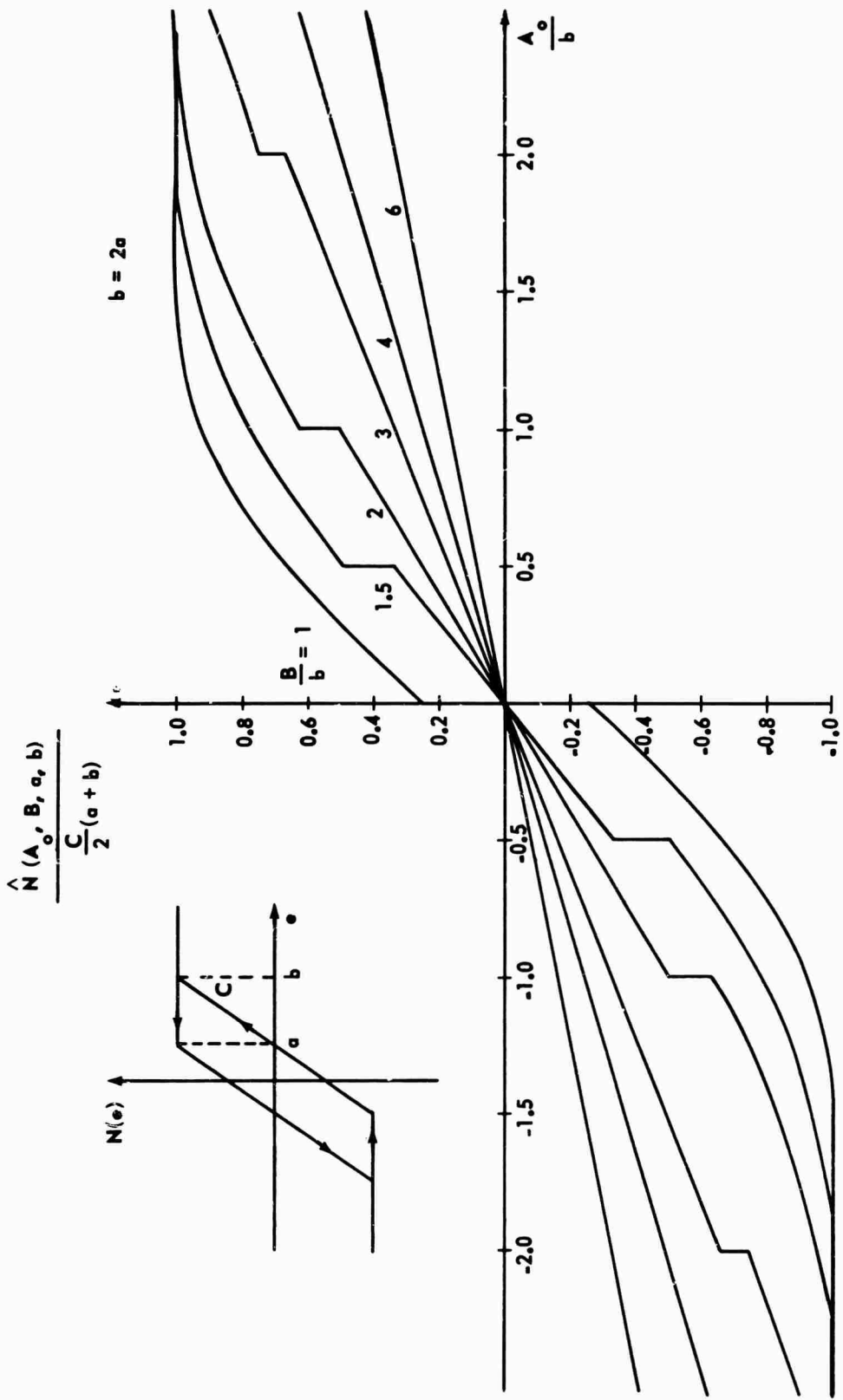


Figure 4.73. Modified Nonlinear Element for Limiter with Hysteresis, Triangle Wave Secondary Signal

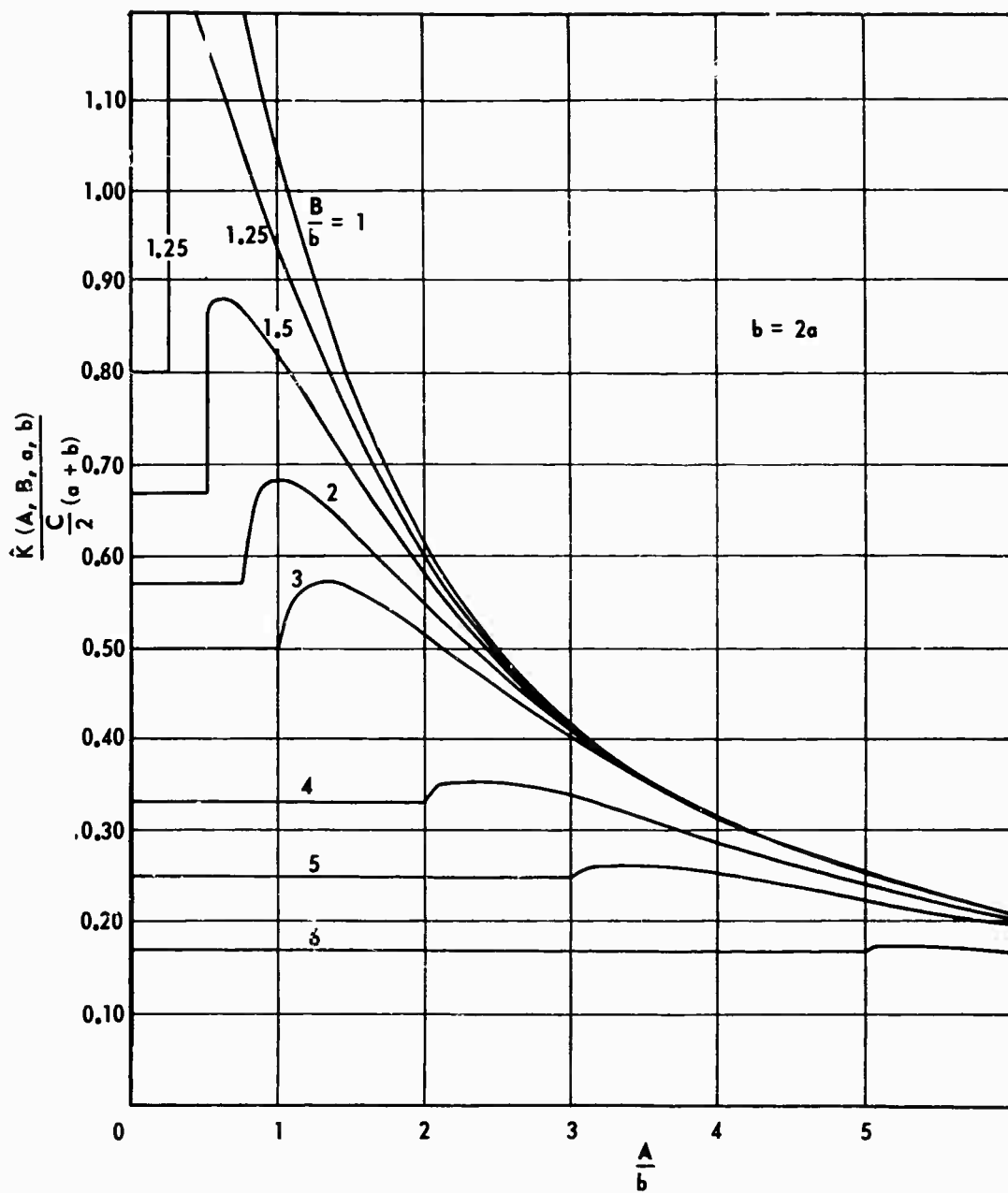


Figure 4.74. DIDF for Limiter with Hysteresis,
Triangle Wave Secondary Signal

$$\begin{aligned}
h_A = \frac{C}{\pi A} & \left[A(\sin^2 \gamma_4 - \sin^2 \gamma_2) - 2b \sin \gamma_4 + a(\sin \gamma_2 + \sin \gamma_3) \right. \\
& + \frac{A}{2} \left(1 + \frac{a}{B} \right) (\sin^2 \gamma_2 - \sin^2 \gamma_3) - \frac{A^3}{3B} (\sin^3 \gamma_2 - \sin^3 \gamma_3) \\
& \left. - \frac{1}{2} \left(B + \frac{a^2}{B} \right) (\sin \gamma_2 - \sin \gamma_3) \right] ; \quad B < \frac{b-a}{2} , \quad (4.129)
\end{aligned}$$

$$\begin{aligned}
g_A = \frac{C}{\pi A} & \left[A(\gamma_2 + \gamma_4 - \sin \gamma_2 \cos \gamma_2 - \sin \gamma_4 \cos \gamma_4 + 2b \cos \gamma_4 \right. \\
& + a(\cos \gamma_2 + 2 \cos \gamma_3 - \cos \gamma_4) + A \left(1 + \frac{a}{B} \right) (2 \gamma_3 - \gamma_4 \\
& - \gamma_2 + \sin \gamma_2 \cos \gamma_2 - 2 \sin \gamma_3 \cos \gamma_3 + \sin \gamma_4 \cos \gamma_4) \\
& - \frac{A^2}{2B} \left(\cos \gamma_2 - 2 \cos \gamma_3 + \cos \gamma_4 - \frac{1}{3} \cos^3 \gamma_2 - \frac{1}{3} \cos^3 \gamma_4 \right. \\
& \left. \left. + \frac{2}{3} \cos^3 \gamma_3 \right) + \left(B + \frac{a^2}{B} \right) (2 \cos \gamma_3 - \cos \gamma_4 - \cos \gamma_2) \right] ; \quad (4.130)
\end{aligned}$$

$$\frac{b-a}{2} \leq B \leq b ,$$

and

$$\begin{aligned}
h_A = \frac{C}{\pi A} & \left[A(\sin^2 \gamma_4 - \sin^2 \gamma_2) - 2b \sin \gamma_4 + a(\sin \gamma_4 + \sin \gamma_2) \right. \\
& + \frac{\pi}{2} \left(1 + \frac{a}{B} \right) (\sin^2 \gamma_2 - \sin^2 \gamma_4) - \frac{A^2}{3B} (\sin^3 \gamma_2 - \sin^3 \gamma_4) \\
& \left. - \frac{1}{2} \left(B + \frac{a^2}{B} \right) (\sin \gamma_2 - \sin \gamma_4) \right] ; \quad \frac{b-a}{2} \leq B \leq b . \quad (4.131)
\end{aligned}$$

Case b (Figure 4.62)

$$(B \geq b)$$

$$N_4 = C \left(\frac{a+b}{2} \right) \frac{A_0}{B} ; \quad A_0 < B - b \quad (4.132)$$

$$N_5 = \frac{C}{4} \left[2 \left(1 + \frac{a}{B} \right) A_0 - \frac{A_0^2}{B} - B + 2b - \frac{a^2}{B} \right]; \quad (4.133)$$

$$B - b \leq A_0 \leq B + a$$

$$\hat{N}(A_0, B, a, b, c) = M; \quad A_0 > B + a \quad (4.134)$$

$$\begin{aligned} \hat{K}(A, B, a, b, c) = & \frac{C}{\pi} \left(\frac{a+b}{B} \right) (-\gamma_4 + \sin \gamma_4 \cos \gamma_4) \\ & + \left(1 + \frac{a}{B} \right) (\gamma_3 + \gamma_4 - \sin \gamma_4 \cos \gamma_4 \\ & - \sin \gamma_3 \cos \gamma_3) - \frac{A}{B} (\cos \gamma_4 - \cos \gamma_3 \\ & + \frac{1}{3} \cos^3 \gamma_3 - \frac{1}{3} \cos^3 \gamma_4) \\ & + \frac{1}{A} \left(2b - B - \frac{a^2}{B} \right) (\cos \gamma_4 - \cos \gamma_3) \\ & + \frac{2}{A} (b + a) \cos \gamma_3 \Big]; \quad B > b \quad (4.135) \end{aligned}$$

Square Wave Secondary Signal (Figures 4.75 and 4.76)

Case a (Figure 4.77)

$$(B < b)$$

$$N_3 = \frac{C}{2} (A_0 + b - B); \quad B - b < A_0 < B + a \quad (4.136)$$

$$g_A = \frac{c}{\pi A} \left[\frac{A}{2} (2\gamma_4 + \gamma_2 + \gamma_3 - 2 \sin \gamma_4 \cos \gamma_4 - \sin \gamma_2 \cos \gamma_2 - \sin \gamma_3 \cos \gamma_3) \right. \\ \left. - 2b \cos \gamma_3 + a(\cos \gamma_2 + \cos \gamma_3) + B(\cos \gamma_3 - \cos \gamma_2) \right];$$

$$B < \frac{b-a}{2} \quad (4.137)$$

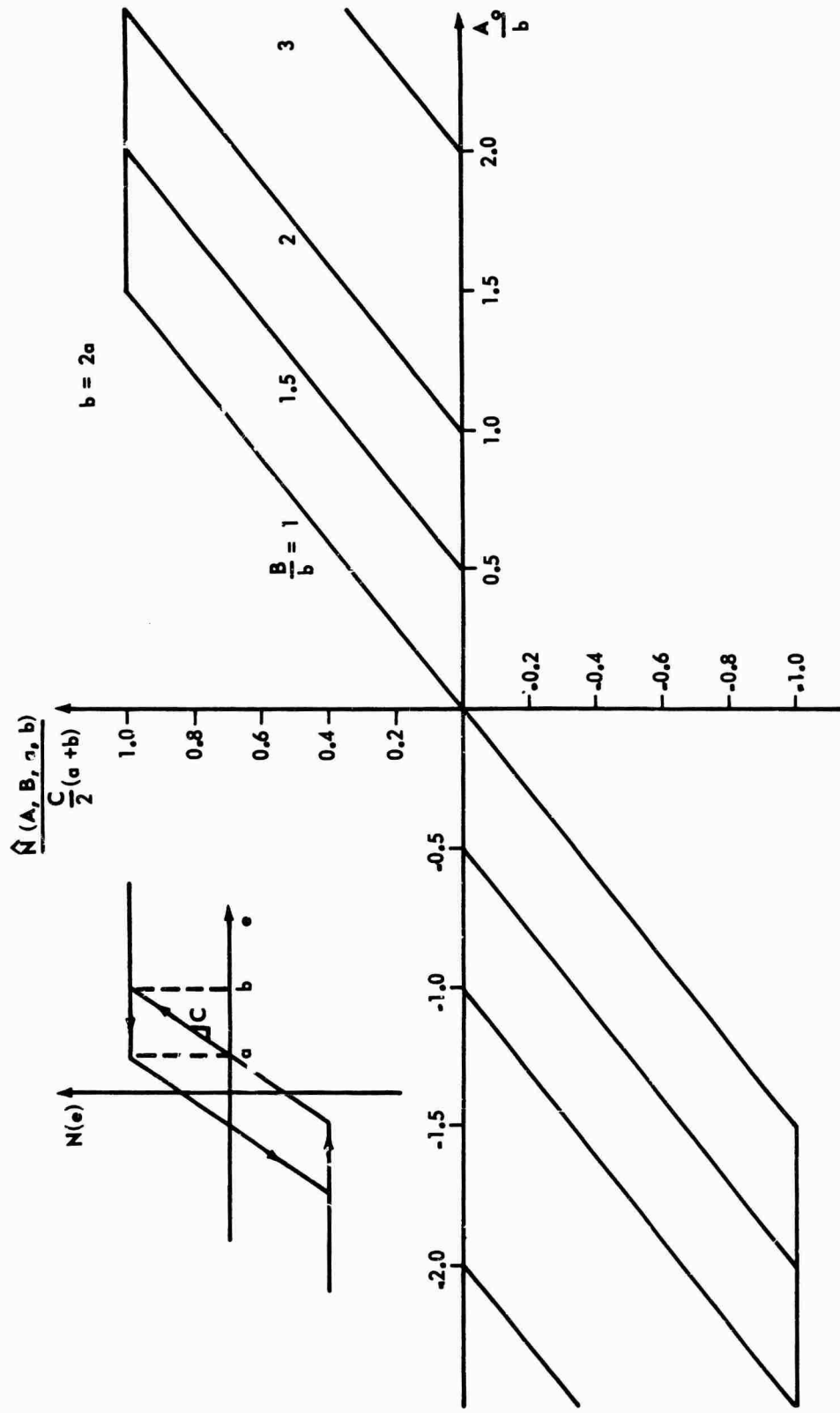


Figure 4.75. Modified Nonlinear Element for Limiter with Hysteresis, Square Wave Secondary Signal

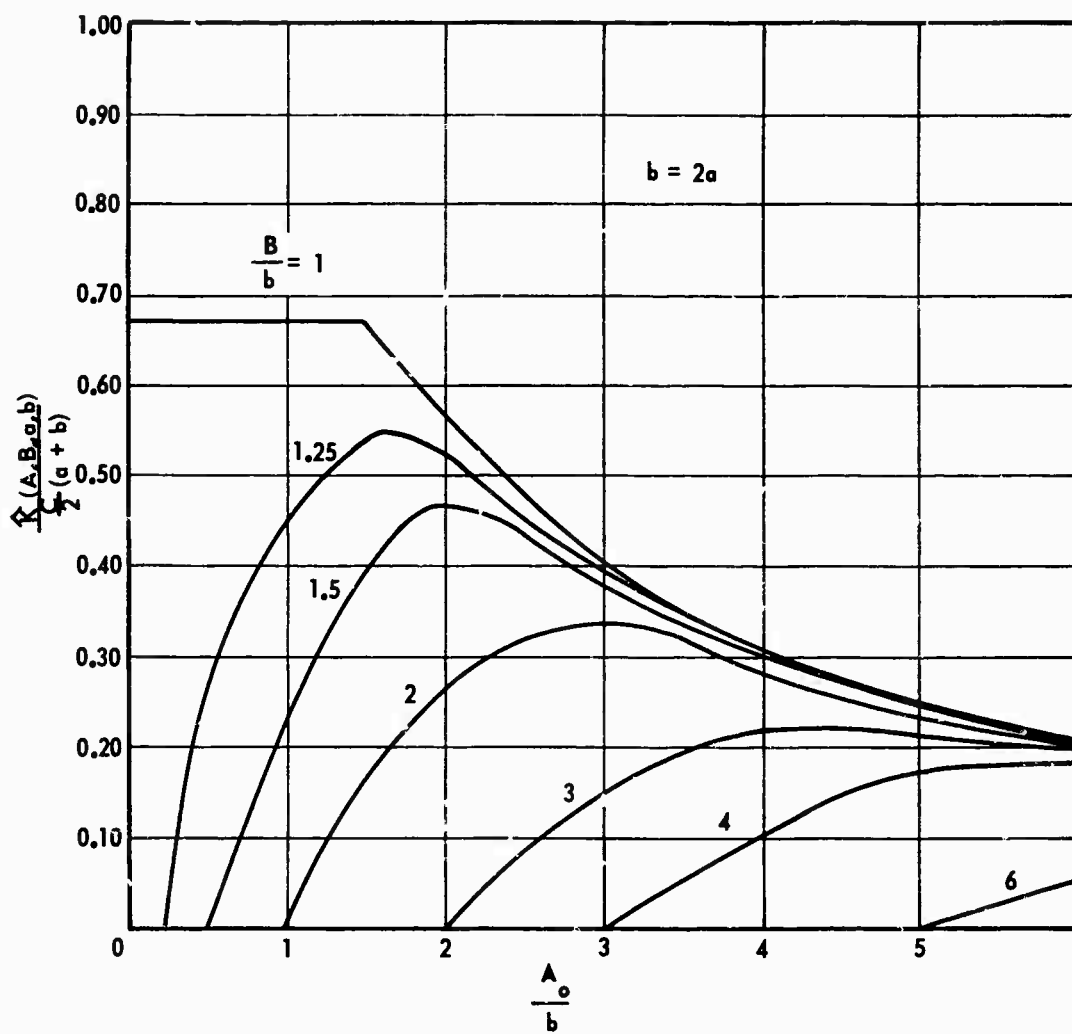


Figure 4.76. DIDF for Limiter with Hysteresis, Square Wave Secondary Signal

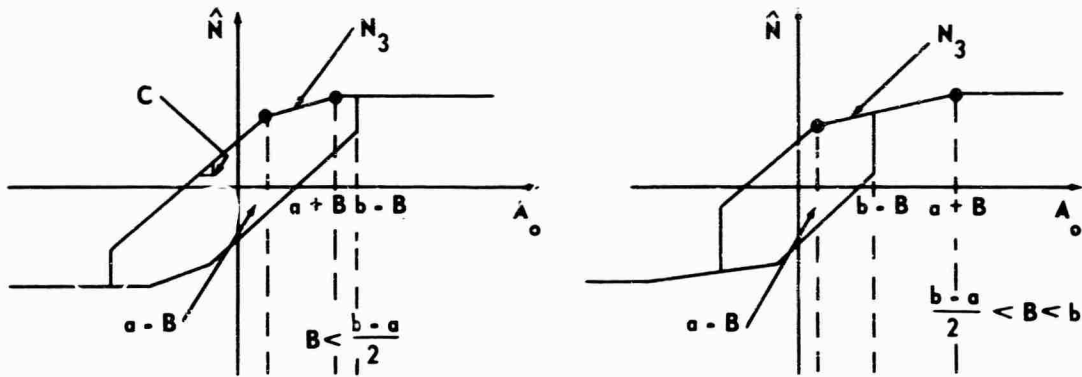


Figure 4.77. Modified Nonlinear Element When $B < b$ for the Square Wave Secondary Signal

$$h_A = \frac{C}{\pi A} \left[\frac{A}{2} (2 \sin^2 \gamma_4 - \sin^2 \gamma_2 - \sin^2 \gamma_3) + b(\sin \gamma_4 - \sin \gamma_2) + a(\sin \gamma_4 + \sin \gamma_3) + B(\sin \gamma_3 - \sin \gamma_2) \right] ;$$

$$B < \frac{b-a}{2} . \quad (4.138)$$

$$g_A = \frac{C}{\pi A} \left[\frac{A}{2} (\gamma_4 + \gamma_2 + 2\gamma_3 - \sin \gamma_4 \cos \gamma_4 - \sin \gamma_2 \cos \gamma_2 - 2 \sin \gamma_3 \cos \gamma_3) + \frac{b}{2} (3 \cos \gamma_4 - \cos \gamma_2 - 2 \cos \gamma_3) + a(\cos \gamma_2 - \cos \gamma_4) \right] ;$$

$$\frac{b-a}{2} < B < b , \quad (4.139)$$

$$h_A = \frac{C}{\pi A} \left[\frac{A}{2} (\sin^2 \gamma_4 - \sin^2 \gamma_2) + \frac{b}{2} (3 \sin \gamma_2 - 2 \sin \gamma_3 - 3 \sin \gamma_4) + \frac{a}{2} (3 \sin \gamma_2 - 2 \sin \gamma_3 + \sin \gamma_4) + B(\sin \gamma_4 - \sin \gamma_2) \right] ;$$

$$\frac{b-a}{2} < B < b . \quad (4.140)$$

Case b (Figure 4.78)

$$(B \geq b)$$

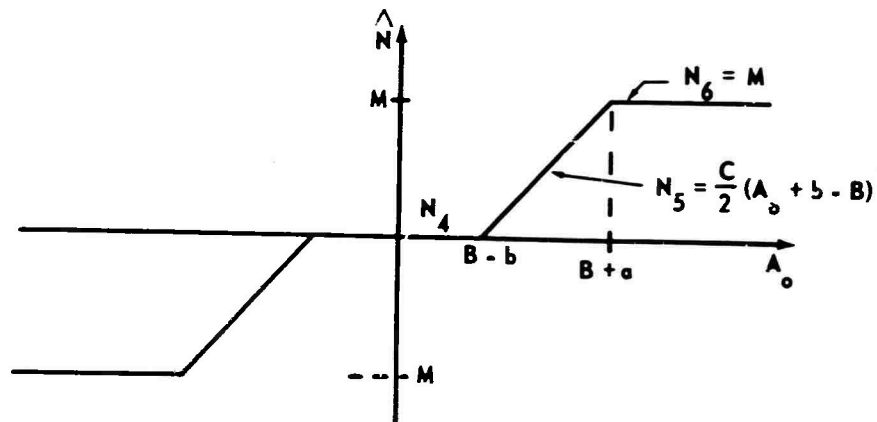


Figure 4.78. Modified Nonlinear Element When $B > b$ for the Square Wave Secondary Signal

$$\hat{N}(A, B, a, b) = \frac{C}{2} \left[(B + a) \text{sat} \left(\frac{A_0}{B + a} \right) - (B - b) \text{sat} \left(\frac{A_0}{B - b} \right) \right] \quad (4.141)$$

$$K(A, B, a, b) = \frac{2C}{\pi A} \left[\frac{A}{2} (\gamma_3 + \gamma_4 - \sin \gamma_3 \cos \gamma_3 - \sin \gamma_4 \cos \gamma_4) + b \cos \gamma_4 + a \cos \gamma_3 + B(\cos \gamma_3 - \cos \gamma_4) \right] ; \quad (4.142)$$

$$B > b$$

CHAPTER V

TWO-SINUSOID INPUT DF FOR RELAY WITH HYSTERESIS

In this chapter the TSIDF is calculated for the relay with hysteresis, taking into account the frequency ratio of the input components. This is done by using the "Average DIDF" method explained in Chapter II. The nonlinear element is defined in Figure 5.1 and the essential mathematical steps are indicated in the following equations:

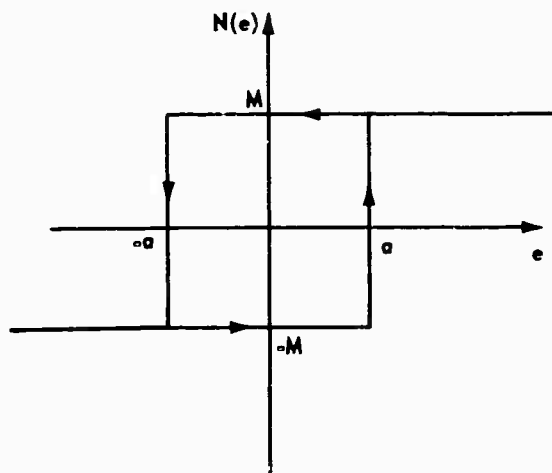


Figure 5.1. Relay with Hysteresis

$$K_r = \hat{K}_r(A, B, n) = \frac{1}{2\pi^2 A} \int_0^{2\pi} d\phi \int_0^{2\pi} N[A \sin p\omega t + B \sin (q\omega t + \phi)] \sin p\omega t d\omega \quad (5.1)$$

$$K_i = \hat{K}_i(A, B, n) = \frac{1}{2\pi^2 A} \int_0^{2\pi} d\phi \int_0^{2\pi} N[A \sin p\omega t + B \sin (q\omega t + \phi)] \cos p\omega t d\omega \quad (5.2)$$

$$|\hat{K}| = \sqrt{K_r^2 + K_i^2} \quad (5.3)$$

$$\angle \hat{K} = \tan^{-1} \frac{K_i}{K_r} \quad (5.4)$$

where K_r , K_i , $|\hat{K}|$, and $\angle \hat{K}$ are the real part, imaginary part, magnitude, and phase, respectively, of the DIDF. The primary component in the input signal is

$$e_1 = A \sin p\omega t \quad (5.5)$$

and the secondary component of the input signal is

$$e_2 = B \sin (q\omega t + \phi) \quad (5.6)$$

It is not necessary to identify input frequencies p and q since only the frequency ratio $n = q/p$ is important. However, they have been included in the formulation for computational purposes. This will be explained further in the discussion which follows.

It was stated in Chapter II that the average DIDF as computed for multivalued nonlinear elements has meaning only when n is an irrational number. However, only integers are chosen for p and q in this analysis and it must be kept in mind that the resulting DIDF holds only for irrational frequency ratios in close proximity to the chosen n . Although a closed form solution can be found for the DIDF when n equals one, it is doubtful that the integrals of Equations (5.1) and (5.2) can be solved analytically when n is other than one. It would be an important contribution if only the first indicated integration could be performed analytically as in the modified

nonlinear element method. However, it appears that even this cannot be done and for this reason a double integration by some numerical technique is usually required. Therefore, when a DIDF is calculated with a digital computer, one can expect to use a relatively large amount of computer time.

In this chapter, the results of a digital computer solution are presented in the form of graphs. Nine values of n and four values of B/a are chosen. A table of seventeen ϕ 's was set up for "averaging" the DIDF and performing the second integration. The $\Delta\omega t$ increments used for carrying out the first integration were approximately one degree. It was found that the size of the $\Delta\phi$ increments did not affect the accuracy of the final answer to the same extent as the size of the $\Delta\omega t$ increments. The increment for the second integration was chosen as $\Delta\phi = 2\pi/16$ because of limited available computer time.

Several restrictions must be kept in mind when working with the multivalued nonlinear elements. First, the nature of the nonlinear element requires that each succeeding ωt increment in the integration routine be larger than the previous one; that is, ωt must always increase (decrease). Some integration routines are thus not suited for integrating multivalued functions. Second, a different answer is obtained for any one particular integration depending upon the assumed initial output state of the nonlinear element when the integration limits are 0 to 2π . This is apparent even in sinusoidal DF analysis where the correct procedure is obvious. The correct procedure in the DIDF case required finding the angle ωt_1 ($0 \leq \omega t_1 \leq 2\pi$) where the first "switch," if any, occurred at the nonlinear element output (Figure 5.2). The integration

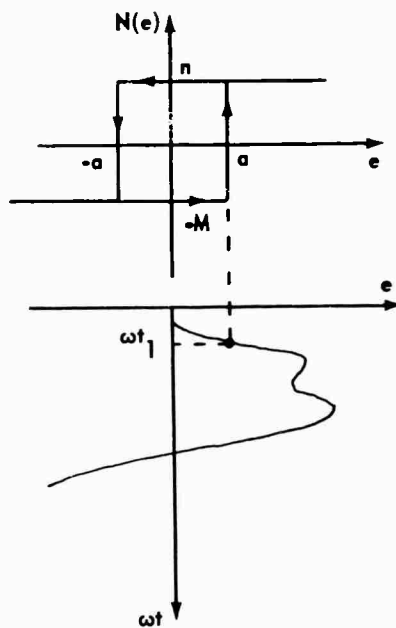


Figure 5.2. Composite Input Signal for Defining Switching Point

interval in this case was $\omega t = \omega t_1$, to $2\pi + \omega t_1$. There are certain values of A , B , and ϕ for which ωt_1 cannot be found and the integral is zero. The program was also run with the integration limits $\omega t = 0$ to $\omega t = 2\pi$, where the hysteretic relay output was set to $-M$ at the beginning of each integration cycle. Some discrepancy was noted for the parameter ranges $1 < A + B < 2$ where n was close to one. Otherwise both procedures gave essentially the same results.

Fourier Series analysis requires that the integration limits be over an entire period. Thus when $n \geq 1$, p was set to one and q was made to take on integer values. When $n < 1$, q was set to one and p was made to take on integer values. The resulting DIDF's are shown in Figures 5.3 to 5.11. It is seen that the magnitude of the DIDF shows relatively little dependence on the frequency ratio n when $n > 3$. However, the phase angle of the DIDF is

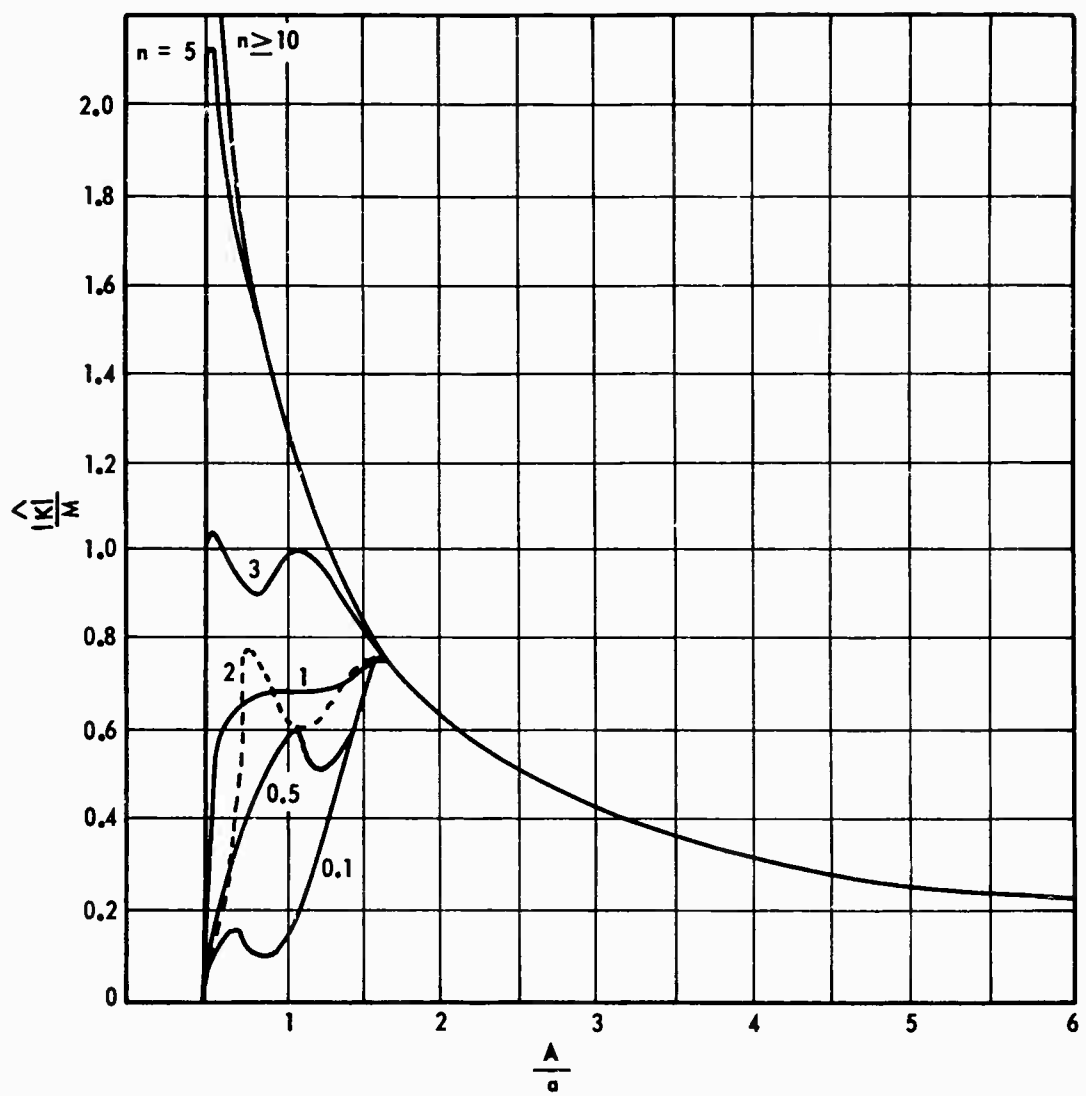


Figure 5.3. Magnitude of DIDF of Relay with Hysteresis When $B/a = 0.5$

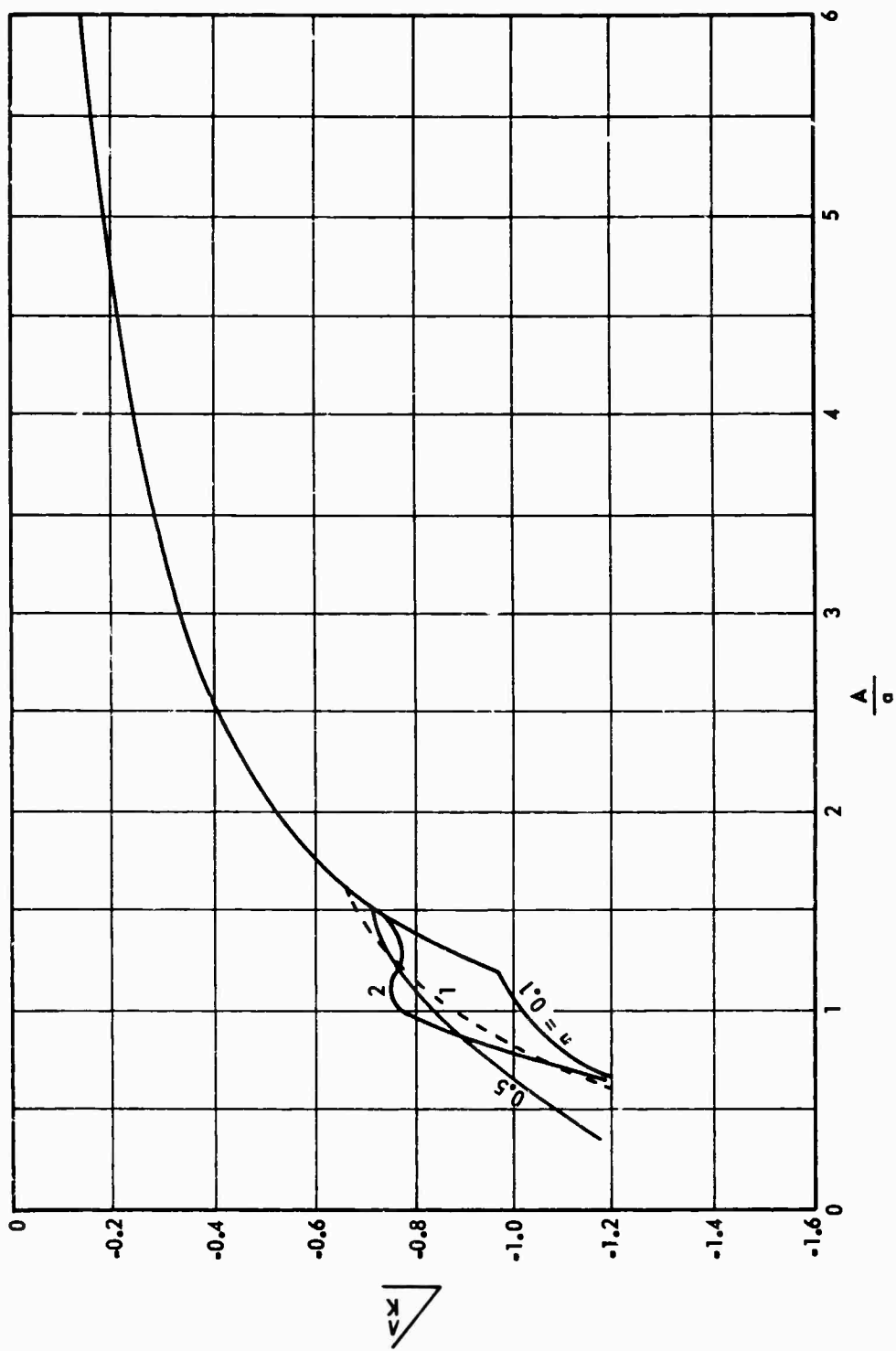


Figure 5.4. Phase of DIDF of Relay with Hysteresis When $B/a = 0.5$

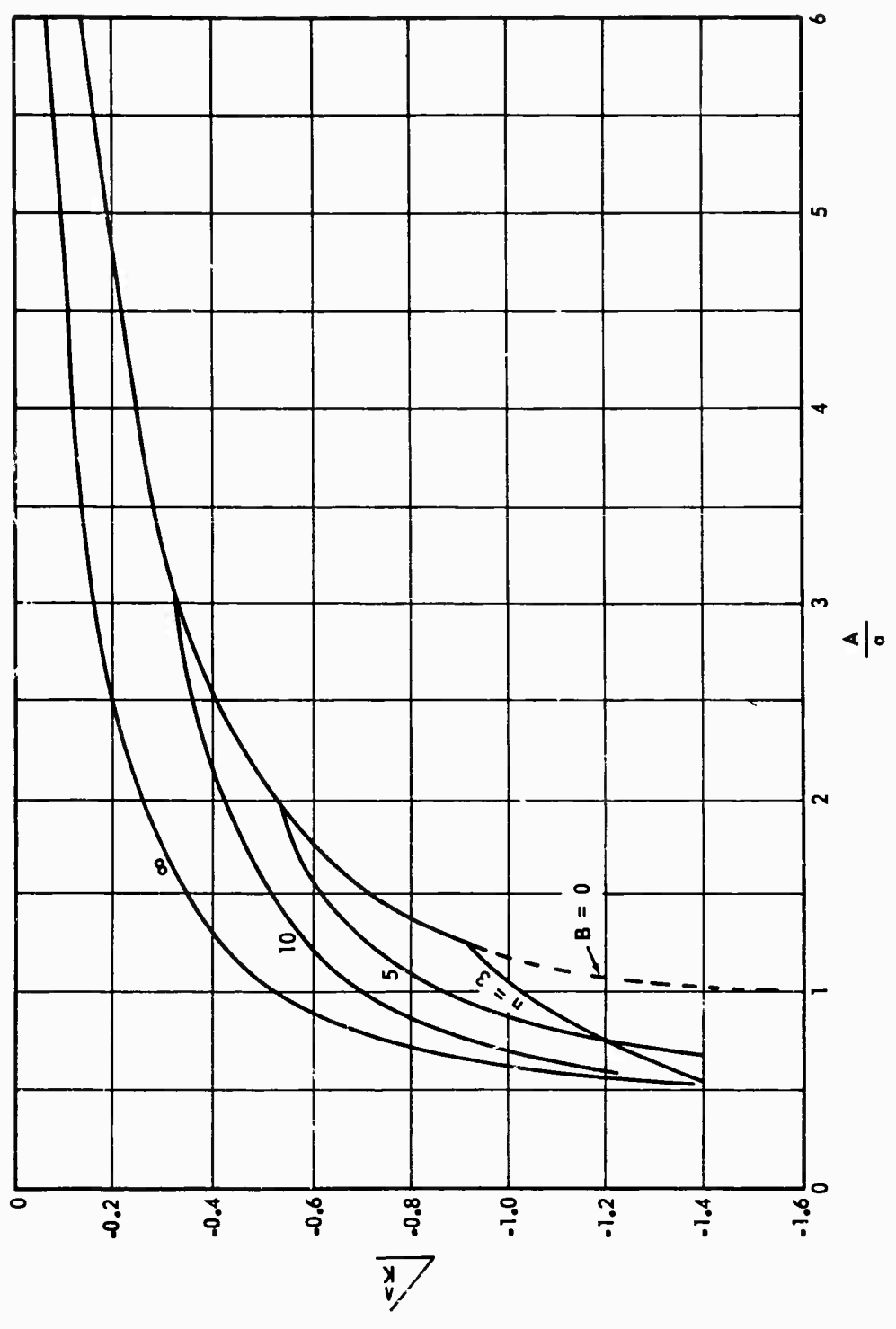


Figure 5.5. Phase of DIDF of Relay with Hysteresis When $B/a = 0.5$

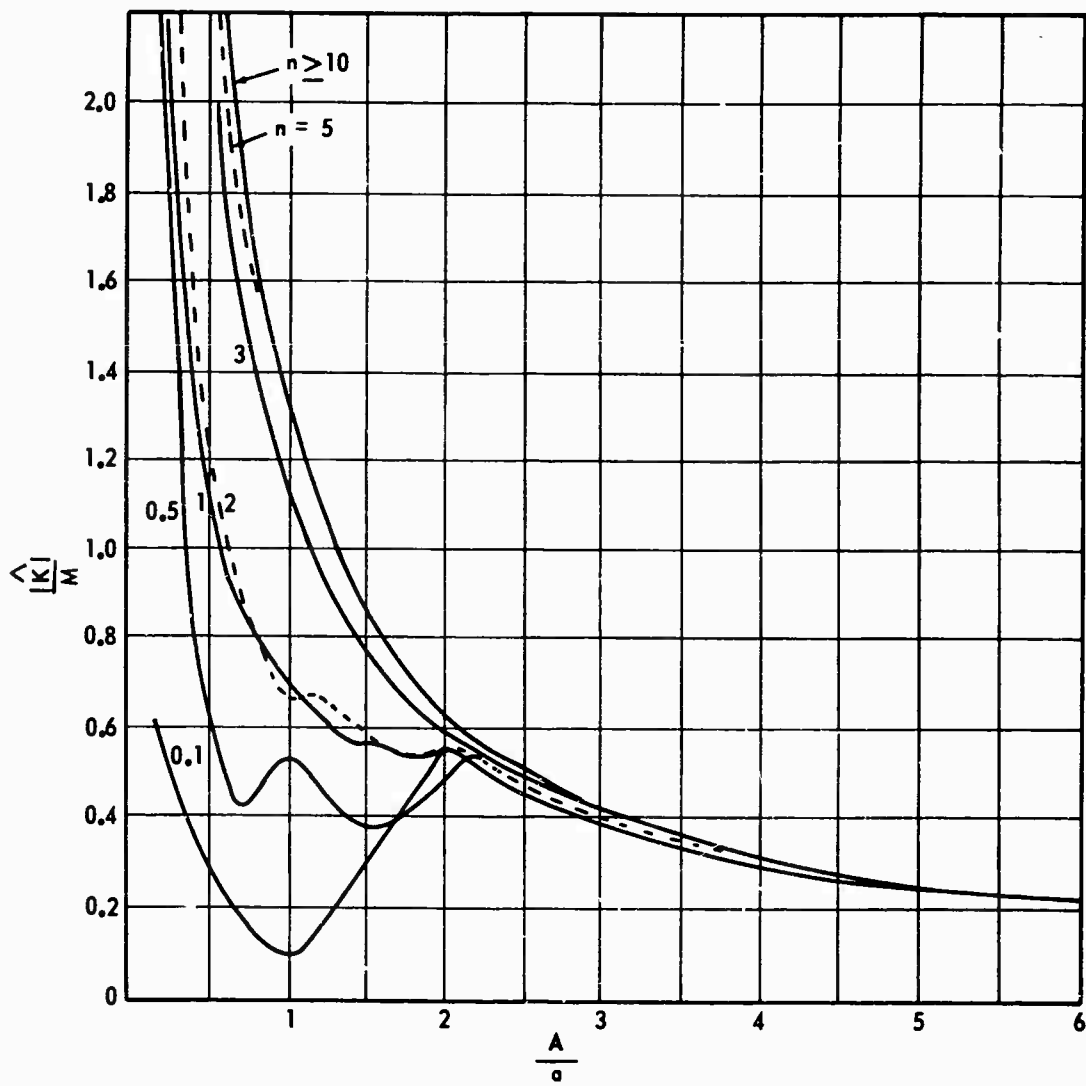


Figure 5.6. Magnitude of DIDF of Relay with Hysteresis When $B/a = 1.0$

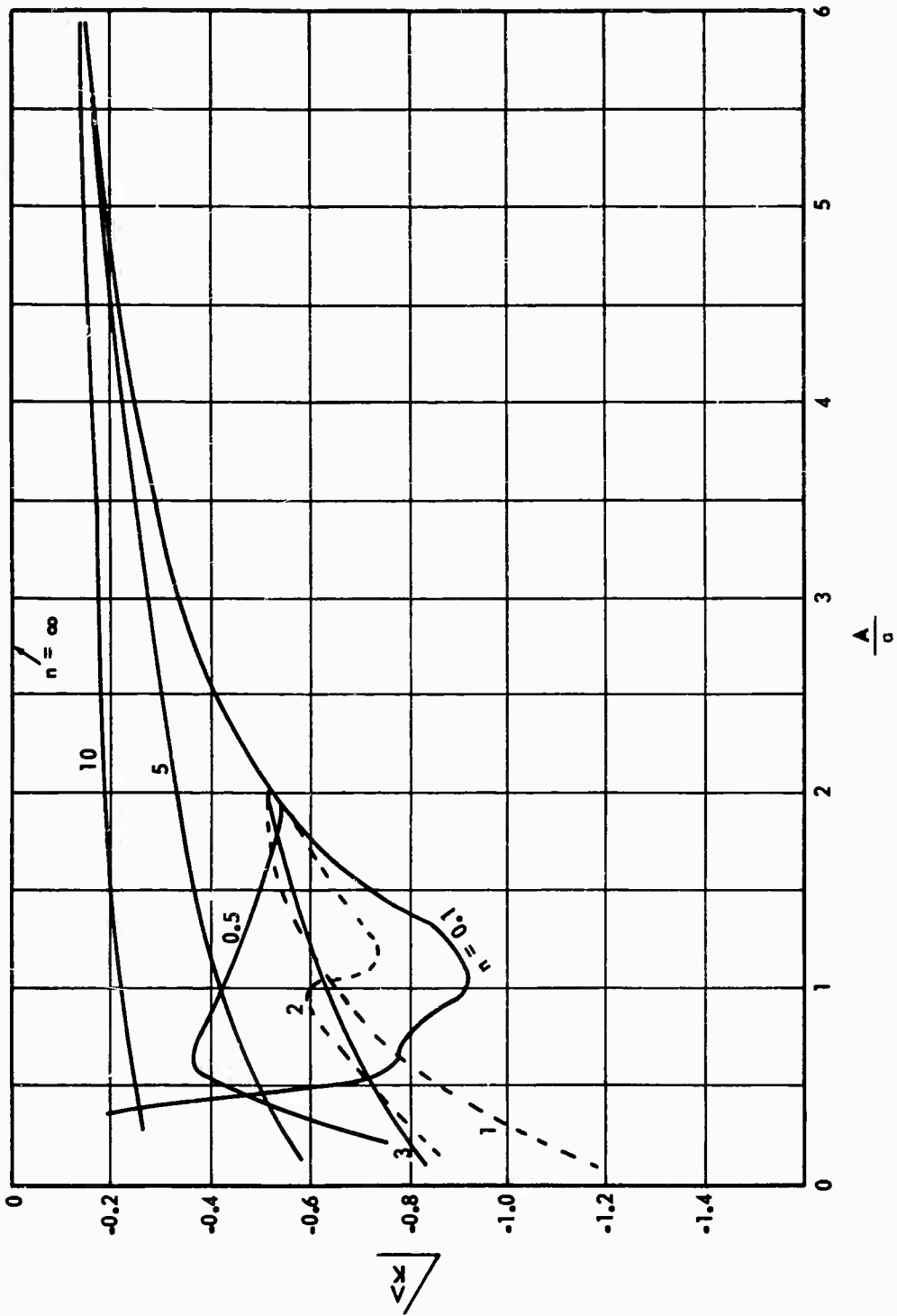


Figure 5.7. Phase of DIDF of Relay with Hysteresis When $B/a = 1.0$

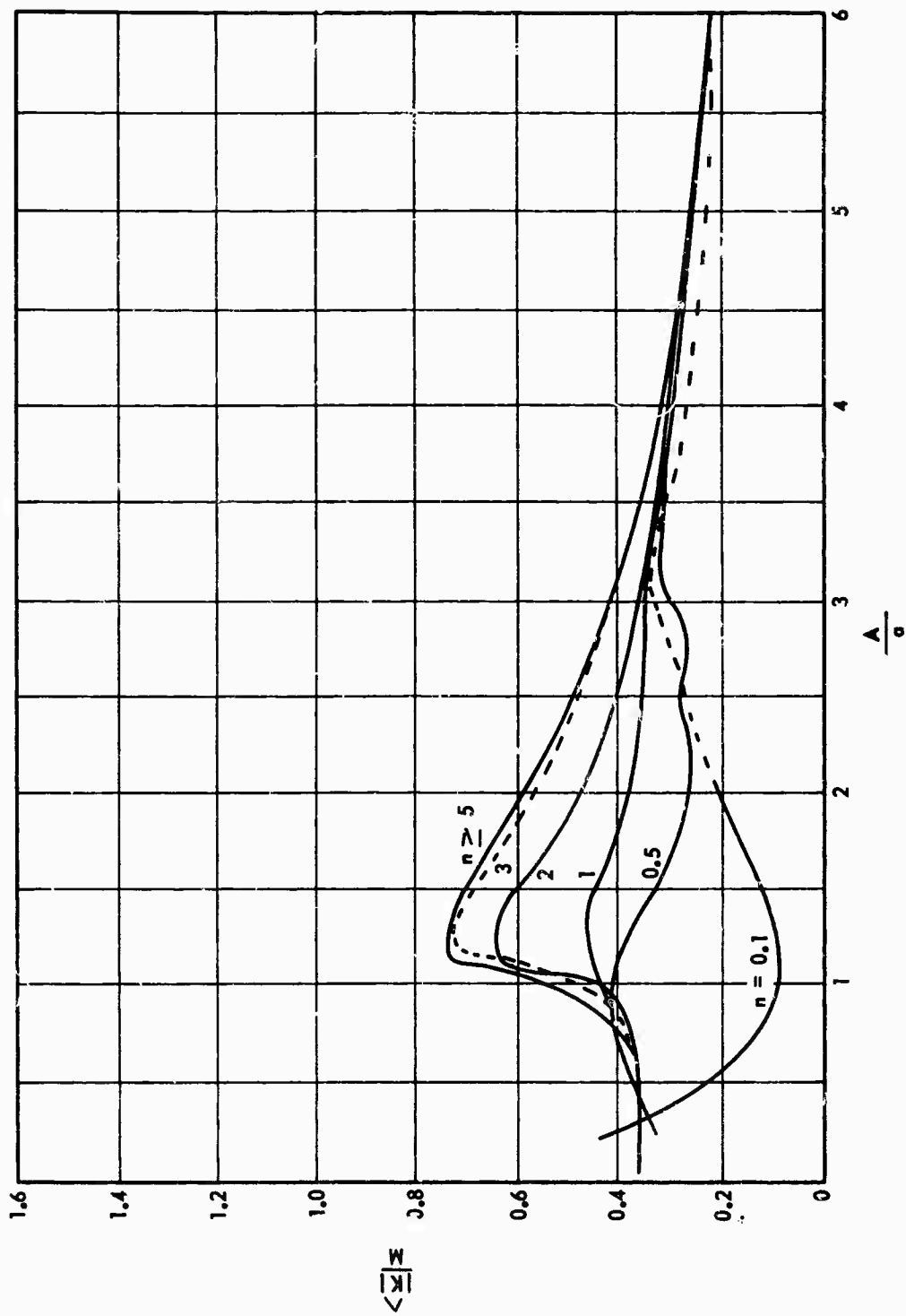


Figure 5.8. Magnitude of DIDF of Relay with Hysteresis When $B/a = 2.0$

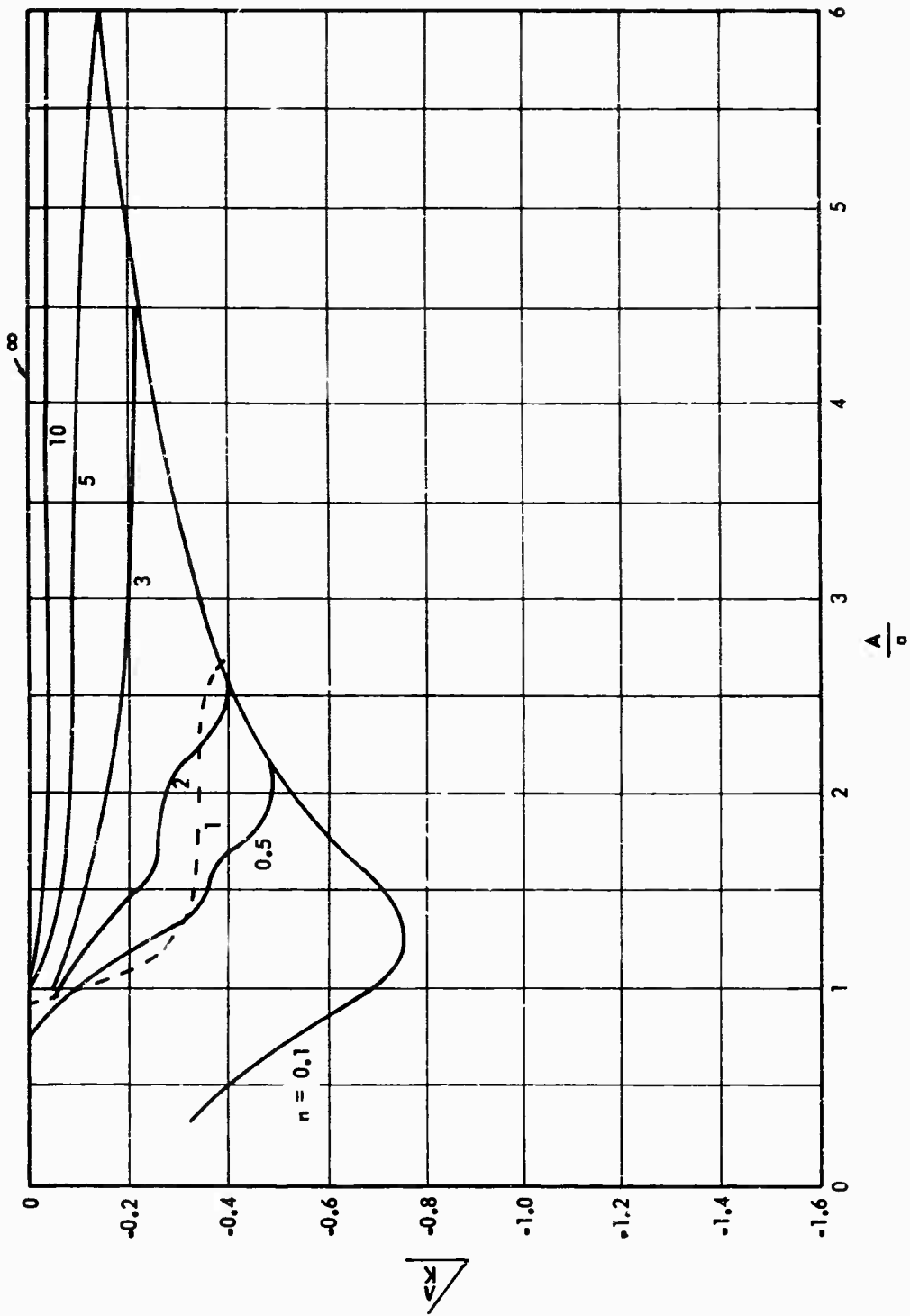


Figure 5.9. Phase of DDF of Relay with Hysteresis When $B/a = 2.0$

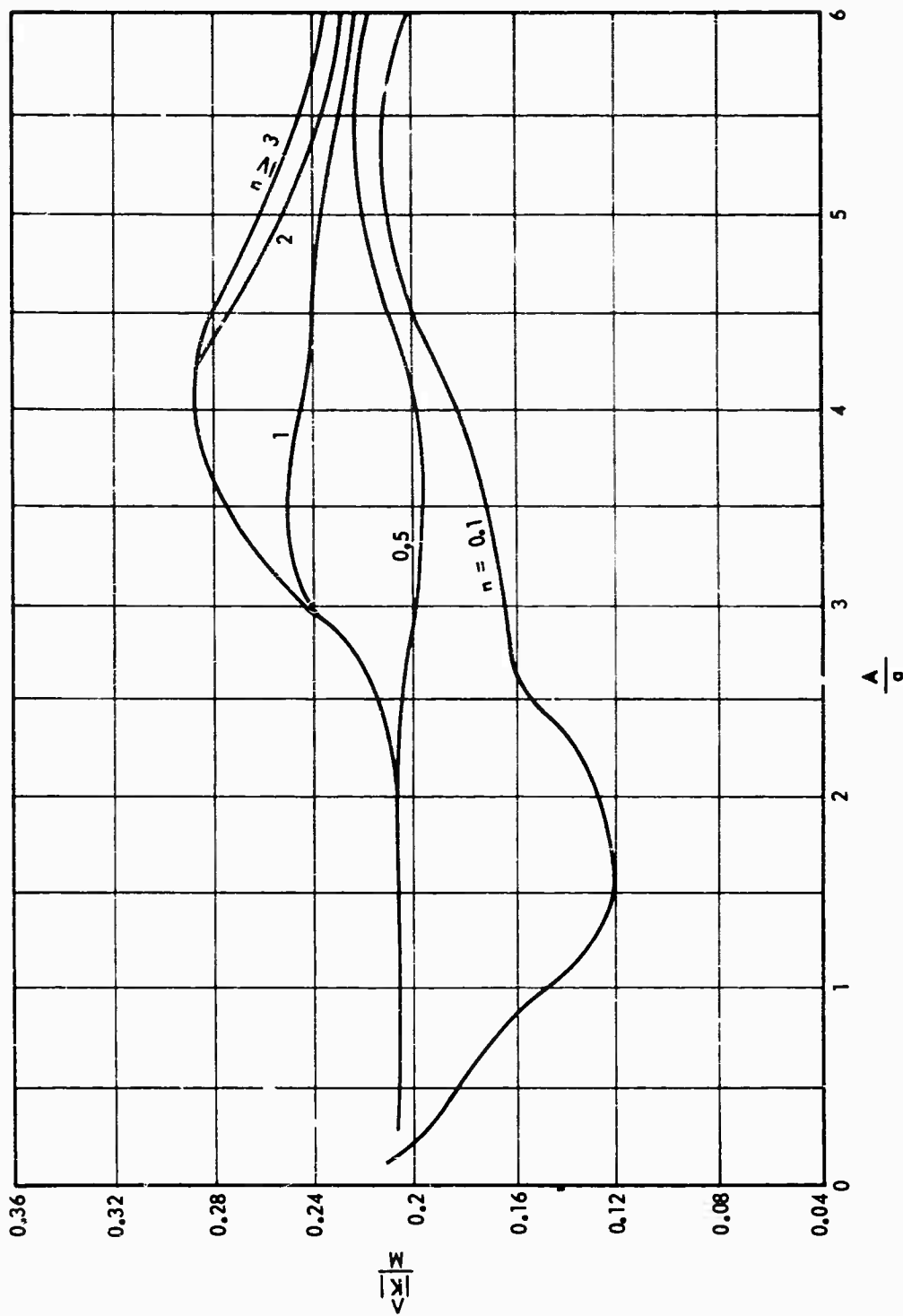


Figure 5.10. Magnitude of DIDF of Relay with Hysteresis When $B/a = 4.0$

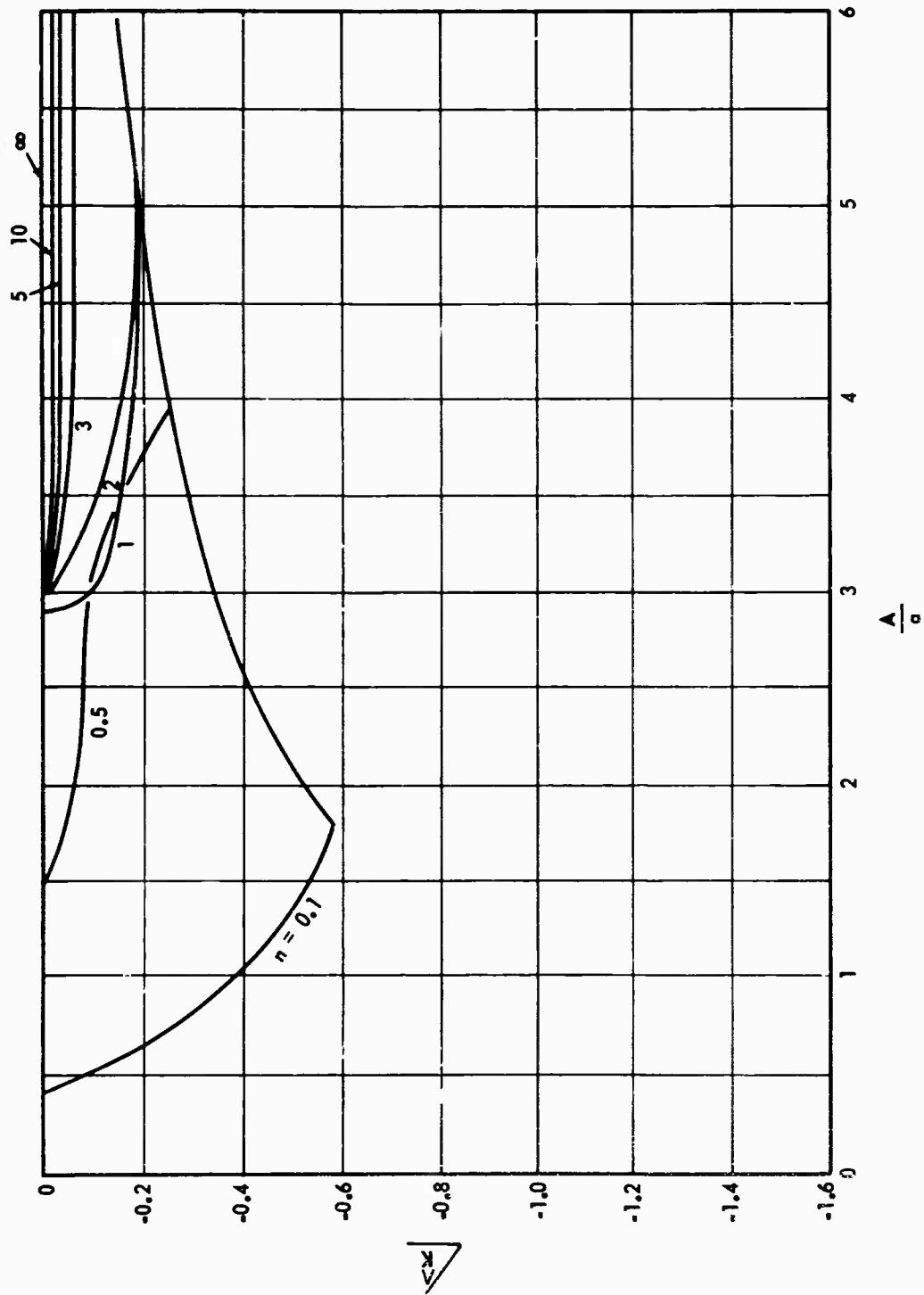


Figure 5.11. Phase of DIDF of Relay with Hysteresis When $B/a = 4.0$

strongly dependent upon n , especially when $B/a < 4$. It is noted that when n becomes sufficiently large, the DIDF of this method approaches that obtained with the modified nonlinear element method. In that case the phase shift across the nonlinear element goes to zero for the relay with hysteresis when $B/a \geq 1$. It has been implied by previous investigations [10,40,41] that the modified nonlinear element is valid for multivalued nonlinear elements when $n \geq 10$. The DIDF's given in this chapter show that a more severe restriction is required in some cases. For example, when $B/a = 1$, $A/a = 1.5$, and $n = 10$, the average phase shift of the DIDF is -11.4 degrees, whereas the modified nonlinear element method predicts that the average phase shift will be zero.

The DIDF presented in this chapter in graphical form does not agree with the one given by Mahalanabis and Oldenburger [31] because the frequency ratio n does not appear in their DIDF. Therefore, the DIDF of Mahalanabis and Oldenburger is adequately presented by only one graph sheet showing the magnitude and one graph sheet showing the phase. The authors imply that the frequency of the secondary signal may be either higher or lower than the primary component frequency. It appears, however, that their approximate DIDF expression is only correct for a band limited noise secondary signal with a low frequency spectrum. Their phase curves appear to compare with those given in this chapter when n is somewhere between 1 and 2.

CHAPTER VI

CONCLUSIONS AND RECOMMENDATIONS FOR FUTURE WORK

The author's literature search of the published methods for calculating the DIDF revealed that the modified nonlinear element concept, first proposed for single valued nonlinear elements by Sommerville and Atherton [9], is still one of the most widely used methods. It is especially useful when the secondary signal is a nonsinusoidal deterministic function. However, its use in determining the DIDF for multivalued nonlinear elements is much more restricted than for single valued nonlinear elements.

It appears that the inverse DIDF problem as posed in Chapter III will be difficult to apply in the case of a general nonlinear element. This inverse DIDF problem consists of finding the waveform of a secondary signal which will result in a specified modified nonlinear element. This problem was solved for a restricted class of nonlinear elements and it was shown that a general equation for the DIDF of certain nonlinear elements may be found without regard to the waveform of the secondary signal. In particular it was shown that only the coefficients in the equation are altered (not deleted) when the waveform of the secondary signal is changed. If the order of the equation describing $N(e)$ is p then the order of the equation describing the modified nonlinear element is not

lower than $p - 1$, although it may be larger than p . Thus when the order of the predominant terms in the equation describing $N(e)$ is large, the secondary signal waveform has little effect on the appearance or characteristics of the modified nonlinear element. Such examples serve to indicate that the use of the inverse DIDF procedure as a synthesis tool will be of limited value. In this connection it was observed that a very wide range in the characteristics of the modified nonlinear element of the relay function [$N(e)$ is zero order] could be affected by a change in the secondary signal waveform. Thus the proposal of Oldenburger and Ikebe, in which a relay function is inserted ahead of a given nonlinear element in conjunction with the secondary signal of Equation (3.20) in this thesis, provides a versatile synthesis tool with which to change existing nonlinear characteristics to desirable ones.

The modified nonlinear element and DIDF curves given in Chapter IV suggest that undesirable nonlinear characteristics may often be modified to give acceptable characteristics by the proper choice of a secondary input signal. These DIDF and modified nonlinear element curves should be beneficial in certain synthesis problems.

The average DIDF method given in Chapter II provides an alternate procedure for calculating the DIDF. This method reduces to a fairly simple and compact form when the nonlinear element is single valued and both components of the input are sine waves. Examples show that in such a case the average DIDF method may involve less computational work than the modified nonlinear element method. The average DIDF method also complements the modified nonlinear element method in giving physical interpretation to the DIDF,

although the intermediate step of the latter method is more useful.

The literature search revealed that very few useful results have been published on effective procedures for calculating the DIDF for multivalued nonlinear elements. One exception is the application [16,30] of the modified nonlinear element method which is limited to the case when $n \gg 1$ or its extension [16] which holds when $n \ll 1$. In this thesis the incorrectness of some of the alternative procedures which have been proposed in previous publications has been demonstrated. Mahalanabis and Oldenburger [31] have recently published a paper in which they offer a new procedure based upon an "envelope" description of the dual input. In this way, they obtain a single expression for the DIDF which does not include n as a parameter but which, they assert, holds for both $n > 1$ and $n < 1$. It would seem to this writer that if the modified nonlinear element is incorrect for multivalued nonlinear elements, then any correct method must include the frequency ratio n in the analysis and final answer.

The average DIDF method offers such a procedure. It suffers from the amount of computer time required to give a complete solution and the number of graphs required for presentation in graph form. The TSIDF of the relay with hysteresis was calculated by this method and presented in Chapter V. Unfortunately the order of integration cannot be reversed in the double-integral formulation [Equations (2.12) and (2.13)] when $N(e)$ is multivalued. However, this is in essence what is done when the modified nonlinear element method is incorrectly applied to multivalued nonlinear elements and results in the same answers. An approximate method for solving the first or both

integrals by analytical means would be very helpful. Further studies in this area might prove fruitful.

Some experimentally determined DIDF's for common-multivalued type nonlinear elements would be of benefit to the control engineer. For example in pulse width modulation (PWM) control systems incorporating a controller actuator which is characterized by a relay with hysteresis or saturation with hysteresis, it is not uncommon to have an n of 6 or 8. However, the secondary signal would usually be a triangle wave in the PWM system.

The average DIDF method may be extended to incorporate an input consisting of the sum of three or more sinusoidal functions. Some useful approximate results might be obtained in such an investigation if one restricts attention to single valued nonlinear elements where the parameter n may be set equal to unity.

APPENDIX

EXAMPLE CALCULATIONS OF THE MODIFIED NONLINEAR ELEMENT AND DIDF

The modified nonlinear element method as explained in Chapter II is used to find the DIDF of the absquare when the secondary signal is a triangle or square wave. The average DIDF method developed in Chapter II is used to calculate the TSIDF. The procedures given in the following detailed example were followed in deriving the DIDF's tabulated in Chapter IV. The cases where the secondary signal is a sine wave are the most difficult to solve and the average DIDF method provides some labor savings in these cases. The approximate solutions for the TSIDF of dead band, limiter, and limiter with dead band given in Chapter IV were found by the approximate trapezoidal integration rule in solving the second integral of the average DIDF method.

A. Sine Wave Secondary Signal

The equation describing the absquare nonlinear element is

$$N(e) = e^2 \operatorname{sgn}(e) \quad . \quad (A-1)$$

The DIDF is found by Equations (2.29) and (2.31) which are repeated here for convenience.

$$g(A, B, \phi) = \frac{A + B \cos \phi}{D} \cdot \frac{1}{\pi A} \int_0^{2\pi} N(D \sin \omega t) \sin \omega t \, d\omega t \quad (\text{A.2})$$

where

$$D \triangleq \sqrt{A^2 + B^2 + 2AB \cos \phi} \quad (\text{A.3})$$

and

$$\hat{K}(A, B) = \frac{1}{2\pi} \int_0^{2\pi} g(A, B, \phi) \, d\phi \quad (\text{A.4})$$

Substituting Equation (A.1) into Equation (A.2) gives $g(A, B, \phi)$ for the absquare.

$$g(A, B, \phi) = \frac{1 + \frac{B}{A} \cos \phi}{D} \cdot \frac{2}{\pi} \int_0^{\pi} D^2 \sin^2 \omega t \, d\omega t \quad (\text{A.5})$$

or

$$g(A, B, \phi) = \frac{8D}{3\pi A} (A + B \cos \phi) \quad (\text{A.6})$$

The DIDF becomes

$$\hat{K}(A, B) = \frac{4}{3\pi^2 A} \int_0^{2\pi} (A + B \cos \phi) \sqrt{A^2 + B^2 + 2AB \cos \phi} \, d\phi \quad (\text{A.7})$$

The integrand is symmetrical about $\phi = \pi$ and is solved by separating the integral into two parts which are easily identified as elleptic integrals.

$$\begin{aligned} \hat{K}(A, B) &= \frac{8}{3\pi^2 A} \int_0^{\pi} \sqrt{A^2 + B^2 + 2AB \cos \phi} \, d\phi \\ &+ \frac{8}{3\pi^2} \frac{B}{A} \int_0^{\pi} \cos \phi \sqrt{A^2 + B^2 + 2AB \cos \phi} \, d\phi \quad (\text{A.8}) \end{aligned}$$

The solution of the first integral of Equation (A.8) is found to be

$$Q_1 = \frac{16}{3\pi^2} (A + B) E\left(\frac{\pi}{2}, k\right) \quad (\text{A.9})$$

where

$$k = \frac{2\sqrt{AB}}{(A + B)^2} \quad (\text{A.10})$$

and $E\left(k, \frac{\pi}{2}\right)$ is the complete elliptic integral of the second kind. The second integral of Equation (A.8) is denoted by Q_2 .

$$Q_2 = \frac{8}{3\pi^2} \frac{B}{A} \int_0^{\pi} \cos \phi \sqrt{A^2 + B^2 + 2AB \cos \phi} \, d\phi \quad (\text{A.11})$$

or

$$Q_2 = \frac{8}{3\pi^2} \left(\frac{B}{A} \sin \phi \sqrt{A^2 + B^2 + 2AB \cos \phi} \right) \Big|_0^{\pi} + \frac{8B^2}{3\pi^2} \int_0^{\pi} \frac{\sin^2 \phi \, d\phi}{\sqrt{A^2 + B^2 + 2AB \cos \phi}} \quad (\text{A.12})$$

The solution of Equation (A.12) is shown by Byrd and Friedman [38] to be

$$Q_2 = \frac{8B^2}{3\pi^2} \left(\frac{8}{A + B} \right) \left(\frac{1}{3k^4} \right) [(2 - k^2) E(k) - 2(k')^2 F(k)] \quad (\text{A.13})$$

where

$$(k')^2 = 1 - k^2 \quad (\text{A.14})$$

The modulus k is given by Equation (A.10) and $F\left(\frac{\pi}{2}, k\right)$ is the complete elliptic integral of the first kind. Equation (A.13) may be written

$$Q_2 = \frac{8}{9\pi^2} \frac{(A + B)}{A^2} [(A^2 + B^2)E - (A - B)^2 K] \quad (\text{A.15})$$

where, according to standard notation,

$$E \triangleq E\left(\frac{\pi}{2}, k\right) = E(k) \quad (\text{A.16})$$

and

$$K \triangleq F\left(\frac{\pi}{2}, k\right) = F(k) \quad (\text{A.17})$$

Adding Q_1 and Q_2 gives the DIDF of absquare.

$$\hat{K}(A, B) = \frac{8(A + B)}{9\pi^2 A^2} [(7A^2 + B^2)E - (A - B)^2K] \quad (\text{A.18})$$

The modified nonlinear element $\hat{N}(A_o, B)$ is explained in Chapter II. The expression for $\hat{N}(A_o, B)$ is given by the integral

$$\hat{N}(A_o, B) = \frac{1}{2\pi} \int_0^{2\pi} N(A_o + B \sin \beta t) d\beta t \quad (\text{A.19})$$

Equation (A.19) is separated into two parts for the absquare; i.e.,

$$\hat{N}(A_o, B) = \frac{1}{2\pi} \int_{-\theta_1}^{\pi+\theta_1} (A_o + B \sin \beta t)^2 d\beta t - \frac{1}{2\pi} \int_{\pi+\theta_1}^{2\pi-\theta_1} (A_o + B \sin \beta t)^2 d\beta t, \quad (\text{A.20})$$

where

$$\theta_1 = \sin^{-1} \left[\text{sat} \left(\frac{A_o}{B} \right) \right], \quad (\text{A.21})$$

Evaluating Equation (A.20) gives

$$\hat{N}(A_o, B) = \frac{1}{\pi} \left[(2A_o^2 + B^2) \theta_1 + 4A_o B \cos \theta_1 - B^2 \sin \theta_1 \cos \theta_1 \right] \quad (\text{A.22})$$

The DIDF could have been found by using the modified nonlinear element of

Equation (A.22) as the first stage of the two-stage evaluation process

(Chapter II). However, the mechanics of solving the integrals are somewhat

more involved, but the same final expressions may be worked out. Equation

(A.22) simplifies to

$$\hat{N}(A_o, B) = \begin{cases} \frac{1}{\pi} \left[(2A_o^2 + B^2) \sin^{-1} \theta_1 + 3A_o B \sqrt{1 - \left(\frac{A_o}{B} \right)^2} \right]; & A_o < B \\ (A^2 + \frac{1}{2} B^2); & A \geq B \end{cases} \quad (\text{A.23})$$

The input and output signals are shown in Figure A.1. A multiplying factor c may be inserted to add to the generality of the absquare.

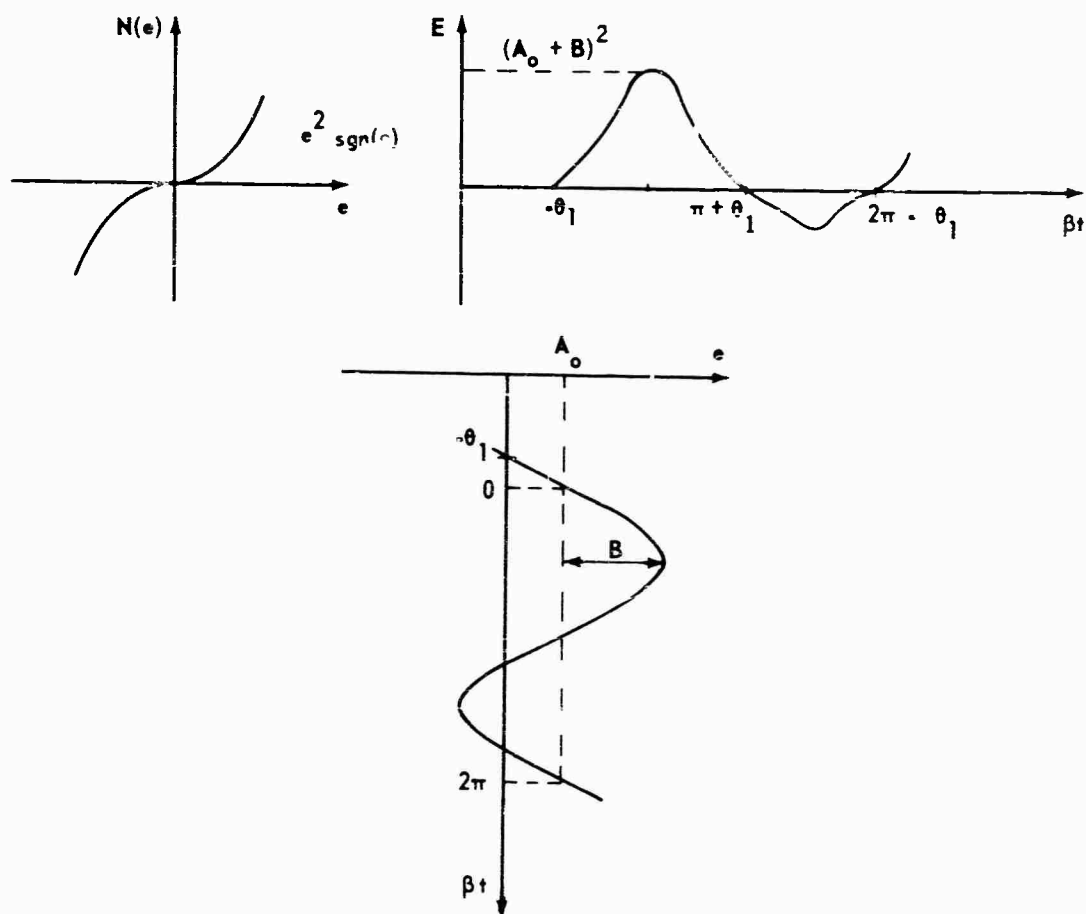


Figure A-1. Input and Output Signals of Absquare for Computing Modified Nonlinear Element

B. Triangle Wave Secondary Signal

The application of the modified nonlinear element concept is very straightforward when the secondary signal is either a triangle wave or square wave. In many instances the "stabilizing" property of these secondary signals is not very different than that of a sine wave [32]. However, the resulting effective gain may be very different, as was shown in Chapter III and

elsewhere [16,33]. The modified nonlinear element is first found as follows:

Assume the triangle wave $\sigma(\beta t)$ and the dc bias A_0 shown in Figure A-2.

The equation for the triangle wave secondary signal is

$$\begin{aligned} \sigma(\beta t) &= B \left(\frac{\beta t}{\pi/2} \right) ; & -\pi/2 \leq \beta t \leq \pi/2 \\ & B \left(\frac{\pi - \beta t}{\pi/2} \right) ; & \pi/2 \leq \beta t \leq \frac{3\pi}{2} \end{aligned} \quad (\text{A.24})$$

The integral form for the modified nonlinear element is

$$\begin{aligned} \hat{N}(A_0, B) &= \frac{2}{2\pi} \int_{-\theta_1}^{\pi/2} \left(A_0 + \frac{2B}{\pi} \beta t \right)^2 d\beta t \\ &\quad - \frac{2}{2\pi} \int_{\pi-\theta_1}^{3\pi/2} \left[A_0 + B \left(\frac{\pi - \beta t}{\pi/2} \right) \right]^2 d\beta t \quad (\text{A.25}) \end{aligned}$$

The last integral of Equation (A.25) is best simplified so that

$$\hat{N}(A_0, B) = \frac{1}{\pi} \int_{-\theta_1}^{\pi/2} \left(A_0 + \frac{2B}{\pi} \beta t \right)^2 d\beta t - \frac{1}{\pi} \int_{\theta_1}^{\pi/2} \left(A_0 - \frac{2B}{\pi} \beta t \right)^2 d\beta t \quad (\text{A.26})$$

$$\hat{N}(A_0, B) = \frac{1}{\pi} \left[2A_0^2 \theta_1 + \frac{4A_0 B}{\pi} \left(\frac{\pi^2}{4} - \theta_1^2 \right) + \frac{8B^2}{3\pi^2} \theta_1^3 \right] \quad (\text{A.27})$$

The angle θ_1 is found from the relation

$$\sigma(\theta_1) = A_0 \quad (\text{A.28})$$

or

$$\theta_1 = \left(\frac{\pi}{2} \right) \text{sat} \frac{A_0}{B} \quad (\text{A-29})$$

Substituting for θ_1 in Equation (A.27) results in the following relationships:

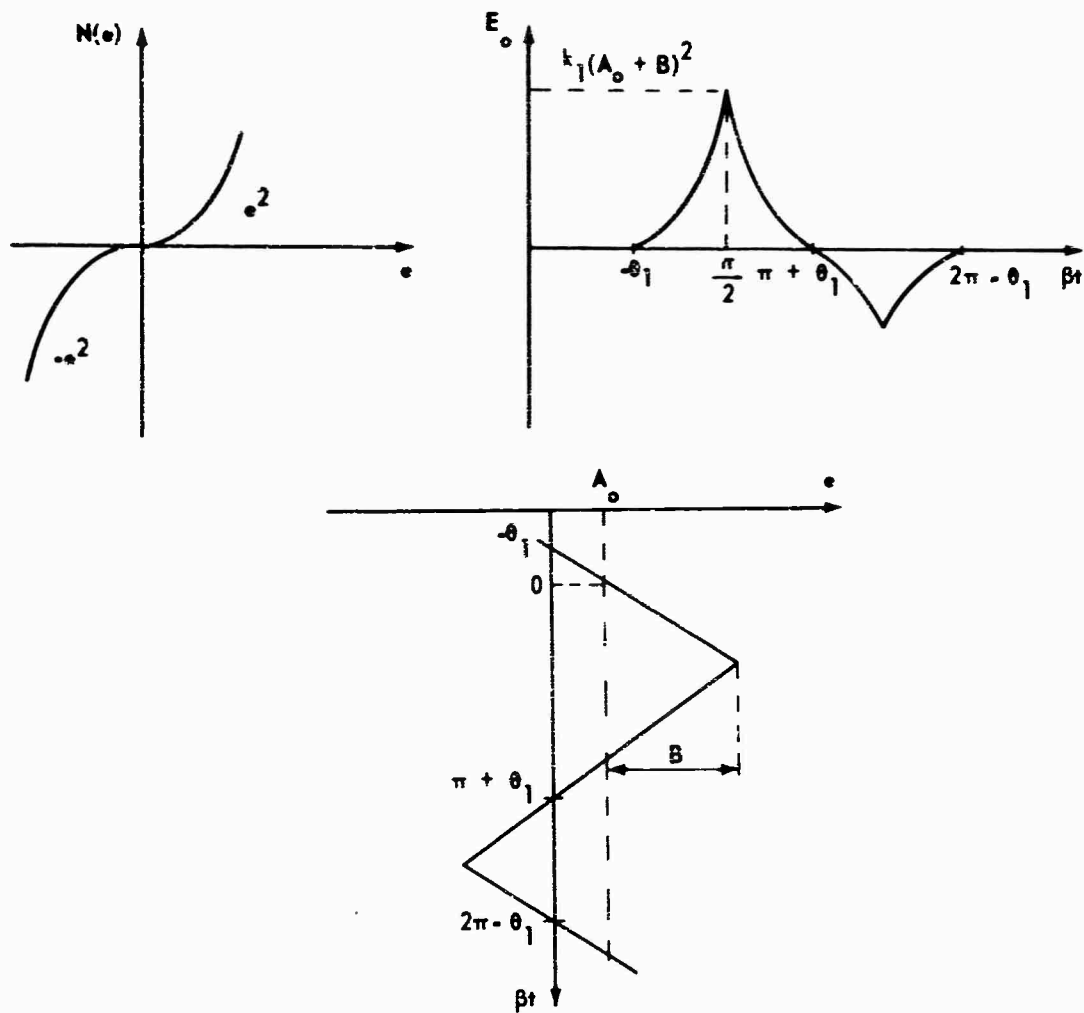


Figure A-2. Input and Output Signals of Absquare Nonlinear Element for Determining the Modified Nonlinear Element

$$\hat{N}(A_o, B) = \begin{cases} A_o B + \frac{A_o^3}{3B} & ; \quad A_o \leq B \\ A_o^2 + \frac{B^2}{2} & ; \quad A_o > B \end{cases} \quad (\text{A.30})$$

The DIDF is found with the signal $A \sin \omega t$ as the primary component of the input to the modified nonlinear element $\hat{N}(A_o, B)$ (Figure A-3). It should be noted that Equation (A.30) would have to be modified slightly to hold for

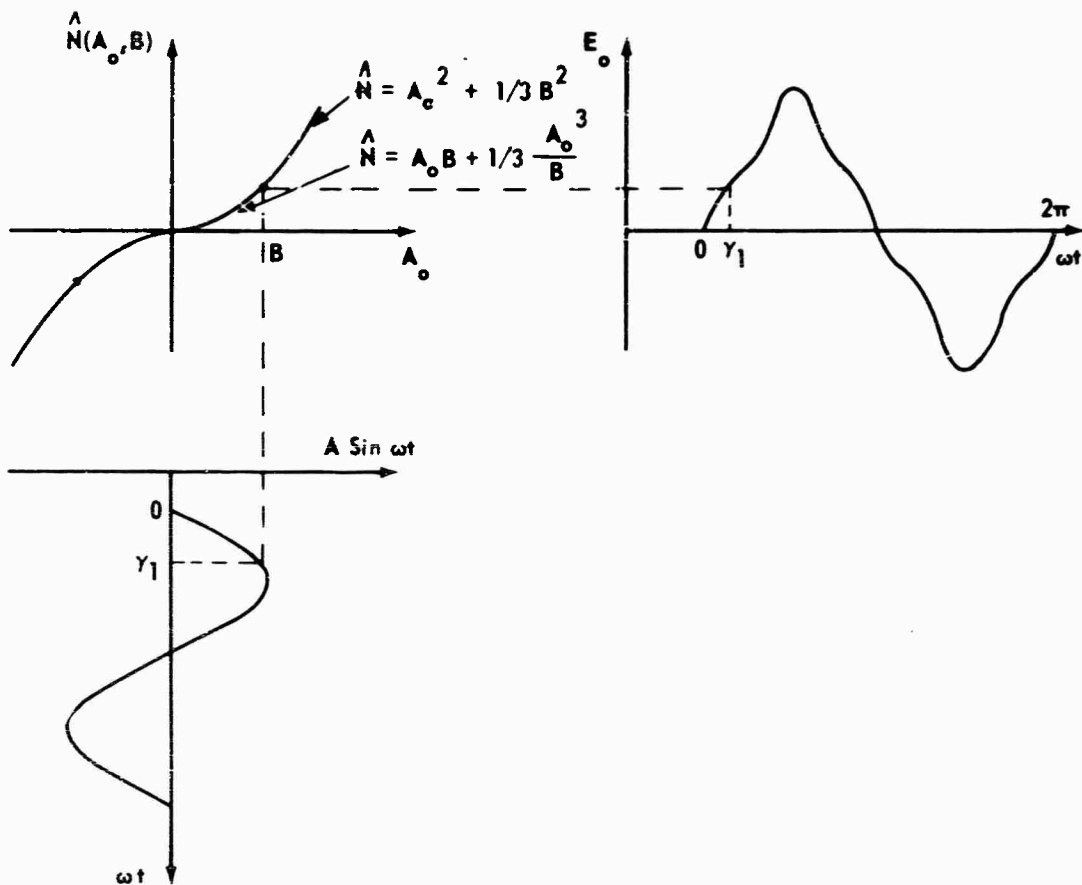


Figure A-3. Modified Nonlinear Element for Absquare with Triangle Wave Secondary Signal, Shown with Primary Input Signal

negative values of A_0 . This will hold true for most of the modified nonlinear elements to be derived and will be neglected hereafter.

The DIDF is found by using Equation (2.5) which is restated here.

$$\hat{K}(A, B) = \frac{1}{\pi} \int_0^{2\pi} \hat{N}(A \sin \omega t, B) \sin \omega t \, d\omega t \quad (A.31)$$

Therefore,

$$\hat{K}(A, B) = \frac{4}{\pi A} \int_0^{\gamma_1} \left(AB \sin \omega t + \frac{1}{3} \frac{A^3 \sin^3 \omega t}{B} \right) \sin \omega t \, d\omega t$$

$$\begin{aligned}
& + \frac{4}{\pi A} \int_{\gamma_1}^{\pi/2} \left(A^2 \sin^2 \omega t + \frac{1}{3} B^2 \right) \sin \omega t \, d\omega t \\
\hat{K}(A, B) & = \frac{1}{\pi} \left[B \left(2\gamma_1 - 2 \sin \gamma_1 \cos \gamma_1 \right) \right. \\
& + \frac{A^2}{B} \left(\frac{\gamma_1}{2} - \frac{2 \sin \gamma_1 \cos \gamma_1}{4} - \frac{\sin^3 \gamma_1 \cos \gamma_1}{3} \right) \\
& \left. + A \left(\frac{4}{3} \cos \gamma_1 - \frac{4}{3} \cos^3 \gamma_1 \right) - \frac{4}{3} \frac{B^2}{A} \cos \gamma_1 \right] , \tag{A.33}
\end{aligned}$$

where

$$\gamma_1 = \sin^{-1} \text{sat} \left(\frac{B}{A} \right) . \tag{A.34}$$

Substituting this value for γ_1 into Equation (A.33) gives

$$\hat{N}(A, B) = \begin{cases} \frac{1}{\pi} \left[\left(2B + \frac{A^2}{2B} \right) \sin^{-1} \left(\frac{B}{A} \right) + \sqrt{1 - \frac{B}{A}} \left(\frac{B^2}{3A} - \frac{13A}{6} \right) \right] ; & A > B \\ B + \frac{A^2}{4B} ; & A \leq B . \end{cases} \tag{A.35}$$

C. Square Wave Secondary Signal

In this case γ_1 is always zero (Figure A-1). The square wave signal is shown in Figure A-4.

The modified nonlinear element is described by the relation

$$\hat{N}(A_o, B) = \frac{1}{2\pi} \int_0^{\pi} (A_o + B)^2 d\beta t + \text{sgn}(A_o - B) \frac{1}{2\pi} \int_{\pi}^{2\pi} (A_o - B)^2 d\beta t . \tag{A.36}$$

Evaluating these integrals shows the modified nonlinear element to be

$$\hat{N}(A_o, B) = \begin{cases} 2BA_o ; & A_o \leq B \\ A_o^2 + B^2 ; & A_o > B . \end{cases} \tag{A.37}$$

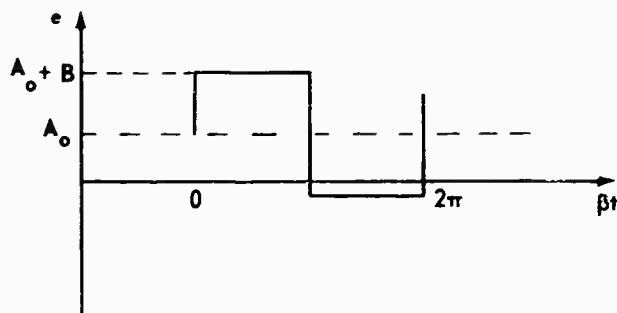


Figure A-4. Bias and Square Wave Secondary Signal

Again the DIDF is found by assuming the signal $A \sin \omega t$ as the input to $\hat{N}(A_0, B)$ and determining the fundamental output (Figure A-3)

$$\begin{aligned} \hat{K}(A, B) &= \frac{4}{\pi A} \int_0^{\gamma_1} 2AB \sin^2 \omega t \, d\omega t \\ &+ \frac{4}{\pi A} \int_{\gamma_1}^{\pi/2} (A^2 \sin^2 \omega t + B^2) \sin \omega t \, d\omega t \quad , \end{aligned} \quad (\text{A.38})$$

where again

$$\gamma_1 = \sin^{-1} \text{sat} \left(\frac{B}{A} \right) \quad . \quad (\text{A.39})$$

The DIDF is found to be

$$\hat{K}(A, B) = \frac{4}{\pi} \left[B \sin^{-1} \text{sat} \left(\frac{B}{A} \right) + \frac{1}{3} \left(2A + \frac{B^2}{A} \right) \sqrt{1 - \text{sat} \left(\frac{B}{A} \right)^2} \right] \quad . \quad (\text{A.40})$$

Separating the last equation into two parts results in the following simplified expressions:

$$\hat{K}(A, B) = \begin{cases} \frac{4}{\pi} \left[B \sin^{-1} \left(\frac{B}{A} \right) + \frac{1}{3} \left(2A + \frac{B^2}{A} \right) \sqrt{1 - \left(\frac{B}{A} \right)^2} \right] ; & B < A \\ 2B ; & B \geq A \quad . \end{cases} \quad (\text{A.41})$$

This shows the linear range mentioned in Chapter III [Equation (3.31)].

REFERENCES

1. L. A. McColl, Fundamental Theory of Servomechanisms (New York: D. van Nostrand, 1945), 78-87.
2. J. C. Lozier, "Carrier-Controlled Relay Servos," Electrical Engineering, 69 (December 1950), 1052-1056.
3. L. C. Goldfarb, "On Some Nonlinear Phenomena in Regulatory Systems," Avtomatika Telemekhanika, 8 (1947), 349-3831, reprinted in Frequency Response (New York: MacMillan, 1956).
4. A. Tustin, "The Effects of Backlash and of Speed Dependent Friction on the Stability of Closed-Cycle Control Systems," IEEE Journal (London), 94 (1947), 143-151.
5. Ralph J. Kochenburger, "A Frequency Response Method for Analyzing and Synthesizing Contactor Servomechanisms," Trans AIEE, 69 (1950), Part 1, 270-284.
6. N. Kryloff and N. Bogoliuboff, Introduction to Non-Linear Mechanics (Princeton: Princeton University Press, 1943).
7. J. C. West, J. L. Douce, and R. K. Livesly, "The Dual-Input Describing Function and Its Use in the Analysis of Nonlinear Feedback System," Proc IEEE, 103 (1956), Part B, 463-474.
8. R. Oldenburger, "Signal Stabilization of a Control System," Trans ASME, 79 (1957), 1869-1872.
9. M. J. Sommerville and D. P. Atherton, "Multi-Gain Representation for a Single-Valued Non-Linearity with Several Inputs, and the Evaluation of Their Equivalent Gains by a Cursor Method," Proc IEE, 105 (July 1958), Part C, 537-549.
10. R. Oldenburger and R. C. Boyer, "Effects of Extra Sinusoidal Inputs to Nonlinear Systems," Trans ASME (December 1962).

11. J. E. Gibson and R. Sridhar, "A New Dual-Input Describing Function and an Application to the Stability of Forced Nonlinear Systems," Trans AIEE, Applications and Industry, 66 (May 1963), 65-70.
12. W. R. Bennett, "New Results in the Calculation of Modulation Products," Bell System Technical Journal (1935), 228-243.
13. R. M. Kalb and W. R. Bennett, "Ferromagnetic Distortion of a Two-Frequency Wave," Bell System Technical Journal, 4 (1935), 322-359.
14. B. E. Amsler and R. E. Gorozdos, "On the Analysis of Bi-Stable Control Systems," IRE Trans on Automatic Control, AC4 (December 1959), 46-58.
15. R. Sridhar and R. Oldenburger, "Stability of Nonlinear Feedback Systems in the Presence of Gaussian Noise," Trans ASME (March 1962), 61-70.
16. D. P. Atherton and G. F. Turnbull, "Response of Nonlinear Characteristics to Several Inputs and the Use of the Modified Nonlinearity Concept in Control Systems," Proc IEE, III (January 1964), 157-164.
17. A. Gelb and N. E. Vander Velde, "On Limit Cycling Control Systems," Trans IEEE, AC8 (April 1963), 142-157.
18. A. Gelb and W. E. Vander Velde, Multi-Input Describing Functions and Nonlinear System Design (New York: McGraw-Hill, 1968).
19. A. K. Mahalanabis and A. K. Nath, "On the Compensation of Hysteresis Effects in Relay Control Systems by Using Positive Hysteresis," Journal of Electronics and Control, 17 (1964).
20. A. K. Mahalanabis and A. K. Nath, "On the Statistical Equivalent Gain of Memory Type Nonlinearities," IEEE International Convention, Proc on Automatic Control (March 1964).
21. A. K. Mahalanabis and A. K. Nath, "A Method of Finding the Equivalent Gains of Double-Valued Nonlinearities," International Journal of Control, I (1965), 281.
22. D. P. Atherton, "A Note on Nonlinearities in Series," International Journal of Control, II (1965).
23. A. K. Mahalanabis and A. K. Nath, "On a Note on Nonlinearities in Series," International Journal of Control, IV (1966).

24. A. K. Mahalanabis and A. K. Nath, "Stability of a Hysteretic System with Random Signal Inputs," International Journal of Control, II (1965), 135.
25. A. K. Mahalanabis and A. K. Nath, "On the Stability of a Hysteretic System Under Sinusoidal Excitation," International Journal of Control, II (1965), 551.
26. A. K. Mahalanabis and A. K. Nath, "On the DIDF of a Nonlinear Element with Memory," IEEE Trans on Automatic Control, AC11 (January 1966), 138.
27. A. K. Mahalanabis and A. K. Nath, "A Multiple-Input Quasi-Linearization Method with Applications," International Journal of Control, IV (1966).
28. A. K. Nath and A. K. Mahalanabis, "Method of Statistical Linearization, Its Application for Evaluation of the Response of a Hysteretic System to Gaussian Inputs," Proc IEE, 113 (December 1966), 2081.
29. M. Ananda Mohan and G. Krishna, "On Some Aspects of Statistical Linearization of Nonlinear Elements," International Journal of Control, III (1966), 541-555.
30. G. E. Cook, Determination and Application of the Dual-Input Describing Function for Multivalued Nonlinearities, PhD. Thesis, Vanderbilt University (Ann Arbor, Michigan: University Microfilms, Inc., 1965).
31. A. K. Mahalanabis and R. Oldenburger, "Signal Stabilization of a Memory Type Nonlinearity," Trans ASME, Journal of Basic Engineering, 89 (June 1967), Series D.
32. R. Oldenburger and T. Nakada, "Signal Stabilization of Self-Oscillating Systems," IRE Trans on Automatic Control, AC6 (1961), 319-325.
33. O. I. Elgerd, "Continuous Control by High Frequency Signal Injection," Instruments and Control Systems (December 1964), 87-91.
34. J. E. Gibson, J. C. Hill, E. S. Ibrahim, and E. G. di Tada, Describing Function Inversion: Theory and Computational Techniques (Lafayette, Indiana: Purdue University, July 1961), Technical Report TR-EE62-10, also J. E. Gibson, Nonlinear Automatic Control (New York: McGraw-Hill, 1963), Appendix E, 565-571.

35. N. Nikiforuk and J. C. West, "The Describing-Function Analysis of a Non-Linear Servo Mechanism Subjected to Random Signals and Noise," Proc IEE, 104 (November 1956) 193-203.
36. A. Gelb and W. E. Vander Velde, "Discussion of the Double Input Describing Function for Unrelated Sinusoidal Signals," IEEE Trans on Automatic Control (April 1964), 197-198.
37. A. K. Mahalanabis and A. K. Nath, "On the Dual-Input Describing Function of a Nonlinear Element," Trans IEEE, AC10 (1965), 203-204.
38. Paul F. Byrd and Morris D. Friedman, Handbook of Elliptic Integrals for Engineers and Physicists (Berlin: Springer-Verlag, 1954).
39. Erdélyi, Magnus, Oberhettinger, and Tricomi, "Higher Transcendental Functions," Bateman Manuscript Project, (New York: McGraw-Hill, 1953), 2.
40. R. Oldenburger and Y. Ikebe, "Linearization of Time-Independent Nonlinearities by Use of an Extra Signal and an Extra Nonlinearity," Trans ASME, Journal of Basic Engineering (June 1967).
41. S. Ochiai and R. Oldenburger, "The Second Describing Function and Removal of Jump Resonance by Signal Stabilization," Trans ASME, Journal of Basic Engineering, 89 (June 1967), Series D.

BIBLIOGRAPHY

- Atherton, D. P., "The Evaluation of the Response of Single-Valued Non-Linearities to Several Inputs," Proc IEE (October 1961), 146-157.
- Bass, R. W., "Mathematical Legitimacy of Equivalent Linearization by Describing Functions," Proc of the First Congress of the International Federation of Automatic Control, Moscow (1960), 895-905.
- Bocton, R. C., "The Analysis of Nonlinear Control Systems with Random Inputs," Symposium on Nonlinear Circuit Analysis, Polytechnic Institute of Brooklyn (April 23-24, 1953), 369-391.
- Douce, J. L., "A Note on the Evaluation of the Response of a Non-Linear Element to Sinusoidal and Random Signals," Proc IEE (October 1957), 88-92.
- Douce, J. L., and King, R. E., "Instability in a Nonlinear Conditionally Stable System Subjected to a Sinusoidal Input," Trans AIEE, Applications and Industry (January 1959), 665-670.
- Elgerd, O. I., High-Frequency Signal Injection: A Means of Changing the Transfer Characteristics of Nonlinear Elements (University of Florida, 1963), Technical Paper No. 240, XVI.
- Elgerd, O. I., A Study of Asynchronously Excited Oscillations in Nonlinear Control Systems (Hughes Aircraft Company, August 1959), TM-619.
- Gibson, J. E., and Sridhar, R., "The Response of Nonlinear Closed-Loop Systems to Random Inputs," Trans ASME, Journal of Basic Engineering (March 1964), 132-138.
- Grief, H. D., "Describing Function Method of Servomechanism Analysis Applied to Most Commonly Encountered Nonlinearities," Trans AIEE, Applications and Industry (September 1953), 243-248.
- Johnson, E. C., "Sinusoidal Analysis of Feedback-Control Systems Containing Nonlinear Elements," Trans AIEE, Applications and Industry (July 1952), 169-181.

- Irdu, Ramu, and Deekshatulu, B. L., "Analysis of Systems with Backlash and Resolution," International Journal of Control, 4 (1966), 325-336.
- Kochenburger, R. J., "Limiting in Feedback Control Systems," Trans AIEE, Applications and Industry (July 1953), 180-194.
- Loeb, J. M., "A General Linearizing Process for Nonlinear Control Systems," ed. by A. Tustin, Automatic and Manual Control (London: Butterworth Scientific Publication, 1952), 275-283.
- Oldenburger, R., and Liu, C. C., "Signal Stabilization of a Control System," Trans AIEE, 59 (May 1959), 96-100.
- Oldenburger, R., and Sridhar, R., "Signal Stabilization of a Control System with Random Inputs," Trans AIEE (November 1961), 260-268.
- Oldenburger, and Nicholls, R. E., "Stability of Subharmonic Oscillations in Nonlinear Systems," Trans ASME, Journal of Basic Engineering (March 1964), 116-120.
- Sen, A. K., "A Note on Complex Equivalent Gain," Trans IEEE, Automatic Control (October 1967), 620-621.
- Sen, A. K., "The Use of an RMS Describing Function for the Study of Low-Order Systems Incorporating Backlash," International Journal of Control, 6 (1967), 75-80.
- Turnbull, G. F., Atherton, D. P., and Townsend, J. M., "Method for the Theoretical Analysis of Relay Feedback Systems," Proc IEE, 112 (May 1965), 1039-1055.
- Tustin, A., "A Method of Analysing the Effect of Certain Kinds of Nonlinearity in Closed-Cycle Control Systems," Journal IEE, 94 (1947), 152-160.
- West, J. C., and Nikiforuk, P. N., "The Frequency Response of a Servomechanism Designed for Optimum Transient Response," Trans AIEE (September 1956), 234-239.
- West, J. C., and Nikiforuk, P. N., "The Behavior of a Remote-Position-Control Servomechanism with Hard Spring Nonlinear Characteristics," Proc IEEE (1964), 481-492.

DISTRIBUTION

	No. of Copies		No. of Copies
U. S. Army Missile Command Distribution A	79	Flight Controls Project Office, Data Systems Division, Autonetics, a Division of North American Rockwell Corporation	
Defense Documentation Center Cameron Station Alexandria, Virginia 22314	20	ATTN: Harold L. Ehlers, Flight Controls Project Engineer	1
North American Aviation, Inc. Columbus Division ATTN: Ralph C. A'Harrach 4300 E. Fifth Avenue Columbus, Ohio 43219	1	Dept. 344-17, Building 221 3370 Miraloma Anaheim, California 92803	
Cornell Aeronautical Laboratory 4455 Genesee Street ATTN: J. Normal Ball Head, Flight Research Dept. P. O. Box 235 Buffalo, New York 14221	1	The Johns Hopkins University Applied Physics Laboratory ATTN: Robert E. Fischell 8621 Georgia Avenue Silver Spring, Maryland 20910	1
Thompson-Ramo-Wooldridge, Inc., Systems Division ATTN: E. P. Blackburn, Manager, Electronic Systems Laboratory 1735 I Street, NW Washington, D. C. 20006	1	Northrop Corporation/Norair Division 3712/31 ATTN: John E. Glenn, Controls Research Engineer 3901 West Broadway Hawthorne, California 90250	
Honeywell, Inc., Aerospace Division ATTN: Boris Boskovich, Project Engineer 2600 Ridgway Road Minneapolis, Minnesota 55413	1	Johns Hopkins University Applied Physics Laboratory ATTN: Dr. Walter A. Good 8621 Georgia Avenue Silver Spring, Maryland 20910	1
General Electric Company Ordnance Department ATTN: Charles E. Bradford Consulting Development Engineer 100 Plastics Avenue Pittsfield, Massachusetts 01201	1	Princeton University Room 302, Sayre Hall Forrestal Campus ATTN: Professor Dunstan Graham Princeton, New Jersey 8540	1
Martin Marietta Corporation, Denver Division, Mail No. 0451 ATTN: Dr. A. J. Bradt, Chief of Guidance and Controls P. O. Box 179 Denver, Colorado 80201	1	Martin Marietta Company Electromechanical ATTN: Philip C. Gregory, Department Head MP-172, P. O. Box 5837 Orlando, Florida 32805	1
Stanford University, Department of Aeronautics and Astronautics ATTN: Dr. Daniel B. DeBra Senior Research Assistant Stanford, California 94305	1	Lockheed Georgia Company Engineering Department 72-49, Zone 248 ATTN: John E. Hart, Manager, Flight Controls Marietta, Georgia 30060	1
Grumman Aircraft, West Coast Operations ATTN: Fred A. Donnebrink 999 N. Sepulveda Boulevard, Suite 510 El Segundo, California 90245	1	Lear Siegler, Inc., Astronics Division ATTN: Kenneth G. Hart, Director of Flight Control Engineering 3171 South Bundy Drive Santa Monica, California 90405	1
Collins Radio Company Mail Stn. 106-20, Avionics and Applied Science Division ATTN: Kenneth E. Dunning, Group Head Cedar Rapids, Iowa 52406	1	TRW, Inc., Systems Group Building R-2, Room 1170 ATTN: Dale P. Hoffman One Space Park Redondo Beach, California 90710	1

DISTRIBUTION (Continued)

	No. of Copies		No. of Copies
North American Rockwell/LAD Flight Dynamics Group ATTN: William L. Holladay Los Angeles International Airport Los Angeles, California 90009	1	General Dynamics Convair Division ATTN: David R. Lukens, Dynamics Group Engineer MZ 966-7, P. O. Box 1128 San Diego, California 92112	1
Honeywell, Inc., Honeywell Aero Division ATTN: Lincoln Hudson 2600 Ridgway Road Minneapolis, Minnesota 55413	1	General Electric Company, Mail Drop 130, Aircraft Equipment Division Avionic Controls Department ATTN: Michael F. Marx, Consulting Engineer P. O. Box 5000 Binghamton, New York 13902	1
Bell Aerosystems Company ATTN: Charles Janoff, Assistant to Director of Engineering P. O. Box 1 Buffalo, New York 14240	1	Data Systems Division Autonetics, D347-1, BD 32 ATTN: Dr. R. N. McCoy 3370 Miraloma Avenue P. O. Box 4171 Anaheim, California 92803	1
Advanced Flight Control Systems, Lockheed-California Company ATTN: George Kachel, Group Engineer Box 551 Burbank, California 91503	1	Hughes Aircraft Company Guidance and Control Systems Laboratory, Space Systems Division ATTN: Robert J. McElvain, Head, Systems Analysis Staff 1950 Imperial Highway El Segundo, California 90245	1
Teledyne Systems Company ATTN: Lawrence A. Kaufman, Vice President 19601 Nordhoff Street Northridge, California 91324	1	Systems Technology, inc. ATTN: Duane T. McRuer, President 13766 S. Hawthorne Boulevard Hawthorne, California 90250	1
Raytheon Company Missile Division ATTN: Richard W. King, Jr., Assistant Plant Manager Woburn Street Lowell, Massachusetts 01852	1	Honeywell, Inc., Military Products Group, Aeronautical Division ATTN: D. L. Mellen, Section Head, Advanced Flight Systems 2600 Ridgway Road Minneapolis, Minnesota 55413	1
McDonnell-Douglas Company, Eastern Division Department 238 ATTN: Fred Krachmalnick, Head, Aircraft Group Box 516 St. Louis, Missouri 63166	1	The Boeing Company Org. 2-7838, M/S 8H-40 Space Division, Aerospace Group ATTN: Warren I. Mitchell, Senior Group Engineer, G&C Systems Technology P. O. Box 3985 Seattle, Washington 98124	1
The Boeing Company Missile and Information Systems Division Aerospace Group ATTN: L. E. Leistikow, Senior Group Engineer P. O. Box 3999 Seattle, Washington 98124	1	The Bendix Corporation Flight Control Navigation and Control Division ATTN: Kurt Moses, Assistant Chief Engineer 43 Williams Avenue Teterboro, New Jersey 07608	1
General Dynamics Corporation, Fort Worth Division ATTN: E. C. Livingston, Chief, Stability and Control and Flight Controls P. O. Box 748 Fort Worth, Texas 76101	1		

DISTRIBUTION (Continued)

	No. of Copies		No. of Copies
McDonnell Douglas Astronautics Company Eastern Division ATTN: Arnold G. Mueller, Chief Guidance and Control Mechanics Engineer Box 516 St. Louis, Missouri 63166	1	McDonnell Douglas Astronautics Company Western Division Research and Development Department A-830, BBEO/MAIL ATTN: Dr. W. K. Waymeyer Chief Engineer, Guidance and Advance Flight Mechanics 3000 Ocean Park Boulevard Santa Monica, California 90406	1
North American Rockwell Autonetics Division ATTN: Dr. E. A. O'Hern, Chief Scientist, Systems 3370 Miraloma Avenue Anaheim, California 92803	1	General Dynamics/Convair Division, Mail Zone 585-0 ATTN: R. A. Westerwick, Design Specialist Leary Villa Road P. O. Box 1128 San Diego, California 92112	1
Aerospace Corporation Guidance and Control Subdivision ATTN: Dr. A. J. Schiewe, Associate Director 2350 El Segundo Boulevard P. O. Box 95085 El Segundo, California 90045	1	Massachusetts Institute of Technology Room 33-115 ATTN: Professor H. Philip Whitaker 77 Massachusetts Avenue Cambridge, Massachusetts 02139	1
Litton Systems, Inc. Guidance and Control Systems Division ATTN: Dr. Alfred F. Schmitt, Director, Digital Computer Lab Mail Station 67/31 5500 Canoga Avenue Woodland Hills, California 91364	1	Honeywell, Inc. Aeronautical Division ATTN: William T. Wright 2600 Ridgway Road Minneapolis, Minnesota 55413	1
The Boeing Company Commercial Airplane Division MS 44-02, Org. 6-7000 ATTN: Richard L. Schonman Renton, Washington 98055	1	Air Force Flight Dynamics Laboratory, FDCC ATTN: R. O. Anderson, Control Analysis Group Leader Wright-Patterson Air Force Base Ohio 45433	1
Hughes Aircraft Company Building 359, MS 500 ATTN: Dr. Lawrence Schwartz P. O. Box 90919 Los Angeles, California 90009	1	NASA Headquarters, RVA ATTN: Raymond F. Bohling Chief, Guidance and Control Design Criteria Washington, D. C. 20546	1
University of California Department of Engineering Boelter Hall 3732D ATTN: Dr. Edwin B. Stear Associate Professor of Engineering Los Angeles, California 90024	1	U. S. Army Electronics Command, Avionics Laboratory ATTN: AMSEL-VL-F, Sylvanus Bracy Fort Monmouth, New Jersey 07703	1
TRW, Inc. Systems Division 1220/RS ATTN: Mitch Streicher One Space Park Redondo Beach, California 90278	1	U. S. Air Force, ASNFD-30 ATTN: John W. Carlson Wright-Patterson Air Force Base Ohio 45433	1
Sperry Rand Company Instrumentation and Electromechanical Equipment, Sperry Flight Systems Division ATTN: E. R. Tribken, Engineering Manager P. O. Box 2529 Phoenix, Arizona 85002	1	U. S. Naval Weapons Center Code 557 ATTN: E. G. Cozzens, Head, Weapon Systems Management Division China Lake, California 93555	1
		AFIT-SEE, Air Force Institute of Technology ATTN: Maj. Russell A. Hannen Wright-Patterson Air Force Base Ohio 45433	1

DISTRIBUTION (Concluded)

	No. of Copies		No. of Copies
National Aeronautics and Space Administration		NASA, S&E-ASTR-NE, Mr. Z. Thompson	1
Electronics Research Center		AMSMI-F, Dr. McDaniel	1
ATTN: Edwin H. Hilborn	1	-RG, Mr. Huff	1
575 Technology Square		Mr. Leonard	1
Cambridge, Massachusetts 02139		-RGC, Mr. Griffith	8
		-RGN	1
Air Force Flight Dynamics Laboratory (FDSC)		-RGX, Mr. Gambill	1
ATTN: Capt. Robert P. Johannes	1	-RES	1
Wright-Patterson Air Force Base		-RBL	5
Ohio 45433		-RPR	1
		-RPA (Record Set)	1
Department of the Air Force			
Air Force Flight Dynamics Laboratory (AFSC)			
ATTN: John H. Kearns	1		
Wright-Patterson Air Force Base			
Ohio 45433			
SEFC			
ASNSFF - Aeronautical Systems Division			
ATTN: Henry F. Knecht	1		
Wright-Patterson Air Force Base			
Ohio 45433			
Naval Air Systems, Command Headquarters			
AIR 5301, Airframe Division			
Department of the Navy			
ATTN: William Koven, Head,	1		
Aero Hydro Branch			
Washington, D. C. 20360			
NASA/Langley Research Center			
Mail Stop 217A			
ATTN: Dr. Peter R. Kurzhals	1		
Head, Stability and Control Section			
Hampton, Virginia 23365			
Naval Air Systems, Command Headquarters			
Department of the Navy			
ATTN: R. S. Niemczyk	1		
Washington, D. C. 20360			
Air Force Flight Dynamics Laboratory (FDSC)			
ATTN: Morris A. Ostgaard,	1		
Principal Scientist			
Wright-Patterson Air Force Base			
Ohio 45433			

UNCLASSIFIED

Security Classification

DOCUMENT CONTROL DATA - R & D		
<i>(Security classification of title, body of abstract and indexing annotation must be entered when the overall report is classified)</i>		
1. ORIGINATING ACTIVITY <i>(Corporate author)</i> Army Inertial Guidance and Control Laboratory and Center Research and Engineering Directorate (Provisional) U. S. Army Missile Command Redstone Arsenal, Alabama 35809		2a. REPORT SECURITY CLASSIFICATION Unclassified
		2b. GROUP N/A
3. REPORT TITLE DUAL INPUT DESCRIBING FUNCTIONS		
4. DESCRIPTIVE NOTES <i>(Type of report and inclusive dates)</i> Technical Report		
5. AUTHOR(S) <i>(First name, middle initial, last name)</i> Gordon D. Welford		
6. REPORT DATE 28 October 1969	7a. TOTAL NO. OF PAGES 203	7b. NO. OF REFS 41
8a. CONTRACT OR GRANT NO.	9a. ORIGINATOR'S REPORT NUMBER(S) RG-TR-69-16	
b. PROJECT NO.		
c.	9b. OTHER REPORT NO(S) <i>(Any other numbers that may be assigned this report)</i>	
d.	AD _____	
10. DISTRIBUTION STATEMENT This document has been approved for public release and sale; its distribution is unlimited.		
11. SUPPLEMENTARY NOTES None	12. SPONSORING MILITARY ACTIVITY Same as No. 1 above	
13. ABSTRACT A study was made of Dual Input Describing Functions (DIDF) for nonlinear elements with a view toward the synthesis problem where the characteristics of the DIDF are specified a priori. The study included a literature survey and an analytical investigation of the DIDF. Improved methods for calculating DIDF's were sought. The problem of defining the DIDF in such a way that it is valid for multivalued nonlinear elements was also considered and one method of solution is proposed. The effect of changes in the secondary signal waveform on the DIDF for nonlinear elements was also investigated.		

DD FORM 1473 1 NOV 68 REPLACES DD FORM 1473, 1 JAN 64, WHICH IS OBSOLETE FOR ARMY USE.

UNCLASSIFIED

Security Classification

UNCLASSIFIED

Security Classification

14. KEY WORDS	LINK A		LINK B		LINK C	
	ROLE	WT	ROLE	WT	ROLE	WT
Dual input describing functions						

UNCLASSIFIED

Security Classification